Cape Peninsula University of Technology

APPLICATION AND EVALUATION OF ELECTROCOAGULATION TECHNIQUES FOR THE TREATMENT OF DYEHOUSE EFFLUENTS

By

ANDILE THOLE

Thesis submitted in fulfillment of the requirements for the degree

Master of Technology Chemical Engineering

In the Faculty of

Engineering

At the **Cape Peninsula University of Technology**

Supervisor: Prof D. Ikhu-Omeregbe

Co-supervisor: Mr U. Narsingh

Bellville

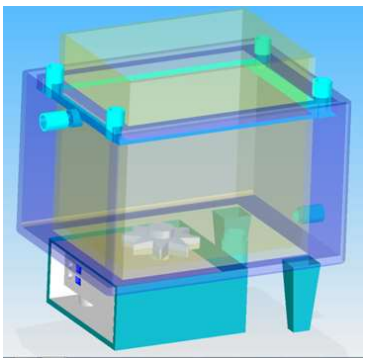

August 2015

DECLARATION

I, Andile Thole, declare that the contents of this thesis represent my own unaided work, and that this thesis has not previously been submitted for academic examination towards any qualification. Furthermore, it represents my own opinions and not necessarily those of the Cape Peninsula University of Technology.

Signed

15 August 2015

Date

ABSTRACT

Wet textile processing (WTP), is faced with many challenges that are related to operating costs and market competiveness. WTP uses large amounts of water and electricity, which constitute a big portion of operating costs of dyehouses and other costs are related to releasing large quantities of water, high concentrations of dyes and chemicals into the textile effluents with possible effluents discharge limits (EDL) penalty charges if EDL are exceeded. EDL penalty costs had become a normative part of the operating costs for some WTP textile factories, making the EDL penalties, a monthly cost item, because water utilities and the effluent discharge are not controlled and optimized. Cotton dyeing is a complicated chemi-physical-sorption process that is not easy to perform efficiently. Inefficient dyeing (off-shades and un-level dyeing) sometimes results in several reprocessing steps, leading to mega litres of water and chemical usage. Inefficient dyeing can also lead to higher concentrations of dyes and chemicals in the dyeing effluents.

The main objectives of this study were to investigate the applicability of electrocoagulation (EC) in treatment of reactive dyes textile effluents for safe discharge into sewers or for reuse and also to evaluate EC reaction kinetics in removal of various pollutants from reactive dyes textile effluent with a batch electrocoagulation reactor (ECR). To achieve these objectives; textile effluents to be used had to be created instead of using factory effluents because textile effluents vary between dyeing batches and reaction kinetics study require constant and consistent composition of effluents. This was done by following the standard commercial sample cotton-dyeing procedures. The dyeing and pre-bleaching procedures were formulated from literature sources. The dyeing and pre-bleaching were done to create the reactive dyes textile effluents with commercial sample dyeing machines; Washtec-P and Pyrotec-MB2 at liquor ratios of 10:1 and 20:1.

The reactive dyes textile effluents coming out of a pre-bleaching and dyeing at a 10:1 liquor ratio were characterized as having highest water pollution levels compared to pre-bleaching and dyeing at a 20:1 liquor ratio. The average values were found to be 3500 mg/L for COD; total suspended solids (TSS) of 141 mg/L; turbidity of 77 NTU; pH of 8.6; electrical conductivity (κ) of 8.3 mS/cm; absorbance of 1.4; and resistivity of 205 Ω.m. Most of these reactive dyeing textile effluents would have met the requirements set City of Cape Town (CCT) industrial effluent discharges limit (EDL) by-law without further treatment. This shows that with correct textile dyeing methods; it is possible for the dyehouses to archive effluent discharge limits as set in the current CCT bylaws. However, further treatment could lower the effluent discharge pollution loads and the treated effluent could be recycled in the dyehouses.

The reactive textile effluents from 20:1 liquor ratio dyeing were treated with iron electrocoagulation (IEC) process for removal of COD; $C\ell^-$; TSS; turbidity; free (f-$C\ell_2$) and total chlorines (t-$C\ell_2$) in a batch electrocoagulation reactor (ECR) at temperatures between 25°C and 55°C. The analyses for ferrous and total iron; free and the chlorine; total suspended solids (TSS); chemical oxygen demand (COD); chlorides ($C\ell^-$); and hazen colour chemical analyses of the effluent before and after EC were done with standard HACH DR 2800 uv-spectrophotometer procedures.

The batch ECR performed well in removing a variety of pollutants from the textile at temperatures between 35°C and 45°C. The highest COD removal efficiency was 81%, archived with experiments at 40°C, lowering COD from 2800 mg/L to 500 mg/L (0.0156 mol/LO_2). The lowest COD that was achieved was ±500 mg/L (0.0156 mol/LO_2) for experiments at 25°C, 30°C, and 35°C. In addition, a 99% absorbance removal was achieved with experiments at 40ºC. The highest removal efficiency of TSS; turbidity and chlorides were 92% (13.2 mg/L) at 30°C; 88% (7.5 NTU) at 35°C and 96 % $C\ell^-$ (13.0 mg/L$C\ell^-$) at 25°C respectively.

The determination of reaction constants (k_c) were performed with the integral method for COD, total chlorines [t-$C\ell_2$]; [$C\ell^-$], and absorbance ($A_{\lambda 560nm}$) at various temperatures. The reaction constants for COD ($k_{c\text{-}COD}$) removal for experiments between 25°C and 40°C were between 1.17 x10^{-4}/s and 1.51 x10^{-4}/s and between 3.19x10^{-4}/s and 4.69 x10^{-4}/s for experiments between 45°C and 55°C. The absorbance removal also followed first order reaction kinetics model with k_{c1} values between 7.71 x10^{-4} /s and 1.69 x 10^{-3} /s and the mass transfer coefficients (k_m) were between 5.08 x10^{-4} cm/s and 2.3 x10^{-4}cm/s.

The activation energy (E_A) and enthalpy of the transition state ($\Delta H^{\#}$) for COD removal were found to be -39 kJ/mol and -42 kJ/mol respectively. The total chlorines removal followed zeroth order with (k_c) values ranging from 1.4 x10^{-8} at 25°C to 2.25 x10^{-8} at 50°C; E_A= -15.7 kJ/mol; $\Delta H^{\#}$ = -13.3 kJ/mol entropy of the transition state ($\Delta S^{\#}$) were= -438.8 J/K or total chlorine. Chlorides removal followed first order model with $k_{c\text{-}C\ell}$ values between 7.0x10^{-4} /s at 25°C and 4.0x10^{-4} /s at 45°C, with the same $E_{A\text{-}C\ell}$ and ($\Delta H^{\#}$) of -32 kJ/mol.

ACKNOWLEDGEMENTS

I would like to thank God, the Almighty for giving me strength and courage.

I would like to extend my gratitude to the following for their assistance and support of this study:

My supervisors: Prof D. Ikhu-Omeregbe and Mr U. Narsingh

Chemistry Departments (Dr. B.J. Ximba; Mrs N. Mthembu) for providing laboratory space and some equipment. Dr K. Ngam; Mrs G. Fennessy-Yan and Mr L. Mnyaka.

Cape Peninsula University of Technology and my HOD, Prof D. Ikhu-Omeregbe for kindly providing me with an opportunity to be a Khula Programme recipient.

AProf M. Sheldon and Dr D. de Jager for assistant COD analysis.

Cape Peninsula University of Technology-University Research Fund (URF)

Technology Station in Clothing and Textile, (TSCT), for the provision of Commercial Sample Dyeing Machines and the Laboratory (Mr Shamil Isaacs and Mr Nelson Mali)

Dr M. Nduna; Ms S. Deyi; Dr M. Thamae; Ms M. Nkohla; Mrs I. Erdogan and Mrs L. Budler for various drafts editing and proof reading.

DEDICATIONS

To my wife, Alleta, and my mother, Nomvulo

Mr Sinford Ndinisa

To my schoolteacher who initiated me into science and technology education.

TABLE OF CONTENTS

LIST OF FIGURES

LIST OF TABLES

GLOSSARY OF ACRONYMS AND SYMBOLS

Acronyms

C.E.	Current efficiency,
C.I	Chemical Index
CCT	City of Cape Town.
CD	Chlorine Demand,
CEPT	Common Effluent Treatment Plant
CEPT	Common Effluent Treatment Plants
COD	Chemical Oxygen Demand, (mg/L O_2)
CSIR	Council of Scientific and Industrial Research
DTI	Department of Trade and Industry
DWAF	Department of Water Affairs and Forestry-South Africa
EC	Electrocoagulation
ECR	Electrocoagulation Reactor
ECT	Electrocoagulation Technology
EDL	Effluent Discharge Limit
EDTA	Ethylenediamine Tetraacatic Acid
$E_{H.}$	Equivalent Hydrogen
FAO	Food and Agriculture Organization
GAC	Granular Activated Carbon
ISO	International Standards Organization.
NHE	Normal Hydrogen Electrode
NTU	Normal Turbidity Unit
NWA	National Water Act.
ORP	Oxidation Reduction Potential
ORP	Oxidation Reduction Potentials
Pt-Co	Platimun-cobalt
RSA	Republic of South Africa
SA	South Africa
STE	Synthetic Textile Effluents
TDS	Total Dissolved Solids (mg/L)
TFSA	Textile Federation of South Africa
TMDF	Textile Manufacturing Dyeing and Finishing,
TOC	Total Organic Carbon
TSS	Total Suspended Solids (mg/L)
TWQR	Target Water Quality Range
US-EPA	United State Environmental Protection Agency
WHO	World Health Organization
WSA	Water Services Authority
WSAct	Water Services Act.
WSP	Water Services Provider
WTP	Wet Textile Processing.
WWP/W	Wastewater Treatment Plants/Works.

Symbols Description

A	Absorbance
a	Cross sectional area conductivity meter cell
A_e	Effective Surface area of the electrocoagulator electrodes, (cm^2).
d	Distance between the conductivity cell electrodes
d_e	Distance between electrodes (cm).
C_t	Concentration particles at time (t),
C_0	Concentration particles at time 0,
C^{bulk}	Concentrations particles or ions in the bulk solution
C^{surf}	Concentrations particles or ions at near surface of the electrodes
ΔE_{rev}	Change in Reversible or equilibrium potential difference, in V
ΔG^0	Change in Gibbs free energy at standard conditions.
$E_{act,}$	Activation overpotential
E_{app}	Applied voltage in V;
E_A	Activation Energy in kJ/mol,
$E°_{cell}$	Cell potential at standard conditions
$E_{Conc,}$	Concentration Overpotential at the Anode
E_{out}	Voltage output in V;
E_Ω *or* E_{IR}	Overpotential caused by solution resistance or IR-drop (V).
$\mathcal{F}$	Faradays constant 96485 $C.mol^{-1}$
h	Planck's constants (6.63×10^{-34} m^2kg/s)
I	Current
i	Current Density (A/cm^2).
i_{App}	applied current density (A/cm^2).
i_L	Limiting current density (A/cm^2).
k_B	Boltzmann's constants ($91.38x10^{-23}J.K^{-1}$)
kc_1	First order reaction constant
kc_2	Second order reaction constant
$k_{m,O}$	Mass Transfer Coefficient for Oxidation (O) Reaction
$k_{m,R}$	Mass Transfer Coefficient for Reduction (R) Reaction
K_w	the water auto-ionization constant)
M^{z+}	Metal Ions in Aqueous Phase With z Charges
m	Mass (g or mg)
R	Universal Gas constant = 8.314 J/mol.K
t	Time in (s) or min
T	Temperature in ^oC or K
u	electrophoretic velocity of the particles
V_e	Electrodes Volume, (cm^3).
V_R	Volume of the reactor.
w	Amount of Electrode Material (g/cm^2).

Greek Symbols

ε	Absorptivity
κ	Conductivity (mS/cm);
(λ_{max})	Maximum wavelength (nm);
ρ	Solution resistivity (Ω.m);
μ	Viscosity of the continuous medium

DEFINITIONS OF BASIC TERMS AND CONCEPTS

Electrocoagulation: is the process whereby the coagulants are generated within a coagulation vessel by electrolysis oxidation of an appropriate anode material. During this process, charged ionic species, or otherwise, are removed from wastewater by allowing them to react (1) with an iron having opposite charge, or (2) with floccs of metallic hydroxides generated within the effluent (Acar & Eren, 2006).

Liquor Ratios: is defined as a ratio of the total volume of water in the dyeing machine to the mass of the material to be dyed. It is the practice of textile technologists and dyers to use low liquor ratios to minimize water, chemicals and dyes use. A 'high liquor ratio' has less concentrations of pollutants but high volumes of water, whereas a 'low liquor ratio' has high concentration of pollutants in less quantity of water (Lacasse & Baumann, 2001).

Dyebath: is a liquid volume that contains dyes and auxiliary chemicals inside the dyeing machine in which the textile material is immersed. Depending on the dyeing machine, the fabric may be rotated within the dyebath to properly mix the dyes and auxiliary chemicals with the textile material (Lacasse & Baumann, 2001).

Sample Dyeing Effluent: In the textile industry, sample dyeing is used in developing new dyeing procedures, which are used to produce a shade of fabric according to customer specifications. These new procedure are then carried out in commercial sample dyeing machines. If the new procedure is successful, it is then sent to the main dyehouse for bulk dyeing under similar processing conditions. Therefore, the effluent coming out of the commercial sample dyeing machines should be similar to the effluent from bulk dyeing.

Levelling is migration dye molecules in the fabric to achieve uniform distribution of dye in a fabric. When the fabric has uneven distribution of dyes, the fabric is un-level. (Lacasse & Baumann, 2001)

Exhaustion Rate (*E*) is defined a measure of difference between concentration of dyes or chemicals in the dyebath and after dyeing. It is represented as a fraction (degree of exhaustion) or a percentage and as the difference between the initial dye concentration, (C_o) and final dye concentration (C_f) in the dyebath divided by initial dye concentration (Hamdaoui, *et al*., 2012)..

1.1 Introduction and Theses Outline

Chapter 1 presents an introduction and background information about the evaluation of the performance of the iron electrocoagulation (IEC) process in the removal of pollutants from reactive dyebath textile effluents. This chapter covers research statement, project objectives, project rationale for electrocoagulation technology (ECT) in textile effluent treatments, and then examines ECT strengths and challenges.

Chapter 2 presents a comprehensive literature review in which ECT is discussed and compared to other industrial effluents treatment technologies. The choice of a wastewater treatment technology is determined from the characteristics of wastewater or industrial effluents; therefore, the rest of Chapter 2 focuses on the characterization of textile effluents and industrial effluents standards. This characterization was very important for formulation of dyeing procedures that were used to generate textile effluents for use in this study. Water, wastewater and industrial effluent quality standards were reviewed (as shown in Table 2.1) and were found to be different from country to country from municipality to municipality (as informed by By-Laws) and as well as globally as informed by ISO and WHO.

Chapter 3. A theoretical framework for the ECT review was performed to clarify some theoretical assumptions and problems that are associated with these assumptions. A literature review of various reactions and electrocoagulation processes mechanisms that are taking place during EC was also highlighted in this chapter. The ECT proved to be a broad field of study with multi-modal mechanism at a reaction kinetics models and process mechanisms models as demonstrated in Figure 3.3 and Figure 3.2.

Chapter 4. This chapter describes procedures; equipment's and chemical reagents that were used in this study. The procedures for operating commercial sample dyeing machines (Washtec-P and Roaches Pyrotec-MB2) to generate sample textile effluents were described.

Chapter 5. discusses the pre-bleaching, dyeing and finishing textile effluent pollutants in comparison with City of Cape Town's, (CCT) industrial effluent discharge limit by-laws and other effluent discharge standards (as shown in Table 2.1, 2.3 and 2.4). The data from the sample dyeing experiments are presented in appendix A and as graphs showing all three sets of experiments. The chapter also discusses the determination of reaction kinetic parameters such reaction kinetic constant, k_c, mass transfer coefficient, k_m, and consequently, activation energy, E_a.

Chapter 6. discusses conclusions and recommendations.

1.2 Research Problem Statement

Problems of pollution can sometimes emanate from the inefficiencies of the dyeing processes such as low exhaustion rate dyes, lack of textile laboratory to dyehouse reproducibility, inefficient dyeing process and faulty processing equipments. An industrial activity of this nature has negative impacts on the environment, both in terms of pollutant discharge (and associated penalties), excessive water and energy consumption. Although the volumes of water used and the wastewater that is generated are dependent largely on the specific type of textile processing operation, in general, the TMDF operations exert the greatest water utility demands (Yildiz, *et al*., 2007).

Currently, a number of research findings have indicated that effluents originating from textile dyeing operations could be successfully treated by electrocoagulation (EC) processes (Acar & Eren, 2006; Adinew, 2012; Aslam, et al., 2004; Maharaj, et al., 2002; Barclay, et al., 2005; Savin & Butnaru, 2008; Okafor, J. O. et al, 2011 and Yusuff, R. O. & Sonibare, J. A., 2004). Therefore, treatability of textile effluents by electrochemical coagulation and flotation processes is no longer a question, but current studies are focusing on the effectiveness of the ECT and reaction kinetics. However, some of these studies have mainly been carried out with “synthetic textile effluents” that are created by simple additions of chemicals and dyes without fabric dyeing or least simulation of the real dyeing processes (Arslan, 2001; Avlonitisa I, *et al*., 2008; Montiel, 2008 and Spagni, *et al*., 2010).

The dye molecules are hydrolysed and their chemical properties are altered during the actual dyeing process (Sala & Gutiérrez-Bouzán, 2012 and Hussain, *et al* 2012). This study is about the evaluation of the removal efficiencies of various textile effluent pollutants by iron electrocoagulation and determination of absorbance, COD and chlorides reaction kinetics parameters in a batch electrocoagulation reactor (ECR).

1.4 Aims and Objectives of the Study

The main aim of this research was to determine the effectiveness of electrochemical coagulation treatment as a means of removing pollutants such as colour (absorbance and true-hazen colour (Pt-Co)); COD; turbidity; TSS; chloride and total and free chlorines from reactive dyebath textile effluents. To make this study possible, the following deliverables needed to be achieved to:

- Formulate of pre-bleaching and dyeing procedures in order to generate textile effluents.

- Determine removal efficiencies for colour (hazen colour (Pt-Co) and absorbance), COD, chlorides, free and total chlorines, turbidity and TSS removal in a batch electrochemical reactor were determined.
- Determine reaction constants (k), mass transfer coefficients (k_m) and energies of the transition state for COD, absorbencies, total chlorines and chlorides removals were determined.

1.3 Research Questions

In this study, the following questions are answered:

- How was the actual real textile effluent generated?
- Did the treatment of dyehouse effluents by electrochemical coagulation technology achieve industrial effluent discharge limits (EDL) standard (CCT bylaw) or reusable water quality standards or environmental discharge standards?
  - What were the values of electrochemical coagulation reactor reaction kinetics parameters such as reaction constants (k_c); mass transfer coefficients (k_m) for chemical oxygen demand (COD); Chlorides ($C\ell^-$); Absorbance; and total chlorines (t-$C\ell_2$) that were determined in a batch iron electrochemical coagulation reactor?
  - What were the energies of the transition state such as activation energies (E_A), enthalpies ($\Delta H^{\#}$) and Entropies ($\Delta S^{\#}$) that were determined in a batch iron electrochemical coagulation reactor (ECR)?

1.5 Rationale to the Research Problem

Wet textile processing (WTP) effluents are associated with dark colour; high COD; high pH; high conductivity; moderate biological oxygen demand (BOD) and high concentrations of total suspended solids (TSS) and total dissolved solids (TDS) (Maharaj, *et al*., 2002 and Yusuff & Sonibare, 2004). It is estimated that 10% - 20% of the total amount of dyes used worldwide are eventually discharged into the effluent stream (Yildiz, *et al*., 2007). It is common practice that textile effluents are routed to the wastewater treatment plants/works (WWTP/W) through sewage pipe networks (WWSPN) for treatment prior to release into the environment (Gilfillan, 1997). Textile effluents can be poisonous to the biomass that is used in the WWTP/W and to the environment because of high pH, heavy chemicals (high COD) pollutants and Azo dyes present in the textile effluents (Chequer, *et al*., 2013).

The WWTP/W practitioners and Water Services Authorities (WSA) are aware of the challenges associated with discharging textile effluents into WWTP/W. Textile companies are not allowed to discharge dark coloured, high conductivity, extremely low or high pH and high COD effluents into WWTP/W; otherwise, a heavy effluent discharge limits (EDL) penalty fine

is imposed by WSA (Salunke, *et al*., 2005). However, penalties do not remove threats that are imposed by industrial effluents on effectiveness and efficiencies of the WWTP/Ws, as sometimes it results in WWTWs bioreactors poisonings, resulting in untreated or partially treated effluents that eventually discharged into the rivers.

Treatment and reuse of textile effluents could not only reduce environmental impact of textile pollution but reduce wastewater generation in textile industry that could be 2.5 $x10^9$ L/annum or 177 kL/ton of fabric processed hence reduce WWTWs untreated effluent overflows. This can also reduce process water intake from municipality water supply that is about 159 kL/ton of fabric (Gilfillan, 1997). In addition to China imports, water could have resulted in closures of several clothing and dyehouse factories, especially in the Western Cape, resulting job losses is an evidence of challenges faced by this industry. For example[1], Landsdowne Textile Industries (LTI); SBH Cotton Mills; Rex Truform; Puma; BMB textile; Meritex; Romatex; SA Fine; Colourboss; Table Bay Textiles; Court Fabrics; Maximore; Calibre and South Africans Nylon Spinners are amongst those textile factories that had shutdown in the past two decades.

The textile manufacturing, dyeing and finishing (TMDF) industry is a major contributor to the South African (SA) economy. TMDF industries contribute 11% to the employment rate and 0.6% to the economic growth rate (DTI, 2007). Between 2011 and 2012, there was some sectorial employment growth of 56985 jobs from December 2011 to 58000 in jobs in 2012. Government subsidy of about R112 million to 105 companies, and production incentives of R624 million was approved for 199 companies (DTI, 2007). Proper treatment methods and technologies for industrial effluent recycling or reuse and safe disposal practices for such effluents are therefore necessary to prevent environmental pollution and ensure sustainable water utilities (Maharaj, *et al*., 2002).

1.6 Electrochemical Coagulation Technology and Research Background,

As shown in Figure 1.1, a number of techniques have traditionally been used to treat dyehouse effluents. Anaerobic biological processes have been successful in degrading the organic matter present in textile effluents and Vandevivere, *et al.*, (1998) had demonstrated in Figure 1.1 that, anaerobic biological has advanced to pilot plant scales. Physical and/or chemical treatment processes (coagulation/flocculation, adsorption, flotation, and oxidation-reduction) have also been applied in full scale (dark shaded in Figure 1.1) with varying

[1] Personal interview one dyehouse managers

degrees of successes in removing the pollutants in textile effluents. Most of the chemical treatment methods, however, require the addition of chemicals, which substantially increases operating costs (Mahvi, 2007).

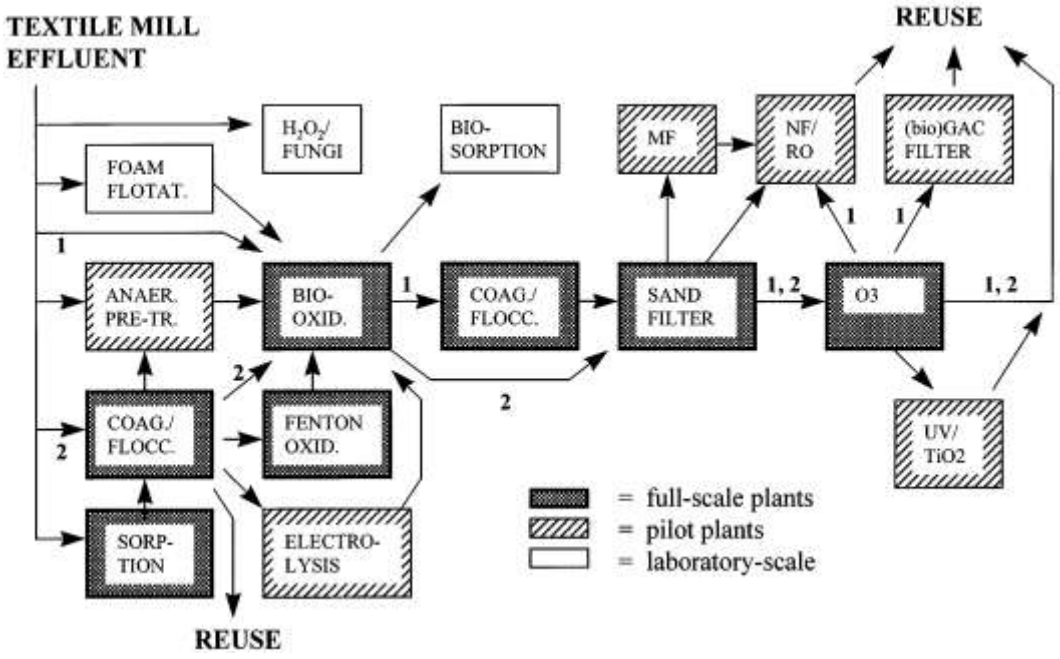

Figure 1.1 Textile Effluent Treatment Processes (Vandevivere, *et al*., 1998)

Electrochemical coagulation oxidation or electrocoagulation is an electrochemical cell that is composed of from two electrodes up to many electrodes; paired or unpaired electrodes that are connected either to monopolar series or parallel and bipolar series or parallel to an electrical power supply (Moreno-Casillas, *et al*., 2007). The monopolar is preferred if electrode passivation is a problem because this changes the polarity of the electrodes at a predetermined frequency. The electrodes are dipped into a textile effluent. EC requires an electrolytic environment (high TDS or conductivity) (Daneshvar *et al.,* 2006 ; Kim *et al.,* 2002 and sheng & Peng 1996)

In recent years, electrochemical oxidation methods have been proposed as an alternative wastewater treatment method because it can deliver a high effluent quality at relatively low capital and operating costs (Elefsiniotis *et al.,* 2007, Lin *et al.,* 2006 and Mollah, *et al*., 2004). Electrochemical techniques had been applied successfully for the treatment of potable water by Holt, (2002), Lechevallier, *et al*., (1981), Jiang, *et al*., (2002) and Vasudevan, *et al*. (2009). Chen, (2004), Cheng, *et al*., (2006) and Ersoy, *et al*., (2009) demonstrated that EC could successfully treat urban wastewater. Heavy metal laden industrial effluents were treated with EC by Henrik , *et al.,* (2006), Khue, *et al*., (2014), Ganesan, *et al*., (2012), Mahvi, *et al,* (2007), Yilmaz *et al* (2005). Textile effluents effluents (Acar & Eren, 2006, Adinew, 2012, Ali, *et al*., 2009, Ahmed & Saad , 2013, Arslan-Alaton, *et al*., 2007, Azzi, *et al.,* 2006) including surfactants contaminated WW (Mahmoud & Ahmed, 2014 and Ebru, 2007) and oily

wastewater (Fouad, 2008, Rincon, 2011, Sparks, *et al*, 1999) are also treatable with electrocoagulation.

In addition, several investigations on economic feasibility of EC as a treatment technology for textile effluents by Kobya, *et al.*, (2007), Mahvi, *et, al*. (2007), Elefsiniotis et al, (2007), Lin *et al.,* (2006), Ribordy P. *et al.,* (2007) and Vlyssides *et al.,* (2000) revealed that electrocoagulation (EC) is economically feasible with low capital and operating costs. Therefore, TMDF industry can save water or at least minimize EDL penalties by utilising electrocoagulation technology (ECT).

The concept of EC is more than a century old technology, conceptualized in England in 1889 in treatment of wastewater added with seawater (Holt *et al*., 2004). Electrocoagulation was first patented by Dietrich in 1906. While EC studies remained dormant for a number of years thereafter, various patents began to reappear in the mid-1970s in the patents of Ramirez, (1976) and Gnieser *et al.*, (1978). An area of opportunity for EC was created by the fact that ECT is very effective in removing a wide range of fine colloidal particles found in industrial effluents and its simplicity in design and operation (Beagles , 2004, Chaturvedi, 2013, Holt *et al.,* 2004, Mollah, *et al*., 2004).

1.7 Electrocoagulation Power Supply Challenges and Solutions

In South Africa, electricity is a scarce resource with occasional load shedding in 2009 and recently. Electricity prices are increasing every year, therefore the ECT might be challenged. Load shedding disrupts EC operations and electricity price increases make EC less competitive. However, EC uses low DC power, making EC amenable to be powered via solar photo voltaic cells as in the works of Valero, *et al*., (2008) and Drouiche, *et al*., (2009) or other renewable energies such as wind and hydropower. Electrocoagulation's ability to use DC allows direct application of photovoltaic cells as a power source without inverters, which is a notable cost saving. EC technology can be applied in small units of water and wastewater treatment systems that can be used in rural areas (Beagles, 2004).

EC does not need a lot of power per cubic metre of water treated. Kobya, *et al*., (2007) reported 0.63 kWh/m^3 for Fe and 0.7 kWh/m^3 for Al electrodes with series connection 0.680 kWh/m^3 for Al and 0.72 kWh/m^3 Fe electrodes with parallel connection and 20.0 kWh/kgAl (Jiang, *et al*., 2002).

1.8 Comparisons between Electrocoagulation and Chemical Coagulation

There are fundamental differences and similarities between electrocoagulation or electroflotation and conventional chemical coagulation and flocculation. The chemical

process mechanisms such as destabilization and neutralization; enmeshment and precipitations of colloids are the same in both electrocoagulation or electroflotation and conventional chemical coagulation and flocculation (Pernitsky, 2003). Both processes require rapid mixing of coagulants; pH and temperature control. Electrolyses gases can create enough turbulence that could mix coagulants and colloids (Jiang, *et al.;* 2002 and Holt, *et al.;* 2002). Also fluid pumping in continous mode electrocoagulators can provide enough mixing of coagulants with colloids (Sheng, et, al.; 1996). Therefore EC can be used without an agitator. The conventional chemical coagulation, flocculation, and electrocoagulation are further compared in Table 1.1:

Table 1.1. Differences between Electrocoagulation and Chemical Coagulation

Parameters comparisons	Chemical Coagulation (CC)/ Flocculation (CF)	Electrocoagulation or Electroflocculation	Comments and References
Chemicals Requirements	✓ Chemical Addition	No chemical addition, except for pH adjustments only	Costs saving (Mahvi, (2007));
Operating Cost Capital costs	✓ $14.18/gal ✓ More costs	$1.69/gal Less	(Powell., 2001), Chaturvedi, 2013).
Sludge production	✓ More sludge ✓ Dewatering plants	✓ Less sludge ✓ Less water bound to sludge ✓ No dewatering plants	(Beagles , 2004) and (Chaturvedi, 2013)
Cleaner Production Technology	✓ Relatively cleaner technology	cleaner technology	Jiang (2002) and Rodriguez *et al*. (2007)
Fitness to the treatment task	✓ Limited to certain pollutants	Colour, turbidity, and TDS, but also COD and bacteria. EC removes COD better than CC Muthikumara *et al*. (2007)	Sheng, *et al*., (1996), Hector, *et al*., (2009) Moreno-Casillas*, et al*., (2007)WW in including
Reactor Design	✓ Many process units	simple, no moving parts only circulation pumps and less mixer	(Beagles , 2004) and (Chaturvedi, 2013)

EC produces electrolyses gases such oxygen and hydrogen. Hydrogen can be recovered as fuel source for hydrogen fuel cell. As previously mentioned, EC uses electricity that can be a challenge as South Africa is currently having load shading. This can be overcome by using solar powdered electrocoagulators (Cho, *et al.,* 2014; Drouiche, *et al*., 2009 and Valero, *et al*., 2008) and wind power. Although EC is a most preferred technology because it requires no addition of chemicals as in conventional chemical coagulation (Mahvi, 2007; Alinsafia, *et al*., 2005; Daneshvar, *et al*., 2006 and Holt, 2002), however it requires additions of electrolytes and pH adjustments chemicals. Another challenge of EC is passivation of electrodes; however, this can be overcome by periodical chemical or mechanical cleaning of electrodes or using pulsed mode power supplier (Cifuentes, *et al*., 2001).

Chapter 2 - LITERATURE REVIEW

2.1 Global Water Problems

Water scarcity is an international dilemma with South Africa (SA) identified as one of the water-stressed countries, described, as the 26th most water stressed country (water-stress threshold is 1 700 m^3/capita/yr.) for available water per person (DWAF, 1997). Currently, only 87% of world's population has access to drinkable standard water (www.100people.org/, 1990) of which 13% comes from 1.7 billion rural dwellers (UNICEF, 2009). The freshwater (e.g. from streams, dams and lakes) is, however, not of readily drinkable quality standard. A large portion, 10% of the world's water, is used in Africa (Food and Agriculture Organization (FAO), 2013). As shown in Figure 2.1, the fresh water resources are only 2.6% of the total available water. This limited resource is also contaminated by domestic, agricultural and industrial activities and treatment before it can be used. Water use by industrial and agricultural processes need to be conserved, controlled, optimized and considering new water sources such as reuse of treated water from municipality wastewater plants, onsite effluent treatment and recycling, use of grey water for irrigations and rainwater harvesting. As shown in Figure 2.1, 97.4% of water in the world is saline in the oceans and is not drinkable because of high chlorides content (Clariant Colour Chronicle, 2005).

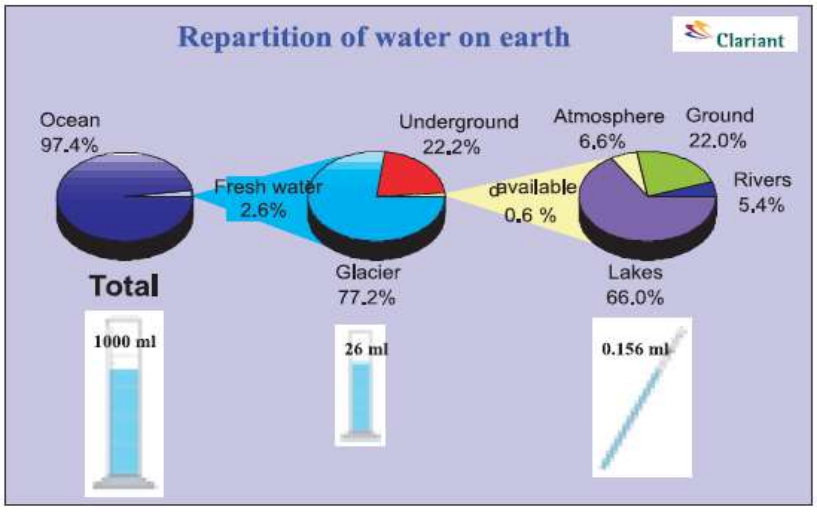

Figure 2.1 Water Balance (Clariant Colour Chronicle, 2005)

Although, there are no current studies that are focused in treatment of seawater with electrocoagulation. Seawater is electrolytic and it might be easily treatable with EC than current conventional reverse osmosis and electro-dialysis technologies.

2.2 Wastewater Policies and Discharge Standards

According to the white paper on National Water Act (NWAct) of 1998 (DWAF, 1999), it is an absolute human right for every person to receive 25 L/day; while 10% of the available water must

be reserved for the aquatic life and the ecosystem. Water management in South Africa (SA) is controlled by NWAct of 1998 and Water Services Act (WSAct) No. 108 of 1997 (Department of Water Affairs of South Africa (DWAF-SA), 1997). According to the DWAF-SA (1997), the City of Cape Town (CCT) is a Water Services Authority (WSA) and a Water Services Provider (WSP) for supply, delivery and control of water pollution within the Western Cape. The CCT enforces industrial effluent discharge by-law/s according to "Provincial Gazette no 5582 dated 15/9/2000" (CCT, 2006). Industrial effluent discharge by-law values for the CCT are shown in the second row in Table 2.1 with values of COD = 5000 mg/L, TSS = 1000 mg/L; TDS = 4000 mg/L; chlorides and sulphates = 1500 mg/L and others. The EC process must treat textile effluent to below the set standard for release into the sewers; otherwise DWAF category 4 of the EDL, Target Water Quality Range (TWQR) (DWAF, 1996) must be applied (first row in Table 2.1), if the treated effluent is to be discharged into the environment.

However, the treated effluent by EC does not need to be discharged into the environment. It can be re-used in the dyehouse if it meets Category 2 of Characterization of Industrial Water Use (DWAF, 1996)**;** General and Special standard, Regulation No. 991, 18 May 1984 (https://www.dwaf.gov.za/, Date accessed, 08/12/2014). The rest of Table 2.1 is a comparative literature review of the South African water and effluent standards to the other multi-nationals and international standards. US-EPA uses units of kg/kkg fiber for each textile processing area, over 30 days limits (US-EPA, 2013). After assessing typical textile effluent composition in this literature review, it was found that the CCTs industrial effluent by-law is a reasonable standard and it is possible to achieve these standards if efficient dyeing or at least if appropriate treatment technology are applied.

2.3 Literature Review of Textile Dyeing Processing

The high conductivity in reactive dyebath effluents comes from the electrolytes that are added as dyeing auxiliary chemicals. Typical electrolytes are sodium chloride, (NaCℓ) and sodium sulphate, (Na_2SO_4). Dyehouse effluents contain heavy metals, ammonia, alkali salts, toxic solids and large amounts of pigments, many of which are toxic. About 40% of globally used colorants contain organically bound chlorines (combined chlorine) (Saravanan, *et al*., 2010). Mordents are substances that are used to 'fix' the colour onto the fabric (such as chromium in metal complex) are very toxic.

Table 2.1 A Comparative literature review of national standards for textile effluents

Parameters	T	CN	P/ PO_4^-	pH	κ	TDS	Al/Zn	TSS	COD	f-Cl_2/$C\ell^-$	Cd /Na^+	t-Fe^{2+} /Fe^{3+}	S^-/SO_4^{2-} /SO_3^{2-}	Ph-OH	Cr^{3+} /Cr^{6+}	Cu /Mn
Units	°C	ppm	ppm		mS/cm	mg/L	mg/L	mg/L	mg/L	mg/L	mg/L	mg/L	mg/L	mg/L	mg/L	mg/L
DWAF (1996)		0.02		5,5-9,5	70	70		25	75		0.005/	0.3	1.0/500	0.2	0.05	0.01
CCT[2]	0-40	20	/25	5.5-12	500	4000[3]	/30	1000	5000	/1500	5/1000	50	50/1500	50	10	20
NEMA-Uganda[4]	20-35	0.1	/10	6.0-8.0		1200	/5.0	100	100	1.0/500		10/				
NTPA (Savin, *et al*., 2008)[5]	40	1.0	3.0/	6.8-8.5					500	0.5/	0.3/		1/600/2	30	1.5	
FMENV[6] (Yusuff, *et al*., 2004)	40	-	/5	6-9	-	2000	1.0/1.0	30	80	1.0/				10		1/5
(US-EPA, 2013)[7]	-	-	-	6.0–9.0	0.75			35.2	163.0				0.28/	0.14	0.14	
WHO(Okafor, 2011)	21	0.07		6.5-8.5		1000		25								
Pakistan NEQS, (Ali, *et al*., 2009)	40	-	-	6.0-9.0	-	3500	/5	200-400	150-400	-	0.1	2/	-	-	1	1/1.5
ISO (AAFA)[8] 2010	37	0.2	2.0	6.0-9.0			1.0	30.0	100		0.1					

[2]**Cape Metropolitan Council** Provincial Gazette no 5582 dated 15/9/2000: By-law relating to wastewater and industrial effluent
[3]At 105 °C
[4]The National Environment Management Act of Uganda (Standards for Discharge of Effluent into Water or on Land) Regulations, S.I. No 5/1999
[5] Romania Maximum Allowable Limits, however the author did not describe the abbreviation NTPA
[6] Nigerian Environmental Maximum allowable limit however the author did not describe the abbreviation FMENV
[7] US-EPA uses units of kg/kkg fiber, which translate to g pollutant/kg fiber. US-EPA standards are particular for each textile processing area, Her standards have an equivalent of 30 days limits. (US-EPA, 2013) 40CFR125.30 chapter 410.27
[8]Global Textile Effluent guidelines used by WHO, European National Standards and US-EPA

Table 2.2 shows the processing stages of textile materials along with different types of pollutants that are generated. High pH comes from sodium carbonates (Na_2CO_3) and sodium hydroxide (NaOH), are shown in Table 2.2., which are added as auxiliary chemicals during the dyeing process.

Table 2.2 Wet textile process pollutants (Yusuff, *et al*., (2004)) and (Maharaj, *et al*., (2002))

Process	Effluent	Composition Nature
Sizing	Starch, waxes, carboxymethyl cellulose (CMC), polyvinyl alcohol (PVA), Wetting agents.	High BOD, COD
Desizing	Starch, CMC, PVA, fats, waxes, peptins	High in BOD; COD; TSS;TDS
Bleaching	Sodium hypochlorite, Cl_2, NaOH, H_2O_2, acids, surfactants, $NaSiO_3$, sodium phosphate, short cotton fibre.	High alkalinity, high TSS
Mercerizing	Sodium hydroxide, cotton wax	High pH, low BOD, high DS
Dyeing	Dyestuffs urea, reducing agents, oxidizing agents, acetic acid, detergents, wetting agents	Strongly coloured, high BOD, TDS, low TSS, heavy metals
Printing	Pastes, urea, starches, gums, oils, binders, acids, thickeners, cross-linkers, reducing agents, alkali	Highly coloured, high BOD, oily appearance, TSS slightly alkali

2.3.1 Reactive Cotton Dyes Characterization

The materials that are normally dyed are synthetic, natural fibres and combination textiles and each uses different dyes and auxiliary chemicals. Reactive, direct, disperse acid and vat dyes are applied to the fabrics with various auxiliary chemicals as required. Reactive dyes can be classified by their reactive strengths as low, medium and highly reactive. The addition of an alkaline is based on the reactive strength of the reactive dyes. Soda ash is added to medium reactive dyes. Combinations of soda ash and caustic soda or caustic soda ash only are used for dark shades. Table 2.3 shows characteristics of C.I. Reactive Red 18 and C.I. Reactive Red 239. Levafix Brilliant Blue 181 (Levafix Brilliant Blue 150% EFFN) is medium reactive an anthraquinone reactive dye that is used for dyeing wool, silk, and cotton, which are natural fibres (DyStar, 2007).

Table 2.3 C.I. reactive red 18 characteristics

Dyes CI name	Molar Mass (g/mol)	Particle Size(nm)	Wavelengths λ_{max} (nm)	Source
C.I. Reactive Red 18	1086.178	1.2	541	(Asouhidou, *et al.*, 2009)
C.I. Reactive Red 239	1136.32	www.acecontracting.co.za, Date :contacted 22/10/2011		

Reactive dyes are anionic. Basic dyes are cationic, very soluble in water and are used for cotton dyeing. Disperse dyes are non-ionic (Acar, *et al*., 2006*).* Up 100g/L NaCℓ or Na_2SO_4, 15 g/L of soda ash and 5.0 g/L of NaOH and other electrolytic species are added into the dyebath during cotton dyeing. DyeStar (2007) recommends that only 1.7 g/L of 50% of caustic soda and 70 g/L of NaCℓ should be used for dark shades at 10:1 liquid to fabric ratio.

The dye molecules are classified as colloids. Colloids are particles that are too small to settle in water bodies, they remain suspended in water bodies for long periods. Davis, *et al.,* (2008) describes ccolloids as stable if they are very small, possess a negative (-ve) surface charge (reactive dyes are anionic) and a zeta potential of -25 (Yildiz & Koporal, 2007). Colloids are destabilized by a coagulation process, defined by Davis and Cornell (2008) as the process of "altering the colloids so that they will be able to approach and adhere to coagulants to form large floccs".

2.3.2 Cotton Dyeing Chemistry with Reactive Dyes

Sala, *et al*., (2012) reported reactions that take place in the cotton reactive dyeing process as in reaction R2.1(a) to R2.1(c). Therefore, as shown in equation R2.1 (a) below, the leftover dyes in the textile effluents contain chlorides bound into the dye molecule and hydrochloric acid.

$$Dye\text{-}C\ell + HO\text{-}Cellulose \Rightarrow Dye\text{-}O\text{-}Cellulose + HC\ell \quad \text{R2.1(a)}$$

$$Dye\text{-}C\ell + HO\text{-}Cellulose \Rightarrow Dye\text{-}OH + C\ell^- + Cellulose \quad \text{R2.1(b)}$$

$$Dye\text{-}C\ell + H_2O \Rightarrow Dye\text{-}OH + C\ell^- \quad \text{R2.1(c)}$$

Estimates of dyes that remain in the fabric after dyeing are between 10 and 15% (Shi, *et al*., 2007) and 20% (Daneshvar*, et al*., (2006)).

2.3.3 Cotton Dyeing Process Fabric to Liquor Ratio

A liquor ratio is defined as total volume of water in the dyeing machine to the mass of the material to be dyed. It is the practice of textile technologists and dyers to use low liquor ratios to minimize water, chemicals and dyes use. A 'high liquor ratio' carries less amounts of pollutants, but high levels of water per quanties of a pollutants. Whereas a 'low liquor ratio' carries higher conncetrations of pollutants in a less quantity of water utilised.

The liqour ratio is a very important dyeing processes parameter. A very low liquor ratio (5:1) can be achieved with Thies dyeing machine (Clark, (2011). Dyeing at low liquor ratio is what all dyers want to achieve but the machine liqour or fabric circulation rates, fabric and water contact is a determining factor. The extreme low liquor ratios of 1:3 can be achieved with ecoMaster dyeing machine (DyStar, 2010) and very high 25:1 are possible (DyeStar, (2007) and The Indian Textile Journal, (2014)). Liquor ratios are chosen according to machines capacities, capabilities and shade requirements. The conventional dyeing liquor ratios range between 10:1 and 20:1 for Thies and Jet dyeing machines (Kazakevičiūtė, *et al*., 2004)

2.3.4 Cotton Dyeing Process Description

Figure 2.2 show a textile material pre-bleaching, dyeing and fabric softening process block flow diagram. Acetic acid is added in step 6(a) and 6(b) to neutralize the fabric, thereby lowering the pH of the resulting effluents. Acetic acid also protects the fabrics from metal contamination by chelating metals in the dyebath, as it is known that cotton has impurities like copper, iron and manganese (CSIR, 1991). After all the required chemicals are added in step (1), the pre-bleaching liquor is heated at controlled rate (1.0ºC/min) in step (2) to the pre-bleaching temperature of 95°C. Various numbers of cold water rinsing (4) and one hot rinse (5) follow the pre-bleaching step. Not all dyes and chemicals that are added in the dyeing process will be fixed onto the fabric.

If the fabric comes out off-shade or un-level, the fabric will be re-dyed repeatedly until the right shade is achieved. The off-shade and un-level dyeing could lead to big volumes effluent discharge through reprocessing. The Clothing & Textile Environmental Linkage Centre quantified activities that could generate savings of about R4.98 m by 12 companies in water and effluent discharge (790 000 kL) in the textiles sector (Barclay, *et al.,* 2005). In terms of “right first time dyeing”, it is estimated that most dyehouses are 50-80% efficient (Mbolekwa & Buckley, 2008). The “Right first time dyeing” is a terminology that is used in the dyeing industry to express the efficiency of a dyeing process. If textile material is dyed right, the first time it was dyed; that is without reprocessing such as adding extra dyeing steps such levelling if the fabric is un-level or striping off dyes if the fabric is overdyed.

The broken arrow lines in Figure 2.2 represent process optional steps. For example, process route B involved desizing or scouring which is the removal of the excess chemicals, lubricants, fats and fluff. Foure *et al.* (2006) estimated that up to 80% savings could be achieved with effluents treatment in textile processing.

2.4 Low Dye Exhaustion Rate in Reactive Textile Dyeing

Dye exhaustion rate (*E*) is defined a measure of a difference between the concentration of dyes or chemicals in the dyebath and after dyeing.

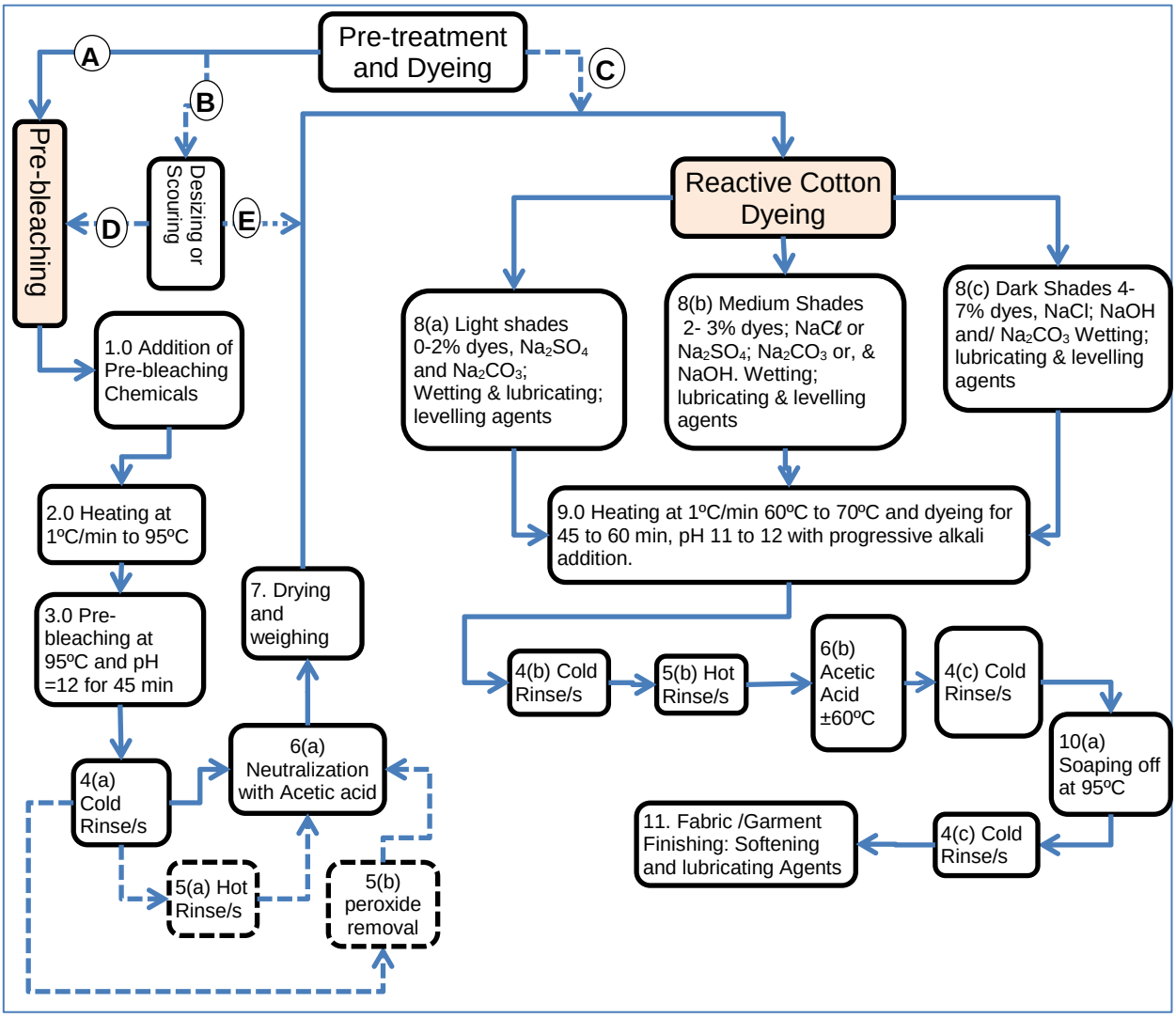

Figure 2.2.Textile preparation; dyeing and finishing block flow process diagram

It is represented as a fraction (degree of exhaustion) or a percentage and as the difference between the initial dye concentration, (C_o) and the final dye concentration (C_f) in the dyebath divided by initial dye concentration (Hamdaoui, *et al*., 2012).

$$\%E = \frac{C_o - C_f}{C_o} \times 100 \qquad 2.1$$

Dye exhaustion rates depend on the type of dyeing machines, textile processing operations, dyeing procedures, quality and types of dyes and chemicals that are used;

and sample dyeing to dyehouse reproducibility. Exhaustion rates as low as 50% are reported in Greentech, (2009).

2.5 Electrolytic Nature of Textile Effluents

Textile effluents are made electrolytic by addition of sodium chloride or sodium sulphates and other ionic species during dyeing. Ionic species provide an electrolytic environment that is favourable for EC (Daneshvar *et al.,* 2006; Kim *et al.,* 2002 and Sheng & Peng, 1996). Electrolytic environments in most electrocoagulation studies were created by the addition of sodium chloride or sodium sulphates. Kim *et al* (2002) studied the electrolyte effects on EC extensively and found NaCℓ as having an effect at low salt concentrations (± 25 mM) for COD and colour removal. NaCℓ produces chlorine that causes carcinogenic by-products such as chloroform and bromo-dichloromechane (Yildiz & Koporal, 2007). Some researchers recommended use of Na_2SO_4, H_2O_2 and Fe_2SO_4 as electrolytes (Ebru, 2007). However, sulphates create sludge problems while chlorides decrease passivation of electrodes (Ebru, 2007). Sheng and Peng (1996) also suggested that adjustment of pH using H_2SO_4; and NaOH would provide enough electrical conductivity for electrocoagulation. Electrical conductivity (κ) is inversely proportional to resistivity (ρ) as given by Waddley, *et al*., (1997) in equation 2.2.

$$k = \frac{d}{\rho a} \qquad 2.2$$

Where, κ (mS/cm) is the electrical conductivity; $\rho\ (\Omega.m)$ is the solution resistivity; $a\ (cm^2)$ is the cross sectional area conductivity meter cell and $d\ (cm)$ is the distance between the conductivity cell electrodes. Therefore, according to equation 2.2; low resistivity EC materials of construction such as copper wires, electrodes and ionic solutions have high conductivity this will give low electrical resistance and better EC performance. Some multi sensor conductivity meters e.g. Hanna HI4522 are available these days to measure conductivity, TDS and resistivity (ρ) simultaneously. Considerable amounts of up to 100 g/L of salt are added as a fixing agent in cotton dyeing with reactive dyes due to low exhaustion rates that are associated with reactive dyes. As report by Daneshvar *et al.* (2003 and 2006), salt enhances the electrical conductivity of the textile effluents which is required for electrocoagulation,

The Ohmic overpotential (E_{ohmic}) is caused by solution resistance or IR-drop (E_{ohmic}) drop can be minimized with higher electrical conductivity, κ, by shorter electrode distances (d_e)

and large electrodes surface area, (A_e). Equation 2.3 means that electrodes with big cross sectional high electrical conductivity will have lower Ohmic overpotential.

$$E_{ohmic} = I\frac{d_e}{A_e \cdot \kappa} \quad 2.3$$

Where E_{ohmic} is the ohmic overpotential; κ (mS/cm) is electrical conductivity; d_e (cm) is distances between electrode and A_e (cm^2) is the surface area of the conductivity cell electrodes. Unlike the resistant ($\mathcal{R}$) of the material, resistivity (ρ) is material's intrinsic electrical characteristic property of the materials or solution that does not depend on the shape and size of the EC cell. Resistance ($\mathcal{R}$) is given in Pouillet's law (Beesabathuni,, *et al.*, 2013) shown in equation 2.4. This is important for the determination of the resistances of wires, electrodes and solution resistances. According to Pouillet's law in equation 2.4, longitudinal (wide) (***L***) EC bath will have high solution resistance than narrower EC bath (*A*).

$$\mathcal{R} = \rho\frac{L}{A} \quad 2.4$$

2.6 Textile Effluents Pollutants Complexity

Dyehouse effluents have complex chemicals whose compositions vary from dyehouse to dyehouse, and even within the same dyehouse as dyeing demands change daily. Many chemical products such as detergents, surfactants, plasticizers, mineral oils, dyes, dye carriers and auxiliary products are used in textile mills operations. There is not a single dyehouse that produces a constant effluent composition because of different dye types and auxiliary chemicals that are used for different fabrics or yarn materials in a single dyehouse. For this reason, there is a wide variety of pollutants that are emerging from dyehouses and textile mills.

Water Services Authorities (WSAs) are aware of these textile effluent complexities and single out certain parameters as representative of the pollutant cocktails such as COD. WSAs measure electrical conductivity of textile effluents first then if the conductivity is high, it is followed by COD analysis. As shown in Figure 2.3; COD is a measure of many oxygen demands contributions. Its reduction and reaction kinetics has been studied mostly in electrocoagualtion but not correlated to the electrodes related reaction kinetics. The chemical oxygen demand (COD) as characterized by Moreno-Casillas *et al.* (2007) contains many other oxygen demands as shown in Figure 2.3. COD and high conductivity is an indicator of the many inorganic and organic salts that are present in the textile effluents.

A large proportion of these chemicals and dyes do not get totally fixed into the dyed fabric but end in the textile effluent as harmful chemicals such as detergents, emulsifiers, wetting and dispersing agents. Textile companies are penalised for dark colours, high conductivity and COD (Moran, 1997). Mazumder, (2011), reported the highest COD of 5272 mg/L, TDS of 5848 mg/L- and TSS of 5138 mg/L for textile effluents.

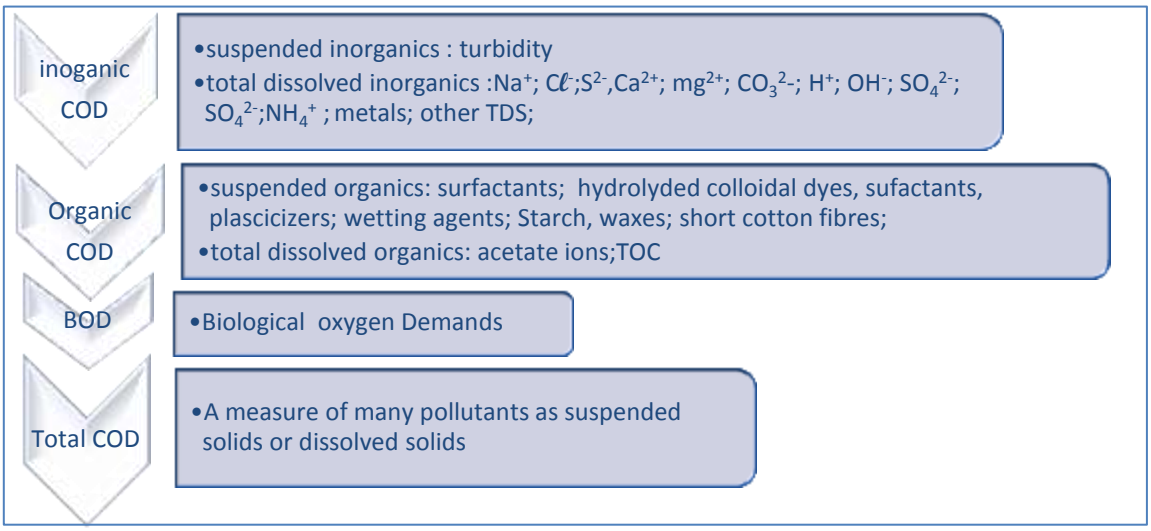

Figure 2.3 Various COD contributions sources (Moreno-Casillas *et al.,* 2007)

2.7 Characterization of Textile Effluents for Electrocoagulation

From Table 2.4; it can be seen that the textile effluent pH and chlorides are very high. TDS of up to 7180 mg/L were recorded by REDDY, *et al*., (2006); however with low COD of 3200 mg/L for TDS recorded. High chlorides and heavy metal content of 7800 mg/L $C\ell^-$ and 0.79 mg/L, respectively might cause the high TDS.

In contrast, chlorides can be as high as 27069 mg/L $C\ell^-$ and may contribute low COD of 485 mg/L (Azzi, *et al*., 2006), therefore chlorides could not be the only contributor of COD. As shown in Table 2.4; the pre-bleaching step alone contributes about 2689 mg/L COD (Savin *et al*., 2008). BOD is relatively low in textile effluents. Without the neutralization, step, the textile effluent would have a pH ranging from 9.8 to 11.8 (Babu, *et al*., 2007). From this review it can be deduced that CCT's industrial effluents by-laws are reasonable and within the practical possible discharge levels of the textile industry.

2.8 Colour Pollution and Absorbance

Dark colour; high salinity; conductivity; high turbidity; COD; pH and heavy metals characterize textile effluents. Strong dark coloured textile effluents can obstruct light transmissions into the water bodies if released to the environment without prior treatment.

Table 2.4 Combined Textile Effluent Characterization

Parameters	*T*	*pH*	*κ/TDS*	*Ca/ Mg/*	*TSS*	*Colour*	*COD*	*BOD_5*	*$frCl_2/Cl^-$*	*Cd /Zn/*	*Tot/Fe^{2+} /Fe^{3+}*	*S^-/SO_4^{2-} SO_3^{2-}*	*NO_3^- /NO_2^-*	*NH^+_4*
Source	*^oC*		*(mS/cm); /mg/L*		*mg/L*	*Pt-Co*	*mg/L*	*mg/L*	*mg/L*	*mg/L*	*mg/L*	*mg/L*	*mg/L*	*mg/L*
Yusuff, *et al*.,(2004)	*35.7*	*11.5*	*/2200*		*1200*	*4637*	*2430*							
Reddy, *et al.,* (2006)		*8*	*/7180*		*320*		*3200*	*560*	*/3800*	*0.7900*				
Arslan-Alaton, *et al.*, (2007)		*11.2*	*27.63/ >1000*		*220*		*>100 0*		*/7800*					
Azzi, *et al*., (2006)	*100*	*10.6*	*42.6/70*	*260*	*70*		*485*	*80*	*/27069*	*0.5965*	*0.92*			
Mazumder, (2011)		*11.3*	*/5848*		*5138*		*5272*							
Ali, *et al*., (2009)	*40.4*	*9.4*	*3.57/ 2512.6*		*5497*		*1652*	*174.7*	*/0,25*					
Savin, *et al*., (2008)		*8.06*			*499.4*		*1907*	*170*	*/213.2*			*1.62/-/*	*6.06/*	*14.3*
Roy, *et al.,* (2010),		*9.8*	*4.82/3392*		*278*	*1890.8*	*2304*	*151.2*		*0.0006/0.085*				
(Ntuli, et al., 2009)	*41.7*	*8.8*	6.385/3193		521		5849		/879		2.6	/133/		

Table 2.5 Textile Effluent from Cotton Bleaching Only

Parameters	T	pH	Color	COD	BOD_5	$frCl_2/Cl^-$	$S^-/SO_4^{2-}/SO_3^{2-}$	NO_3^-/ NO_2^-	NH_4^+
Source	^oC		Pt-Co	mg/L	mg/L	mg/L	mg/L	mg/L	mg/L
Savin, *et al*., (2008)	-	11.6	288.5	2688.5	184	/516	5.44/ - / -5	1.45/	8

Reactive dyes chromospheres are made up of the azo groups, a group known to be carcinogenic (Adinew, 2012). Wastewater colour pollutants from textile mills and paint factories could be visible at wastewater plants even after many dilutions by many industrial and wastewater streams along the way to WWTP. It is important to consider colour analysis in characterizing reactive dyes because colour can be detected by human eye even at very low concentrations of 0.005 mg/L of dyes and concentration of up to 800 mg/L of dyes remains water after dyeing (Ali, *et al.*, 2009 and Adinew, 2012). Absorbance (A) of each dye has its own characteristic maximum wavelength (λ_{nm}) that can be determined uv-spectrophotometer. Absorbance at a maximum wavelength ($A_{\lambda max}$) can be used to determine the exhaustion rate, ($\%E$) for dyeing efficiency.

$$\%E = \left[1 - \frac{A_{\lambda_{max,2}}}{A_{\lambda_{max,1}}}\right] \times 100\% \qquad 2.5$$

Where, $A_{\lambda max,\,1}$ and $A_{\lambda max,\,2}$ are absorbencies of before dyeing and after dyeing respectively.

2.8.1 Oxidizability and Reducibility of Textile Effluent

Textile effluents are electrolytic with high electrical conductivity (κ) and oxidation-reduction potentials (ORP) because of chlorides or sulphates that are known reducing agents (Cho, *et al*., 2014). ORP and κ are important electrochemical of ionic and charge transfer processes parameters for the electrocoagulation. The electrodes standard potentials are well known and are reported in literature for a limited range of conditions of temperature, concentrations; pressure and for single electrolytes that are not easily applicable to the EC process. However, if the references potential of the ORP sensor is known, ORP can be used to indirectly determine an equivalent of a normal hydrogen electrode (NHE), potential called an equivalent hydrogen electrode, ($E^o_{H.}$) (Banchuen 2002). The ORP is easily measured by an inert ORP electrode (usually platinum electrode) and a reference silver/silver-chloride electrode (Kurt, *et al*., 2008). The ORP can be converted to or recorded as an equivalent hydrogen (E_h) potential if the reference standard potential, (E^o_{ref}) of the reference electrodes is known.

$$E_h = ORP + E^o_{ref} \qquad 2.6$$

The reference potentials (E^o_{ref}) are supplied with ORP electrodes at various temperatures.

Equivalent hydrogen potential (E_H) measurements by this method have their own challenges compared to the conventional potentiometric measurements against NHE. However,

according Banchuen (2002), the conversion of ORP measurements into E_H is acceptable as long as all possible sources of electrode contamination are isolated.

2.8.2. Chlorines compounds in textile effluents – a synergy for electrocoagulation.

After the dyeing process, chlorides are released into the dyebath. As shown in Figure 2.4 depending on the pH, chlorides may be present as many other forms of chlorine compounds such as the hydrochloric acid, free, combined chlorines and aqueous chlorine ($C\ell_2$) (). At low pH (between pH 0 and 5) aqueous chlorine ($C\ell_2$) and chlorides exists as free chlorine (f-$C\ell_2$). At medium to high pHs, chlorine compounds are transformed to other forms free chlorine compounds such as hypochlorous acid ($HOC\ell$) and chlorate ions (Cho, *et al*., 2014).

The hypochlorous acid forms equilibrium with chlorides at pKa 7.46 (Lahav, *et al*. 2009). As shown in Figure 2.4, at pH above 8 the hypochlorous acid dissociates (Ahmed & Saad , 2013).

$HOC\ell_{(aq)} + H_2O_{(l)} \rightleftharpoons -OC\ell^-_{(aq)} + H^+_{(aq)}$, pH = 7.5 to 14, pK = 7.57 R2.2 (a)

and

$C\ell_{2(aq)} + H_2O_{(l)} \rightleftharpoons HOC\ell_{(aq)} + H^+_{(aq)} + C\ell^-_{(aq)}$ pH = 4 to 8; pK = 4.6 R2.2(b)

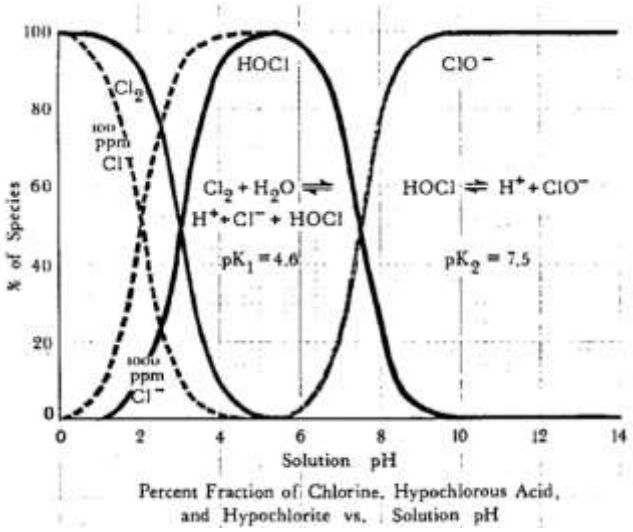

Figure 2.4 Free Chlorine Percentage –pH diagram (IC Controls, 2005)

It can be seen that chlorine chemistry depends strongly on the pH, at pH 4 to 9 (Sengil & Ozacar, 2008). Chlorine alone; with or without electrolysis is used to treat water. This is so because chlorine ($C\ell_2$) is an oxidizer and it can also produce various oxidizers such as a

variety of superoxide radical (O_2^-) (as shown in reaction, R2.2 (a), and hypochlorite ($C\ell O^-$) (by reactions R2.2 (b) to R2.2 (c). According to Quader (2010) every 71g Cl_2 produce 16 kg O_2 to treat textile effluents without electrolysis.

$$C\ell_2 + H_2O \rightleftharpoons 2HC\ell + [O] \qquad R2.2\ (c)$$

As shown in reaction R2.2 (d), other reactions that produce chlorate ions ($OC\ell^-$) are electrolysis of residual chloride ions (Sala, *et al*., 2012). Chlorides are reduced at the anode.

$$2C\ell^- \rightleftharpoons C\ell_2 + 2e^- \qquad R2.2(d)$$

Reaction 2.2 (e) to (f), show hydrolysis of active chlorines ($C\ell_2$) (Sala *et al.*, 2012, Mahmoud & Ahmed, 2014 and Sengil & Ozacar, 2008).

$$C\ell_2 + H_2O \rightleftharpoons C\ell O^- + 2C\ell^- + 2H^+ \qquad R2.2(e)$$

$$C\ell_{2(g)} + H_2O_{(\ell)} \rightleftharpoons HOC\ell + C\ell^-_{(aq)} + H^+_{(aq)} \qquad R2.2(f)$$

The free chlorine enhances EC by converting aqueous ferrous aqua-hydroxo complex into ferric aqua-hydroxo precipitates that depending on the density are readily settle-able or floatable.

$$Fe(H_2O)_4(OH)_{2(aq)} + HOC\ell \Rightarrow Fe(H_2O)_3(OH)_{3(s)} + H_2O_{(\ell)} + C\ell^-_{(aq)} \qquad R2.3$$

2.8.2.1 Free Chlorines Chemistry

Free chlorine is a very strong oxidizing agent. The combination of $C\ell^-$, Cl_2, $HOC\ell_{(aq)}$ and $OC\ell^-_{(aq)}$ is called free chlorine (f-$C\ell_2$). Free chlorine predominantly exists in two forms; hypochlorous acid ($HOC\ell$) and hypochlorite ion, $OC\ell^-$ (Harp, 2002). Free chlorine analyses must be done at pH between 6.3 and 6.5, as the N,N,-diethyl-p-phenylenediamine, (DPD) reagent has a buffering effect at these pHs. The reaction of DPD with chlorine $C\ell_2$ is given in Figure 2.5 (Hach, 2011) or reaction R2.4

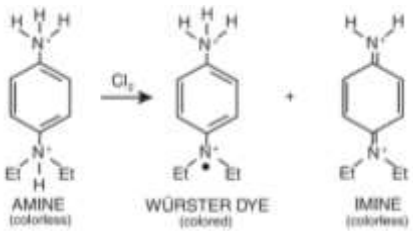

R2.4

Figure 2.5 DPD Reactions with Chlorine. (HACH, 2013)

With DPD, reagent free chlorine forms a bright pink colour with at a maximum wavelength, λ_{max} of 530 nm. Therefore, free (f-Cℓ_2) and total chlorine (t-Cℓ_2) are measured calorimetrically by spectrophotometer at maximum wavelength of 530 nm with N,N-Diethyl-p-Phenylenediamine (DPD) powder pillows reagents.

2.8.3 Turbidity.

Turbidity is another water pollutant parameter that measures the light transmittances through the water. According to Lechevallier, *et al*., (1981) turbidity is related to other water pollutants such as total organic carbon (TOC) and chlorine demand, (CD) by the following equations:

$$\mathrm{CD} = 0.040 + 0.086 \times \mathrm{NTU} \qquad 2.7$$

$$\mathrm{TOC} = 1.070 + 0.153 \times \mathrm{NTU} \qquad 2.8$$

$$\mathrm{CD} = 1.36 + 0.525 \times \mathrm{TOC} \qquad 2.9$$

Chlorine demand (CD) is the chlorine that reacts with organic and inorganic material, metals and other compounds present in water prior to disinfection.

2.9 Various Textile Effluent Treatment Processes

As presented in Figure 2.6, colour bearing industrial effluent including textile effluent treatment has been at the centre of industrial effluent treatment research (Babu, *et al.,*2007; Sala, *et al*., 2012); Vandevivere, *et al*.1998) and. Sala, *et al*.,(2012), characterized the available textile technologies and Vandevivere, *et al*.,(1998) characterized the application levels of these technologies. Sala, *et al*., (2012) had categorized available colour removing industrial effluent technologies into, namely: (1) microbiological, (2) electrochemical, (3) physo-chemical, (4) enzymic methods and (5) chemical oxidation. Traditionally, textile effluent treatment has been done by activated carbon which is a physo-chemical application technology, (as shown in block 7 in Figure 2.6) with successes in removing colour from textile effluents between 80% and 100% colour removal (Mbolekwa & Buckley, 2008). However, this process technology has proved to be expensive (Geethakarthi, *et al*., 2011).

Nanofiltration (block 8 in Figure 2.6) is also a promising textile wastewater treatment technology with colour removal efficiencies of about 70% (Avlonitisa *et al.,* 2008). Moran C.

et al (1997) had proved that 70% of textile effluents are aerobically, bio-treatable (block 1 in Figure 2.6) but Carliell C, (1993) confirms the inability to aerobically remove colour in textile effluent with azo group bearing dyes.

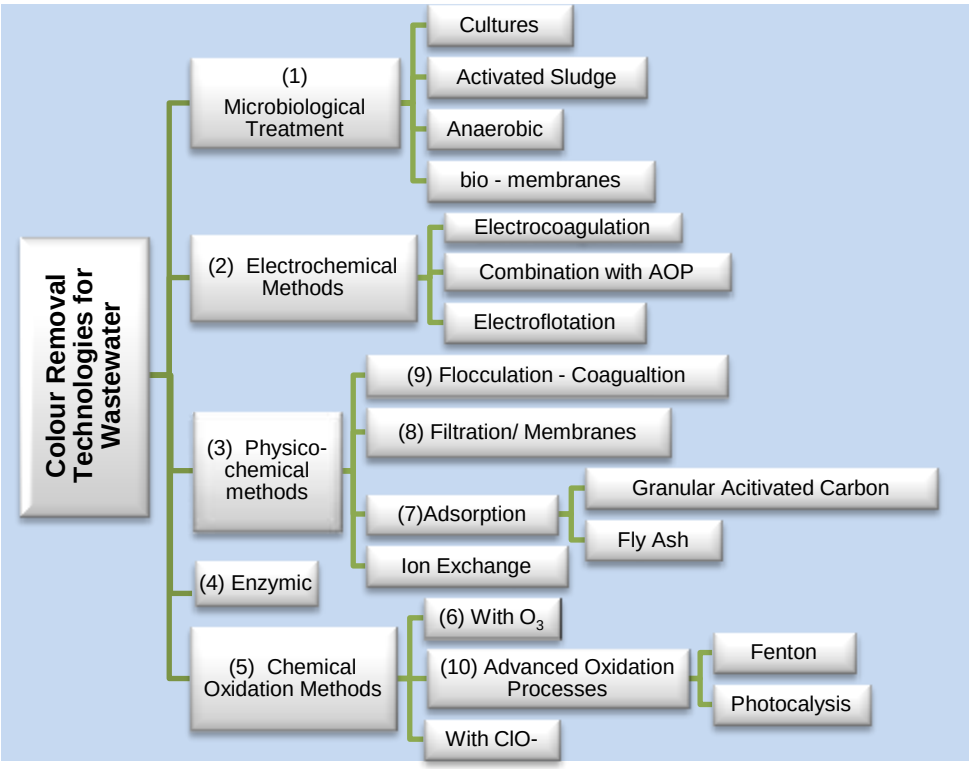

Figure 2.6 Textile effluent treatment technologies (Sala, *et al*., 2012)

Azo dyes are, therefore, fairly biodegradable with aerobic digestion and better degradable with anaerobic biodegradation (Carliell, C. 1993). Anaerobic digestion of textile effluents is very slow and produces aromatic amines that are toxic and carcinogenic (Joshi, *et al*., 2003). Bonakdarpour, *et al*. (2011) achieved a 95% colour removal on simulated reactive dyeing effluent under an-aerobic conditions. Electrocoagulation (EC) is part of blocks 2, 9 and 7 mechanisms and can be combined with some advanced oxidation processes (block 10). As shown in Figure 2.6 reactive textile dyebath contains chlorides and free chlorine that are converted by electrochemical oxidation to be oxidizers that contribute to chemical oxidation methods such as those categorized in block 6 (Sala, *et al*., 2012).

2.9 Electrocoagulation Industrial Effluent Treatment Technologies

Electrochemical coagulation oxidation (as referred to in Kim, *et al*., (2004)) or electrocoagulation and electroflotation process has been applied and proved successful in removing colour and COD in the textile effluents (Canizares, *et al*.; 2004; Sheng, *et al* 1996;

Hector, *et al*., 2009 and Moreno-Casillas, *et al*., 2007). ECT is the application of electrochemical processes to produce coagulants, other oxidizers and floccs within the effluent that is being treated. The floccs are floated by electrolysis gases that are also produced hence referred to as electroflotation. EC can treat raw water, domestic wastewater, and many other industrial effluents either to allowable effluent discharge limits (EDL) or for industrial re-use.

As shown in Figure 2.7 effluent treatment by electrochemical methods is not limited to pure electrocoagulation. There are various other electrochemical methods that can be applied with EC in effluent treatments (Sala, *et al*., 2012). Electrocoagulation, more especially of effluents with chlorine compounds such as found in reactive textile dyebath can follow the process flow diagram until block 3. Electrocoagulation can include many complex process mechanisms as shown in Figure 2.6. Process steps 1(a) and 1(b) are taking place simultaneously (redox reactions).

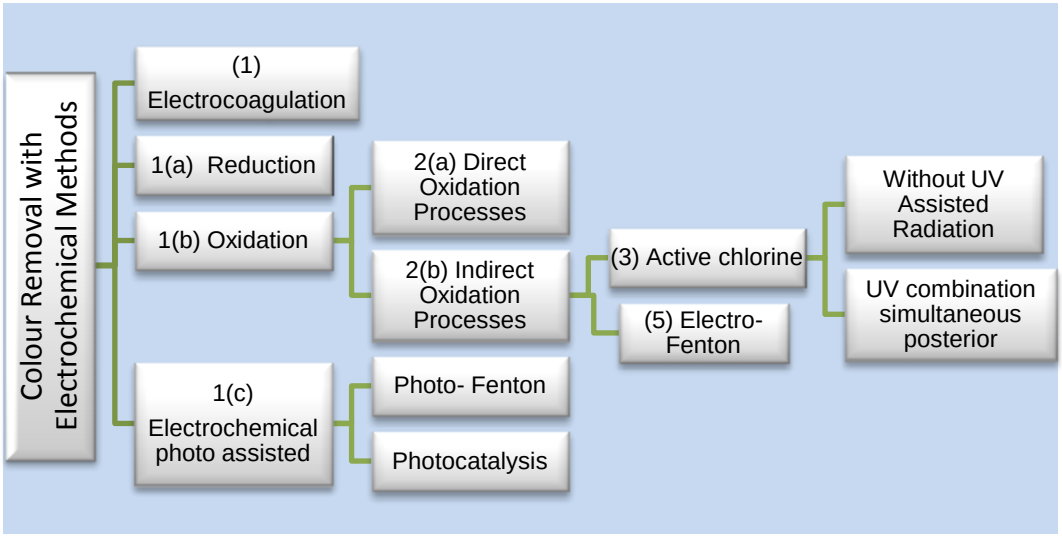

Figure 2.7 Electrochemical methods effluent treatment (Sala, *et al*., 2012)

Oxidation does not only happen electrochemically but it can take place indirectly in step (2b) caused by other oxidizers. Most common oxidizers are ozone (O_3), hydrogen peroxide (H_2O_2), triplet oxygen ($3O_2$), and a variety of superoxide radical (O_2^-), chlorine ($C\ell_2$), hypochlorite ($C\ell O^-$), and nitrate (NO_3^-) (IC Controls, 2005). Previous research had focused only on treatability of various textile effluents by electrocoagulation.

In their studies, Yang and McGarrahan (2005) studied removed colour from textile effluents with residual acid, disperse and reactive dyes with iron and aluminium electrodes electrocoagulation. Arslan-Alaton *et al.* (2007) treated real reactive textile effluent with stainless steel and aluminium electrodes successfully achieving 99-100% colour removal in

15 minutes and 80% and 70% COD removal with aluminium and stainless steel electrodes respectively. Daneshvar *et al.* (2006) decolourized exhaust reactive dyebath with acid and basic dyes with aluminium electrodes in 5 min at current densities of between 6.0 mA/cm^2 and 8.0 mA/cm^2 and COD removal was 75 to 99%. COD and colour removal can be improved with the addition of the Fenton reagent (H_2O_2) during the electrocoagulation, as determined by Esteves and Cunha (2005).

Further, a literature review of various textile effluent treatment technologies is shown in Table 2.6. The removal percentages are mostly colour (absorbance removal), otherwise COD as stated. In the literature review in Table 2.6, it is shown that EC alone or assisted seem to be amongst the best performing such as activated carbon adsorption, anaerobic, Fenton reagent and advanced oxidation processes with colour removal percentages of up to 100% and COD of 98.4 %.

Table 2.6 **Literature review of treatment processes for textile effluents treatments**

REMOVAL TECHNIQUE	REMOVAL PARAMETERS	REMOVAL %	SOURCES	COMMENTS
Adsorption	58.823 mg dye/gPAC[9]	80	(Acar, *et al*., 2006)	Expensive (Geethakarthi, et al., 2011)
	7.936 mg dye/g Fly Ash	100	(Acar, *et al*., 2006)	
	PAC type 53C		(Suteu, *et al*., 2005)	
	F400 GAC[10], varied dose		(Mbolekwa, *et al*., 2008)	pseudo-second order model
Nanofiltration	Good removal efficiencies	70	Work of Chakraborty *et al.,* 2003 quoted in (Adinew, 2012) review on Nanofiltration in Zahrim, *et al*., (2011)	Very promising because it removes a large variety of pollutants (Adinew, 2012)Problems of fouling
Biodegradation	*Bacillus megaterium* N7A	50.7	Ali, et al., (2009)	"difficult to biodegrade and unsuitable for conventional WWTP" (Adinew, 2012)
	Bacillus subtilis N4A	66.7	Ali, et al., (2009)	
Anaerobic biodegradation	Anaerobic sludge from WWTP	±95 95 colour removal	Mbolekwa, *et al*.,(2008); Carliell C, (1993) Bonakdarpour *et al*. (2011)	Generation of aromatic amines. Large scale application
Membrane bioreactors (MBRs)	activated sludge from WWTP, the reactor had aerobic, anoxic and anaerobic compartment		Bonakdarpour, *et al*., (2011) Spagni, et al., (2010)	slow and produce toxins
Reverse Osmosis	Remove all components of reactive dyeing effluents.		Adinew, (2012)	High energy requirements
Coagulation–flocculation	Adding a polyelectrolytes Aluminum sulphate and Ferric Sulphates	86 % 50% COD	Seif, et al., (2001) Zahrim, *et al*., (2011)	Large volume of sludge generation
Fenton's reagent		90 COD	Adinew, (2012)	Sludge production
		99 dye	Kim, *et al*., (2004)	
Photochemical Advanced Oxidation	• $UV/TiO_2/H_2O_2$; (O_3; O_3/H_2O_2, O_3/UV, UV/H_2O_2 • $O_3/UV/H_2O_2$ and Fe^{2+}/H_2O_2)	89	Adinew, (2012) Venkatesh, *et al.,* (2013)	No sludge production but produces by harmful by- products
Electrochemical EC	Remove all components of textile Effluents reactive dyeing effluents.	100%	Adinew, (2012), (Arslan-Alaton, et al., 2007)	Electricity and sludge generation
	Magnesium as an anode and zinc as a cathode had been used at $0.06A/dm^2$	98.4 COD	Vasudevan, *et al*., (2009).	2nd order adsorption reaction constant.
Combined EC with GAC	Acidic aqueous phenol wastes Stainless steel electrodes	80 COD	Canizares, *et al*., (2004)	

[9] Powdered Activated Carbon
[10] Granular Activated Carbon

Chapter 3 : THEORETICAL FRAMEWORK

3.1. Clarification of Theoretical Assumptions

The theoretical knowledge that involves electrocoagulation (EC) is complex and it is impossible to cover all its aspects completely in one study. May be it is this complexity that has contributed to the lack of progress in development of electrocoagulation technology (ECT). ECT involves many chemical reaction phases (homogenous or heterogeneous) and mechanisms (multimodal reaction mechanisms, kinetic, catalytically, electrochemical and chemi-sorption); physical processes (flotation and sedimentation). Therefore, EC reactions kinetics may be characterised by heterogeneous reactions that taking place as electrodes (solid) react to produce metal ions and production of metal aquo-hydroxo complexes at the electrode surface-liquid interphase (heterogeneous phase) and electrolyses gases.

Textile effluents composition is complex as it contains many pollutants and its chemistry is affected by other electrochemical parameters such pH and conductivity (Yildiz & Koporal A. S, 2007). Textile effluents pollutants removal by EC has multiple removal mechanisms such as chemical reactions; physi-chemical sorption; coagulation and flocculation; mass transport; flotation and settling mechanism (Hector, et al., 2009). In this study, the measurements of the electrochemical parameters and pollutants concentrations are only limited to measurements in bulk solutions, which does not satisfy electrodes reaction kinetics. Electrodes reaction kinetics parameters measurements require controlled special conditions that are impossible to satisfy under the operating conditions of electrocoagulator.

The EC kinetics data such as electrode reaction constants and cell voltages are available only for microelectrodes and it is limited to two electrodes and reference electrodes. This data is also determined under standard conditions of temperature, pressure and concentrations as reported in most electrochemistry text (Bard, *et al*., (2000)) and Barrow, (1988) and electrochemical engineering text (Pintauro, (2007) and Pletcher, *et al*.,(1990)). This data is not usable in EC due to the following deviations from standard conditions:

- Electrocoagulation reactors are not limited to 25°C. EC is performed at high concentrations with electrolytes with many ionic species rather than single electrolytes.
- There are many electrodes in electrocoagulation, therefore measurements electrodes parameters such anodes and cathodic reactions rate constants are difficult (Pletcher & Walsh, 1990).

- Measurements of cell voltages, (E^o) at equilibrium conditions are difficult to achieve and to maintain in bulk electrolysis as there are many electrolysis reactions leading to mixed potential or formal potentials measurements. Nevertheless, measurements of formal potentials are acceptable (Scholz, 2010).
- Electrode kinetics is somehow particular and non-transferable into other electrocoagulation studies because of pollutants variability.
- It is difficult to use available electrodes kinetics data in EC processes; hence the lack of progress in EC reaction kinetics. Other problems that are associated with EC reaction kinetics and possible solutions are explained by Figure 3.1 below.

Another challenge is that the reaction kinetics studies in chemical engineering textbooks and literature do not include EC or electrochemical engineering reaction kinetics. However, there are discussion of reaction kinetics of bulk electrolysis in Pletcher and Walsh (1990), Bard and Faulkner, (2000) and (Barrow, 1988).

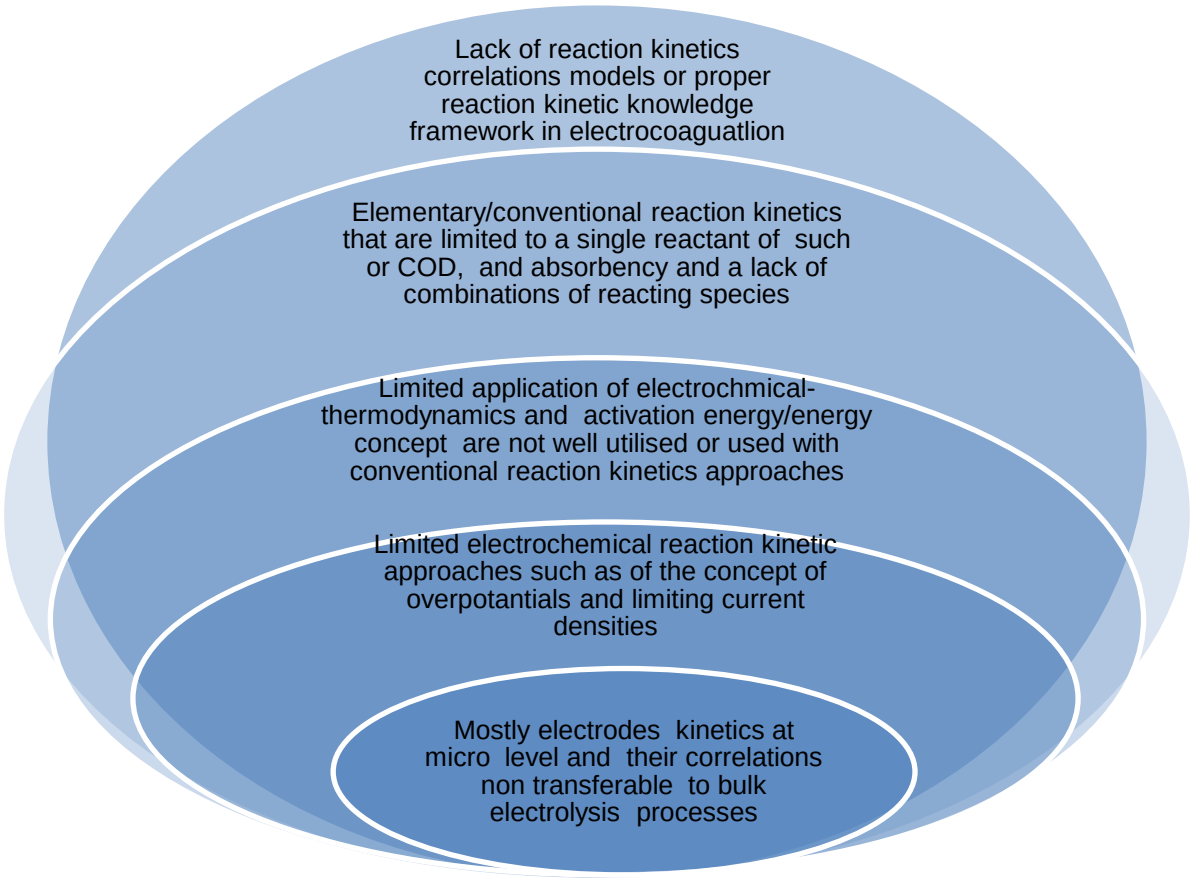

Figure 3.1 Reaction Kinetics Problems in Electrocoagulation Technology

The assumptions for ordinary reaction kinetics studies are based on:

- Irreversible reactions but electrochemical reactions are equilibrium; possibly reversible at some conditions of pH and temperature.
- Chemical reactions follow ordinary elementary chemical kinetics but reaction kinetics may deviate because of coagulation or precipitation reactions or mass transfer controlled reactions.
- Chemical reactions are homogenous liquid or gaseous phase reactions only but other reactions in EC are heterogeneous e.g. electrodes reactions (Nauman, 2002 and Bamford, *et al*., 1986).
- Reaction kinetics that are based on a single or particular reactants but, real processes involved multiple reactions or many parameters such as pH; conductivity; ORP etc. affects EC process (Schmidt, 1998).

Based on these assumptions, deviations from elementary reaction kinetics studies in EC may be possible. Elementary reaction kinetics studies are done by measurements of concentrations of a single species that are degraded or produced during reactions in homogenous phase and there is lack of models that include multiple species. The data is fitted to idealized reaction kinetic models by curve fittings and the success of the reaction kinetics studies is measure by a regression correlations. These models are zeroth; first; second; third orders and fractional lifetime models (Levenspiel, 1999 and Fogler, 2006). The reaction kinetics studies are performed with differential, initial rate and integral curve fitting methods.

3.1.1 The Integral Method

The integral method is easier because it needs less data processing than other methods. The zeroth order is the straight line in the graph of original reacting species molar concentration versus time (Schmidt, 1998). Theoretically, in 100% current efficient electrolyses, electrodes are degraded by zeroth order model (Hmani , et al., 2012).

The first order models can be deduced from the natural logarithmic function of ratios of the reacting species molar concentrations ($[C_i]_t$) to original molar concentrations($[C_i]_o$) versus time graph (Levenspiel, 1999; Rincon, 2011; Schmidt and 1998). The second order model is deduced from a straight graph of the inverse of the reacting species molar concentrations ($[C_i]_t$) versus time.

The reaction constant (k_c) is determined with the integral method under the assumptions that the reaction orders are a perfect fit to the order of the reactions. For various reasons stated above, the dependence of reactions rates on temperature or concentrations, deviations from these reaction order models assumptions are also possible. These are sometimes revealed by deviations of ℓnk versus the inverse temperature plots from a straight line (Arrhenius plots) (Nauman, 2002 and Sparks , 1999). The downward curve reveals that order is in fact a second order if the original assumption was for first order and vice versa. The curvature can also be due to fractional, third and higher orders.

3.2. Iron Electrodes Reaction Mechanisms

There are many chemical reactions that take place during electrocoagulation. Most of these reactions are well known standard electrodes reactions that can be deduced from knowledge of the electrode used. However, reaction mechanisms needs to be understood. Iron reaction mechanisms II) and (I are well understood (Larue, 2003; Daneshvar, *et al*. 2003; Zoulias, *et al*., 2001 and Gurses, *et al.* 2002).

Mechanism I (Basic medium)

$Fe_{(s)} \rightleftharpoons Fe^{2+}_{(aq)} + 2e^-$	at the anode	R3.1 (a)
$Fe^{2+}_{(aq)} + 2OH^-_{(aq)} \Rightarrow Fe(OH)_{2(s)}$	near the anode	R3.1 (b)
$2H_2O_{(\ell)} + 2e^-_{(aq)} \rightleftharpoons 2OH^-_{(aq)} + 2H_{2(g)}$	at the cathode	R3.1 (c)
$Fe_{(s)} + 2H_2O_{(\ell)} \Rightarrow Fe(OH)_{2(s)} + 2H_{2(g)}$	Overall reactions	R3.1

Mechanism II (Acidic medium, pH < 4,) (Sengil & Ozacar, 2008))

$4\,Fe_{(s)} \rightleftharpoons 4\,Fe^{2+}_{(aq)} + 8e^-_{(aq)}$	at the anode	R3.2(a)
$4\,Fe^{2+}_{(aq)} + 10\,H_2O_{(l)} + O_{2(g)} \rightleftharpoons 4\,Fe(OH)_{3(s)} + 8H^+_{(aq)}$	near the anode	R3.2(b)
$8\,H^+_{(aq} + 8e^-_{(aq)} \rightleftharpoons 4\,H_{2(g)}$	at the cathode	R3.2(c)
$4\,Fe_{(s)} + 10\,H_2O_{(l)} + O_{2(g)} \Rightarrow 4Fe(OH)_{3(s)} + 4\,H_{2(g)}$	overall Reaction	R3.2

The source of hydrogen (H^+) and hydroxyl ions (OH^-) in reactions R3.1 (c) and (R3.2 (c) are from water decomposition reactions that take place at the cathode in neutral to alkaline medium (Khue, *et al*., 2014) and at the anode in acid medium (Raju, *et al.*, 2008) as in reaction R3.3 and 3.3(a) below.

3.3 Electro-Oxidation, chemical oxidation (oxygen) and other oxidizers

Electrochemical processes produce oxygen by water decompositon. Water decomposition reactions can take place at the anode (Raju, *et al*., 2008):

$$2H_2O..\Rightarrow \quad O_{2(g)} + 4H^+_{(aq)} + 4e^-_{(aq)} \qquad E°(O_2/H_2O) = +1.23\ V \qquad R3.3$$

In the presence of chlorides as in reactive dyebath textile effluents, molecular oxygen ($O_{2(g)}$) is converted into active oxygen ($O_{2(aq)}$) and other strong oxidizers such hydrohygen peroxide, (H_2O_2) and ozone (Raju, *et al*., 2008).

$$4H_2O + 2O_{2(aq)} + 4e^-_{(aq)}. \Rightarrow 4OH^-_{(aq)} + H_2O_2 \qquad R3.3\ (a)$$

and ozone at voltages more than 1.5V (Raju, *et al*., 2008).

$$H_2O + O_{2(aq)} \Rightarrow O_{3(aq)} + 4H^+_{(aq)} + 4e^-_{(aq)} \qquad R3.3\ (b)$$

Water can also decompose as follows:

$$2H_2O_{(l)} + 2e^-_{(aq)}{}^- \rightleftharpoons H_{2(g)} + 2OH^-_{(aq)} \qquad E°(2H^+/H_2O) = -0.83\ V \qquad R3.3\ (c)$$

As shown in reaction, R3.4, at the anode, the hydroxyl ion (OH^-) are further consumed and their reductions contributes to increase in pH; produces oxygen and releases 4 electrons.

$$4OH^- \rightleftharpoons 2H_2O + O_{2(g)} + 4e^- \qquad R3.4$$

In acidic bulk soultion more hydrogen gas is produced at the cathode from the reduction of the hydrogen ions (H^+)

$$H^+_{(aq)} + 2e \rightleftharpoons H_{2(g)} \quad \text{(acidic)}, \qquad E°\ (2H^+/H_2) = 0.00V \qquad R3.5$$

In acidic bulk solution ferrous iron is oxidize to ferric iron (Khue, *et al*., 2014).

$$O_{2(g)} + 4Fe^{2+}_{(aq)} + 4H^+_{(aq)} \Rightarrow 4Fe^{3+}_{(aq)} + 2H_2O_{(l)} \qquad R3.6$$

8 electrons are used with one 1.0 mol of oxygen in neutral to alkaline bulk solution to oxidize same stoichiometric quantities of Fe(II) to F(III) irons (Khue, *et al*., 2014)

$$O_{2(g)} + 4Fe^{2+}_{(aq)} + 2H_2O_{(\ell)} \Rightarrow 4Fe^{3+}_{(aq)} + 4OH^-_{(aq)} \qquad \text{R3.7}$$

Direct oxidation of the ferrous iron by molecular oxygen is rare, it happens with addition of an acid, as in reaction, R3.6 and in hydrolysis as in reaction, R3.7.

Depending on the pH, the acqueous ($4Fe^{3+}_{(aq)} + 4OH^-_{(aq)}$) will precipitate leading to further reduction of pH. Since the textile effluents contain chlorides, chlorides are oxidised as in reaction R3.8 (Lakshmana, et al., 2009). Depending on pH the chlorines ($C\ell_{2(g)}$) can be converted to other powerful oxidants, the hypochlorous acid ($HOC\ell$) (IC Controls, 2005) and other free chlorine compounds.

$$C\ell^-_{(aq)} \quad \rightleftharpoons \quad C\ell_{2(g)} + 2e^- \qquad \text{R3.8}$$

Chlorine electrolysis gases increase the activation overpotential and they are unavoidable side reactions in electrolysis, with a ratio of $C\ell_2$ to O_2 exchange current densities of 1.0 x 10^3 to 1.0x 10^7 (Abdel-Aal, *et al*., 2010 and Zoulias, *et al*., 2001). In their studies, Czarnetzki and Janssen (1992), Steininger and Pareja (1996) and Zayas *et al.* (2007) showed that chlorine reacts with iron according to reaction R3.8 (a).

$$C\ell_2 + 2Fe^{2+} \Rightarrow 2\,C\ell^- + 2Fe^{3+} \qquad \text{R3.8(a)}$$

3.3 Dye Degradation Processes

According to Cheng, *et al*., (2006) and (Sala, *et al*., 2012) during EC in the presence of oxygen containing chlorine compounds, dye molecules are degraded by reaction 3.9 (a) and 3.9(b) to form carbon dioxides and dye molecules intermediates.

$$OC\ell^- + \text{Dye} \Rightarrow \text{Dye-intermediate} + C\ell^- + O_2 + H_2O \qquad \text{R3.9 (a)}$$

$$^-OC\ell + \text{Dye} \Rightarrow \text{Dye-intermediates} + C\ell^- + CO_2 + H_2O \qquad \text{R3.9(b)}$$

3.4 Hydrolysis Processes

Hydrolysis reactions take place near the surface of the electrodes and in the bulk solution such (Sengil & Ozacar, 2008). The electrodes mechanisms II and I showed that electrode

reactions produce mainly ferrous irons (Fe(II)). Lakshmana, *et al*., (2009), showed the same hydrolysis mechanisms after the formation of the ferrous iron as follows:

$$Fe(s) \xrightarrow{electrolysis} Fe^{2+} \xrightarrow{hydrolysis} Fe(OH)_{2(s)}$$

$$Fe(s) \xrightarrow{electrolysis} Fe^{2+} \xrightarrow[and\ oxidation]{hydrolysis} Fe(OH)_{3(s)}$$

$$Fe(s) \xrightarrow{electrolysis} Fe^{2+} \xrightarrow{hydrolysis} Fe(OH)_{3(s)}$$

The ferrous irons are converted to ferrous-aquo hydroxo complexes or ferric-aquo hydroxo complexes hydroxide and to their precipitates by pH changes. Ghanim, *et al*., (2013) suggest a third electrocoacoagulation hydrolysis mechanism. Electrolysis and hydrolysis reactions near the electrodes as shown in reactions R3.10 and R3.12 (Ghanim, *et al*., 2013) and solid forms in the bulk solution (Lahav, *et al*., 2009); at pH between 4 and 9 (Sengil & Ozacar, 2008).

Mechanism III (Ghanim, *et al*., 2013)

$$Fe_{(s)} + 6H_2O_{(\ell)} \Leftrightarrow \left[Fe(HOH)_4(OH)_{2(aq)}\right] + 2H^+_{(aq)} + 2e^-_{(aq)} \Downarrow Fe(HOH)_4(OH)_{2(s)} + H_{2(g)} \quad \text{R3.4}$$

$$Fe_{(s)} + 6H_2O_{(\ell)} \Leftrightarrow \left[Fe(HOH)_3(OH)_{3(aq)}\right] + 3H^+_{(aq)} + 3e^-_{(aq)} \Downarrow Fe(HOH)_3(OH)_{3(s)} + H_{2(g)} \quad \text{R3.5}$$

$$Fe(HOH)_3(OH)_{3(s)} \Rightarrow Fe_2O_3(HOH)_{6(s)} + 3H_2O \quad \text{R3.10(b)}$$

Studies of iron reaction mechanisms with iron dissolution products are also shown in Moreno-Casillas *et al*. (2007) and the overall cathodic reaction at moderate acid to alkaline conditions are given in reaction equation R3.11:

$$6Fe(s) + (12 + x)H_2O \Rightarrow \tfrac{1}{2}(12 + x)H_2 + xFe(OH)_3 \cdot (6 - x)Fe(OH)_{3s} \quad \text{R3. 6}$$

The general chemical formula for green rust was presented by Hector, *et al*., (2009) as follows: $[Fe^{II}_{6-x}Fe^{III}_x(OH)_{12}]^{x+}\left[(A)_{x/n} \cdot yH_2O\right]^{x-}$

where x = 0.9 to 4.2 and y = 2 to 4; interlayer of water in an n-valent ion, $C\ell^-$; SO_4^{2-} and CO_3^{2}

3.5 Overview of Electrocoagulation Processes Mechanisms

As shown in Figure 3.2 below, there are many physico-chemical reactions and process mechanisms in electrocoagulation. The main process and reaction mechanisms are described in this section and some are illustrated by Figure 3.2. Figure 3.2 was adapted from (Barrow, 1988, Lekhlif, *et al*., 2013, Hector, et al., 2009 and Martinez, et al., 2012).

The following mechanisms take place in electrocoagulation:

1. Electrodes reaction mechanisms (I and II) (were already discussed in section 3.2.)
2. Electrode side reaction (water decomposition) and formation of electrolysis gas;
3. Diffusion of electrolysis gases and flotation of metal ions to the surface of the bulk solution;
4. Migration of ions from electrodes to the bulk solution;
5. Direct or indirect oxidation by oxygen and other oxidizers in the bulk solution;
6. Direct hydrolysis of ferric iron to aquo-hydroxo ferric complexes
7. Hydrolysis ferrous/ferric irons followed by direct oxidation or precipitations to ferric hydroxides,
8. Coagulation and flocculation mechanisms of electrocoagulation coagulants (the aquo hydroxo ferric complexes) with colloids (the pollutants)
9. Chemi-sorption or physic-sorption mechanisms and precipitation reactions
10. Sludge settling

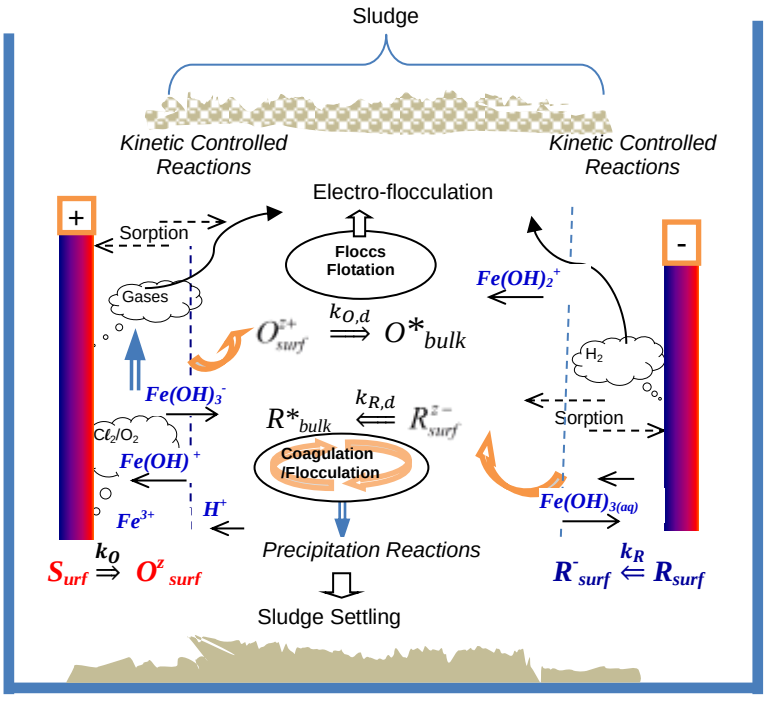

Figure 3.2. Electrocoagulation Processes adapted from (Barrow, 1988); (Lekhlif, *et al*., 2013); and (Martinez, *et al.,* 2012)

3.5.1 Electro-flotation Processes

As the electrolysis gases travel to the top of the bulk fluid, they create turbulence mixing currents for coagulation and flocculation within the bulk solution and lifting (floating) of the formed floccs to the surface of the bulk solution (Jiang *et al.,* 2002 and Holt, 2002). Hence, EC is sometimes called electro-flotation (EF). Small floccs easily rise to the surface of the bulk solution, and once at the surface, where oxygen concentration is high, the metal polyhydroxo complexes are converted to the orange-red, Fe_2O_3. Overtime, the electrolysis gas will form a froth phase with the iron oxide on the surface of the bulk solution. There is more flotation with aluminium electrodes than with iron electrodes and more sedimentation in iron electrodes than in aluminium electrodes EC because of differences densities of the two electrode materials.

3.5.2 Diffusion and Migration Mechanisms

At the electrode-liquid interface, there are two layers of water molecules; the first layer, is predominantly pure water in contact with the electrode surface and the secondary layer is a layer of solvated cations of aquometal complexes of the form, $M(H_2O)_n^{z+}$ and possibly $Fe(H_2O)_6^{z+}$ for iron electrodes. These two layers together are referred to as a double layer (Barrow, 1988). Within the double layer, there are diffusing electrolysis gases; oxygen, (O_2) and chlorine (gas), since textile effluent contian chloride) at the anode and hydrogen at the cathode (Zoulias, *et al*., 2001).

The diffusion of gases is driven by a diffision gradient that is created by the difference in concentration of gases between the surface of the electrode and the bulk solution. If the EC reactor has a mixer the diffusion gradient is normally assumed to be neglible (Barrow, 1988). The cations, anions and their products (Hector, *et al*., 2009) migrate electrophoretically from the electrode surface through the double layer to the bulk solution. The migration of ions is a charge transfer, kinetic reactions mechanisms and mass transport control. The reduced (R^-)^{surf} or oxidized (O^+)^{surf} ions migrate through a thin double layer to the bulk solution and migrate to the anode or cathode respectively.

$$R^{z-}{}_{surf} \rightleftharpoons R^{z-}{}_{bulk}$$

and

$$O^{z+}{}_{surf} \rightleftharpoons O^{z+}{}_{bulk}$$

Various species of total iron are shown in Figure 3.3. As the metal cations (M^{z+}) migrate from electrodes through boundary water layer, they react with water (hydrolysis) to form

aquometalhydro complexes of the form, $M(H_2O)_n^{z+}$ and typically, $Fe(H_2O)_6^{z+}$ for iron electrodes. The water of hydrolysis in $M(H_2O)_n^{z+}$ is replaced by various OH^- ions during electrolytic reactions to form hydroxometal-complexes of the forms $M(H_2O)_{6-n}(OH)^{zn-n}$.

According to Figure 3.3, the freshly produced ferric ions at the anode diffuse towards the cathode while undergoing various hydrolysis reactions forming various ferric polymeric hydroxo complexes such as $Fe(H_2O)_3(OH)_3^0$; $Fe(H_2O)_6^{3+}$; $Fe(H_2O)_5(OH)_2^+$; $Fe(H_2O)_4(OH)_2^+$; $Fe_2(H_2O)_8(OH)_2^{4+}$; $Fe_2(H_2O)_6(OH)_4^{4+}$ etc. (Martinez, *et al*., 2012). Figure 3.3 also show that these polymeric hydroxometal complexes are mainly positively charged, so they migrate towards the cathode while undergoing other electrocoagulation mechanisms such as:

- Electrostatic attracting the negatively charged pollutants and other ionic species,
- Coagulating and flocculating with pollutants,
- Oxidation by dissolved molecular oxygen,
- Chemical and, or physical sorbing pollutants and into their gelatinous structure.

As shown in Figure 3.3, (Martinez, *et al*., 2012), the ferric hydroxides ($Fe(OH)_3^-$) are negatively charged and are formed near the cathode. They migrate towards the anode and become neutral charged, $(Fe(OH)_{3(aq)},$ and depending on the pH they precipitate (Martinez, *et al*., 2012).

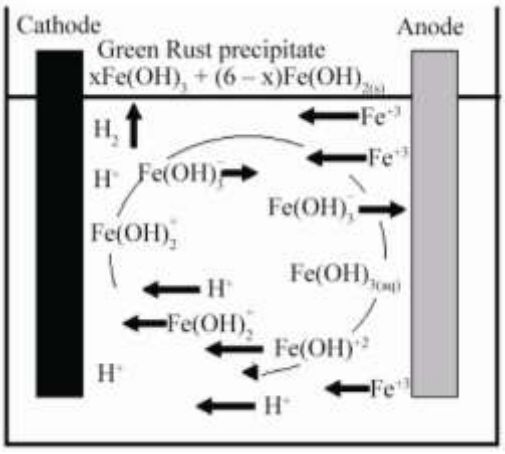

Figure 3.3 Dissolved iron ions during iron electrocoagulation (Martinez, *et al*., 2012)

3.6. Chemi-Physisorption, Coagulation and Complexion Reaction

Adsorption of the solid pollutant particles (colloids); heavy metals and normal organic pollutants onto the gelatinous metallic complexes ions can take place by two adsorption mechanisms that is chemisorption and physisorption mechanisms. Chemisorption is

characterised by low activation energy ranging from 0 to 88 kJ/mol and 88 to 88-400 kJ/mol for physic-sorption (Fil, *et al*., 2014).

These hydroxometal complexes are responsible for destabilization and neutralization of the charge of the colloids (Water Services , 2000 and Lekhlif, *et al*., 2013). These hydroxo-complexes are mostly positively charged. The pollutants that are in the effluent are normally negatively charged and therefore experience weak van der Vaal's forces of electrostatic attractions (Larue, 2003). According to Sengil, *et al*., (2008), dyes can also be removed by adsorption onto the solid polyhydroxo complex iron and iron precipitates.

$$R–SO_3Na + (OH)_3(H_2O)\,Fe \Rightarrow R–SO_3–(OH)_2H_2OFe + Na^+ + OH^- \quad \text{R3.7}$$

The formation of metal hydroxides and aquometalhydroxo complexes depends on pH. Near the anode hydrolysis, mechanism II reaction was shown above (Lopes, *et al*., 2004).

$$4Fe^{2+} + 6H_2O \rightleftharpoons 4(OH)OFe + 8H^+ \quad \text{R3.8}$$

The solid ferric hydroxide can remove dyes by the reactions R3.14.

$$(OH)OFe + Dye\text{-}H \rightleftharpoons DyeOFe + H_2O \quad \text{R3.9}$$

3.6.1. The Concentration Overpotential.

According to Yun, *et al.* (2012); Pintauro, (2007) and Pilatowsky, *et al*.,(2011), the concentration overpotential depends on the applied current density i (A/cm^2) and limiting current i_L (A/cm^2)

$$E_{conc} = \frac{RT}{z\mathcal{F}} \ln\left(\frac{i_L}{i_L - i}\right) \quad 3.1$$

Where, E_{conc} is the concentration overpotential; *R* (J/mol) is the universal constant; z is the number charges; $\mathcal{F}$ is the Faraday constant (C/mol); T is the temperature in K.

3.7 Electrochemical Kinetics Parameters

Electrodes reactions kinetics are well understood as are found in most electrochemistry literature; however under ideal conditions. For example, at a 100% current efficiency, the amount of electrode material (w) dissolution during EC can be estimated by Faradays law (Ghanim, *et al*., 2013 and Lakshmana, *et al*., 2009):

$$w_{theo} = \frac{i \cdot t \cdot M}{z\mathcal{F}} \quad 3.2$$

where, (w_{theo}) is the theoretical amount of electrode material (g/cm^2), i; current density (A/cm^2), $\mathcal{F}$; Faraday's constant (96487 coulombs/mol) M; the relative molar mass of the electrode (g/mol), z the number of electrons or charges. The exchange current density (i_o) is the current density that is defined by charge transfer reaction rate that happens when the anodic and cathodic reaction are at equilibrium. At equilibrium; the anodic, (k_a) and cathodic (k_c) reaction rate are equal to the exchange reaction constant (k_o^s). Assuming that all cathodic and anodic reactions (including side reactions) are at equilibrium such that $k_c = k_a = k^o$, charge transfer reaction rate constant for EC can be defined by equation 3.4 (Scherer, *et al*., 1997):

$$k_{ct} = k_s^o e^{\left[-\alpha z \mathcal{F} \frac{(E^o - E^o_{rev})}{\mathcal{R}T}\right]} \quad 3.3$$

where E^o, is the electrode potentials (V); E^o_{rev}, is the equilibrium cell potential (V) at standards conditions; z and $\mathcal{F}$ were previously described above and α is the symmetry factor or charge transfer coefficient (about 0.5) but according to Grygar, (1995) it is affected by concentration of the electrolytes. (E_{conc} - E^o_{rev},) is defined as the deposition or decomposition or polarization voltages or simply and overpotential, (Barrow, 1988). Charge transfer reactions are dependent on mass transfer coefficient,(k_m) and concentration in the bulk solution, (C^{bulk}) and current density (i) (Protsenko , *et al*., (2010) and Scherer, *et al*., (1997)) by the following equation:

$$i_L = z\mathcal{F}k_{m,O}\left(C_t^{\,bulk}\right) \quad 3.4$$

where; $\mathcal{F}$; Faraday's constant (96487 C/mol); (k_m) is the mass transfer coefficient (cm/s); z is the number of electron (e^-) and C^{bulk} is the bulk concentrations 3.3. The charge transfer constant (k_{ct}) also depend on exchange current density (i_o). Similarly, at the surface of the electrode, if there were no concentration overpotential (E_{conc}.) and reverse currents, there would be charge transfer kinetic current density, (i_k) (Protsenko & Danilov, 2010):

$$i_k = zFk_s^o e^{\left[-\alpha z \mathcal{F} \frac{(E^o - E^o{}_{rev})}{\mathcal{R}T}\right]} \quad 3.5$$

under kinetic controlled reactions, $zFk_s^o e^{\left[-\alpha z \mathcal{F} \frac{(E^o - E^o{}_{rev})}{\mathcal{R}T}\right]} \ll k_{m,O}$

The activation energy depends on the charge transfer reactions at the electrodes (Protsenko & Danilov, 2010). However, under mass transfer controlled reactions,

$$zFk_s^o e^{\left[-\alpha z\mathcal{F}\frac{(E^o - E^o rev)}{\mathcal{R}T}\right]} \gg k_{m,O}$$

and activation energy (E_A) does not depend on the electrodes potentials (Protsenko & Danilov, 2010). In addition, when the current efficiency is less than 100% then the electrochemical reactions are mass transport controlled. However, when the applied current is equal to limiting current then electrochemical reactions are current driven.

It is a common practice to assume mass transfer controlled reaction rates in the study of reaction kinetics studies in EC (Abdel-Aal, *et al*., 2010; del Río, *et al*., 2009; El-Shazly, *et al*., 2013a; El-Shazly, *et al*., 2013 b; Hmani , *et al*., 2012; Raju, *et al*., 2008 and Rincon, 2011). The mass transfer coefficient (k_m) depends on bulk concentrations, (C^{bulk}) of the electrode materials or pollutants that are easily measurable in bulk solution at liming current densities (i_{lim}) as:

$$\frac{i_L}{zFA_e} = k_{m,O} C_{i,}^{bulk} \qquad 3.6$$

Where; mass transfer coefficient (k_m) (cm/s); i_{lim} is the limiting current density*;* (A/cm^2). A_e is the cross sectional area of the electrodes (cm^2); z and $\mathcal{F}$ as defined previously.

When the electrochemical cell is reversible at equilibrium, it will give an electrode equilibrium reversible potential (E^o_{rev},). The ions in the solution between the electrodes contribute other potentials such as ohmic potential ($V = IR$) or solution overpotential (E_Ω) or a chemical potential (ΔE_Φ) or reversible potential (E_{rev}). E_{cell} is given as:

$$E_{cell} = E_{rev} + E_{ohmic}, \qquad 3.7$$

assuming that in the beginning of the electrocoagulation, maximum resistance to electrochemical processes is caused by ions in solution (Papagiannakis, 2005,).

$$E_{app} = E_{cell} + E_{ohmic}, \qquad 3.8$$

where, E_{app} is the applied voltage.

3.7.1. Current Efficiencies

If the electrolysis is only charge transfer and kinetic controlled, in the beginning of the electrocoagulation, when limiting current density (i_L) is equal to the applied current density (i_{app}); the EC is 100% faradic efficiency, (CE) (Hmani , et al., 2012) and (del Río, *et al*., 2009) and is given by:

$$CE = \mathcal{F}V\frac{[COD-O_2]_o-[COD-O_2]_t}{zIt} \times 100\% \quad 3.9$$

Where COD are in mg/L but can be converted into mol/LO_2, I is current (A) and V is volume (L). The Faradic efficiency (CE) can also be determined from Equation 3.9 (Ahmed & Saad , 2013).

$$CE = \frac{z\mathcal{F}wV}{ItM} \quad 3.\ 10$$

Where V is the volume of the effluent (L); C is the concentration of the pollutant (mol/L); w is the mass of the pollutant (mg/L) and the other terms have been described above. However; EC is not 100% efficiency (60% to 92%) (Ahmed & Saad , 2013) and therefore the inefficient factor γ

$$CE = \frac{[COD]_t}{\gamma[COD]_O} \quad 3.11$$

3.7.1 Mass Transfer Coefficient and COD Limiting Current Densities

Reaction kinetics in electrocoagulation involves many mechanisms such as elementary chemical reaction kinetics; electrochemical charge transfer reaction rates; mass transfer and adsorption kinetics. Most recently, researchers such as El-Shazly , *et al.*, (2013), (Hmani , et al., 2012), Ghanim, *et al.,* (2013), and Mahmoud, *et al*., (2014) used mass transfer and adsorption kinetics models to study reaction kinetics in electrocoagulation. Electrochmeical oxidation reactions require molecular oxygen and electrochemical oxidation (the number of electron). Both (z) oxidation electrons and stoichiometric oxygen (o) kinetic oxidation can be presented for any species as a limiting current density (Hmani , et al., 2012) for COD

$$i_{\mathrm{L}} = \frac{z_{O_2}}{o_{O_2}}Fk_m[COD]_t \quad 3.\ 12$$

Where; (o) is the coefficient of oxygen in the stoichiometric reactions and (z) the coefficient of the electrons in a balanced electrochemical reaction. $[COD]_t$ is the chemical oxygen demand at time (t) and $[COD]_o$ is the COD before EC (at original concentrations).

In ordinary chemical reactions, COD is removed by direct molecular oxygen oxidation reactions. In electrocoagulation reactions, COD is removed by electrochemical oxidation of electrodes, releasing electrons that are used in water splitting generating molecular oxygen, (O_2). The molecular oxygen, (O_2); is further utilized in other reactions for oxidation reactions (Khue, *et al*., 2014). Therefore, assuming that the COD is via oxidation reactions as shown in the above reactions, in such a way that it can be presented by using the relationship between the limiting current densities and mass transfer coefficient (Hmani , et al., 2012).

$$i_{\mathrm{L}} = 4Fk_m[COD]_t \qquad 3.13$$

i_L = limiting current (A/cm^2); $\mathcal{F}$ = Faradays constant (96486 C/mol); 4 = is the number electrons or charges transferring in the main oxidation reaction to one mole of molecular oxygen (O_2) and k_m = mass transfer constant (cm/s)

3.8 Reaction Rates

Electrochemical reaction rates, (***r***)*,* are expressed in terms of current densities,(***i***). The reaction kinetics studies can easily be done by few potential or current controlled electrochemical experiments at different applied current densities, (***i***). As by equation 3.14, first order reaction rates are normally the first assumption about reaction rates in electrochemical reactions (Schmidt, 1998).

$$r_a = r_c = r = \frac{z_e \mathcal{F} I}{A_e} \qquad 3.14$$

where; r_a and r_c are anode and cathode equilibrium reaction rates respectively; $\mathcal{F}$; Faraday's constant (96487 C/mol); I is applied current (A); z is the number of electrons that are transferred in the reactions and A_e is the electrodes surface area.

$$-\frac{A_e}{V_R}\frac{d[C]}{dt} = \frac{i}{z_e \mathcal{F}} = r \qquad 3.15$$

Where, $\boldsymbol{i}$ is the current density (A/cm^2), $\mathcal{F}$ is Faradays constant = 96482 C/mol; z is the number of charges; A_e (cm^2) is the electrode area and V_e (cm^3) volume of the electrode. The intergral form of the equation is given in terms of mass transfer coefficient k_m (cm/s) because the concentration (C^{bulk} , mol/L) that are measured in bulk solution, (Raju, *et al*., 2008); (El-Shazly, *et al*., 2013); (Lopes, *et al*., 2004) and (Hmani , et al., 2012).

$$ln\left(\frac{C_o}{C_{(t)}{}^{bulk}}\right) = \left(-\frac{A_e}{V_e}k_m\right)t \qquad 3.16$$

The mass transfer coefficient (k_m) is the slope in the curve of $ln\left(\frac{C_o}{C_{(t)}{}^{bulk}}\right)$ vs time for first order reactions. Also, the above equation can be presented as below.

$$C_t^{Bulk} = C_O \cdot e^{-\left(\frac{A_e}{V_e}k_m\right)t} \qquad 3.17$$

C_t^{bulk}, is bulk soluiton concentration (mol/L) at any time during the electrocoagulation; C_o is concentration (mol/L) before EC and k_m (m.s^{-1}) is mass transfer coefficient. Other researchers Raju, *et al*., (2008) and Essadki, *et al*., (2007) use the mass transfer coefficient, (k_m) in their reaction kinetics. Therefore, $k_m\frac{A_e}{V_e}$ is observed reaction constant as EC include electrode surface kinetic reaction constants, (k_s) such cathode, k_R and k_O electrode surface reactions constant and standard reaction kinetic reaction constant k_o which are determined under special electrochemically controlled conditions that are beyond the scope of this theses.

$$k_c = k_m\frac{A_e}{V_e} \qquad 3.18$$

However, knowing all reaction constants are important to determine if the reaction is kinetic or mass transfer controlled. Nevertheless, the relationship between the mass transfer and kinetic controlled reaction rates is given by reaction 3.19 (Scherer, *et al*., 1997).

$$\frac{1}{k_{obs}} = -\frac{1}{k_s} - \frac{1}{k_m} \qquad 3.19$$

Where k_s is a first order heterogeneous kinetic and charge transfer reaction constant at the surface of the electrodes; k_{obs} is the observed; apparent, or mixed control reaction constant and k_m is the mass transfer coefficient. Second order reactions are also possible because conversional coagulation and flocculation normally follow second order reaction (Pernitsky, 2003). In their studies, Mahmoud & Ahmed, (2014) and Rincon, (2011) reported a second order model. For second order electrochemical reaction, the second order reaction constant

can be determined from the gradient of the plot of $\frac{t}{C_{(t)}^{bulk}}$ versus electrolysis time (t). Equation 3.20 is the equation that describes the relationship between time and concentrations.

$$\frac{t}{C_{(t)}^{bulk}} = \frac{1}{k\left(C_{max}^{2}\right)^{bulk}} + \left(\frac{1}{C_{max}}\right)t \qquad 3.20$$

Where C(t) is the concentrations at time (t); C_{max} is the maximum removed concentrations and k is part of the gradient $\frac{1}{k\left(C_{max}^{2}\right)^{bulk}}$

In conventional chemical coagulation the rate of electrophoretic migration of particles follow second order reaction kineitcs that is describe by equation $\frac{dC}{dt} = k_1 C^2\left(1 - e^{-k_2 t}\right)^2$

3. 21 (Chaturvedi, 2013).

$$\frac{dC}{dt} = k_1 C^2\left(1 - e^{-k_2 t}\right)^2 \qquad 3.\ 21$$

where

μ = the viscosity of the continuous medium

u = the electrophoretic velocity of the particles

$k_2 = u/x$ (x being the geometric parameter of the electrode size),

$k_1 = 4k_BT/3\mu$

k_B = the Boltzmann's constant), C = the concentration at time t; ,

t = coagulation time and T = coagulation temperature

3.9 Activation Energy and Other Transition State Parameters

Another objective of this research was to determine the activation energy. The activation energy in electrochemical system can be determined by voltage and current density measurements. From the voltage and current density data, the activation energy can be determined from the Tafel plots as activation overpotential, (E_{act}) where the E_{act} is converted to energy by its relationships to Gibbs free energy of activation.

$$\Delta\mathbf{G}^{\#} = -z_e\mathcal{F}E_{act} \qquad 3.\ 22$$

Where z_e is the number charges or electrons transferring in electrodes reactions, $\Delta G^{\#}$ (J/mol) is the Gibbs free energy of activation and $\mathcal{F}$ is the Faradays. Also for charge transfer

electrodes reactions, the activation overpotential (E_{act}) depends on the equilibrium potential (ΔE_{rev}) and kinetic overpotential (E_k)

$$E_{act} = E_k - \Delta E_{rev} \qquad 3.\ 23$$

Both activation overpotentials and reversible potentials are not easy to measure in bulk electrolysis. Activation overpotential (E_{act}) can also be derived by manipulating Tafel equation (Barrow, 1988; Pilatowsky, *et al*., 2011; Papagiannakis, 2005; Pletcher & Walsh, 1990) and Yun, *et al*., 2012).

$$E_{act} = \frac{RT}{\alpha \mathcal{F}} ln\left(\frac{I}{I_o}\right) \qquad 3.\ 24$$

Where α is a symmetry factor usually 0.5 but it depends on the electrolyte (Grygar, 1995) and I_o *(A)* is the exchange current at equilibrium, when anode and cathode reactions rates are the same and I *(A)* is the applied current. However, these methods are only applicable to special controlled conditions of electrode reactions; electrolytes concentrations and temperatures. In electrocoagulation, determination of activation energy involves Arrhenius plot of natural logarithmic function of reactions constants (ℓnk) vs the inverse of temperature (1/T) (Hmani , et al., 2012).

$$\ell \mathrm{n}\, k(T) \quad = \frac{R.T}{z\mathcal{F}} \ell \mathrm{n}\, A - \frac{E_a}{R.T.} \qquad 3.\ 25$$

Where, *A*, is the Arrhenius factor ($\Omega^{-1}.m^{-2}$), E_a is the activation energy (kJ), *R* is the universal gas constant (J/mol.K) and T is the reaction temperature (in K). Other parameters of the equation where previously described. The activation energy is the part of the slope $-\frac{E_a}{R}$ in the slope of a plot of ℓnk vs 1/T. Other reaction rate parameters relate reactions to the thermodynamics parameters such as Entropy ($\Delta S^{\#}$) and enthalpy ($\Delta H^{\#}$). Entropy ($\Delta S^{\#}$) and enthalpy ($\Delta H^{\#}$) of activation are, in addition to activation energy, other transition energy state parameters that are determined by Eyring's Law plot of the natural logarithmic function ratio of the reaction constant to the temperature of reaction versus inverse of temperature (Clayden , *et al*., 2000).

$$\ell n\left(\frac{k}{T}\right) = -\frac{\Delta H^{\#}}{R} \cdot \frac{1}{T} + \left(\frac{\Delta S^{\#}}{R} + \ell n\left(\frac{k_B}{h}\right)\right) \qquad 3.\ 26$$

$$y = -m \cdot x + c$$

$$\Delta S^{\#} \quad = \quad R(intercept - \ \ell n\left(\frac{k_B}{h}\right))$$

Where k_B is Boltzman's constant and h is Planck's constant therefore:

$$\ell n\left(\frac{k_B}{h}\right) = 23.76$$

$$\Delta S^{\#} \quad = \quad R\left((intercept - \ \ell n\left(\frac{k_B}{h}\right)\right)$$

Entropy is significant because open circuit voltage is not easy to determine in bulk electrolysis.

$$\Delta G^{\#} \quad = \Delta H^{\#} - T\Delta S^{\#} \qquad 3.\ 27$$

and

$$E_{ocv} = \Delta\mathcal{E}^{0} + \frac{\Delta S^{0}}{z\mathcal{F}}(\mathrm{T} - \mathrm{T}_0) \qquad 3.\ 28$$

Chapter 4 - Research Methodology

In this study, the analytical instruments that were utilised namely: 1) HACH DR2800 uv-spectrophometer; 2) Hanna HI4522 pH-Ec multi-parameter meter; and 3) HANNA HI-93414 Turbidity–chlorine meter. There are certainly numerous significant factors (control parameters) involved in EC and it is impossible to consider all of them in one study. Efforts were made to consider very important factors such as conductivity (κ), pH, temperature (T), initials concentration of pollutants, chlorides ($C\ell^-$), concentrations of electrodes materials (ferrous, Fe (II) and total (t-Fe) iron), applied voltage (U_{app}), applied current density (i_A) and free (f-$C\ell_2$) and total chlorines (t-$C\ell_2$) and chlorides ($C\ell^-$).

The purpose of iron EC was to reduce the concentrations of textile effluent pollutants such as chemical oxygen demand (COD); total dissolved solids (TDS); total suspended solids (TSS); true/apparent colour (P_t-Co,); ORP; absorbance ($A_{\lambda max}$) and turbidity, (NTU). Some of these parameters were measured continuously during EC for example pH, conductivity (κ), total suspended solids (TSS), temperature (T) with data logging system instruments. The initial phase of the experiments entailed the creation of pre-bleaching and dyeing samples. The pre-bleaching and dyeing procedures that were created were used to make textile effluents with commercial dyeing machines, Washtec-P or Pyrotec-MB2 at 10:1 and 20:1 liquor ratios. Triplicate samples for each dyeing step (pre-bleaching, dyeing, soaping off and softening steps) were taken and analyzed for both 10:1 and 20:1 liquor ratios.

As previously explained in chapter 2, liquor ratio is the ratio of the mass of the textile material to be processed to the liquor volume to be used in the dyeing machine. The choice between 10:1 and 20:1 is based on the dyeing industry operating liquor ratios mostly at 10:1 (Kazakevičiūtė, *et al*., 2004) and the 20:1 liquor ratio is based on allowing for dilutions by several rinsing steps.

Triplicate EC experiments at 25°C, 30°C, 35°C, 40°C, 45°C, 50°C, and 55°C were performed at a current density of 9.5 mA/cm^2 for an hour. Twelve samples at intervals of 5 min minutes; pre and post EC treatment were taken and analyzed for COD, dissolved irons, chlorines, chlorides, turbidity, absorbance ($A_{\lambda max}$), true colour (Pt-Co) and TDS.

4.1 Analytical Instruments

The following are the main instruments that were used:

- HACH-2100P turbidity meter was used to measure turbidity.
- DR-2800 uv-spectrophotometer, was used to do the following tests:
  - TSS test was done as soon as samples were centrifuged with DR2800, HACH method 8006.
  - Absorbencies ($A\lambda_{560nm}$) were measured with DR-2800, at a maximum wavelength, λ_{max} of *560* nm.
  - Total and free chlorines.
  - Chemical oxygen demand, and
  - Total and ferrous irons.
  - All the procedures for the DR2800 spectrophotometer could be found in the DR2800 manual (HACH, 2007).

- YSI-5000 Dissolved Oxygen (DO) Meter was used to measure DO in the EC bath.
- HANNA HI 98703 meters also was used to measure turbidity and total and free chlorines.
- Hanna HI-4522 pH-Ec multi-probe was integrated to the computer data logging system as shown in **Error! Not a valid bookmark self-reference.**, label 1; with the following probes (label 6 in **Error! Not a valid bookmark self-reference.**):
  - The conductivity, (κ); resistivity (Ω); salinity; TDS; pH; temperature (T), electrodes and ORP with $Ag^{+}/AgC\ell$**//** Pt_s -electrodes for determination of E_h.
- HACH DR-200 heating block.
- Dc power supplier (EA-PS-8016-20T, 16V-20A), label 2 in (**Error! Not a valid bookmark self-reference.**)
- The GC-001 computer console, GC[11]-001; label 3 in (**Error! Not a valid bookmark self-reference.**) console data logging system connected to Hanna HI-4522 pH-EC labels 1a (mode 1) and 1b (mode 2) in **Error! Not a valid bookmark self-reference.** and Dc power supplier for data logging.

[11] The acronym stands for "glass chem", not "gas chromatography"

- The HI-4522 pH-Ec multi-probe (**Error! Not a valid bookmark self-reference.**) and the DC power supply were connected to the GC-001(3) computer console for data logging.
- Magnetic stirrer, label 7 in **Error! Not a valid bookmark self-reference.**.
- 6 x 318 stainless 3.0 mm x 95 mm x 90.0 mm, as shown in label 5 in **Error! Not a valid bookmark self-reference.**
- The electrocoagulator. label 8 in **Error! Not a valid bookmark self-reference.**
- The thermostatically controlled water bath label 4 in Figure 4.1.

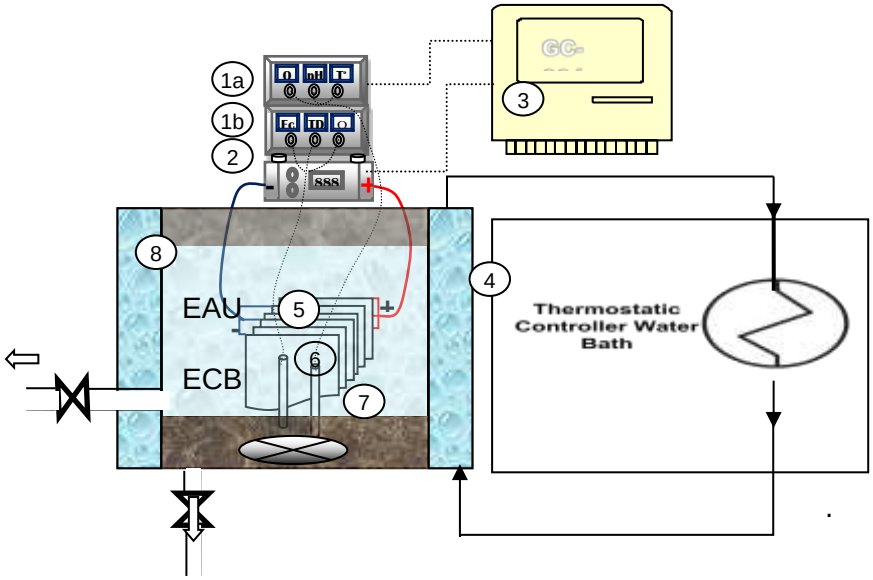

Figure 4.1 Process Flow Diagram

4.2 Chemical Reagents Used

4.2.1 Chemical Reagents for Analyses

- The 50 mL samples and 16 mL sample bottle (bought from United Scientific)
- 45 μm membrane filter (bought from Chemix (Pty))
- 32% HCℓ for 1.0 N HCℓ or NaOH pallets for 1.0 N NaOH to neutralize samples for hazen colour (Pt-Co) analysis with HACH method 8025.
- Merck Spectroquant CODs reagents for the medium range and medium high range.
- The following reagent were bought from Agua Africa:
  - 1,10 Phenanthroline powder pillows reagent, to measure ferrous irons with method Hach method 8146.(were bought from Agua Africa)
  - FerroVer® powder pillows reagents to measure total irons with HACH method 8008

- N,N-diethyl-p-phenylenediamine (DPD) powder pillows reagent to measure free chlorines with, HACH method 10069. (were bought from Agua Africa)
- N,N-diethyl-p-phenylenediamine (DPD) powder pillows reagent to measure total chlorines with, Hach method 10070.
- Ferric iron and mercuric thiocyanate solutions measure chlorides with Hach method 8113.

4.2.2 Pre-bleaching Chemicals

(all dyeing chemicals were obtained from a local dyeing company)

- Antiform (Rusto BXB) (mL/L)
- Wetting agent(Rucogen BFL-Z) (mL/L)
- Sequestering agent (g/L), EDTA
- Caustic Flakes (NaOH)
- 50% Hydrogen Peroxide, only (mL/L)
- Acetic Acid

4.2.3 Dyeing Chemicals

(all dyeing chemicals were given by a local dyeing company)

- Antifoam (Rusto BXB)
- Rucogen BFL-Z (Wetting agent),
- Verolan (Lubricant (anti-crease))
- Rucotex T-Z (Levelling)
- Common salt , (NaC*ℓ)*
- Soda ash (Na_2CO_3)
- 50% **c**austic soda (NaOH)
- Remazol Brilliant Red 3BS (100%), from Dysta South Africa
- Levafix) Brilliant Blue (E-FFN; (150%) Dysta South Africa
- Cibacron Yellow C-R

4.3 Sample Dyeing Methodology

Commercial sample dyeing machines, Pyrotec-MB2 and Washtec-P are shown in Figure 4.2 (a) and (b). Commercial sample dyeing machines are used in the textile dyeing laboratory for dyeing test runs for every fabric to be dyed before being routed to the main dyehouse for bulk dyeing and finishing processes. Commercial sample dyeing machines

can carry up to 16/12 stainless steel beakers as shown in Figure 4.2 that could be filled up to 200.0 mL for Pyrotec-MB2 (Figure 4.2(a)) or 500.0 mL for Washtec-P (Figure 4.2(b)) respectively. These stainless steel beakers generated enough effluent for at least four to five EC experiments at 3.5 L each. Sample dyeing dyebath effluents were created by pre-bleaching and dyeing fabric pieces in 10, of the 16, 200.0 ml stainless steel beakers. This was done at 10:1 and 20:1 as liquor ratios (X).

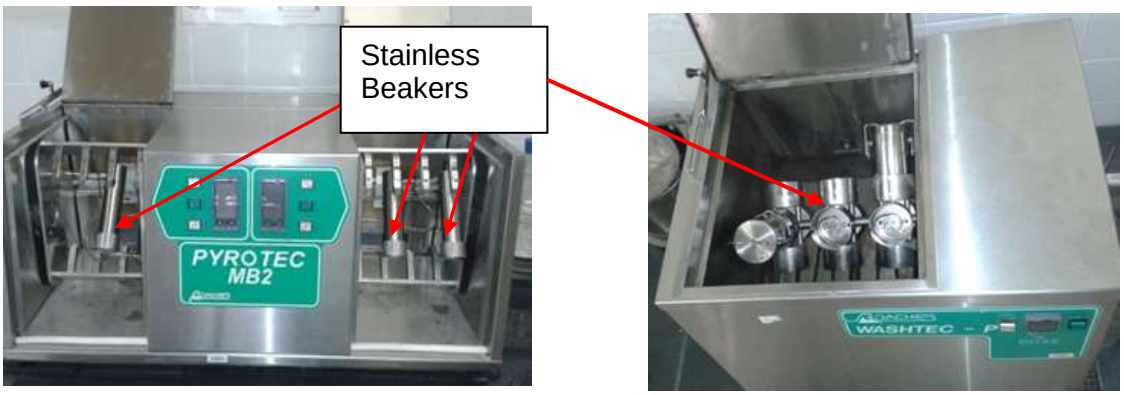

(a) Pyrotec-MB2 (b) Washtec-P

Figure 4.2. (a) Pyrotec-MB2 and (b) Washtec-P Showing Stainless Steel Beakers.

4.3.1 Pre-bleaching Chemicals and Procedure

The quantities of chemicals that were required for pre-bleaching at 10:1 liquor ratio were calculated by equation 4.1(a) and calculated results were presented in Table 4.1. The chemical quantities that were required for pre-bleaching were based on a 20:1 liquor ratio and were calculated by equation 4.1**:**

$$V_{stocksol} = \frac{\text{x (g/L)} \times Liq\,vol(L) \times 100\%}{Stock\ Solution\ \ Conc.} \qquad 4.1(a$$

where $V.$ is the volume of the stock solution required for the pre-bleaching; $\boldsymbol{x}$ (g/L) or x (mL/L) or (as percentage for dyes) is the ratio of grams or (mL) of the chemical per litre of the liquor volume ($Liq\ vol.$) $\boldsymbol{x}$ (g/L) is determined by trial runs in the dyeing laboratory. Stock Solution Concentration. is the available concentration of the stock solution. For example hydrogen peroxide is provided by suppliers at a concentration of 50%. Peroxide requirements for pre-bleaching at a liquor ratio of 20:1, were calculated as follows: A liquor ratio of 20:1 means 20 L of pre-bleach liquor was used to pre-bleaching 1 kg of fabric. 100g of fabric, 2 L of water were required.

The required hydrogen peroxide was calculated as:

$$Peroxide = \frac{5.0\,\text{mL/L} \times 2.0L \times 100\%}{50\%.} = 20.0\,mL\ peroxide \qquad 4.1\ (b)$$

All other chemicals were calculated the same way and presented in Table 4.1**.** EDTA was applied as it is used in textile industry to the keep all metals within the pre-bleaching liquors; otherwise, metals will stain the fabric.

Table 4.1 Pre-bleaching Chemicals at 10:1 liquor

PRE-BLEACHING	Stock %	Ratios (g/L)	Amount (g)	
			g	mg
Antifoam (Rusto BXB) (mL/L)	100	0.20	0.20	200
Wetting agent (Rucogen BFL-Z) (mL/L)	100	1.00	1.00	1000
Sequestering agent (g/L), EDTA	100	1.00	1.00	1000
Caustic Flakes (NaOH) (pH = 12) g/L	100	4.00	4.00	4000
50% Hydrogen Peroxide (mL/L)	50	5.00	10.00	10000
Acetic Acid	99	1.00	1.01	1010.1

4.3.2 Pre-bleaching Chemicals and Procedure

All the chemicals in **Table 4.1** were weighed. All auxiliary chemicals were added to 100.0 mL of water for (10:1) or 200.0 ml for (20:1) in 10 stainless steel beakers, making a total of 1000 mL volume for the liquor ratio of 10:1; 2000 mL for the liquor ratio of 20:1. The fabric pieces, or hanks, were weighed and added to each of the stainless beakers. The beakers were hand shaken and then inserted into the commercial sample-dyeing machine. The stainless steel beakers were clamped into a rotating shaft and rotated inside the machine's water bath or radiant heating medium. It was noted that the beakers were even-numbered inside the commercial sample-dyeing machine.

The machine was programed for a gradual temperature rise of 1°C/min from ambient temperature (±25 °C) to 95°C for pre-bleaching. The commercial sample-dyeing machine was programed to run at 95 °C of bleaching for 45 minutes. After 45 minutes, the machine was stopped and allowed to cool down for about 10 minutes or to a temperature cold enough to be poured into the beakers. The sample-dyeing machine was then opened to recover the effluents.

The fabric was taken out and the pre-bleaching effluent was recovered. The fabric was rinsed with cold water twice. This was followed by 1g/L acetic acid rinse at 95°C and at a liquor ratio of 10:1 to neutralize the fabric to about a pH of about 6. DyeStar (2007)

recommends pH of 6 for the dyes that were utilised. All other rinses were done at liquor ratio of 20:1 to allow for dilutions that are possible in a real dyehouse.

4.3.3 Rinsing and Effluent Preparation and Recovery

The effluents from all the stainless beakers were mixed in a 5-litre bucket by an overhead stirrer for five minutes and a 50 mL the samples were taken. In the meantime, while effluents were being mixed, the fabrics were placed in 2000 mL water in a 5 L bucket for the first and second rinse procedures steps. After each rinsing step, a 50 mL effluent sample was taken. The rinsing effluent were added into the 20 L effluent mixing bucket with the pre-bleaching liquor and mixed for five minutes. A 50 mL sample was taken again.

4.3.4 Dyeing Chemicals

Auxiliary chemicals were calculated by equation 4.1 but dyes were calculated differently with Equation 4.2. Up to 5% of total dyes were used for dark shades. All the dyeing auxiliary chemicals and dyes are shown in table 4.2. Calculations, of Levafix Brilliant Blue with 3% dye addition to the fabric were done as shown in equation 4.2.

$$Dye(g) = \frac{\%dye \times mass of\ fabric}{\%dyeConc.} \qquad 4.2(a)$$

For example

$$Dye(g) = \frac{3.0\% \times 100g}{150\%.} = 2.0g\ Blue\ dye \qquad 4.2\ (b)$$

150% refers to the concentration of the dye molecule. It means 150% granular concentrations of dye is more concentrated in water than 100% dyes in solid form.

4.3.5 Dyeing Procedure

The entire chemicals and dyes list are shown in Table 4.2 and were weighed and added to the sample dyeing machine stainless steel beakers. The machine was programed to raise the temperature at 1.0 ^{0}C/min starting from ambient temperature to 70^{o}C. The dyeing process was allowed to proceed for 10 minutes, after which 50% of the total caustic was added. The dyeing process was continued for another 10 minutes and the remaining caustic was added. The fabric dyeing was continued for 45 min, after which the sample-dyeing machine was stopped and beakers were allowed to cool for about 10 min.

After dyeing, the fabric had a lot of excess dyes and chemicals that were trapped in it. The residual dyes and chemicals were rinsed off by several rinsing steps with water and industrial surfactants. The acetic acid was used to neutralize the fabric and the EDTA as a chelating agent. The first and second cold rinsing steps were followed by a hot rinse at 60 ^{c}o. The rinsing step effluents from each rinsing step were sampled and added to the original pre-bleach liquor that was mixed for five minutes and another 50 mL was taken.

Table 4.2 Dyeing Chemicals at 10:1 liquor ratio

REACTIVE DYEING		% Conc. Stock	Ratios g/L(ml/L)	Amount g
Antifoam (Rusto BXB) (g/L)		100	0.2	20
Wetting agent,(Rucogen BFL-Z) (g/L)		100	1	2.4
Lubricant (anti-crease) (Verolan) (x%)		100	2	4.7
Levelling (Rucotex T-Z)1.0 ml/L		100	1	2.4
Common Salt , NaCℓ(g/L) (5-80)		100	70	165.8
Combinations (NaOH and Na_2CO_3)	50%NaOH (ml/L)	50	0.9	426.4
	Na_2CO_4 (g/L)	100	3	7.1
1% Remazol Brilliant Red 3BS (100%),		150	1	0.7
3% Levafix) Brilliant Blue (E-FFN,(150%)		150	3	2.
1.0% Cibacron Yellow C-R		100	1	1.

The effluent was recovered and the same procedures for sampling and rinsing as in section 4.2.3 were followed. The soaping off step did the additional residual dye removal step.

Table 4.3 Auxiliary Chemical at 20:1 for Acid And Soaping Rinses

Acid Rinsing and Soaping Off	Conc.(%)	Ratios	Amount (g)
Detergent (NP9) g/L	100	2	9.476
Antifoam (g/L)	100	1	4.738
Acetic Acid (g/L)	32	2.5	37.016
Sequestrate (EDTA) (g/L)	50	1	9.476

As the name implies, in this step, an industrial surfactant was added and the soaping off procedure was carried out at 95°C. At the same time, the acetic acid is also added to neutralize the fabric. Equation 4.1 was used to calculate the chemicals that are shown in Table 4.3. The soaping off step was followed by two cold rinses to remove soap and chemicals from the fabric. The last step was the addition of fabric softener and the fabric softening chemicals are shown in Table 4.4.

Table 4.4 Auxiliary chemical additions at 20:1 liquor ratio for fabric softening

SOFTENING	Conc. (%)	Ratios(g/L)	Amount (g)
Acetic Acid (g/L)	50	2.5	23.69
Softener (%fabric) Persoftal VNO 500%)	500	2	0.9476

The samples were kept in a refrigerator at 4^{o}C in order to preserve the integrity of the solution.

4.4 The Electrocoagulation Equipment

In this study, a batch EC reactor Figure 4.3 was used with vertical electrode configurations. EC reactor was made up of three sections: 1) the electrode assembly unit 2); the electrolysis bath unit as shown by label (**A**) in Figure 4.3 and the cooling jacket unit as shown by label (**E**). The electrocoagulator was made up of a double wall water-jacketed reactor with a 6 mm thick Perspex on the outside and 6 mm thick glass inside wall separating the cooling water from the effluent being treated inside the EC bath unit.

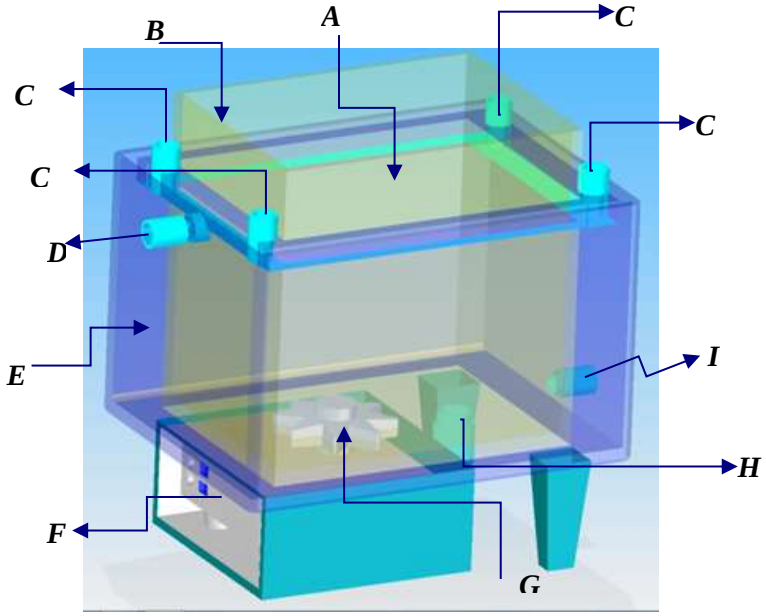

Figure 4.3 The Electrocoagulation Reactor

The thermostatically controlled temperature bath water connected cooling water jacket. Another component of the ECR was an assembly of three pairs of 90 mm x 95 mm and 3 mm stainless steel (318 SS) electrodes that were connected to direct current power supply through a monopolar parallel connection. The reactor was placed over a magnetic

stirrer and mixing was controlled at 125 rpm. The electrode assembly unit (Figure 4.4) was fully immersed into the EC bath unit (**A**) that was containing textile effluent. The EC bath unit (**A**) was separated from the cooling water jacket unit (***E***) by a 3 mm thick glass (**B**). The cooling water was pumped from the water bath circulator to the EC bath unit (**A**) through an inlet into the reactor (***I***). The cooling water exit stream is located at the top of the cooling water jacket unit (**D**).

The temperatures were measured in both the inlet (**D**) and the outlet cooling water streams (**C**), as well as inside the cooling water jacket by (**C)** by four temperature probes pots as shown in Figure 4.4. Below the electrodes assembly unit there is a mixer **(F)** and the magnetic stirrer bar **(G)** Samples of treated effluent were taken at the outlet **(H)**. The cooling water jacket unit, (***E*** in Figure 4.3) was made with clear Perspex material. The total volume of the cooling water jacket unit was 6.7L. There was a 10 mm PVC pipe that went passed the cooling water jacket unit to the inside of the reactor for treated effluent recovery and sampling. The electrode holding mechanism could be fixed onto the bottom of reactor or the electrodes were put individually in the electrode assembly holder as shown in Figure 4.4.

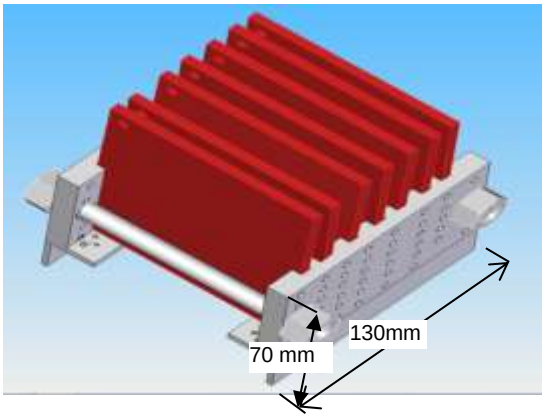

Figure 4.4 The Electrodes Assembly Unit

4.5 Electrocoagulation Preparation and Operation

4.5.1 Electrocoagulation Preparation

The pH, conductivity, TDS and turbidity sensors HI-4522 were calibrated according to the operating procedures. The new iron electrodes were dipped in a 1 M HCℓ for 24 hours to remove the polished surface. The stainless steel (SS-318) electrodes were dipped into a

1. M HCℓ solution for 10 minutes in between experimental runs to remove dirt on the electrode surfaces. The electrodes were rinsed with deionised water.

The EC reactor was put over the magnetic mixer and a 3.5 L of textile effluent to be treated was poured into the EC bath unit. The ECR was connected to the cooling bath water by a 12 mm tubing (Figure 4.4, Label **I**) and the return tubing to the cooling water jacket outlet (**D** in Figure 4.4). The cooling water bath temperature was thermostatically controlled at set temperatures as desired. The ECR was pre- warmed to 5^{o}C more than the desired temperatures because the electrodes would cool the effluent.

The mixer (**G**) was stirred at 125 rpm for all the experiments. EC bath (**A**) was allowed to reach the desired temperatures, while the ECR was temperature adjusted to the required temperatures by the cooling water jacket. The electrode cables were connected by lugs inserted into the electrodes by PVC bolts and nuts were tightened. The electrodes were assembled into an electrode assembly unit as shown in Figure 4.4 above.

The electrode assembly unit was lowered into the EC bath, ensuring that the electrodes assembly unit was fully immersed into the EC bath unit to avoid oxidation of the electrodes at the liquid-air interface. The electrodes were connected in a monopolar series (MP-S) connection. The freshly calibrated pH/EC/ORP probes of the HI-4522-pH/Ec multimeter were inserted into the ECR. The HI-4522-pH/Ec unit was connected to the computer station for data logging.

4.5.2 Electrocoagulation Procedure.

The HANNA HI 4522 multi-meter was used for data logging and the computer station was set to read out pH, TDS, electrical conductivity and resistivity data. Data logging was continued for one minute while recording the initial conditions of the experiment before the power supply was switched on. The EC reactor was started by setting the DC supplier (EA-PS-8016-20T; 16V–20 A) to the required current of 5 A and voltage outputs were displayed on the (EA-PS-8016-20T; 16V–20 A).

16 mL and 50 mL samples were taken at five minutes intervals of 1 hour. At the end of the 60 min, the electrodes assembly unit was taken out of the electrocoagulation reactor (ECR), washed with tap water and rinsed with deionized water. The 16 mL samples vials were centrifuged at 4500 rpm for 10 minutes. 2 mL of the samples from the sample bottles were eluted out into the COD vials for measurements. The COD analysis had first priority of analysis to avoid degradation of samples by other external factors. Otherwise,

COD samples would be preserved with concentrated sulphuric acid at pH 2 and stored at 4^{o}C if analysis were not done on the same day as recommended by Hach, (2007). In this study, the current was fixed and voltage was fluctuating, as was in the study of Moreno-Casillas *et al.* (2007). This power supply unit is programmable for data logging into a PC.

Electrocoagulation experiments were carried out at various temperatures such as 25°C, 30°C; 35°C; 40°C; 45°C; 50°C and 55°C at constant current densities of 0.0195 A/cm^2. Another set of EC experiments were done at various current densities from 3.9 x10^{-3} A/cm^2 at intervals of 9.75 x10^{-3} A/cm^2 to 7.8 x10^{-2} A/cm^2. The original effluents came out at 20:1 liquor ratio dyeing with pHs of about 9 to 11. However, iron reactions were preferred at low starting pHs; therefore pH adjustments were necessary to bring the original effluent pH down with 1M sulphuric acid to lower pH to between 3 and 4, just before the DC supplier was switched on. The final pH was controlled between 8 and 10 initial pH.

4.6 Chemical Analyses

For determinations of chemical reaction rates; triplicate experiments at various temperatures starting from 25^{o}C in increments of 5^{o}C until 55^{o}C were done. The most appropriate parameters measurements were:

- Total and ferrous iron by powered pillow reagents method; 8146
- Free and total chlorine measured by powder pillow reagents method; 10069 and 10070.
- Chloride measurements were done by Mercuric Thiocyanate Method 8113
- COD by method 8000, program number 430/435 (HACH, 2007)
- The ORP was measured by Ag/AgCℓ //Pt ORP sensor.
- Turbidity was measured with the HACH-2100P turbidity meter as per the HACH 2100P and HANNA HI 98703.
- The TSS tests were done with DR-2800, method 8006.
- Absorbencies were measured with DR-2800, at a maximum wavelength, λ_{max} of *560 nm.*

4.6.1 Free and Total Chlorine

Free and total chlorine was determined by colorimetric methods using N, N,-diethyl-p-phenylenediamine, (DPD) (Steininger, *et al*., 1996). With this reagent, free chlorine forms

a bright pink colour at a wavelength, λ_{max} of 530 nm (HACH, 2007). Free chlorine is a very strong oxidizing agent.

A 10 mL sample was put into the square sample cell. The N, N,-diethyl-p-phenylenediamine, (DPD) powder pillows were poured into the sample and it was shaken until it was totally dissolved and showed a bright pink colour. To the second square sample cell; 10 mL distilled water was added to prepare a blank sample. The blank was inserted into the uv-spectrophotometer. The Programme was selected and a light shield was put over the sample compartment free chlorine measurements. The zero button was pressed to set the programme to zero mode. The instrument recorded a "zero" from the blank sample. The blank was taken off and the real sample was put into the uv-spectrophotometer sample compartment for real sample measurement by pressing a start button. The procedure was the same for both the total and free chlorine except the DPD powder pillows and the Uv-spectrophotometer programme numbers.

4.6.2 Chemical Oxygen Demand Analyses Procedure.

COD was determined by dichromate colorimetric method (Hmani , et al., 2012). The HACH DR-200 heating block was used for COD digestion. 1 mL of distilled water was pipetted with 1 mL micro pipette into COD vials for both medium and high ranges. The vial was shaken for a few seconds to allow for reaction to take place. The vials were wiped out on the outside with dry towelling paper to remove any water droplets.

The 16 mL samples were centrifuged at 4500 rpm for 10 minutes. 1 mL of the sample was pipetted out by 1 mL micro pipette pump and added into the third COD vial. The vial with sample was also shaken for few seconds. A number of these samples were prepared so that they can fill up the HACH DR-200 heating block (24 vial compartments) and be done at the same time. All samples were put into the HACH DR-200 heating block for COD digestion at 150°C for 120 min. The measurements of CODs were done in the lower-medium range 300 mg/L to 1500 mg/L for high liquor ratio effluents (20:1). Medium-high range (500 mg/L to 5000 mg/L COD) vials were used for low liquor ratios (10:1).

At the end of the 120 minutes the DR-200 heating block automatically switched itself off and was allowed to cool off for 30 min before taking the digested vials out. The digested vials were taken out of the heating block and placed in the sample rack for further cooling. The COD was done with method 8000; programme number 430/435 with DR 2800 uv spectrophotometer. DR 2800 uv spectrophotometer was switched on and the

appropriate program 430 or 435, low or high range respectively was selected. The blank sample (with distilled water) was inserted into the sample compartment. The zeroing button was selected to zero the spectrophotometer. The real sample was put into the cell compartment and the uv-spectrophotometer recorded the COD value as mg/LO_2.

4.6.3 Total Iron Analyses

The total iron was measured with Hach DR 2800 uv-spectrophotometer, HACH programme 265, and powder pillows method 8008. The spectrophotometer was started to initiate self-calibration. Program 265 was selected from stored programs. The sample was poured into the 10 mL sample cell. The FerroVer® powder pillow reagents were added into the sample cell and swirled for mixing. The timer was switched on to 3 min reaction time. While the reaction was taking place, the blank was prepared by adding 10 mL of sample to the second sample bottle. The blank was put into the spectrophotometer sample cell compartment and was zeroed. The uv-spectrophotometer was set on 3 min timer, for 3 reaction time and when the 3 minutes expired, the real sample was put into the sample cell compartment, covered with the light shield, then the READ button was pressed and the measured values were displayed.

4.6.4 Ferrous Iron Analyses

The total iron was measured with Hach DR 2800 uv spectrophotometer, HACH programme 255, 1.10 Phenanthroline powder pillows, and method 1846. The spectrophotometer was switched on to initiate self-calibration. Program 255 was selected from stored programs and it was left on standby. A clean 50 mL graduated cylinder was filled with 25 mL of sample. 1.10 Phenanthroline powder pillow reagent was added into the measuring cylinder and the measuring cylinder was stopped and mixed by repeated. The timer as switched on to 5 min reaction time.

One sample cell was filled with raw sample for blank preparation. When the 5:00 minutes expired, the sample with reagent was poured into the second 10 mL sample cell. The sample cell with blank was put into the cell compartment and the light shield was closed. The zero button was pressed and the spectrophotometer read 0 mg/L. The second sample cell was put in the uv-spectrophotometer. The same procedure was followed by pressing the read button for the actual sample.

The ferric iron was determined by the difference between total and ferrous irons. Iron concentrations in the original effluents were not measured because iron was not

anticipated to be present in higher concentrations in tap water. However, it was discovered later that there was some residual iron in municipality water

4.6.5 Chloride Analyses

The chlorides were analyzed by Hach mercuric thiocyanate solution and ferric iron solution, method 8113. The samples were prepared by centrifuging them at 4500 rpm or filtering them with 0.45 μm membrane filter sheets to remove or lower turbidity and were neutralized to pH 7.6. The DR2800 uv-Spectrophotometer was switched on to initiate self-calibration. The samples were poured into a 10 mL square sample cell and 10mL deionized water was poured into another 10 mL square sample cell for blank preparation. Programme 70 was selected and 0.8 mL of mercuric thiocyanate solution was pipetted into both sample cells and swirled to mix. 0.4 mL of ferric solution was pipetted into both sample cells and swirled to mix with the sample. The timer was set on 02:00 reaction time. The samples cells were wiped on the outside; the blank was inserted into the sample cells compartment and the sample cell compartment was closed. The zero button on the screen was pressed. The screen displayed 0.0 mg/L. The same procedure was done for the real sample but the read button was pressed. Some sample would be over the range (>25 mg/L). If this was the case, the samples were diluted and done all over again.

4.6.6 Determination of Maximum Absorbance

Absorbance is a good measure of colour. DR2800 uv-spectrophotometer was used to determine the absorbance of the samples before and after EC treatments. Dyes absorbance maximum wavelength **($A_{\lambda max}$)** was determined by mixing dyes quantities as shown in Table 4.5 in 100 mL of dyes mixture.

Table 4.5 Dyes Mixture Quantities for Determination of the Maximum Wavelengths

Reactive Cotton Dyes	Amount (mg)
1% C.I. Reactive Red 239 (Remazol Brilliant Red 3BS (100%),)	3.3
3% C.I. Reactive Blue 181 (Levafix Brilliant Blue (E-FFN,(150%))	10
1.0% Cibacron Yellow C-R	5

The maximum absorbance wavelength (A□max) was determined from the mixture dyes after it was diluted 10 times (1 mL in 10 mL). The diluted samples were put into the 10 mL square sample cell and deionized water was put into the other. The absorbance (A), wavelength (λ) and % transmission modes are default programmes on the DR2800 uv-

spectrophotometer screen. The multiple wavelengths mode was selected (to record 4 wavelengths at a time), from 470 nm to 780 nm at interval of 10 nm. The deionized water (the blank) sample cell was put into the cell compartment and the cell compartment light shield was closed. The zero button on the screen was pressed for zeroing the spectrophotometer. The sample cell with the dye mixture was put into the cell compartment, the cell compartment light shield was closed, and absorbance readings were taken. The same procedure was followed until the whole range of the selected wavelengths was done. The data was plotted in excel spreadsheet to determine a maximum wavelength. The maximum wavelength was read at the maximum peak.

4.6.7 Determination of Absorbance Calibration Curve

The dye mixture sample was further diluted by pipetting 1 mL of dyes mixture into 20 mL; 40 mL; 60 mL; 80 mL and 100 mL. The prepared samples were used to do a calibration curve. The single wavelengths mode was selected and the maximum wavelength as determined above was entered. The 10 ml samples and blanks were poured into two 10 mL square sample cells and the sample cells were wiped. The deionized water (the blank) sample cell was put into the cell compartment and the cell compartment light shield was closed. The zero button on the screen was pressed for zeroing the spectrophotometer. The sample cell with the dye mixture was put into the cell compartment and the cell compartment light shield was closed. The start button on the screen was pressed and the spectrophotometer displayed the absorbance as required.

4.7. Methodology for determination of reaction kinetics parameters

The kinetic reaction constant (k_c) values were determined by the integral method. The reaction constants were determined by plotting the raw data in a concentration vs time axis. This was followed by visual inspection and curve fitting of the raw data on a scatter chart built in excel regression models such as exponential linear models. The excel program was able to predict the suitable curves that best described the data. The linear and exponential curve fittings for zeroth and first order respectively were observable by inspection. The curves mostly became flat towards end of the EC for most parameter and could fit the exponential model.

The integral method was used to linearize the data by plotting natural logarithmic function ratios of concentrations $ln\left(\frac{[C]_t}{[C]_0}\right)$ vs time for first order or inverse of concentration $\left(\frac{1}{[C]_t}\right)$ vs time for second order to determine reaction constants as the gradients of the

linearized equations that were automatically generated by the excel programmes. The integral method was chosen for determination of reaction constant (k_c) because data fitted this method compared to the second order model for most parameter.

However, the gradients on the excel program automatically generated linearized equations could not be used as they were because they showed only one significant figure and in most cases showed the reaction constants for most temperatures such as 25°C; 30°C and 50°C as having the same gradient of 4 x10^{-4} for chlorides. The gradients were manually determined from the chart gridlines and better results were obtained. Consequently the mass transfer coefficients (k_m) were determined by the previously (in equation Section 3.7.1) stated relationship between k_m and k_c.

$$k_c = k_m \frac{A_e}{V_e}$$

Where A_e is the surface area of the electrodes equal to 513 cm^2 and V_e is the volume of the electrodes is equal to 153.9 cm^3.Their ratio of the electrode surface area (specific surface, A_s) A_e/V_e was A_s = 3.33 cm^{-1} therefore the direct gradient was k_c and the mass transfer coefficient k_m was k_c divided by 3.33 cm^{-1}

Chapter 5 : RESULTS AND DISCUSSION

5.1 Discussion of Results of Textile Effluent Characterization Experiments

Industrial textile effluents vary from dyeing batch to dyeing batch and from dyehouse to dyehouse, therefore, to do reaction kinetics studies with real industrial textile effluents could be affected by variability. However, The textile industry does textile fabrics or yanks pilot dyeing process (procedures) to create new dyeing procedures (dyeing recipes) in the textile dyeing laboratory before the bulk dyeing process in the main dyehouse known as "sample dyeing". "Sample dyeing[12]" is performed by small pieces of fabrics or hanks between 100 g and 10 kg in "commercial sample dyeing machines". The commercial dyeing machines are small dyeing machines ranging from 200 mL[13] machine to 100 L[14] (10 kg capacity). Nevertheless, 200 mL and 500 mL sample dyeing machines were used in this study. Many sample-dyeing batches were done because only one dyeing batch could produce effluents for three to four EC experiments.

Therefore, to maintain effluent quality and consistency for the reaction kinetics experiments, "commercial sample dyeing" techniques were used to create textile effluents for use in EC experiments; the bulk textile dyeing process was closely simulated by creation of textile effluent using commercial sample dyeing machines. The first part of the discussion of results is about how the textile effluent characterization using a sample dyeing technique compares to bulk dyeing dyehouse textile effluents as found in literature, thereby, providing some background information about how sample-dyeing machines can be used for textile effluents generation for use in textile effluent research.

5.1.1 TDS pH and conductivity of Textile Effluents for 10:1 and 20:1 Liquor Ratios.

It was observed that even though sample-dyeing techniques were carefully followed to avoid effluent variability between sample dyeing effluents, textile dyeing proved to be a delicate and sensitive process, as revealed by the variability of data some pollutant parameters as shown in Figure 5.1. The data in Figure 5.1 **is** arranged in such a way that it is easy to observe similarities and differences between the presented parameters in 10:1 and 20:1 liquor ratios. A slight change in the pH, conductivity and temperature and dye liquor

[12] Sample dyeing is dyeing of a small fabric piece/s in the textile laboratory to test if the required shade will be achieved in the main dyehouse.
[13] CPUT textile institute, these capacity machines were used in this study.
[14] Thies dyeing machines at Lansdowne textile Industries, The Company I worked for the period 1998 to 2001.

circulation (mixing of fabrics and dye liquor) could affect the dyeing processes. Figure 5.1 is a chart of the average values of triple pre-bleaching, dyeing and finishing experiments at 10:1 and 20:1 liquor ratios. The average values were calculated from the actual values in Appendices A1 and A2. For detailed data, refer to Appendices A1 for 10:1 and Appendix A2 for 20:1 triplicate pre-bleaching and dyeing experiments. In these appendices, the average and standard deviation values are also presented.

As shown in Figure 5.1 pH trends of 10:1 and 20:1 fabric to liquor ratios are relatively the same, except for hot and acetic acid rinsing steps which are lower for 10:1 fabric to liquor ratios. This may be because dyes and chemicals were adsorbed into the fabrics better for 10:1 than in 20:1. The pH trends are ranging between 10 and 12 during the cold and hot rinsing steps. In fact, the hot rinsing step raises the pH to almost the original pH. This is because; the purpose of hot rinsing is to desorb the residual hydrolysed dye (Hussain, 2012) (for the dyeing liquors) and chemicals (for the pre-bleaching liquors) from the fabric, which includes the caustic soda hence higher pH. The acetic acid rinsing steps lower the pH to about 4 for both the pre-bleaching and dyeing liquors.

The acid rinses after dyeing has a significant effect on final effluents because the pH was low between 4 for 10:1 and 6 for 20:1 liquor to material ratios until the softener additions. Softener additions raises pH because they are made of aliphatic monoamines that are very soluble in water and could raise the pH to about 9 (Wamser, 2000) and perform better at low pH between 4 and 5 with acetic acid (Parvinzadeh & Najafi, 2008). Hence, some dyers add softener with acid rinsing steps. Obviously, pre-bleaching and dyeing pH depend on the dyeing procedure (pre-bleaching pH 12 and dyeing pH 11) and the neutralization steps. Acetic acid was used for neutralization of the fabric after pre-bleaching and to prevent metallic deposits into sticking into the fabric. Acetic acid additions contributed to neutralization or lowering of pH of mixed effluents. Consequently, the final effluent for 10:1 and 20:1 fabric to liquor ratio of pH, 7.6 and 9.8 respectively was within CCT effluent discharge limit of between pH 5.5 -12 (City of Cape Town, 2006).

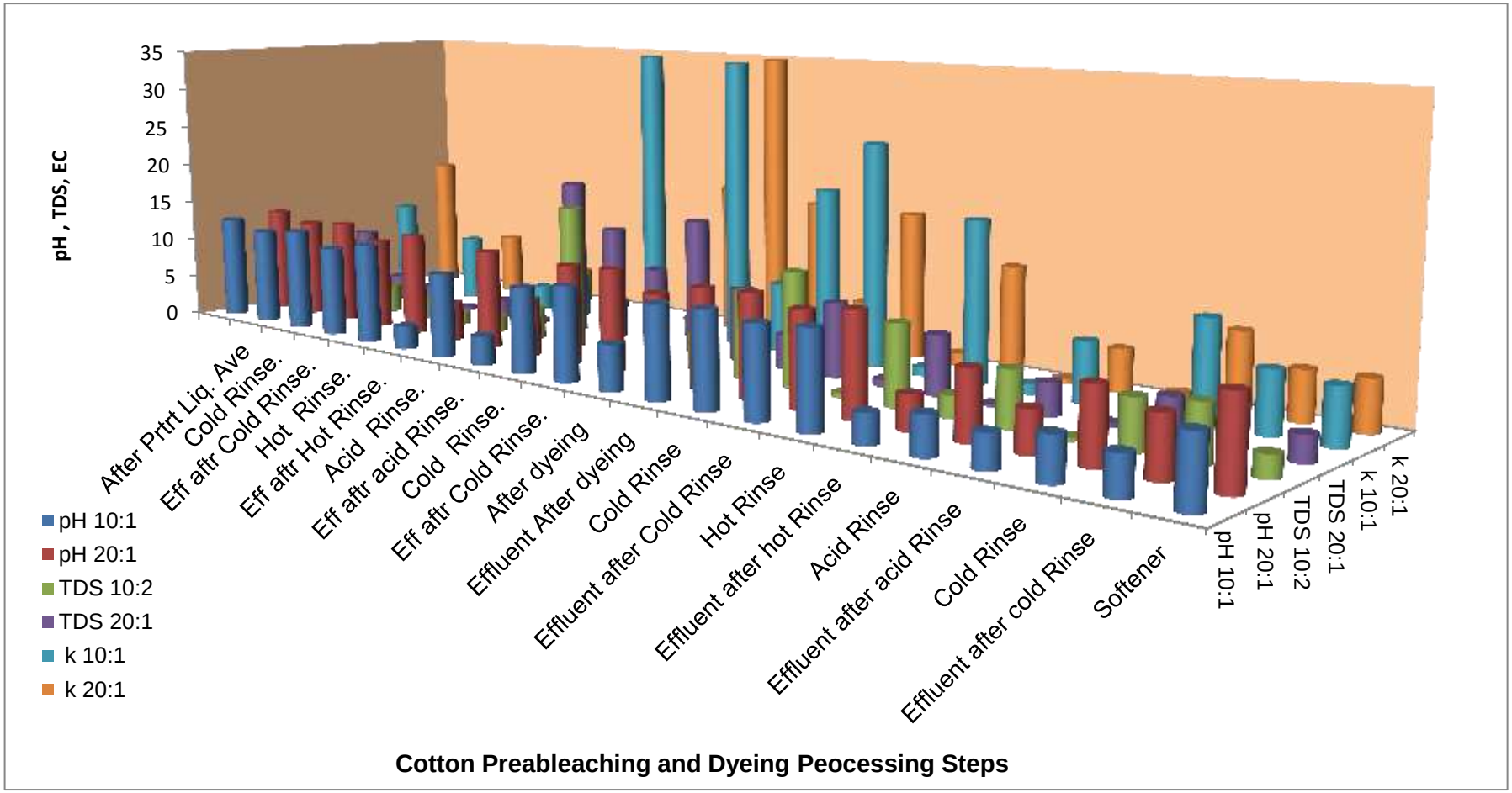

Figure 5.1 Trends for TDS, Conductivity and pH at 20:1 and 10:1

5.1.2 Turbidity and TSS of Textile Effluents for 10:1 and 20:1 Liquor Ratios.

Figure 5.2, shows that the highest TSS and turbidity that are found in textile effluents are generated during the pre-bleaching steps. Up to 320 mg/L TSS of water pollution by textile processing could have been caused by dirt that was on the fabric materials (such as fluff, loose cotton pieces; short fibres; waxes, oils, sizing agents etc.) that are added during cotton milling, weaving and knitting. However, only few studies have been devoted to the characterization of pre-bleaching effluents. The pre-bleaching effluents in this are comparable to the one studied by Saving and Bunter (2008) with TSS of 288.5 mg/L. The softener addition step contributed about 150 mg/L TSS and turbidity of 100 NTU, which is the composition of the final effluent.

It is worth observing and discussing the implications of the TSS and turbidity on electrochemical parameters such as resistivity and conductivity because they seem to have an opposite effect to TSS and turbidity. Resistivity (ρ) is the characteristic solution resistance ($\mathcal{R}$) property that is inversely proportional to the electrical conductivity (κ) of the solution. Solution resistance ($\mathcal{R}$) is an equivalent of metal conductor resistance that yield ohmic resistance in current flow. As shown in Figure 5.2, while the original pre-bleaching bath effluents have high TSS and Turbidity, their resistivities were low. However, the conductivities and TDS were high which imply that the pre-bleaching pollutants were ionic and could have contributed positively to EC process.

The high conductivity in pre-bleaching liquors could be mostly contributed by caustic soda or soda as that is added during pre-bleaching. Hot rinsing pre-bleached fabric produced the highest resistivities of 3602 Ω.m and 2542 Ω.m with lowest conductivity of 0.2 mS/cm and 0.7 mS/cm for 10:1 and 20:1 liquor ratios, respectively. This means that the hot rinsing step was removing mostly non-ionic species from the fabric such as plasticizers, wetting agents, starch, waxes; short cotton fibres that were still remaining in the fabric. Effluent after dyeing had high electrical conductivity of about 35 mS/cm for both liquor ratios with low TSS, turbidity and resistivity. The high conductivity was due to sodium chloride additions during dyeing process. Hot and acid rinses had low conductivity, elevated resistivity but low turbidity and TSS.

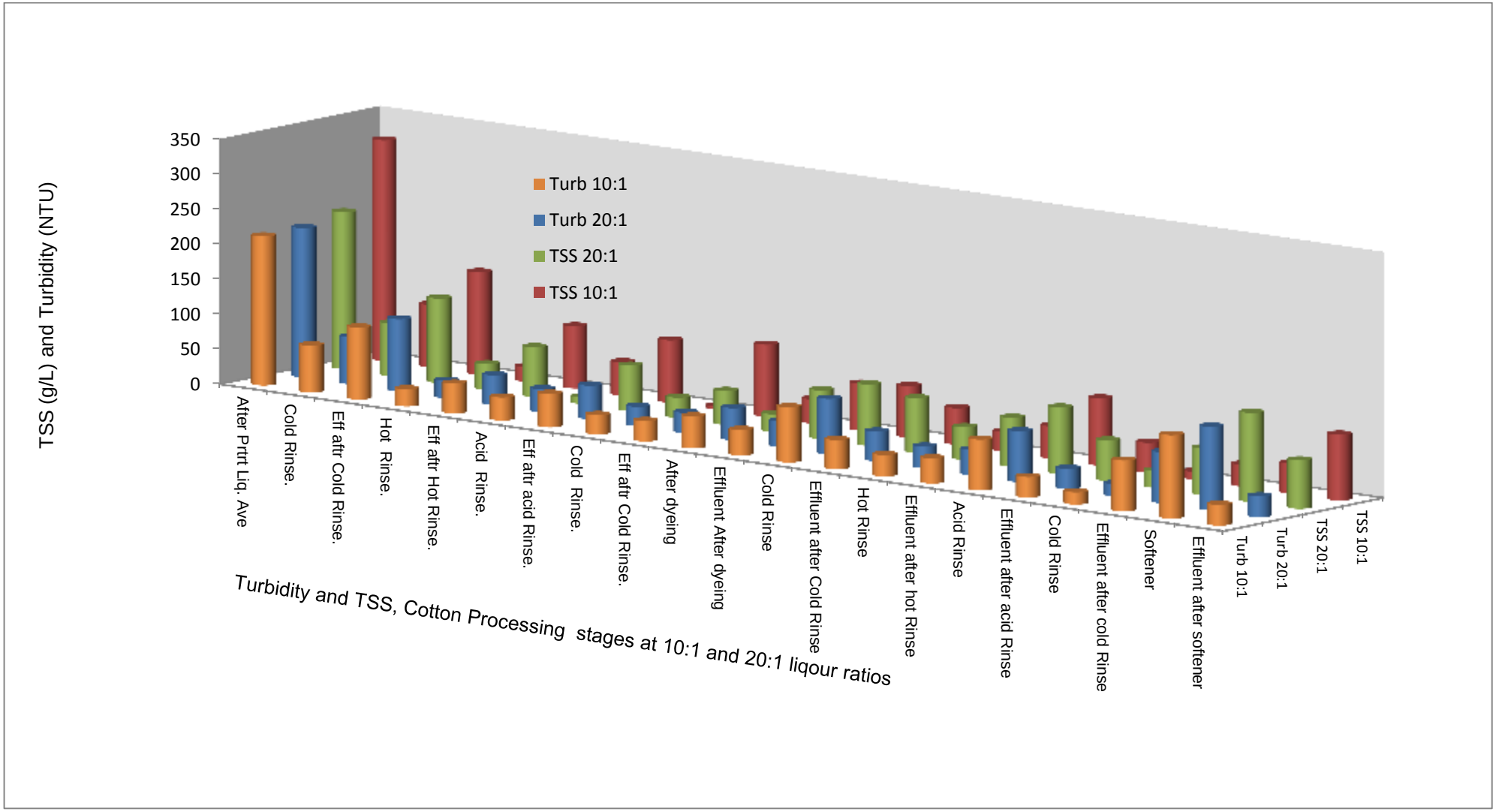

Figure 5.2 Cotton Processing Stages Turbidity and TSS at 10:1 and 20:1 liquor ratios

The textile effluents important parameters have been shown in Table 5.1. The final effluents had low resistivity of about 204.5 Ω.m and 365.7 Ω.m for 10:1 and 20:1 liquor ratios respectively and low conductivities of about 6 mS/cm for both liquor ratios compared to raw pre-bleaching and dyeing bath effluents because of various dilutions by several cold rinses. The conductivity and resistivity of the textile effluents are very significant for determination of the ohmic overpotential both for the operational and design parameters of the electrocoagulators. According to equation 2.4, high electrical conductivity (κ) reduces ohmic overpotential (E_{ohmic}), therefore low voltages losses during electrocoagulation.

$$E_{ohmic} = I\frac{d_e}{A_e \cdot \kappa}$$

High electrical conductivity gives low ohmic potential or low solution resistance; low or no passivation of electrodes and high mobility of ions such as Fe^{+} and Fe^{3+} that are responsible for electrochemical reactions and coagulation of pollutants. Electrodes after EC showed no passivation of electrodes except for EC experiments at high temperatures. Passivation of electrodes could negatively affect EC and reaction rates as the charges and ionic species transfer are impeded by the passivation layer on the electrodes surface (Chaturvedi, 2013).

The resulting final effluents have low electrical conductivities of about 6 mS/cm compared to raw pre-bleaching liquor 12 mS/cm and 16 mS/cm and after dyeing raw liquor of 35 mS/cm for 10:1 and 20:1 fabric mass to liquor ratios respectively. Perhaps, this was an indication that EC treatment of raw pre-bleaching, dying and fabric rinsing liquors separately could yield even better results.

The data of various pollutants in the 10:1 and 20:1 liquor ratio dyeing effluent is presented in Table 5.1, for easy observations of similarities and differences between the two dye liquor to fabric ratios. A fabric mass to dye liquor ratios or simply referred to as “liquor ratio” is a textile industry terminology that refers to the amount (g or kg) of textile material (fabric, yarn, hanks, or garment) to the volume of water (liquor) to be used in the dyeing process. The pre-bleaching steps produce effluents with highest TSS of 314.5 mg/L and turbidity of 223.7 NTU and these are major contributors to the COD. However, the CODs were not measured for pre-bleaching effluents because this was not anticipated. The final TSS for 10:1 and 20:1 liquor ratios are about 110 mg/L and 70 mg/L respectively (Figure 5.2). The TSS of about 150 mg/L is between the values of study of combined textile effluent study by Arslan-Alaton *et al.* (2007), 220 mg/L TSS and 70 mg/L (Azzi, *et al*., 2006).

Table 5.1 Pre-preaching and Dyeing Processing Steps Average Values of Parameters.

Pre-bleaching and Dyeing Processing Steps	pH		Conductivity (mS/cm^2)		Total Dissolved Solids		Resistivity (ρ)		Turbidity		Total Suspended Solids		Absorbance	
	pH 10:1	pH 20:1	κ 10:1	κ 20:1	TDS (g/L) 10:2	TDS (g/L) 20:1	$\rho(\Omega)$ 10:1	$\rho(\Omega)$ 20:1	Turb 10:1	Turb 20:1	TSS 10:1	TSS 20:1	$A_{\lambda 660nm}$ 10:1	$A_{\lambda 660nm.}$ 20:1
After Pre-bleach Liq. Ave	12.700	13.017	11.5	16.9	5.840	8.530	***95.1***	59.0	314.5	212.9	314.5	223.7		
Cold Rinse.	11.827	12.137	1.1	2.1	2.686	3.044	813.0	492.0	89.7	67.0	89.7	75.0		
Eff after Cold Rinse.	12.436	12.662	8.2	7.5	3.435	2.428	234.0	134.3	146.0	102.6	146.0	120.3		
Hot Rinse.	10.938	11.086	0.2	0.7	2.765	0.392	3602.0	2542.0	20.7	24.5	20.7	36.7		
Eff after Hot Rinse.	12.057	12.463	3.0	4.3	1.516	2.157	231.7	243.3	88.6	42.5	88.6	70.7		
Acid Rinse.	2.864	4.719	5.5	0.9	1.910	0.508	1977.3	2740.0	47.4	32.7	47.4	9.0		
Eff after acid Rinse.	10.123	11.857	2.7	32.2	3.905	18.850	414.7	291.3	88.6	47.7	88.6	64.3		
Cold Rinse.	3.498	6.827	34.9	0.2	17.101	13.669	152.7	3693.3	4.6	27.5	4.6	28.7		
Eff after Cold Rinse.	10.115	11.727	2.4	18.2	1.228	9.375	484.0	265.4	102.3	29.0	102.3	48.0		
After dyeing	11.087	12.078	34.6	34.8	2.764	16.035	254.9	136.9	34.3	45.5	34.3	25.0	2.468	2.444
Effluent After dyeing	5.445	10.067	8.3	17.3	4.261	8.606	229.5	72.3	66.5	36.3	66.5	69.0	1.545	1.160
Cold Rinse	10.823	11.609	20.2	5.9	10.151	4.070	131.6	76.1	73.2	78.6	73.2	87.3	1.943	0.880
Effluent after Cold Rinse	11.109	11.883	26.3	17.3	13.183	8.669	149.3	58.3	51.7	42.0	51.7	77.7	4.175	0.984
Hot Rinse	10.547	10.912	1.0	1.5	0.602	0.863	203.8	712.0	27.6	30.5	27.6	46.3	0.883	0.284
Effluent after hot Rinse	11.028	11.787	18.7	12.6	9.272	6.920	55.6	85.4	45.8	35.8	45.8	69.7	1.860	0.750
Acid Rinse	3.404	3.983	1.2	0.6	2.562	0.282	549.3	1259.0	95.4	72.4	95.4	94.3	0.671	0.414
Effluent after acid Rinse	4.416	7.744	7.0	4.9	6.354	3.750	307.5	1887.9	42.4	29.0	42.4	57.3	1.208	0.671
Cold Rinse	3.822	4.732	0.3	1.2	0.455	0.567	352.0	2901.0	11.1	17.5	11.1	24.0	0.116	0.224
Effluent after cold Rinse	4.881	8.254	11.4	8.9	5.711	4.425	94.8	125.4	31.3	72.6	31.3	66.3	1.207	0.302
Softener	4.333	6.622	7.0	5.7	6.354	4.180	307.5	2809.0	42.4	118.8	42.4	126.7	1.208	0.248
Effluent after softener	7.557	9.818	6.4	5.9	2.490	2.933	204.5	365.7	93.7	29.6	93.7	69.0	1.414	0.805

5.1.4 Chemical Oxygen Demand (COD) of the Textile Effluent History

Table 5.2 represents the characteristics of the textile effluent. The CODs were only recorded for the final effluent or effluent after fabric softener addition. The average values of CODs were 3501 mg/L, which is close to the COD of 3784 mg/L for 10:1 and 1720 mg/L 20:1 liquor ratios that were reported for the textile effluents in the studies of Ali, *et al.,* (2009); Arslan, (2001); Reddy *et al.* (2006) and Savin and Butnaru, (2008) (COD of 1907.3 mg/L).

As discussed above in Section 5.1.1 and according to Savin and Butnaru (2008); the pre-bleaching step raises the COD of textile effluents to the equivalent of the COD of the final effluents due to large amount of materials that were removed from the fabric during pre-bleaching such as NaOH; H_2O_2; acids; surfactants; $NaSiO_3$; sodium phosphate and short cotton fibres.

As shown in Table 5.2, the textile effluent would have passed the City of Cape Town effluent discharge standard by-law. The effluent compositions were very close to other textile effluent compositions found in literature (as were previously presented in Table 2.4 and as re-quoted in Table 5.2 fourth and fifth rows) and from the local textile factories.

Table 5.2 Final Textile Effluent Composition

FINAL EFFLUENTS	pH	Cond (mS/cm)	TDS (mg/L)	Resistivity (Ω.m)	Turbidity, NTU	TSS (mg/L)	Absorbance	COD (mg/LO_2)
20:1, Averages	**9.818**	**5.895**	**2.933**	**365.6**	**29.6**	**69.0**	**0.805**	**1720**
10:1, Averages	**7.557**	**6.382**	**2.490**	**204.5**	**74.6**	**112.5**	**1.414**	**2509**
CCT EDL By-Law	5.5 -12	500	4.000			1000		5000
Roy, *et al*., (2010),	*9.8*	4.82	3.392					
Ali, *et al*., (2009)	*9.4*	3.57	2.512			5497		1652
Local dyers 1 Navy Blue --/08/2009	*10.982*	23.37	11.63		34	56		1873
Local dyers 1 Fusia --/08/2010	*10.158*	40.47	20.23		54.6	72	1.251	1096
Local dyers 2 Samples 23/08/2010	*10.44*	40.7			771	1015		1882
Local dyer 2 Samples 02/03/2012	*10.588*	17.49	8.741		17.2	20		1219
Local dyers 2 Samples -/03/2013	*11.75*	14.58	7.336		57.4	110		1698

5.2 The Electrocoagulation Process Results

In this research, a batch EC reactor was used to perform EC experiments that were used to study the reaction kinetics of iron EC for removal of COD, chlorides ($C\ell$), absorbance and total chlorines (t-$C\ell_2$). The reaction constants (k_c) and mass transfer coefficient (k_m) were

determined by assuming that reaction rates and reaction mechanisms follow elementary reaction rate kinetic methods. Other assumptions about the reaction kinetics studies in the electrochemical coagulation were explained in section stated in section 3.1.

The parameters that were measured were COD, total (t-Cl_2) and free (f-Cl_2) chlorines, ferrous (Fe^{2+}) and total (t-Fe) iron, hazen colour, TSS, turbidity, TDS, conductivity, resistivity, pH, ORP, absorbance and chlorides. Triplicate EC experiments were performed at 25°C, 30°C, 35C, 40°C, 45°C, 50°C and 55°C. The reaction kinetics experiments were done at a liquor ratio of 20:1 because even though 10:1 liquor ratio dyeing is practice in textile industry. The resulting textile effluent would be diluted by various sources of dilutions such as other water utilities, machine rinsing, flow washing, reprocessing of reject etc.

The original effluents were pinkish to dark blue with maximum wavelength (λ_{max}) of 560 nm and molar absorptivity of 3.92 x 10^4 M/cm. A white frothy layer was observed on the top of the fluid within a few seconds from the start of electrocoagulation. The froth had pinkish particles on its surface; this means that some dye particles were adsorbed onto the bubbles and floated to the surface of the fluid by electrolysis gases. After 15 min the bulk effluent appeared dark green (green floccs) when viewed through the sides of the glass of the chambers of the EC reactor as shown in Figure 5.3. This demonstrates the formation of green rust or ferrous hydroxide ($Fe(OH)_{2(s)}$). Some green floccs from the bulk of fluid seemed to be constantly being attached to the bottom of the white froth layer. This means that besides floccs being floated by electrolyses gases, some floccs were floated by buoyancy because their densities were less than the density of the bulk fluid. This was possible at low temperatures such as 25°C to 30°C.

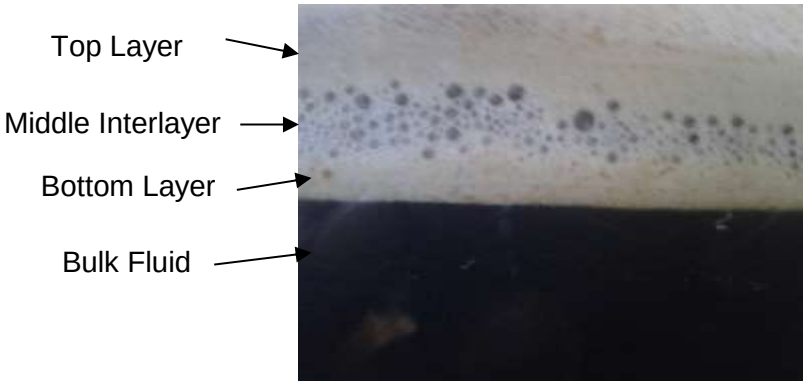

Figure 5.3 Top section of the Electrocoagulation Reactor

The white froth layer on top became orange-brown. This indicates oxidation of ferrous hydroxide ($Fe(OH)_{2(aq)}$ and other forms of ferrous polymeric hydroxyl complexes to $Fe_3O_{2(s)}$ in

the oxygen rich surface. The dark green floccs became larger and dark grey in the bulk of the fluid. The white froth layer, on the air interface became reddish brown indicating formation ferrous oxidation products such as $Fe_2O_{3(s)}$; hence, the top layer of the froth also became thick. The bottom and top layers of the froth phase were separated by a middle layer of bigger bubbles.

5.2.2 Current Efficiencies for COD and Chlorides During Electrocoagulation.

The electrocoagulation reactor (ECR) was operated at an applied constant current of 5.0 A, or applied current density (i_{App}) of 9.75 mA/cm^2 to processes 3.5 L of textile effluents. However, due to mass transfer driven reactions, the applied current densities would reach limiting current densities (i_L). Mass transfer controlled reactions are characterized by low current efficiencies (C.E.) (Hmani , et al., 2012). Therefore, determinations of current efficiencies are very important in electrocoagulations to establish if the reactions are mass transfer controlled or not. The current efficiencies with respect to COD were determined by the equation below. However, the COD was first converted into units of COD molar concentrations units as follow:

$$1900\frac{mg}{L}\times\frac{1.0g}{1000\,mg}\times\frac{1.0\,molO_2}{32.0g}=0.0595\frac{mol}{L}O_2$$

The current efficiency could be determined by the following equation (Hmani , *et al*., 2012 and Cho, *et al*., 2014)

$$\%CE=100\%\times\frac{z\mathcal{F}\left(C_i^o-C_i^t\right)V}{\int_0^t Idt}$$

I = applied current (A) = 5.0 A; $\mathcal{F}$ = Faradays constant (96486 C/mol); t = is the EC time; V = the volume of the reactor (3.5 L)

z = is the number charges transferred 8 for COD and 2 for chlorides

$\left(C_i^o-C_i^t\right)$ = molar concentration difference of species i; for original condition (o) and at any time (t), expressed as mol/L O_2 and

$$\%\,EC_{COD}=96487\frac{C}{mol}\times 3.5L\frac{[0.0595]_o-[0.0466]_t}{8\times 5.0\frac{C}{s}\times 300s}\times 100\%=71\%$$

Current efficiencies (CE) at other temperatures were determined the same way, and data was presented in Figure 5.4 (a) and (b) for chlorides and COD respectively. For comparison purposes, the COD removal influences on applied current are represented with chlorides in

Figure 5.4 (a) and (b) because it is known that chlorides are amongst the powerful oxidizing agents that can oxidize organic materials (dye molecules in this study) (Panizza & Giacomo , 2010).

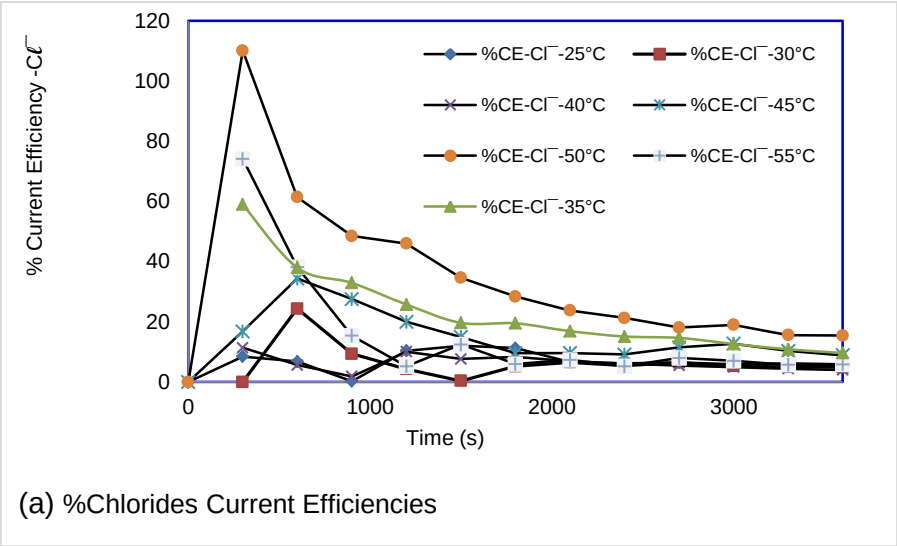

(a) %Chlorides Current Efficiencies

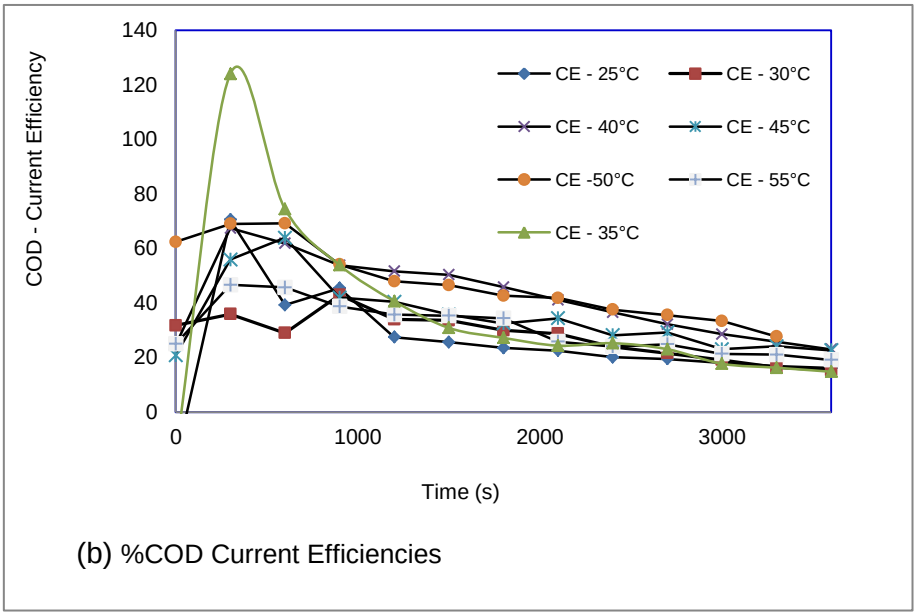

(b) %COD Current Efficiencies

Figure 5.4 (a) Percentage EC-Cℓ⁻ and (b) Percentage EC-COD at various temperatures

Therefore, current efficiency is a quantitative indication of chlorides electrochemical oxidation reactions. The current efficiencies for chloride removal are about 5% to 10% removal towards end of electrocoagulation. COD was found to be comparably higher than chlorides CE, with COD current efficiencies of about 20% to 30% towards the end of the EC and between 40% and 75% for the first 1000 s (16.67 min.). This is an indication that the COD

removal uses a lot of current than Faraday is theoretically possible but still higher than chlorides current efficiencies.

Electrochemical oxidation is production of O_2; OH^- and H^+ through water splitting and hydrolysis reactions; some of these products might have been used up in other side reactions that were not directly contributing to reduction of COD, therefore resulting in low COD removal and low CEs. Experiment at 40°C is amongst the experiments that achieved high percentage COD removal. As it seems, its current efficiency trends are not significantly different from the other current efficiencies trends, except only between 1000 s (16.67 min) and 2000s (33.33 min), where the current efficiency curve is slightly above all others. Therefore, the better removal efficiencies for COD in experiments at 40°C were not driven by better charge transfer reactions.

Only experiments at 35°C showing better current efficiency of up 120% as being the highest removal efficient. Perhaps, this was caused better charge transfer reactions at a low pH of about 6 for from the beginning of the experiment to the 300th s. with a quick COD removal in the first 1200 s. (as shown in Figure 5.5). Similar high electrocoagulation COD trends were observed in Panizza, *et al*., (2010) but with different effluents and electrodes.

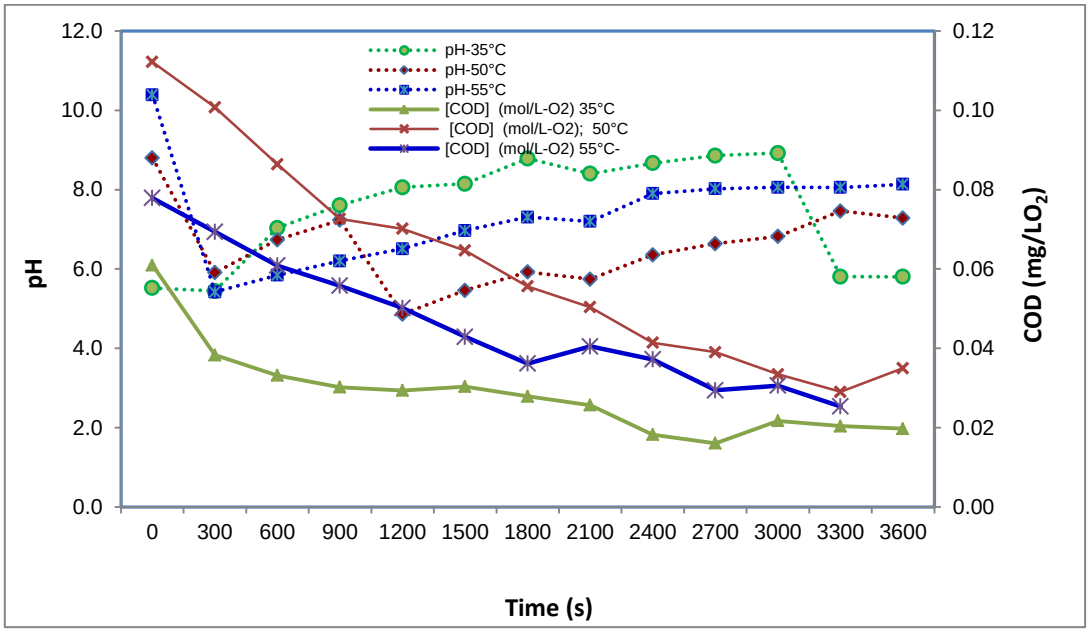

Figure 5.5 Effect of initial pH on COD Removal for 35°C, 50°C; and 55°C

The acetic that was used during pre-bleaching and dyeing and it might have chelated ferrous and other metals in the EC bath, resulting in slow electrochemical reactions and no rise in

pH. H_2SO_4, was used for pH adjustments just before EC as it does not have chelating effects. The major contributor to current losses during the EC was found to be chlorides.

5.2.3 pH adjustment, Turbidity and TSS During Electrocoagulation

The pH trends are shown in Figure 5.6 were recorded during EC for experiments at 45°C. Electrocoagulation (EC) experiments were performed at a constant current density of 9.75 mA/cm^{-2} at low initial (pH_i) of between 3 and 4 and equivalent hydrogen potential, (E_h) 0.031V. The EC pH would increase if it was not controlled as shown by gradually rising pH trends between the 500^{th} sec. and 1800^{th} sec. as shown in Figure 5.6. The rise of pH might have been caused by the generation of the hydrogen ion (H^+) during the water electrolysis splitting and consumption of (OH^-) during the formation of ferrous and ferric hydroxide complexes as was previously discussed in section 3.2. through section 3.3. by the following chemical reactions (R3.1 to R3.4).

$$Fe^{2+}_{(aq)} + 2OH^-_{(aq)} \Rightarrow Fe(OH)_{2(s)} \qquad \text{near the anode}$$

In an oxygen, rich environment the hydrogen ion (H^+) is produced as in the following reaction. (Acidic medium, pH < 4,) as the initial pH were between 3 and 4 (Sengil & Ozacar, 2008)):

$$4\,Fe^{2+}_{(aq)} + 10\,H_2O_{(\ell)} + O_{2(g)} \rightleftharpoons 4\,Fe(OH)_{3(s)} + 8H^+_{(aq)} \qquad \text{near the anode}$$

Possibly via hydrolysis as $Fe^{2+}_{(aq)} + 10\ H_2O_{(\ell)}$ forming various hydrolysis products in less oxygen environment. The oxygen is the dissolved oxygen in the effluent. However, the reaction is an equilibrium reaction, when at higher pH the reaction could shift towards formation of ($Fe^{2+}_{(aq)} + 10\ H_2O_{(\ell)}$)

Or

At the anode, the hydroxyl ions (OH^-) are consumes in production of oxygen

$$4OH^- \rightleftharpoons 2H_2O + O_{2(g)} + 4e^-$$

Even the water splitting reactions that provide abundant hydroxyl ions could not be producing enough hydroxyl ions.

$$2H_2O_{(\ell)} + 2e^-_{(aq)} \rightleftharpoons 2OH^-_{(aq)} + 2H_{2(g)} \qquad \text{(cathode)} \quad -0.83\ V \text{ vs NHE}$$

At the anode (Raju, *et al*., 2008):

$2H_2O_{(\ell)} \Rightarrow O_{2(g)} + 4H^+_{(aq)} + 4e^-_{(aq)}$ $E^\circ (O_2/H_2O) = +1.23$ V vs NHE

$H^+_{(aq)} + 2e^-_{(aq)} \rightleftharpoons H_{2(g)}$ (cathode acidic medium) 0.00V (H^+/H_2) vs NHE

However, output voltage versus equivalent hydrogen (E_h) potential (Ag/AgCℓ, reference electrode) was 3.14 V, which was high enough to support pH observable trends in Figure 5.6.

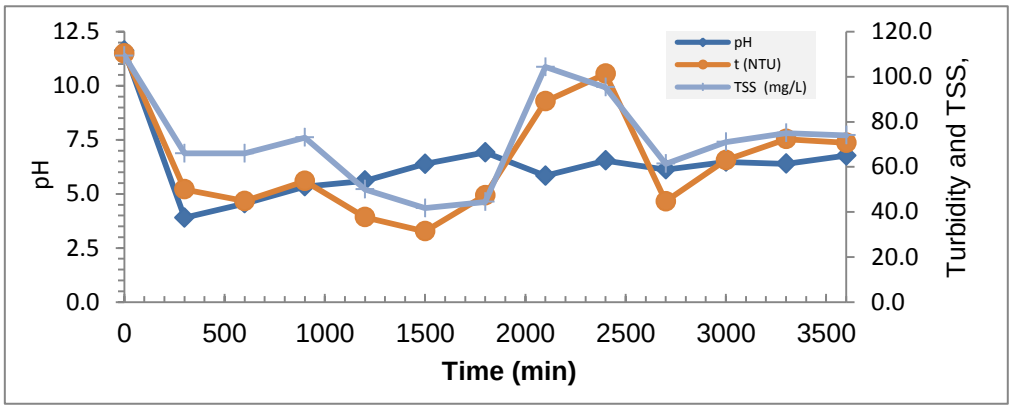

Figure 5.6 TSS, Turbidity and pH Trends During Iron Electrocoagulation @ 45°C

It is known in basic chemistry that hydrogen ion $[H^+]$ and $[OH^-]$ concentrations are related to pH and pOH to the water ionization constant, K_w. The following is a proof of why the pH is increasing during electrocoagulation.

$pK_w = pH + pOH$ and $pH = 14 - pOH$

where: $pK_w = -\log K_w = 14$ (K_w , the water auto-ionization constant) ; $pOH = -\log [OH^-]$ ($[OH^-]$ is molar concentration of the OH^-) and $pH = -\log [H^+]$, ($[H^+]$ is molar concentration of the OH^-). Low initial pH's were preferred because maximum ferrous iron is produced at low pH and effective chemical coagulation starts pH 6.5. pH 6.5 and 8.0 are favourable for ferrous precipitation reactions and formation of green rust (Lakshmana, *et al*., 2009). This is supported by the fact that the TSS and turbidity of the treated effluents reached their lowest level values of 46 mg/L TSS and 32 NTU respectively,

Upon adjusting pH to below 8 at about 1800 s. the TSS and turbidity rise as shown by peaks almost to the original effluent values and then dropped to minimum values. The turbidity followed similar trends as the TSS trends while the pH was stabilized at pH of approximately 6.5. Therefore, turbidity and TSS concentrations were at their lowest values of about 32 NTU

and 46 mg/L TSS at about 1500 seconds (25 min) respectively. This was followed by a rise to almost the original concentrations. This rise of TSS and Turbidity was systematic and consistent, experimental disturbances such as disturbances of floccs (such as break down of already formed floccs) were not likely to be the cause of the peaks because the curves were plotted from averages of triplicate data of values. An increase in TSS and turbidity might have been caused by dissolution of already formed floccs and excessive coagulant loading as the EC process was prolonged without removal of the formed floccs or sludge (Chaturvedi, 2013). The floccs were not removed because the experiments were done in batch mode. It should also be noted that green could have dissolved at pHs outside 6.5 to 8.0 range.

5.2.3 Further Discussion on Turbidity Removal Efficiencies

Figure 5.7 represents data for experiments at 35°C; 25°C; and 30°C with increasing removal turbidity of up to 85% at 2400th sec. (40 min); 88% at 2820th sec (47 min.) at 35°C and 60% at 25°C respectively. These were maximum turbidity removal efficiencies, after which the trends were effectively constant or decreasing towards the end of the electrocoagulation. It can be noted from Figure 5.7 that good turbidity percentage removal efficiencies were only achieved between 1000s and 1500s. During this period, the pH was kept between 5.5 and 7.5.

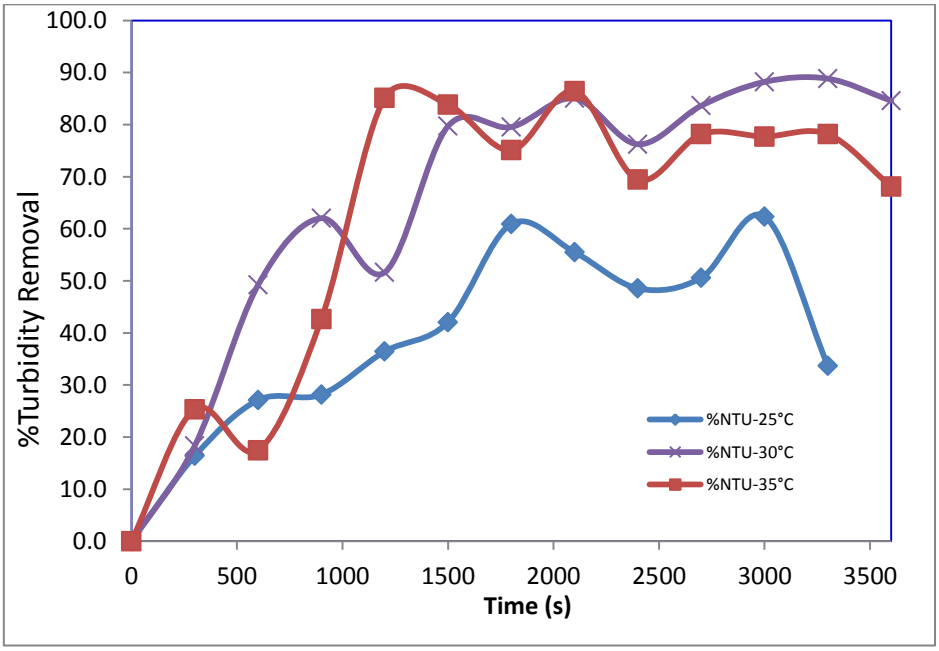

Figure 5.7 %Turbidity Removal at 25° C; 30° C and 35° C

These good removal efficiencies could be linked to the pH. The pH affects the surface charge of the colloids by neutralizing or destabilizing the charges of the colloids (Pernitsky, 2003). The coagulants are responsible for enmeshments of the charged colloids. The pH between 5.5 and 7.5 is the pH, where most ferric and ferrous hydroxo complexes are positively charged and therefore maximum forces of attractions between the negatively charged colloids and positively charged coagulants (Pernitsky, 2003).

After the period between 1000s and 1500s, the percentage removal efficiency remained either constant or decreased. The decreasing trends were more for experiments at 25°C and low turbidity removal percentages might be due to slow reactions and coagulation rates at low temperatures. In addition, this might be because this was a batch mode ECand the particles that were responsible for turbidity pollution might have been accumulating in the EC bath. In addition, because, 25°C might be still a low temperature for the density of water might be still higher than the density of floccs that are suspended in the treated effluent and therefore no settling of the floccs. It is known that, in conventional water treatment turbidity removal is also affected by chlorine demands (Lechevallier, *et al*., 1981).

5.2.4 Further Discussion on Total Suspended Solids Removal Efficiency

TSS removal percentages of up to 95% for experiments at 30°C and 85% for experiments at 35°C at 2820th sec. (47 min.) and 2460 sec. (41 min.) respectively, were observed in Figure 5.8. There appear to be a decreasing removal percentages trends towards the end of the ECfor experiments at 25°C, 30°C and 35°C for TSS as was the case with turbidity as shown in Figure 5.8 and perhaps for similar reasons explained above. It can be noted from Figure 5.8 that good percentage removal efficiencies were only archived between 1000 s and 2000 s.

For the 40^{o}C experiment, the maximum removal efficiency for turbidity was 87% at 30th min. of EC and at the same time, the TSS was 92%. There were 91% NTU (to 10 NTU) and 62% (to 44.4 mg/L TSS) removals at 45°C. Turbidity and TSS removal achieved for experiments at 50^{o}C were up to 75% NTU (down to 23 NTU) and 75% TSS (down to 31.2 mg/L TSS) respectively. However, it was noted that the turbidity and the total suspended solids removal percentages were decreasing with temperatures. So turbidity and TSS removal are affected by temperature. The best COD removal efficiencies of 76% (463 mg/L) for experiments at 25^{o}C and up to 81% (485 mg/L) for experiments at 40^{o}C were achieved. The COD removal

percentage for experiments at 45°C was low with a value of 63.2%; within the same range as experiments at the 50°C, with 64% removal efficiency.

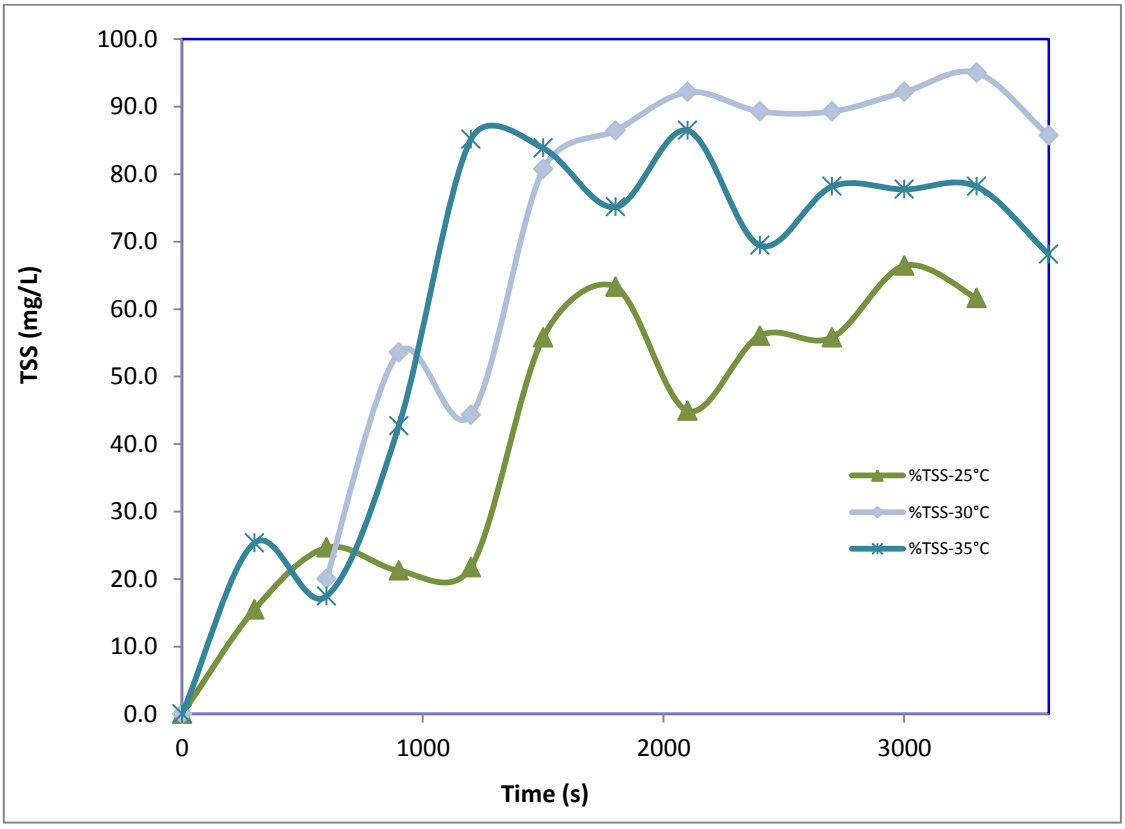

Figure 5.8 TSS Removal Percentages at 25°C; 30°C and 35°C

5.2.3 Removal efficiencies of COD; Turbidity; TSS; Cℓ; Absorbance; True Colour at 25°C; 30°C; 35°C; 40°C;45°C; 50°C and 55°C.

As shown in Figure 5.9. COD removal efficiency seem to be higher from lower to middle temperature ranges and effectively trending down with occasional peaks towards higher temperature range. This may be because of the following:

- The precipitates may have lost stability at higher temperatures and re-dissolved into solution.
- Coagulant overdose and precipitation reactions reverses or the charges get reversed (Vepsäläinen, 2012).
- Coagulants were fully destabilized with zero zeta potential (Pernitsky, 2003).
- In chemical coagulation, destabilization happens at near neutral pH the ending ECpH were higher (pH 8 to 10) (Vepsäläinen, 2012) and (Pernitsky, 2003)

- Low ionic strength, low electrostatic forces of attraction.
- Passivations of electrodes was evident at higher temperatures (Chaturvedi, 2013).

For most of the experiments, removal efficiency were about 70%. Based on this data, it is difficult to confirm if the discrepancies in COD removals were related to changing temperatures because high efficiencies were achieved at, both low (76% at 25°C) and middle temperatures (81% at 40°C). For the same type of effluent and electrode materials at a current density of 22 mA/cm^{-2} (but 9.75 mA/cm^{-2} in this study), Arslan-Alaton *et al.* (2008) achieved 69% COD removal.

The increasing trends of, COD removal efficiency in Figure 5.9 for experiments at 55^{o}C were similar for individual experiments (A, B and C). However, this did not happen in 40^{o}C experiments. Turbidity and Chlorides followed the same trends as those of COD. At higher temperatures more structurally definitive oxides of iron could have been produced as well such Fe_2O_3 (hematite) which known not to have coagulate reactions.

As shown in Figure 5.9, the highest removal efficiencies for turbidity were up to 89 % at 30°C and 80 % at 35°C after which the removal was effectively trending down

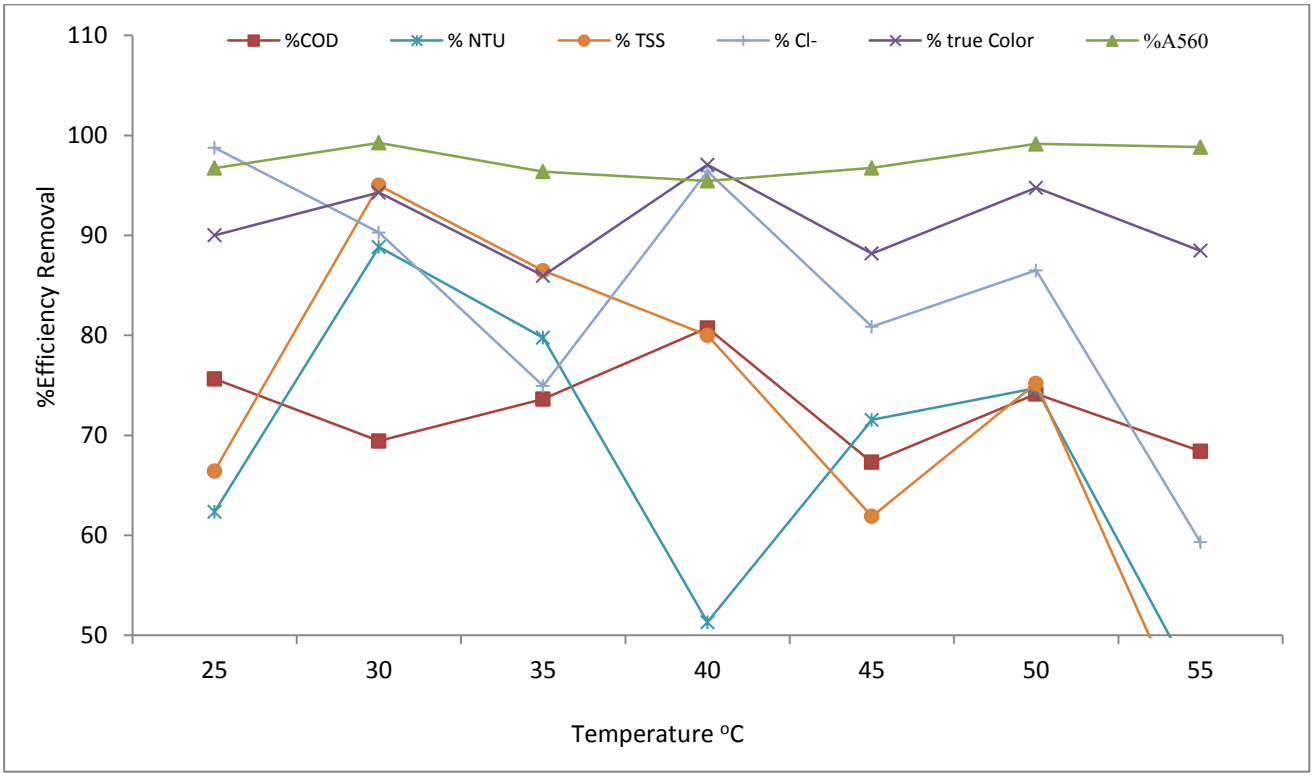

Figure 5.9 Percentage Removal Efficiencies of COD; Turbidity; TSS; Chlorides; Absorbance; True Colour at 25°C; 30°C; 35°C; 40°C;45°C; 50°C and 55°C.

. The TSS highest percentage efficiency removal was 95% at 30°C and continued to drop towards higher temperatures. Chlorides follow the same trend as those of TSS with 99% at 25°C and 90% at 30°C and systematically dropped as the temperatures were raised. However, it can be observed in Figure 5.9; that the removal efficiencies of true colour (Pt-Co); although its trend is effectively constant, it is similar to those of chlorides. May be chlorides had an effect on the removal efficiency of true colour (Pt-Co). However, this could not be investigated further because chlorides doses were not controlled.

Good hazen colour removal efficiencies of up to 93% and the absorbance removal efficiencies of up to 97% were achieved in experiments at 30^{o}C and 35^{o}C in 30 to 50 minutes and 40 to 35 minutes respectively. Absorbance was not affected by temperature. Absorbance removal efficiencies of about 95% to 99% were achieved over the selected range of temperatures. Arslan-Alaton *et al.* (2008) achieved 99% for the similar operating conditions in 30 minutes at 25°C.

5.3 Chemical Oxygen Demand Removal and Reaction Kinetics

5.3.1 Chemical Oxygen Demand Removal

The reaction kinetics studies were done by performing experiments at 25°C, 30°C, 35°C, 40°C, 45°C, 50°C and 55°C with textile effluents that were produced during pre-bleaching and dyeing cotton fabrics with commercial sample dyeing machines. One batch of sample pre-bleaching and dyeing experiments could only cover three to four of 3.5 L ECexperiments. Therefore, some batches were mixed to avoid textile effluent variability. Experiments at 25^{o}C, 30^{o}C and 35^{o}C were performed with the same textile fabric pre-bleach and dyeing batch; experiments at 40 ^{o}C and 55^{o}C were done with another dyeing batch and experiments at 45^{o}C and 50^{o}C were from different sample pre-bleaching and dyeing experiments.

Figure 5.10 represents COD concentration removal trends for the seven set of experiments that were performed at 25°C; 30°C; 35°C; 40°C; 45°C; 50°C and 55°C. There was a COD build up in experiments at 50^{o}C from about 1203 mg/L (0.0376 mol/L O_2) at the 40th min. to 1739 mg/L (0.0543 mol/L O_2) at 60th min. This trend was similar to the trends of experiments at 35^{o}C but the increase in trends did not continue further. The measurements of COD for experiments at 30^{o}C show constant values from the 30th minute to the end, and so were the experiments at 40^{o}C. As shown in Figure 5.10; the lowest COD achieved was ±500 mg/L (0.0156 mol/L O_2) for experiments at 25^{o}C, 30^{o}C, 35^{o}C and at 40^{o}C with trends showing no

further COD removal even if the EC was prolonged except for experiment at 25°C. All experiments were stopped after 3600s (60 min.) of electrocoagulation. This appears to be the maximum removal levels that were achieved in these experiments and there was resistance for further COD removal towards the end of electrocoagulation. However, experiments at 25°C show a continual removal of COD at the 60th min. It was discussed already in section 5.2.3 that low temperatures and high pH as was revealed by high TSS and Turbidity towards the end of negatively affect coagulation mechanisms. TSS and Turbidity could be contributing to low COD removal.

Figure 5.10 shows that experiments at 40°C and 55°C were obtained from the same sample dyeing experiment and experiment at 40°C deviated slightly from experiments at 55°C trends ending with lower CODs than experiments at 55°C**.** The COD concentration trends at different temperatures in Figure 5.10, have high regression, R^2 of about 0.9 for exponential removal of COD except for experiments at 35°C.

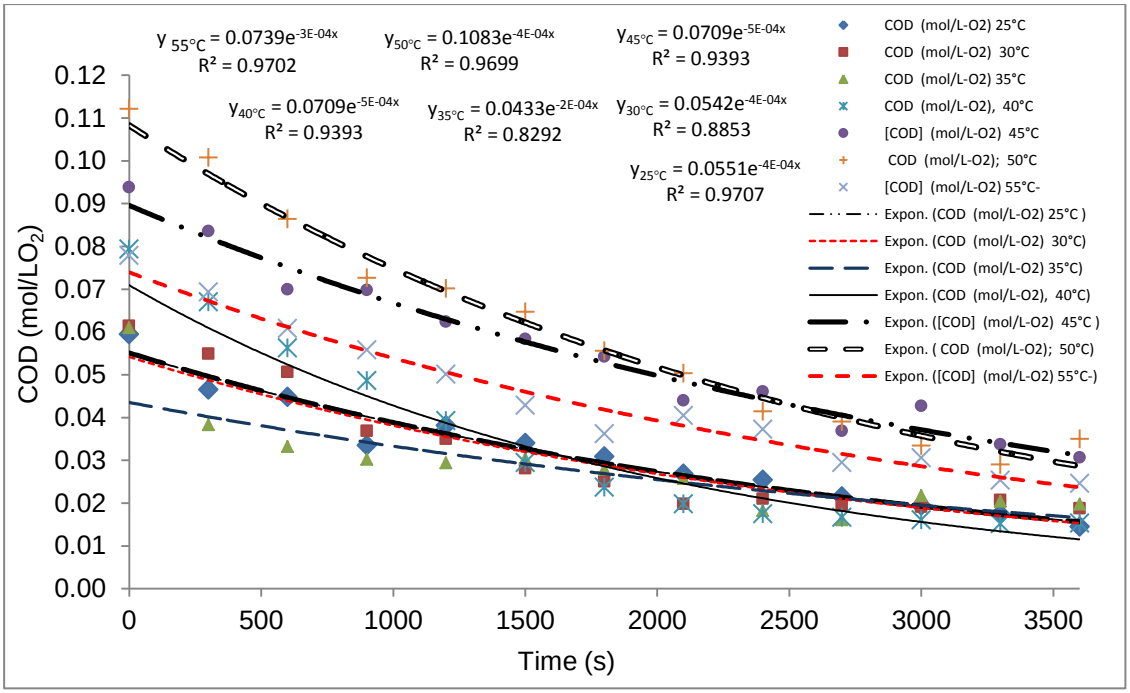

Figure 5.10 COD removal trends at 25°C; 30°C; 35°C; 40°C;45°C; 50°C and 55°C

For those EC experiments with higher initial COD such as 50°C and 45°C, their trends were not flat and still continuing to drop at the end of the EC that might, perhaps indicate that the extent of removal partially depends on initial concentrations of COD. It can be concluded that lower CODs could be achieved at temperatures between 25°C to 40°C and at about 35 min

5.3.2 Chemical Oxygen Demand Reaction Kinetics

To determine reaction constants (k_c), the COD data was linearized by plotting $ln\left(\frac{[COD]_t}{[COD]_0}\right)$ vs time and the reaction constants (k_c) as shown in Figure 5.11. The reaction constants (k_c) were read from gradients of straight-line equations in Figure 5.11. The data shows good fit to the first order reaction rate model with regression correlation of more than 0.9 except for experiments at 35°C, which is 0.83. The previous research confirms that reaction rates for COD removal normally follow first order reaction kinetic model. Arslan-Alaton *et al.* (2007) achieved k_{cCOD} = 8.75 x 10^{-3} s^{-1} for similar effluent and about double the operating current densities of 22.0 mA.cm^{-2} (9.75 mA.cm^{-2} in this study).

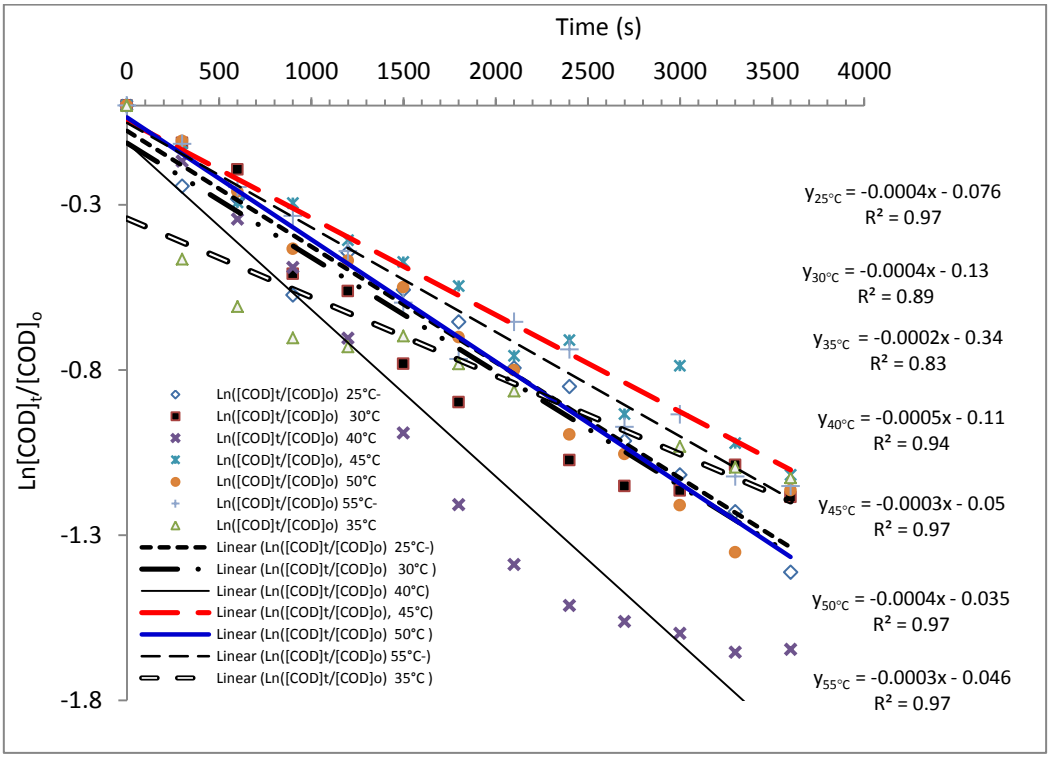

Figure 5.11 Ln ($[COD]_t/[COD]_o$) vs time for 25°C; 30°C; 35°C; 40°C; 45°C; 50°C and55°C

Rajkumar, *et al*., (2006) also reported first order reaction model with k_{cCOD} of about 1.2 x10^{-3}/s for various types azo dyes effluents and Lopes, *et al*., (2004) determined k_{mCOD} to be 5.0 x10^{-6} m/s from the first order reaction kinetics model. Other iron EC systems with similar electrodes showed k_m values of about 2.2 ×10^{-2} cm/s with chlorides to 1.4 × 10^{-4} with nickel redox couple (Martinez, *et al*., 2012)**.** At about the same current density but with different supporting electrolytes, Hmani , *et al*., (2012) reported a first order reaction constant of 2 x

10^{-4} /s for experiments at 30°C and pH of 5. However, EC involves multiple reaction mechanisms for COD removal including chemical coagulation. Chemical coagulation for second order reaction rate models (Hmani , *et al*., 2012 and Pernitsky, 2003). Mahmoud & Ahmed, (2014) reported second order reactions kinetic models for electrolyses of the surfactant water but with a different methodology.

Nevertheless, the assumed reaction rate model (first order) might be incorrect. The data was fitted to the second order model using the integral method. As shown in Figure 5.12, the linearized plot of $\left(\frac{1}{[COD]_t}\right)$ vs time was used to determine reaction constants for COD removal.

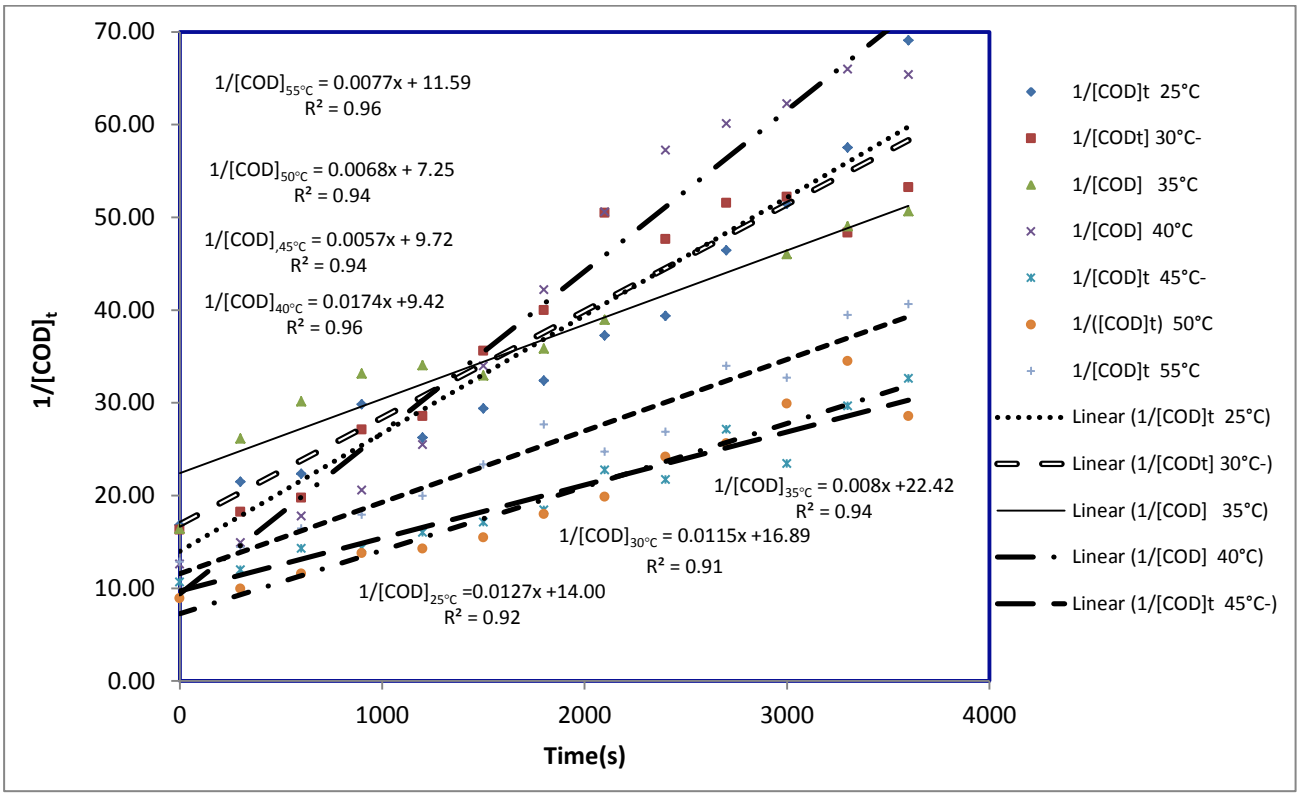

Figure 5.12. $\left(\frac{1}{[COD]_t}\right)$ vs time for determination of 2nd order Reaction Constant.

The data was a close fit for all experiments with regression coefficient values, R^2 = 0.9. However, his model was not accepted because the regression R^2 values were lower compared to the first orders except for experiments at 30°C and 35°C.

The k_{c1} values in Table 5.3 are decreasing from 25°C until 40°C and increasing from 45°C to 55°C. This shows that there are different reaction kinetics mechanisms or other reaction rate models that are taking place at low temperature range between 25°C and 40°C and high temperature range between 45°C and 55°C. Ideal reaction rate models are based uni-molecular, homogenous, and non-catalytic reactions while in fact it might be possible that

this is only true for certain ranges of temperatures. The second reaction rate constant (kc_2) values are shown Table 5.3. The higher values of k may be due to multiple reactions and side reactions that are only possible at temperatures above 45°C.

5.3.3 COD Activation Energy.

To explore dependence of COD removal reaction kinetics on temperature and to determine the activation energy (E_A); Arrhenius plot and Eyrings plots were performed. The data for these plots are shown in Table 5.3 as $\ell n kc_1$ and $\ell n(kc_1/T)$. $\ell n kc_1$ and $\ell n(kc_1/T)$ versus inverse of temperature (1/T) were plotted for Arrhenius and Eyrings plots respectively. For better presentation of the temperature data, 1000/T was used instead of 1/T. Arrhenius Laws was used to determine the activation energy and Eyrings plots to determine the enthalpy of reaction ($\Delta H^{\#}$) and the entropy ($\Delta S^{\#}$) at the transition state.

Table 5.3 Reaction Constant; Mass Transfer Coefficients; Arrhenius and Eyring plots

T°C	T(K)	1000/T (K)	kc_1 (s^{-1})	$k_m = k_c/As$ (cm/s)	ℓnkc_1	$\ell n(kc_1/T)$	kc_2 ($M^{-1}.s^{-1}$)	ℓnkc_2	$\ell n(k/T)$
25	298.6	3.35	$3.89x10^{-4}$	$1.17 x10^{-4}$	7.85	13.55	0.013	4.4	10.1
30	303.5	3.29	$4.19x10^{-4}$	$1.26 x10^{-4}$	7.78	13.49	0.012	4.5	10.2
35	308.4	3.24	$4.50x10^{-4}$	$1.35 x10^{-4}$	7.71	13.44	0.008	4.8	10.6
40	313.5	3.19	$5.03x10^{-4}$	$1.51 x10^{-4}$	7.60	13.34	0.017	4.1	9.8
45	318.7	3.14	$3.19x10^{-4}$	$9.58 x10^{-4}$	8.05	13.81	0.0057	5.2	10.9
50	323.5	3.09	$3.92x10^{-4}$	$1.18 x10^{-4}$	7.85	13.62	0.0068	5.0	10.8
55	328.4	3.05	$4.69x10^{-4}$	$1.41 x10^{-4}$	7.66	13.46	0.0077	4.9	10.7

However, the data did not obey Arrhenius plots for the whole range of experimentally chosen temperatures for this research such as 25°C, 30°C, 35°C, 40°C, 45°C; 50°C; and 55°C. As a result, the data in Table 5.3 is a plot for the low temperature range (25°C; 30°C; 35°C and 40°C) range and high temperature range (45°C; 50°C; and 55°C) as labelled. The gradients were found to be E_A/R = -1581 K and – 4276 K for lower and higher temperature ranges respectively. The activation energies were determined as follows:

$$-E_A/R = \text{-1586K}$$
$$E_A = \text{-1586 x -8.314 = +13186 J/mol = +13.19 kJ/mol}$$

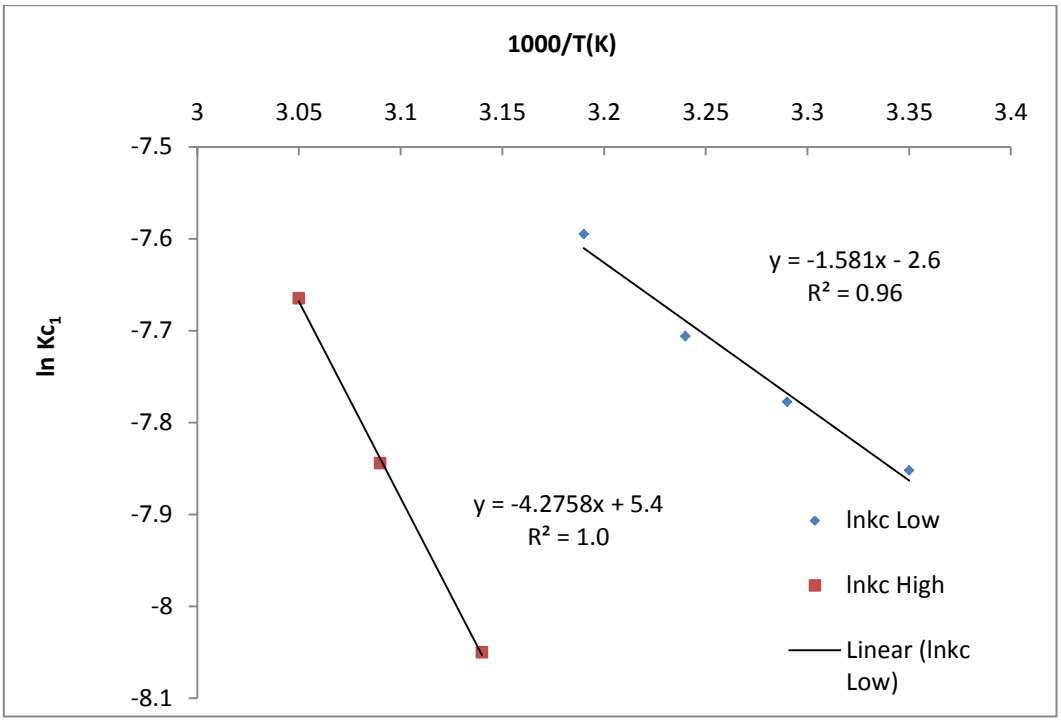

Figure 5.13 Arrhenius Plot for low temperatures 25°C; 30°C; 35°C and 40°C and High temperatures 45°C; 50°C; 55°C with first order model.

The activation energies were found to be +13.2 kJ/mol for lower range of temperature which is less than for the high range with E_A = +34.4 kJ/mol. The following equation describes the parameters.

$$\ell \mathrm{n}\, k(T) \quad = \frac{R.T}{z\mathcal{F}} \ell \mathrm{n}\, A - \frac{E_a}{R} \cdot \frac{1}{T.}$$

The data was substituted for low temperature range between 25°C and 40°C,

$$\ell \mathrm{n}\, k(T)_{low} \quad = (-1581)\frac{1}{T} + \ 2.06 \times 10^{-5} T$$

While determining Arrhenius plot, it became apparent from the curve that the rate constants are responding differently to plot normal plot. The resulting curves showed two opposite straight lines with both perfectly fitting to the Arrhenius plot. The two curves included a set of temperature ranges, 25°C; 30°C; 35°C and 40°C and higher range of temperatures, 45°C; 50°C; and 55°C. The more negative activation energy for the higher temperature range indicates that the reaction rates are lower at higher temperatures. In ordinary elementary reaction rate kinetics reaction rates increase with increasing temperatures. This was true for both temperature ranges but the trends discontinued after 40°C for the lower range. May be the different $k_{c\text{-}COD}$ values over the low and high range of temperatures were due to kinetic controlled reactions at low temperatures because activation energy of 13.2 kJ/mol ≤ 25

kJ/mol and 34.4 ≥ 25 kJ/mol at high temperatures was due to mass transport controlled reaction rates (Robertson, *et al*., 2005).

This abnormality could also have been caused by the following:

(1) Dominancy of mass transfer controlled reactions at high temperatures because of thermal overpotentials (Nauman, 2002).

(2) Other chemical kinetics mechanisms pathways; chemical equilibrium shifts at high temperatures as most EC reactions are equilibrium reactions.

(3) Deviations from elementary reactions are possible by formation of side reactions (multiple reactions) or at higher temperatures (Schmidt, 1998).

(4) There were evidences of passivation of electrodes at high temperatures. Electrodes surfaces appeared black after EC at high temperatures. This colour could not be easily cleaned by a wire brush. This reduces the discharge of charges or ions from the electrodes.

(5) As already discussed in section 5.2.3 and 5.2.4 that turbidity and TSS removal by coagulation mechanisms are low at high pH and temperature, therefore EC reaction rates were slow for high temperature experiments. Turbidity and TSS are components of COD (Pernitsky, 2003).

(6) May be the assumed models is actual fact incorrect. Other researchers (Mahmoud & Ahmed, 2014; Cho, *et al*., 2014; Ganesan, *et al*., 2012; Grygar, 1995 and Ghanim, & Ajjam , 2013) chose the second order model. Hence, the data was also analysed with second order models as shown in Figure 5.13(b).

The second order reaction model gave an activation energy of +28 kJ/mol and -30 kJ/mol for high and low temperature ranges respectively. +28 kJ/mol is about the same as the activation energy for first order reaction model +34 kJ/mol for the high temperature range. This means that the is still a high energy barrier for electrochemical reactions at higher temperatures. Low temperature range still show less dependance on temperature. However, the second order model excluded experiments at 40°C. According to Nauman, (2002) deviations from Arrhenius plot are sometimes caused by less dependency of reaction kinetics on temperature or a shift from kinetic limitation to mass transfer limitation or the activation energy is decreasing with temperature. Reaction rates decrease as the temperature is increased.

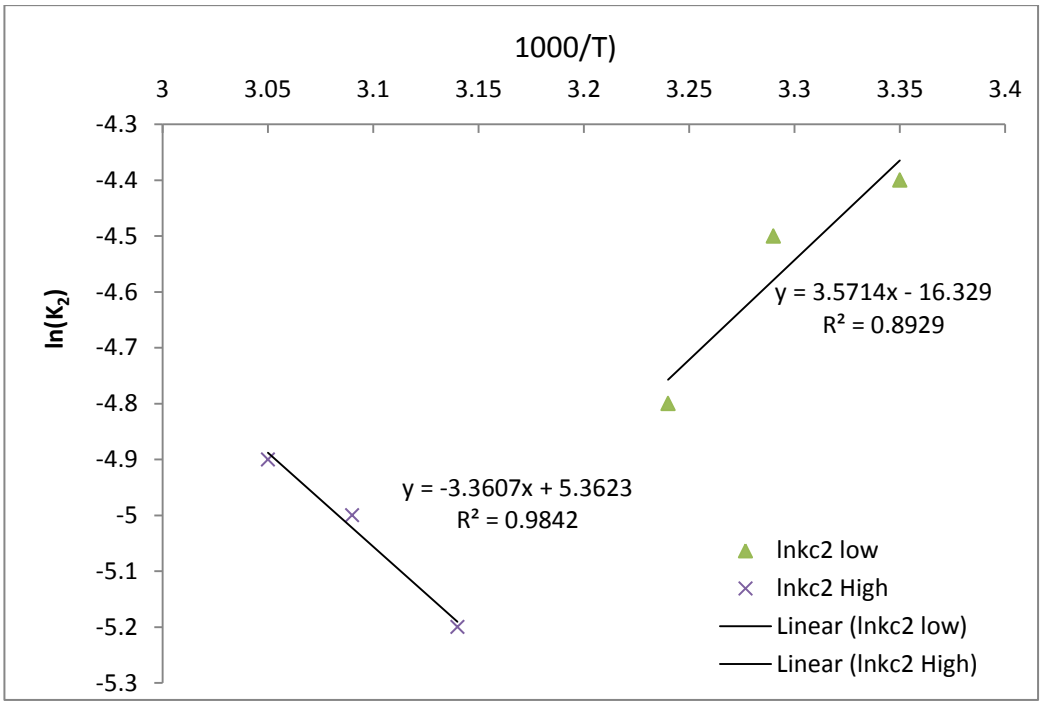

Figure 5. 14 Arrhenius Plot for low temperatures 25°C; 30°C; 35°C and 40°C and High temperatures 45°C; 50°C; 55°C with 2nd order model.

5.3.4. COD Removal Enthalpy ($\Delta H^{\#}$) and Entropy ($\Delta S^{\#}$) of Reaction and Eyring's Law.

The entropy of the transition state $\Delta S^{\#}$ could also be determined from the intercept because Boltzmann's (k_B) and Planck's (h) constants with values, k_B = 1.38x10^{-23}J.K^{-1} and h = 6.63×10^{-34} m^{2}kg/s, respectively (Clayden , 2000).

$$\ell n\left(\frac{k}{T}\right) = -\left(\frac{\Delta H^{\#}}{R}\right)\cdot\frac{1}{T} + \left(\frac{\Delta S^{\#}}{R} + \ell n\left(\frac{k_B}{h}\right)\right)$$

Enthalpy ($\Delta H^{\#}$) and Entropy ($\Delta S^{\#}$) were important for the analyses of the thermodynamic energy relationship more especially in this system. Figure 5.15 is a plot of rate constant vs the inverse of temperatures. The plots were similarly done with low and high temperature ranges as was done in the determination of activation energy. The low temperatures are 25°C; 30°C; 35°C and 40°C and high range temperatures are temperatures 45°C; 50°C; and 55°C respectively. It can be seen in Figure 5.15 that $-\frac{\Delta H^{\#}}{R}$ = -1283 and after multiplication with the universal gas constant R = 8.314 J/mol, the enthalpy, ($\Delta H^{\#}$) was found to be = +11 kJ/mol for the low temperature range.

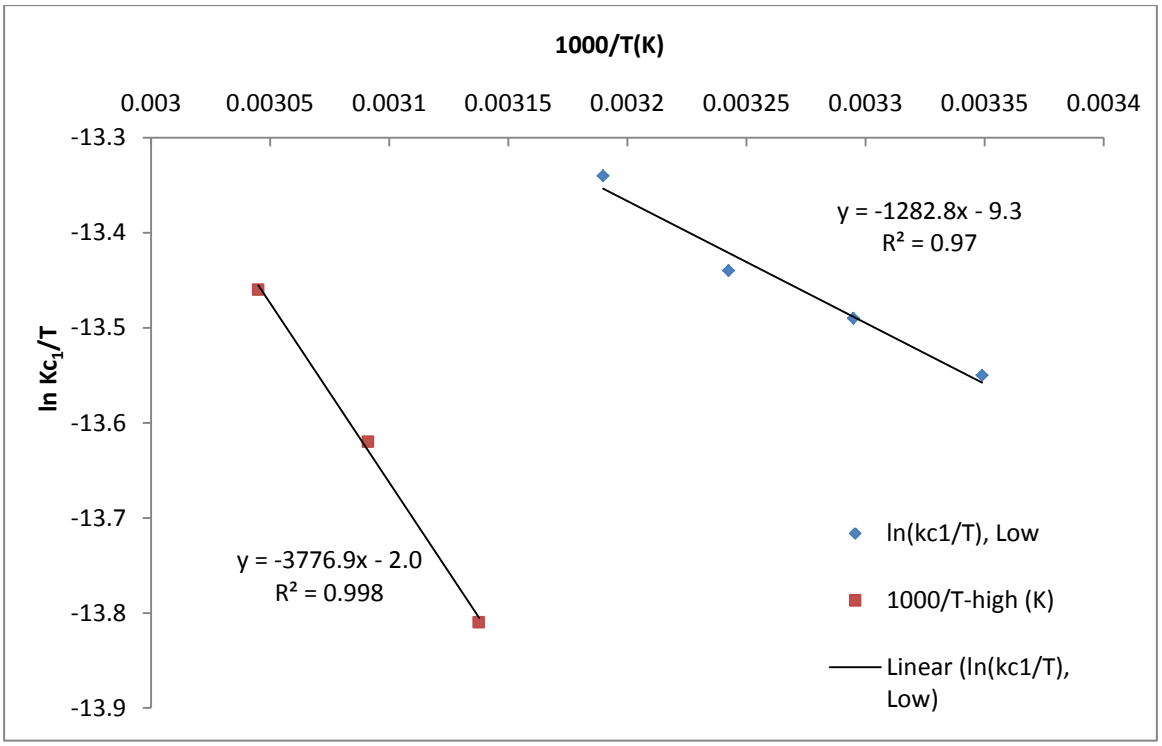

Figure 5.15 Eyrings Plot for low range 25°C to 40°C and High range 45°C to 55°C

Similarly, $-\frac{\Delta H^{\#}}{R} = -3777$, for $\Delta H^{\#}$ = +31 kJ/mol for the high temperature range.

Therefore, the reactions are affected by temperature and are endothermic because the ($\Delta H^{\#}$) is positive. This means that the EC system requires energy for starting up reaction. The energy that is added could be coming from the fact that it is known that electrical current produce heat as joule-heating. Some heat might have been lost into heating up the mass (m) of a bulk solution. However, the temperatures were maintained constant at predetermined temperature values for reaction kinetic studies. The other heat gains and losses could be entropic heat contribution of energy changes between the reactants and products. The entropy could be easily determined from the intercept of the Eyring's law equation. k_B = 1.38x10^{-23}J.K^{-1}and h = 6.63×10^{-34}m^{2}kg/s:

$$\ell n\left(\frac{k_B}{h}\right) = 23.76$$

For the lower range of temperatures (25°C, 30°C, 35°C, and 40°C), the entropy at the transition state was calculated as follows:

$$\Delta S^{\#} = R\left((intercept - \ell n\left(\frac{k_B}{h}\right)\right) = 8.314\,(-9.3 - 23.76) = -274.9kJ/K$$

Similarly at a high range of temperatures (45°C; 50°C; and 55°C), the entropy was found to be -213.34 J/K. The positive entropy of the transition state could mean that some of the reactions are spontaneous in the forward direction (Zumdahl and Zumdahl, 2007). The larger negative entropy at low temperatures than at higher temperatures means that some reactions are reversible at the high temperature ranges.

The extent of the reactions in the bulk solution can be of interest during EC because these concentrations could be equilibrium concentrations more especially towards the end of the electrocoagulation. Gibbs free energy together with equilibrium constant (K) are a good measure of the extent how these reactions could go and the spontaneity of the reactions. The spontaneity of these reactions could be investigated by the following relationship:

$$\Delta G^{\#} = \Delta H^{\#} - T\Delta S^{\#} = \Delta G^{\#}_{high\ Range} = +32\frac{\text{kJ}}{\text{mol}} - T\left(-213.34\frac{\text{J}}{\text{mol.K}}\right) \qquad 5.1$$

Where T (K) is between (45°C and 55°C)

$$\Delta G^{\#}_{Low\ range} = +11\frac{\text{kJ}}{\text{mol}} - T\left(-274.9\frac{\text{J}}{\text{mol.K}}\right) \qquad 5.2$$

where T (K) is between 25°C and 40°C

In both cases, the enthalpies are positive and the entropies are negative which suggests that Gibbs free energy will depend on the value of temperature. If T is large, then Gibbs free energy will be positive, meaning that some reactions might have stopped or reversing ($-\Delta S^{\#}$). This condition will remain the case because of the negative sign of $T\Delta S$. The above relationships (equations 5.1 and 5.2) required very low temperatures, at least for low value of $\Delta G^{\#}$. Hence, experiments at 25°C had good COD removal. However, these reactions never reached equilibrium because $\Delta G^{\#} \neq 0$ and nowhere close. For example experiments at 55°C, showed low removal efficiencies with a positive Gibbs free energy of +102 kJ/mol.

$$\Delta G^{\#}_{high\ Range} = +31.70 \times 10^{3}\frac{\text{J}}{\text{mol}} - 328.4K\left(-213.34\frac{\text{J}}{\text{mol.K}}\right) = +102\ kJ/mol$$

5.3.4. Cell Potential or Open Circuit voltage

Entropy and Gibbs Free energy determinations are very important for calculations of open circuit voltage, (E^{o}_{ocv}) or cell potentials (E^{o}_{cell}) and equilibrium potential E^{o}_{eq}. Open circuit voltage (E^{o}_{ocv}) is very important for calculations of voltage drops during EC if the other potentials are known. The reference potential, (E^{o}_{ref}) were known and provided for the ORP

sensor by the suppliers for all the temperature. The normal hydrogen potential ($E^o_{,NHE}$) could be determined indirectly by ORP measurement and presented as equivalent hydrogen potential (E^o_H) vs the reference electrode potential.

$$\Delta E^0_H = E^0_{ref} + ORP \qquad \Delta\varepsilon^0_H = 0.241V + 0.004V = 0.245V$$

Therefore, the cell potential or open circuit voltage can be determined by the following equation:

$$E_{ocv} = \Delta E^0_H + \frac{\Delta S^0}{z\mathcal{F}}(T - T_0) \qquad E_{ocv} = 0.245\text{V} + \frac{-213.34}{6\times 96485}(298.6 - 273.15) = 0.236V$$

$\boldsymbol{T_o}$ is the reference temperature = 273.15 K and as it is shown in the above calculations, for experiments at 25°C, E^o_H = 0.245 V is the equivalent standard hydrogen potential. The calculations reveal that the EC at 25°C; had an initial positive potential of 0.236V, even before the EC was started hence the reactions were spontaneous.

5.3.5. COD Limiting Current Densities (i_L)

In ordinary oxidation reactions, COD is removed by direct molecular oxygen oxidation of inorganic and organic pollutants. In electrocoagulation reactions, COD is removed by electrochemical oxidation of electrodes, releasing electrons that are used in water splitting, generating molecular oxygen, (O_2), that is further utilized in molecular oxidation reactions of organic and inorganic pollutants (Khue, *et al*., 2014 and Hmani , *et al*., 2012). Therefore, assuming that the COD reduction is via molecular oxidation reactions in such a way that it can be presented by using the relationship between the limiting current densities (i_L) and mass transfer coefficient.

$$i_L = 4\mathcal{F}k_m[COD]$$

i_L = limiting current (A/cm^2); $\mathcal{F}$ = Faradays constant (96486 C/mol); 4 = is the number charge transferring in the main oxidation reactions and k_m = mass transfer constant (cm/s). The following calculations were done below for COD removal in experiments at 25°C. The k_m values were previously determined and presented in Table 5.3 in Section 3.3.2.

$$i_L = 4 \times 96485\ C/mol \times (-1.17 \times 10^{-4} cm/s \left[5.95 \times \frac{10^{-5} mol}{L}\right] = -3.14 \times 10^{-4} A/cm^2$$

The negative sign indicates that the currents are cathodic (Robertson, *et al*., 2005). The same calculations were done for limiting current densities at other temperatures and the

results were plotted against time as shown Figure 5.16. The initial limiting current densities are as low as -5 x10^{-3} A/cm^{-2} to -4 x10^{-3} A/cm^{-2} for high temperature range and gradually rise to -2.5 x10^{-3} A/cm^{-2}.

The initial current densities for low temperature range (25°C; 30°C and 35°C) were higher between -3.2 x10^{-3} A/cm^{-2} and -2.7 x10^{-3} A/cm^{-2}. These current densities were followed by a rapid rise for the first 1000 s (16.7 min) to -2.5 x10^{-3} A/cm^{-2}; which indicates high rates of electrochemical kinetic driven reactions for lower temperature range experiments (25°C, 30°C; and 35°C) compared to high temperature ranges (40; 45°C; 50°C and 55°C). The low temperature trends (25°C, 30°C; and 35°C) followed rather a flat plateau between 1000 s (16.7 min) and 1200 s (20 min) and crisscross at common i_L value of 2.5 x10^{-3} A/cm^{-2} at about 1200 s (20 min). In Figure 5.16 , there is a noticeable second plateau between 2000s (33.3 min) and 3000s (50 min) for experiments at 25°C, 30°C; and 35°C including experiment at 40°C with a limiting current at this plateau is 1.0 x10^{-3} A/cm^{-2} and is still less than applied current density.

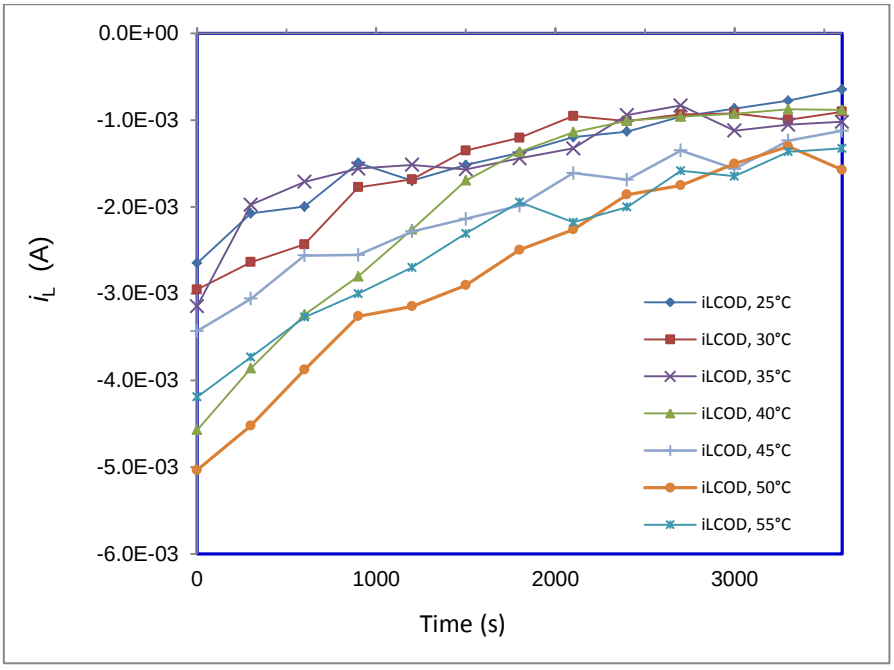

Figure 5.16 CODs Limiting Current Densities at 25°C, 30°C, 35°C, 40°C, 45°C; 50°C; and 55°C

The plateau is a common in current vs potential plots (Ntengwe, *et al*., 2010); Pintauro, 2007; Pletcher & Walsh, 1990; Papagiannakis, 2005; Bard & Faulkner, 2000 and Pilatowsky, *et al*., 2011) and indicates the maximum limiting current density (i_m) of 2.5 x10^{-3} A/cm^{-2}. According to Panizza , *et al*., (2010); if the limiting currents are lower than the applied currents (density in this case) then the electrochemical reactions are mass transport controlled; which is the case here; because 1.5 x10^{-3} A/cm^{-2} is less than 9.75 x10^{-3} A/cm^{-2}.Limiting current densities

for experiments at 45°C; gradually rose with little individual plateaux only for a short period about 300 s between 600 s. and 900 s. Experiments at 40°C and 55°C did not have a lower plateau but converged with others in the upper plateau. Experiments at 45°C and 50°C gave a maximum limiting current of -1.5 x10^{-3} A/cm^2.

The second rise of trends towards the secondary plateau could indicate secondary kinetic reactions such as coagulation, precipitation etc., reactions that are followed by mass transport in the second limiting currents regions. This only happened at lower temperature range. The high limiting current densities,(i_L); indicates, therefore higher rates of COD reduction in the bulk solutions as the reactions are not only driven kinetic reactions but by precipitation, coagulation, flocculation and absorptions reactions at low temperature; diffusion of ion transport that are dependent on concentration overpotential which reduces current leading to low current efficiencies. Probably of all pollutants being removed in this study, COD has the highest limiting current density.

5.3.3 Chemical Oxygen Demand Concentration Overpotential (E_{conc})

The values of limiting current density (i_L) were used to determine concentration overpotential, (E_{Conc}). E_{conc} was determined from the equation that follows and values were plotted as shown Figure 5.17.

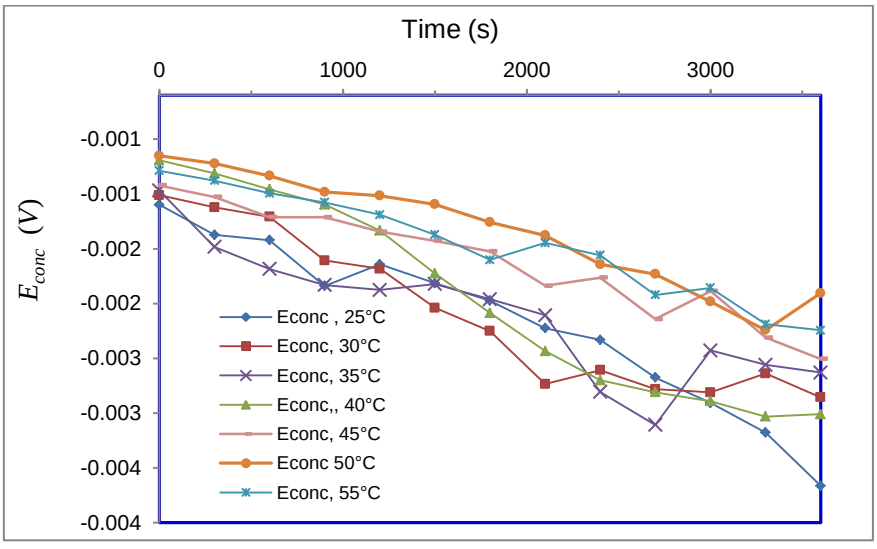

Figure 5.17 COD the Concentration Overpotential,

$$E_{Conc} = \frac{RT}{z\mathcal{F}} ln\left[\frac{i_L}{i_L - i}\right]$$

i = applied current density (A/cm^3); $\mathcal{F}$ = Faradays constant (96486 C/mol) ; z = 4 is the number charges ; $\mathcal{R}$ = 8.413 J/mol.K; $\frac{RT}{z\mathcal{F}} = 2.18 \times 10^{-5} \times T$; T = is temperature (*K*);

$$E_{Conc} = 2.18 \times 10^{-5} T \times ln\left[\frac{i_L}{i_L - 0.00975}\right]$$

As can be seen in the above calculations, E_{conc} depends on temperatures.

The E_{conc} profiles also show the same differences between the high and low temperature ranges that were observed during the determination of activation energy such as the lower temperature (25°C, 30°C, 35°C and 40°C) formed similar trends and (45°C; 50°C; and 55°C) formed similar bottom trends in Figure 5.17. Therefore; as shown Figure 5.17 there is high concentration overpotential at lower temperatures than at higher temperatures.

5.4 Chlorides Removal and Determination of Reaction Rates Parameters

The chlorides concentrations ([Cℓ^-]) were measured during the EC experiments and according to **Figure 5.18** trends; they were removed from the textile effluents. The reaction constant (k_c) were determined from the gradients of the linearized plots of the ratio of the chloride molar concentrations ([Cℓ^-]$_t$) to the original concentrations ([Cℓ^-]$_o$) vs time as shown in **Error! Reference source not found.**. Experiments at 40°C have steeper gradients with k_c alue higher than all the other values. In addition, the experiments at 25°C have similar trends as that of 40°C but its k_c value is lower due to the scatter of the data. As was done with COD, the kinetic reaction constant (k_c) values were determined and consequently k_m values were determined. k_m values were used to calculate the limiting current densities.

5.4.1 Arrhenius and Eyrings Plots for Cℓ^- 25°C, 35°C, 40°C.

In the same way activation energy was determined for COD, the k_c values for chlorides removal were used to determine the activation energy for chlorides removal. According to Panizza , *et al*., (2010), chlorides, sulphates and hydrogen peroxides reactions should obey Arrhenius law. As shown in Figure 5.18; the data did not obey Arrhenius plot and showed a decrease of reaction rate for chloride removal with respect to temperature for a limited temperature range of between 25ºC and 40°C.

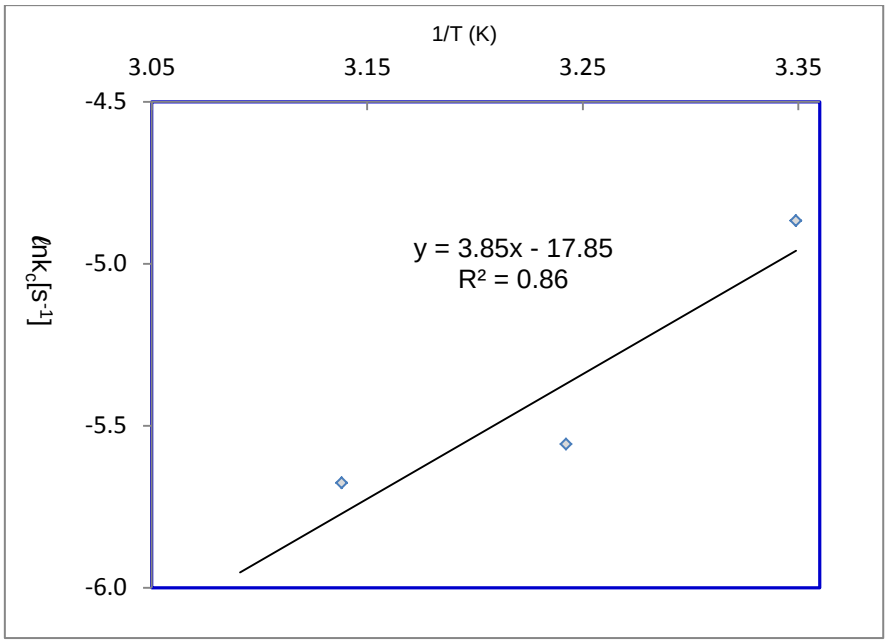

Figure 5.18 Arrhenius Plots for Chlorides removal at 25°C, 35°C and 40°C

As presented in Figure 5.19, the positive enthalpy of reaction is negative which means that the reaction is exothermic, that the reactions do not need heat to start up the reactions or heat must be removed. The entropy of the transition state is the intercept in the equation shown in Figure 5.19.

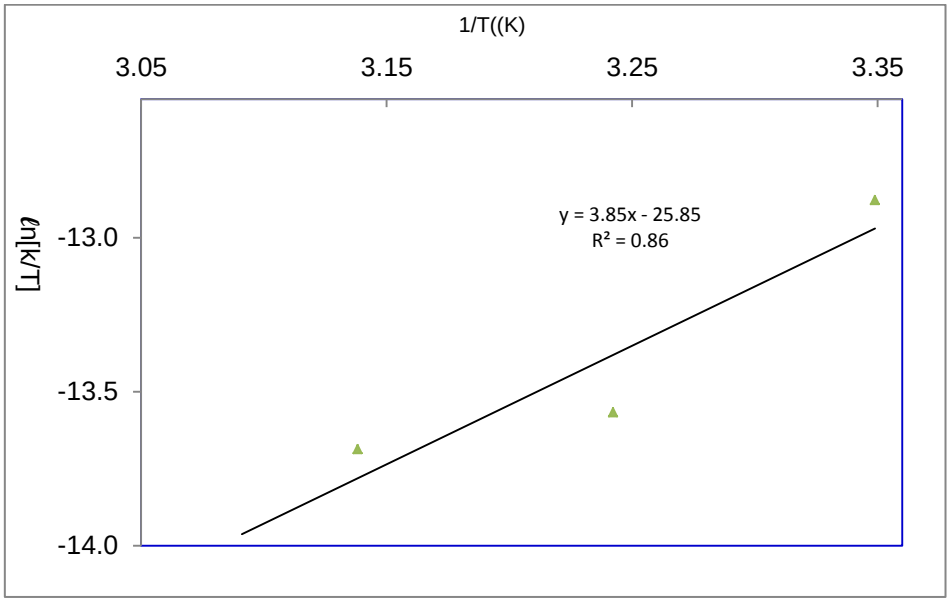

Figure 5.19 Eyrings Plots for chlorides 25°C, 35°C and 45°C

$$\Delta S^{\#} = R\left((intercept - \ell n\left(\frac{k_B}{h}\right)\right) = \quad 8.314\,(-25.85 - \ 23.76) = -412.46 J/K$$

If the entropies and the enthalpies are known, the Gibbs free energy of the transition state for the temperature range between 25°C and 55°C can be calculated.

$$\Delta G^{\#} \quad = \Delta H^{\#} - T\Delta S^{\#} \quad = -32\ \mathrm{kJ} - T\left(-412.46\frac{\mathrm{J}}{\mathrm{K}}\right)$$

It must be noted that the enthalpy of reaction ($\Delta H^{\#}$ = -32 kJ/mol) of the transition state for chlorides removal is the same as that of COD removal for the higher range. Also the cell or open circuit voltage for chlorides redox couple at 25°C was determined to be +0.191 V by the following equation.

$$E_{ocv} = \Delta E_H^0 + \frac{\Delta \mathrm{S}^0}{\mathrm{z}\mathcal{F}}(\mathrm{T} - \mathrm{T}_0)$$

$$E_{ocv} = 0.245\mathrm{V} + \frac{-412.46\mathrm{J/K}}{2 \times 96485\mathrm{C/mol}}(298.6K - 273.15K) = +0.191V\ vs\ Ag/AgC\ell$$

The activation energy for chlorides removal is -32 kJ/mol. This means a deviation from Arrhenius law. It also means that the reactions rate with respect to chloride reaction do not depend on temperature or reaction decrease with increasing temperature, therefore the temperature must be lowered in order to make reactions go faster

5.4.2 i_L and E_{Conc} for $C\ell^-$ at 25°C, 30°C, 35°C, 40°C, 45°C, 50°C and 55°C.

Figure 5. 20, shows that the chlorides removals have similar limiting current densities as those of COD (-1.5 x10^{-3} A/m^2) between -1.8 x10^{-3} A/m^2 and -1.4 x10^{-3} A/m^2 for the first plateau, however, over a long time range of 600s to 2000s than that of COD. The second plateau have a maximum limiting current densities of about the same for both chlorides and COD removal (-1.0 x10^{-3} A/m^2). As shown in Figure 5. 20, i_L trends for experiments at 25°C, 30°C and 40°C are steep in the beginning of EC and reaching almost zero at the end of the electrocoagulation. Two of these experiments achieved better COD removal efficiencies of 76% for experiments at 25ºC and 81% for experiments 40°C. The limiting current densities of these two experiments are higher than the rest and even higher than the applied current density. According to Hmani , *et al*., (2012), when the limiting current is equal to the applied current density, then the reaction are charge and kinetic driven. Although these high limiting

current densities took place in chloride removal, it is possible that the chlorides were consumed in chemical reactions that resulted in reduction of COD

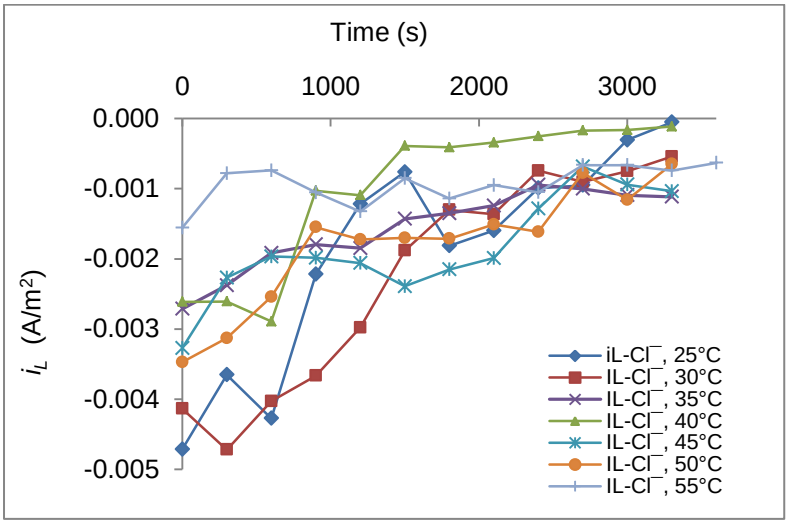

Figure 5. 20 i_L-Cℓ^- at 25°C, 30°C, 35°C, 40°C, 45°C, 50°C and 55°C

Figure 5.21 shows that experiments at 25ºC and 40°C achieved the lowest concentration overpotentials.

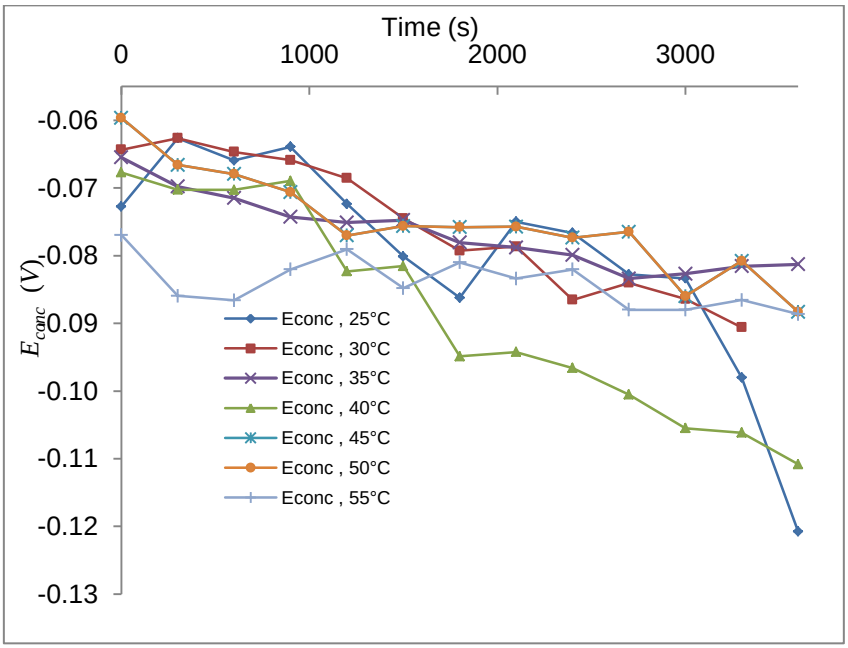

Figure 5.21. E_{conc} for Cℓ^- at 25°C, 30°C, 35°C, 40°C, 45°C, 50°C and 55°C

The concentration overpotential is potential loss due mass transfer, therefore for two experiments there were less voltage losses due to bulk solution concentration gradient but due to concentration differences between the surface of the electrode and bulk solution. For the rest of the other experiment, E_{Conc} are between -0.08 V and -0.09 V and their trends are flat which shows that the concentration gradient was only due to the bulk solution concentration gradient.

5.5. Total Chlorine Reaction Kinetics

The combination of hypochlorous acid (HOCℓ) and chlorate ion (OCℓ^-) is free chlorine (free-Cℓ_2). The combinations of free-Cℓ_2 and combined chlorine (comb.-Cℓ_2) is total chlorine (t-Cℓ_2). Combined chlorine is mostly chloramines. Combined chlorine was not measured in this study. Some of the chlorine gases that do not escape as electrolysis gases are counted in the free chlorine. Figure 5.22 shows reduction of total chlorines to minimum concentrations at 2500 s. The trends are linear with good regression, R^2= ±0.9 except for experiments at 45°C.

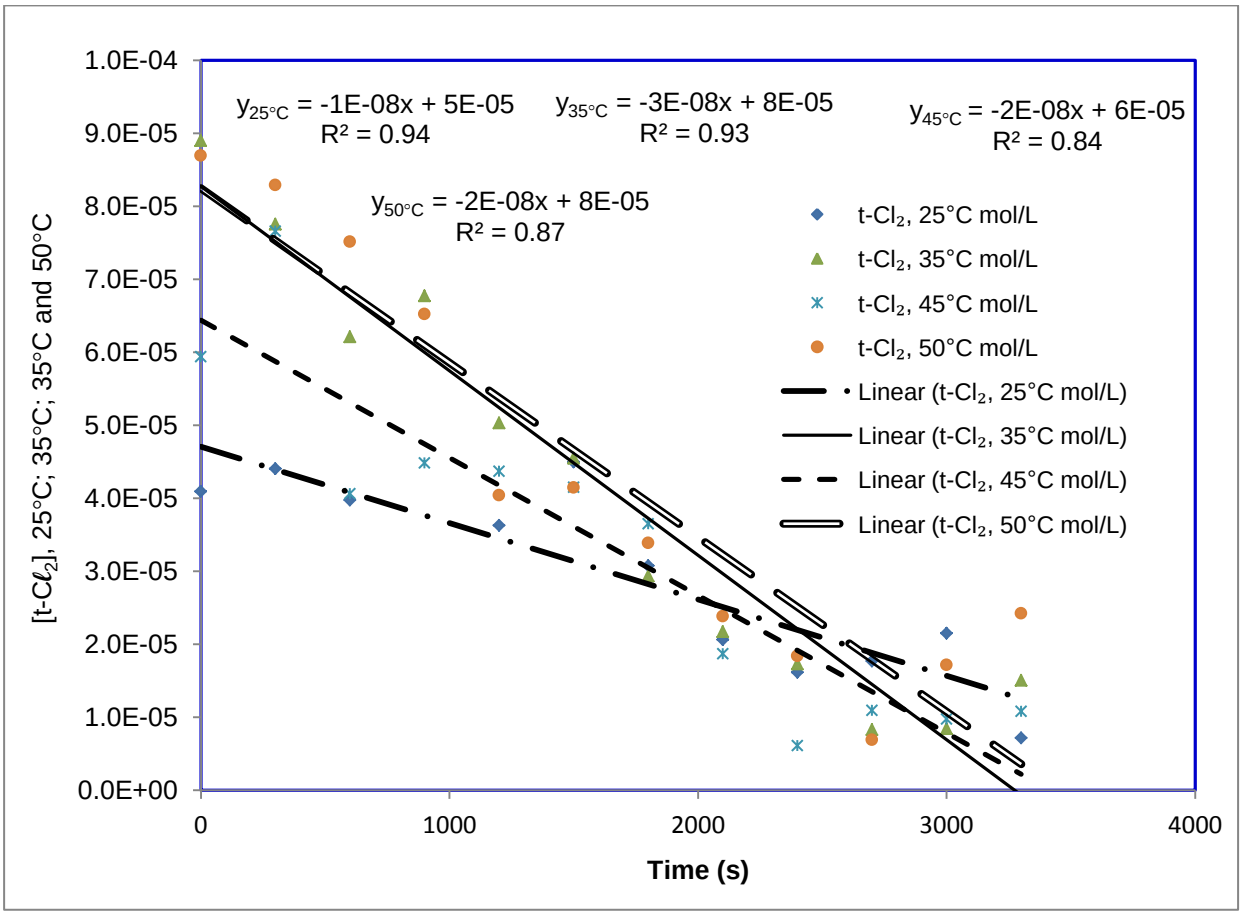

Figure 5.22 Chlorides Removal Trends at 25°C, 35°C, 45°C, 50°C experiments.

However, the trends are flat and tending to go upwards towards the end of electrocoagulation, as was the case with some COD removal experiments. This could be the case because total chlorine is known to have an effect in COD removal (Cho, *et al*., 2014). As shown in Figure 5.22, experiments at 45°C show low fitment of data with linear regression correlation, R^2 = 0.84. The reasons for the scatter of the data for experiments at 45°C was investigated in relations to other EC parameters at 45°C such as free chlorine; absorbance; ferrous and total iron.

Figure 5.23 is a plot of all three experiments (A, B, and C) at 45°C. The cause of the scatter comes from experiment B that has high total chlorine along with ferrous iron between 5 and 40 minutes as shown in Figure 5.23. This shows some relationship of total chlorine (t-Cℓ_2) to ferrous ion because they are having similar trends in Figure 5.23. According to these charts, total residual chlorine might be higher because ferrous iron may not have reacted with any species of total chlorines (t-Cℓ_2). This obviously affected absorbance removal for experiment B at 45°C compared to experiments A and C. The trends for the experiments at 55°C, 40°C, and 30°C are not shown in Figure 5.24 because their trends are different and are not linearly related to time as the trends of experiments at 25°C, 35°C, 45°C and 50°C.

The trends of Cl_2 seem to form a minor trough at about the 400 to 800 s followed by a peak of 8.3 x10^{-5} M at 900 s for experiments at 55°C as shown Figure 5.24. Other peaks are formed at the end of the EC up to 6.1 x10^{-5} mg/L (shown in Figure **5.24**) that can be due to dissolution chlorine products resulting from over-accumulation of total chlorine products. These peaks are probably the reasons for deviations of these trends from zeroth order. The peaks are likely possible because there are many possible reactions that are dependent on pH, temperature and reactions pathways as was discussed in section (2.7.2). Some reactions might reproduce the chloride ions that are recycled into making more total chlorine species hence leading to the build-up of total chlorines.

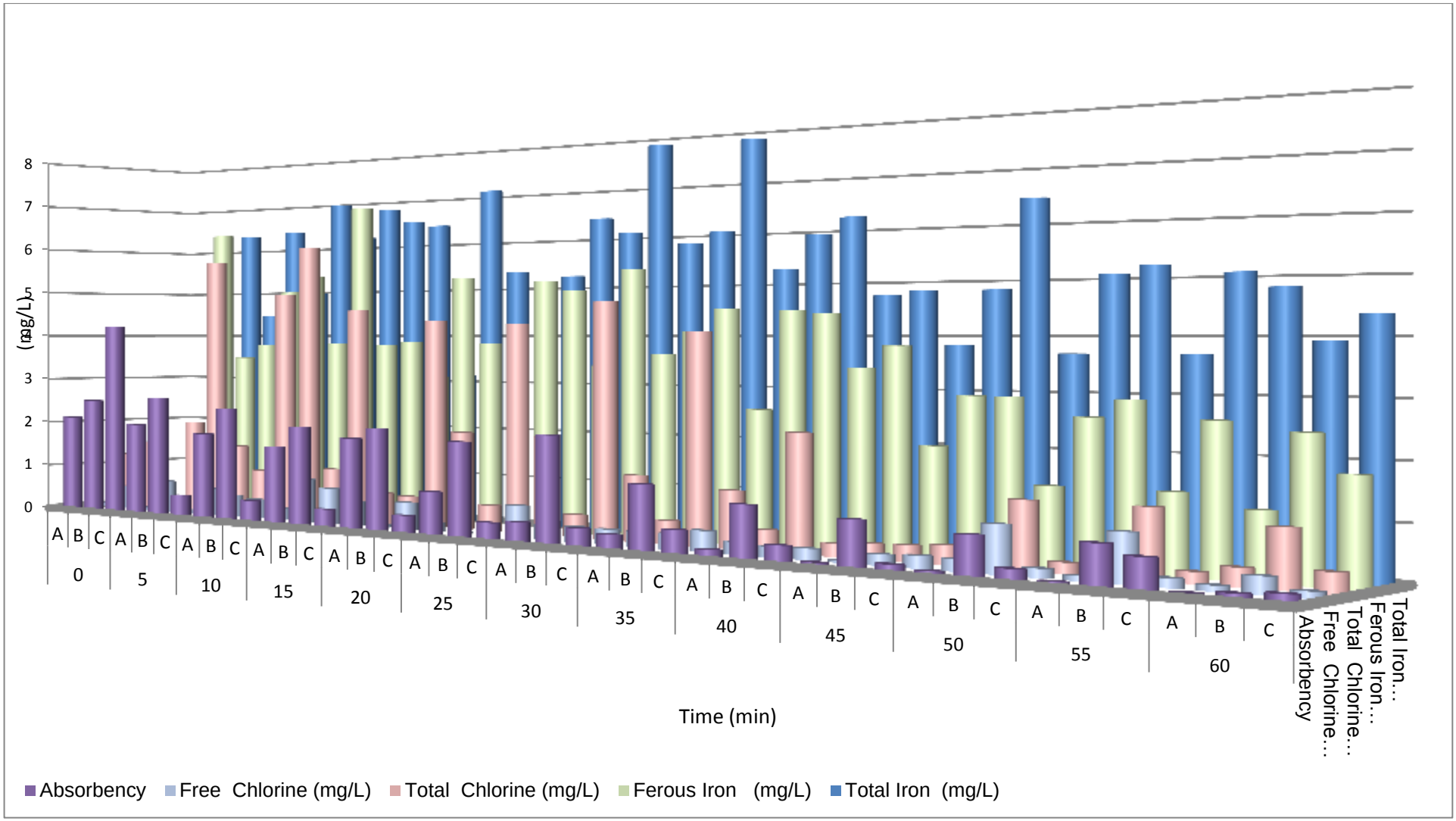

Figure 5.23 Ferrous iron, total and free chlorine for A; B and C experiments at 45°C

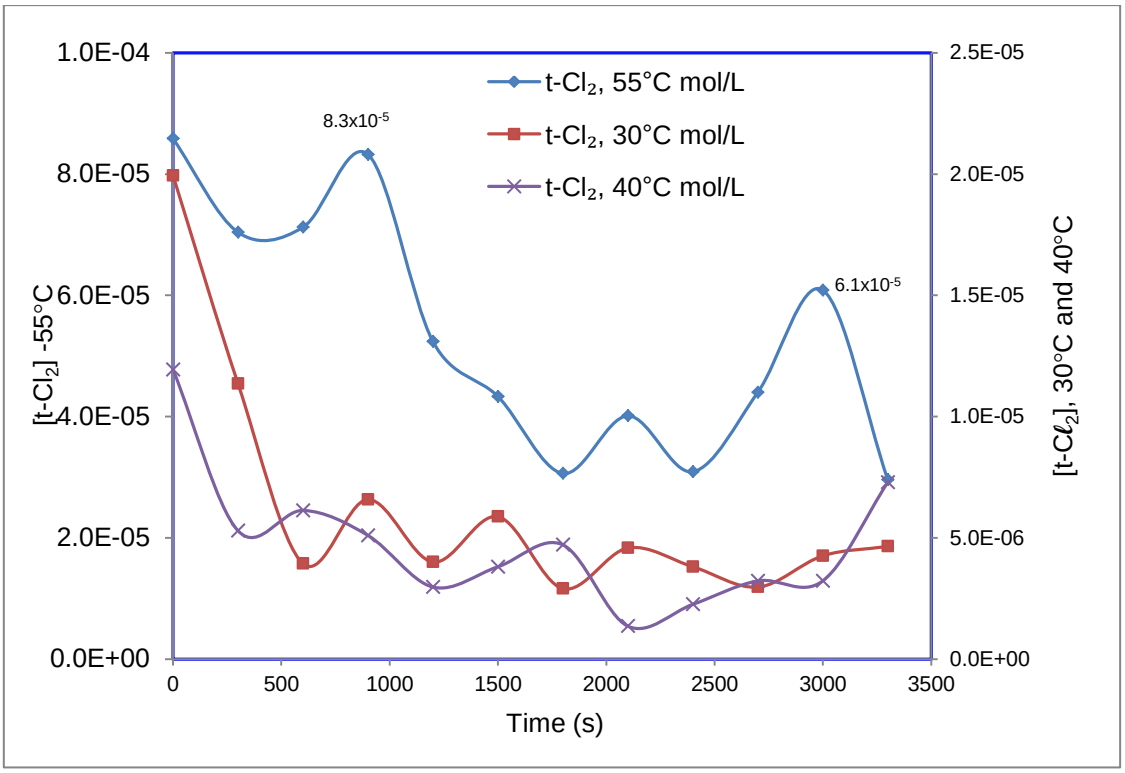

Figure 5.24 Trends t-Cl_2 for experiments at 55°C, 40°C, and 30°C

5.5.3 Total Chlorine Reaction Kinetics

Most electrochemical reactions are near electrodes reactions. Because total chlorine is the product of chloride reaction at the anode, total chlorine removal reaction kinetics follows zeroth order. The k_c values were read in Figure 5.22 gradients and are presented in Table **5.4**.

Table 5.4 k_c values for t-Cℓ_2

T(°C)	T (K)	k_c
25	298.6	1.40×10^{-8}
35	308.4	3.00×10^{-8}
45	318.7	2.48×10^{-8}
50	323.5	2.25×10^{-8}

Figure 5.25 represents the $\ell n k_c$ and ($\ell n k_c$/T) plot against the inverse of temperatures, which are Arrhenius, and Eyring plots respectively. These plots were performed to determine the activation energy, entropy and enthalpy of transition state respectively. The resulting activation energy (E_A), enthalpy ($\Delta H^{\#}$) and entropy ($\Delta S^{\#}$) of the transition state were found to be -15.7 kJ/mol; -13.3 kJ/mol and -438.8 J/K respectively. Total chlorine indicates that the

reactions are exothermic because the heat of reactions is negative. This means that this reaction released the heat that was provided by current flow resulting in positive activation energy.

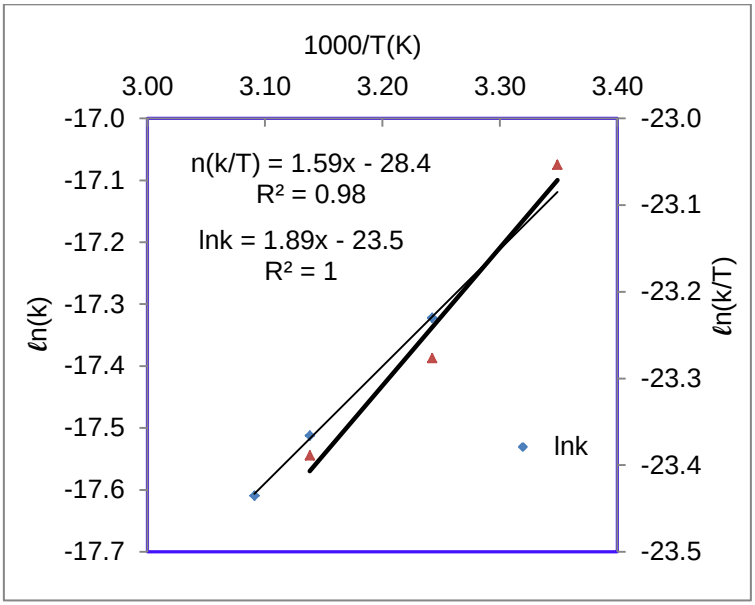

Figure 5.25 Arrhenius and Eyring plots

5.6. Absorbance Removal and Reaction Kinetics

5.6.1 Absorbance Removal Trends

All absorbance measurements were performed at maximum wavelength (λ_{max}) of 560 nm. As shown in Figure 5.26; the range for this maximum wavelength was ranging between 556.5 nm to 563.5 nm.

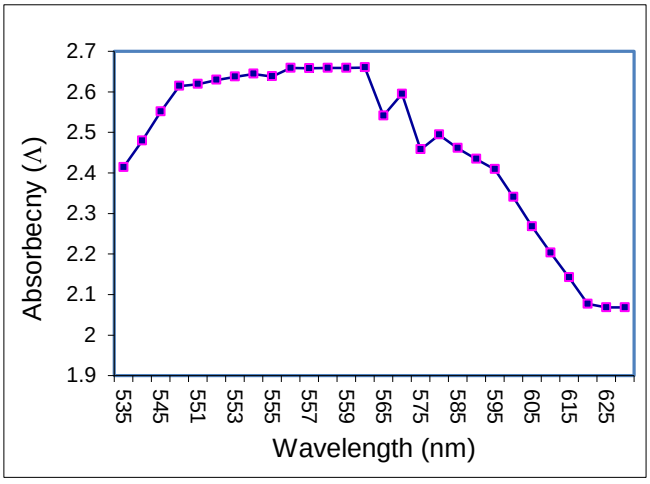

Figure 5.26 Determination of Maximum Absorbance

As shown in Figure 5.27; irrespective of original concentrations; the curves are relatively straight line until about between 1500 s and 2500 s for 25°C; 30°C, 40°C; 50°C and 55°C. This means that if the EC was stopped about these times, the reaction kinetics could have been zeroth order. This behaviour covered a wide range of temperatures for the electrocoagulation, except for experiments at 35°C and 45°C.

However, experiments at 25°C; 35°C and 40°C show some continued removal of absorbance and stopping of EC after about 2000 s (33.3 min) could have resulted in low removal efficiencies. Raghu, *et al.*, (2007), Arslan-Alaton, *et al*., (2007) and Rajkumar, *et al*., (2006) studies, concluded that absorbance removal to be described by first order reaction models for absorbance removal by electrocoagulation. Maximum absorbance removal efficiencies were achieved in the first 20 to 25 minutes for experiments at 30°C, 35°C and 40°C and then the absorbance removal remained constant for the remainder of the time. Absorbance of the textile effluent decreased during the EC as shown Figure 5.27.

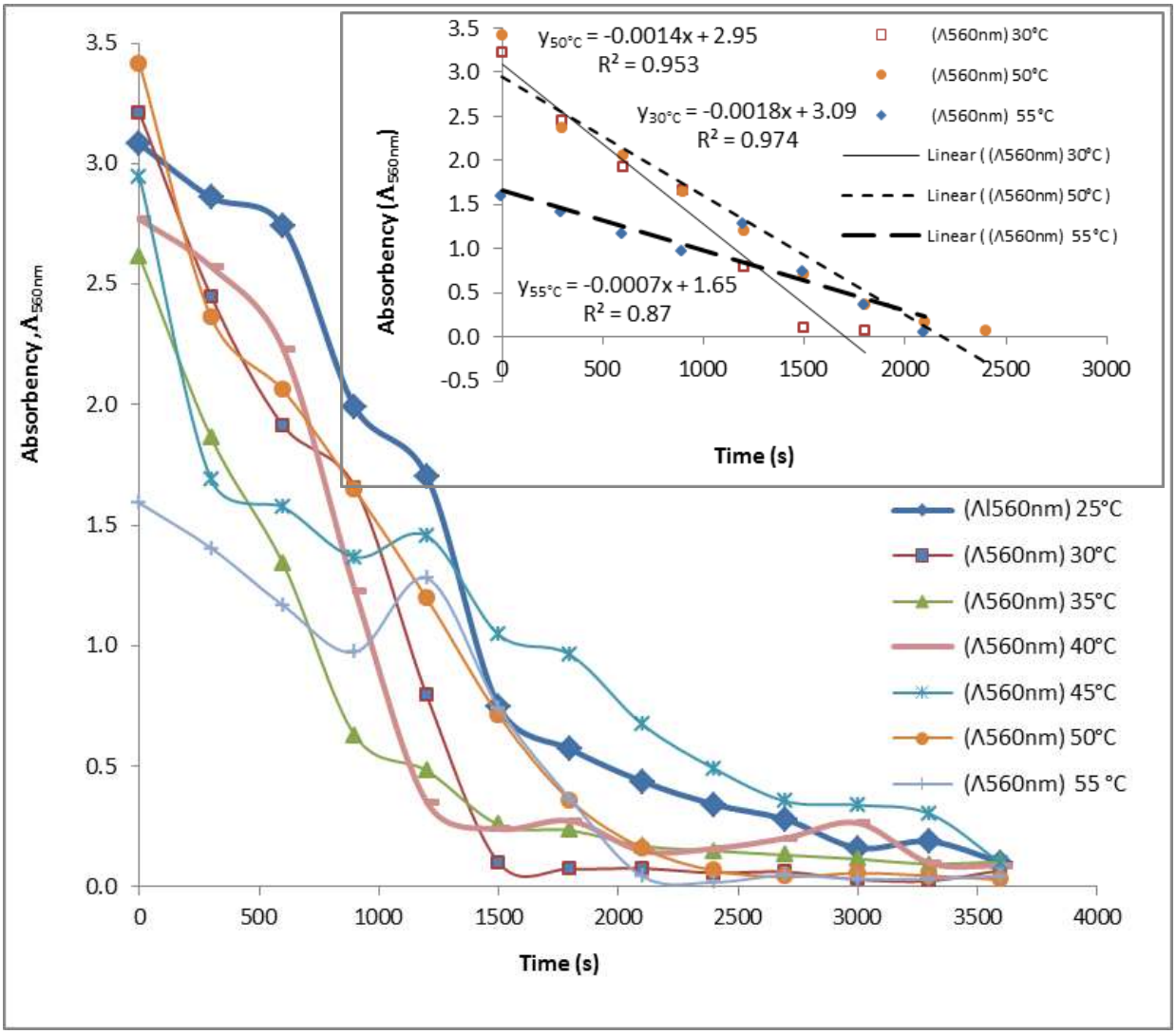

Figure 5.27 Absorbence Removal Trends at 25°C; 30°C; 35°C;40°C;45°C; 50°C and 55°C. A snapshot showing a straight line for 30°C, until 30 min and 50°C 38 min

Both the original concentration curve plot (exponential fit) and the insert curve (linear fit) have good regression of R^2 = 0.87 for the linear and mostly about R^2 = 0.97 for the exponential model curve fit. This suggests that data fit exponential models better than the linear models.

5.6.2. Determination of Reaction Constant for Absorbance Removal

Data in Figure 5.28 seem to follow first order reaction rates with R^2 = 0.9 as shown by excel program generated regression equations. The determination of k_c values was successful for the whole range of temperatures with good regression fit. Although experiments at 55°C and 50°C k-values had good fitness to the first order reaction kinetics, they did not fit the Arrhenius and Eyrings curves. Arslan-Alaton *et al.* (2007) achieved $k_{\lambda 560nm}$ = 1.77 x 10^{-3} s^{-1} for similar effluents and at about doubled the operating current density of 22.0 mA.cm^{-2} (9.75 mA/cm^{-2} in this study), 2.8 x10^{-3}/s for various reactive dyes (Rajkumar & Kim, 2006) which are within the range of the k_c value in Table 5.5.

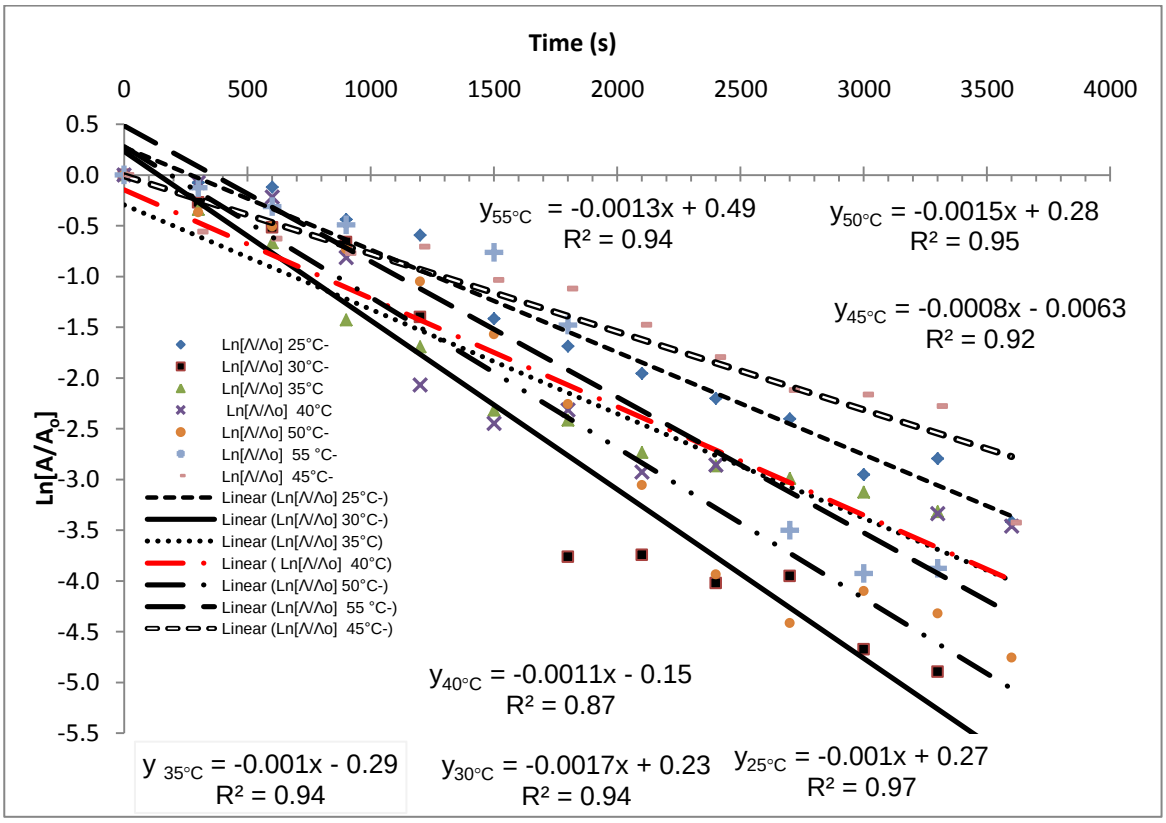

Figure 5.28: $\ln[A_t/A_o]$ vs time plot

Similarly, as was done with COD, chlorides, and total chlorine; the Activation energy (E_A); enthalpy ($\Delta H^{\#}$) and entropy ($\Delta S^{\#}$) for absorbance were determined from linear plot of $\ell n k_c$ vs 1/T and $\ell n(k_c/T)$ vs 1/T from the data in the fourth and fifth columns respectively in Table 5.5.

Table 5.5 A_{560nm} k_c and k_m values along with Data for Arrhenius and Eyring Plot

T°C	Actual T (K)	k_c (/s)	$\ell n k_c$	$\ell n(k_c/T)$	k_m
25	298.6	-1.00×10^{-3}	-6.91	-12.61	-3.00×10^{-4}
30	303.5	-1.69×10^{-3}	-6.38	-12.10	-5.08×10^{-4}
35	308.4	-1.19×10^{-3}	-6.73	-12.46	-3.58×10^{-4}
40	313.5	-1.07×10^{-3}	-6.84	-12.59	-3.21×10^{-4}
45	318.7	-7.71×10^{-4}	-7.17	-12.93	-2.31×10^{-4}
50	323.5	-1.53×10^{-3}	-6.48	-12.26	-4.60×10^{-4}
55	328.4	-1.33×10^{-3}	-6.62	-12.41	-4.00×10^{-4}

However, the data failed to fit into Arrhenius Law linear relationship between $\ell n k_c$ vs 1/T if whole range of temperatures between 25°C and 55°C was used.

Figure **5.29** shows a good data fit between 30°C and 45°C with R^2 = 0.97 and it gave activation energy of -39 kJ/mol.

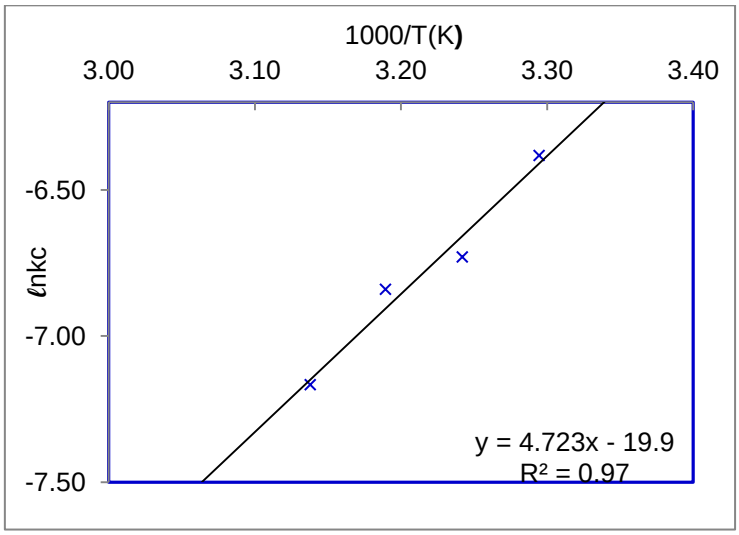

Figure 5.29: Arrhenius Plot at 30°C, 35°C, 40°C and 45°C

As shown in Figure 5.30 the data also obeyed Eyring's plot within the same temperature range and gave a positive enthalpy ($\Delta H^{\#}$) of the transition state of -42 kJ, which indicates exothermic reactions for absorbance removal.

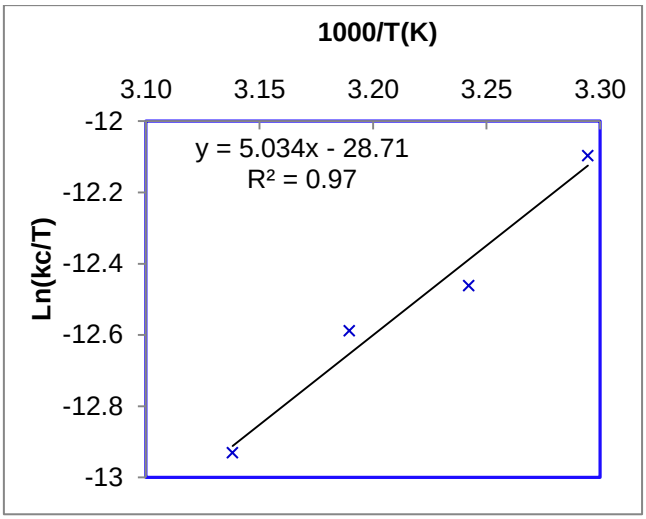

Figure 5.30 Eyring Plot at 30°C, 35°C, 40°C and 45°C

5.7 The summary of reaction kinetics parameters

The mass transfer coefficients were used to estimate limiting current density (i_L) the individual species limiting current density (i_L). The mass limiting current density are also shown in Table 5.6. The mass transfer coefficient is about $\times 10^{-4}$ cm/s, within the range of those found (Martinez, *et al.*, 2012) for nickel-iron electrodes. As a result, the limiting current densities were determined under the assumption that the reaction kinetics are mass transport limiting and the difference between the surface and bulk concentrations of oxidizing or reducing species are very large such that $C_{i.o,}^{surf} <<< C_{i,bulk}$ so that $C_{i,}^{surf} = 0$. This proved to be correct because the ferrous and ferric iron bulk concentrations were less than the theoretical possible Faradic concentrations. This is because once ferrous ion is produced it undergoes very fast multiple reactions such as hydrolysis and oxidations. According to Martinez, *et al.*, (2012) ferrous iron does not exist as a free ion in solution but as various polymeric hydroxides.

Table 5.6 Reaction rate constants at 25°C; 30°C; 35°C; 40°C;45°C; 50°C and 55°C

	Electrochemical Parameters (averages)			COD		Chlorides		Absorbance at λ560nm		Total Chlorine
T, K	*ORP*	κ, (S/m)	ρ	k_c-*COD (1/s)*	k_m-*COD (m/s)*	$k_c Cl^-$ *(1/s)*	$k_m Cl^-$ *(m/s)*	$k_{c\text{-A560nm}}$ *(1/s)*	$k_{m\text{-A560nm}}$ *(m/s)*	k_c-t-Cl_2
298.6	0.103	0.860	103.3	3.89×10^{-4}	1.17×10^{-4}	9.05×10^{-4}	2.71×10^{-4}	1.00×10^{-3}	3.00×10^{-4}	1.40×10^{-8}
303.5	0.088	1.102	88.2	4.19×10^{-4}	1.26×10^{-4}	6.40×10^{-4}	1.92×10^{-4}	1.69×10^{-3}	5.08×10^{-4}	
308.6	0.085	1.151	84.9	4.50×10^{-4}	1.35×10^{-4}	3.47×10^{-4}	1.04×10^{-4}	1.19×10^{-3}	3.58×10^{-4}	3.00×10^{-8}
313.5	0.083	1.170	83.3	5.03×10^{-4}	1.51×10^{-4}	9.62×10^{-4}	2.88×10^{-4}	1.07×10^{-3}	3.21×10^{-4}	
318.7	0.130	0.734	130.1	3.19×10^{-4}	9.58×10^{-5}	3.59×10^{-4}	1.08×10^{-4}	7.71×10^{-4}	2.31×10^{-4}	2.48×10^{-8}
323.5	0.138	0.748	137.9	3.92×10^{-4}	1.18×10^{-4}	4.31×10^{-4}	1.29×10^{-4}	1.53×10^{-3}	4.60×10^{-4}	2.25×10^{-8}
328.1	0.145	0.635	145.4	4.69×10^{-4}	1.41×10^{-4}	2.00×10^{-4}	6.00×10^{-5}	1.33×10^{-3}	4.00×10^{-4}	
i_L (A/m^2)					1.8×10^{-3}		1.40×10^{-3}			
E_A[15]				13.2/34.4		-31.7		39		-13.3
$\Delta H^{\#}$				10.7/ 31.7		-31.7		42		-15.7
$\Delta S^{\#}$				-274/-213.3		-412.5		-436		-438.8

[15] the first value of $E_{A,COD}$ is for low temperature range and high value is for high temperature range

5.8 Residual Total Iron in the Treated Effluent

Although, the effluent samples were clear; upon neutralization from higher pH with 1.0 N NaOH, the green rust ($Fe(OH)_2(s)$) precipitated out at pH less than 7.6. At low pHs, green rust, ($Fe(OH)_2(s)$) obviously undergoes hydrolysis with the water in the effluent forming various ferric and ferrous hydroxo complexes and precipitates of ($Fe(OH)_2(s)$) and ($Fe(OH)_3(s)$) (Kobya, *et al.*, 2007). Total iron is composed of all dissolved monomeric ferric and ferrous ions and their polymeric aquo hydroxo ferric complexes and hydrolysis products such as $Fe(H_2O)_3(OH)_3^0$ $Fe(H_2O)_6^{3+}$, $Fe(H_2O)_5(OH)_2^+$,$Fe(H_2O)_4(OH)_2^+$,$Fe_2(H_2O)_8(OH)_2^{4+}$ and $Fe_2(H_2O)_6(OH)_4^{4+}$

As shown in Figure 5.31; iron EC for experiments at 25°C and 30°C showed a gradual rise in residual dissolved total iron (t-Fe) until a maximum peak at 2100 s for experiments at 25°C and 1200s for experiments at 30°C. The trends show a gradual drop towards the end of electrocoagulation.

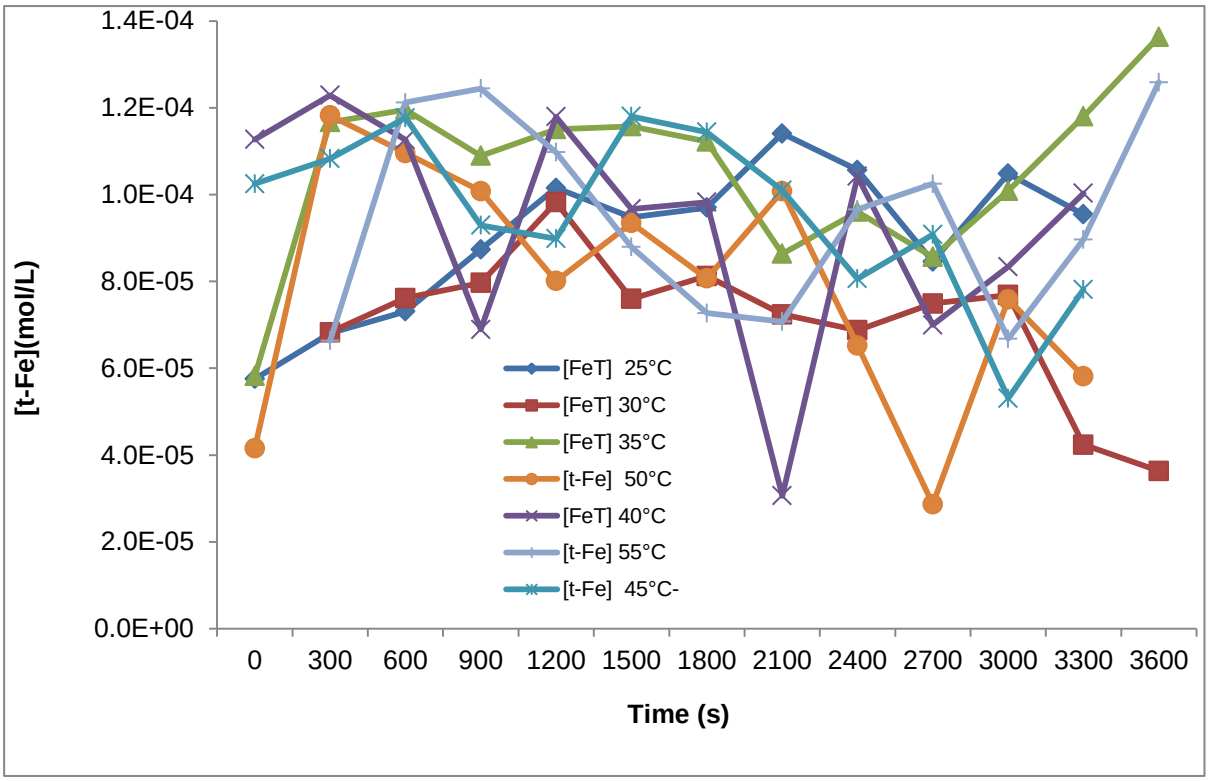

Figure 5.31 Iron Generation During Electrocoagulation

The same behaviour is observable in experiments at 55°C which gave a plateau or a dome shaped graph for total iron until about 600 s and 900 s. The rest of the experiments show maximum residual total iron production in the first 5 min. and gradual reduction towards the

end of the electrocoagulation, except for experiments at 25°C, 35°C and 55°C. The reduction in total iron is due to conversion of total iron products or coagulants into sludge by coagulation (enmeshment of the colloids) or precipitation that were floated to the surface of the treated effluent or settled to the bottom of the electrocoagulator. This is another proof that the reactions were mass transport controlled otherwise according to Faradays law of electrolyses these curves could have been straight lines. The increase in total iron for experiments at 25°C; 35°C and 55°C could be explained in terms of the lack of effective coagulation at higher pH and possible dissolution of the already formed iron precipitates and floccs (Pernitsky, 2003). This observation can also be supported by the fact that, there were the turbidity and the TSS increase towards the end of EC for these experiments. This was discussed in details in sections 5.2.3 and 5.2.4.

5.8.1 The Impact of Residual Total Iron in the Treated Effluent and Reaction Kinetics

Consequently, the increasing total iron towards the end of EC might be the cause for the previously noted deviations to the Arrhenius and Eyring plots, with absorbance and total chlorine for experiments at 25°C and 55°C, k_c values failing to fit into the Arrhenius plot. As previously discussed in section 5.2.3, experiments at 25°C could have been performed at a low temperature and experiments at 55°C, at a high temperature for affective coagulation (Pernitsky, 2003). High TSS, turbidity and total iron towards the end of EC could have been reason for the low COD removal towards the end of the electrocoagulations.

Precipitation of ferric hydroxides or removal could be difficult due to the presence of the stabilizing agents (chelating agents) in textile effluents. Typical stabilizing agents used in the textile industry are EDTA and acetic acid. In this study, 1 g/L EDTA was used in the pre-bleaching step and the same quantity in finishing bath. Both iron forms are known to be insoluble in acetic acid and EDTA and therefore cannot be easily removed by EC (Moreno-Casillas, *et al*., 2007).

5.8.2 Total Iron Reaction Kinetics

Another relevance of knowing the limiting current density is its use in the determination of surface or near electrode surface concentrations, (C^{surf}). Concentrations at the surface of the electrodes rarely are studied because they are difficult to measure (Bamford, *et al*., 1986). Hence, bulk concentrations are used for reaction kinetics though they usually do not tell about actual dissolution rate of electrodes. This is because the electrodes reactions are very fast as the electrons are not much impeded by the double layer at the surface of the electrodes in the beginning of the EC (Bamford, *et al*., 1986). In addition, hydrolysis and

oxidation reactions are faster than the mass transport of species. The following equation was used to determine surface concentration of total iron.

$$C^{surf} = \left(1 - \frac{i}{i_L}\right) C^{bulk} \left(1 - \frac{9.75 \times 10^{-3}}{-1.5\ \text{x}10^{-3}}\right) \times 9.0\ \text{x}\ 10^{-4}\ M = 6.8 \times 10^{-4} M$$

Using the average bulk concentration of 9.0 x 10^{-4} *M* for experiments at 25°C and a limiting current density of -1.5 x10^{-3} A/m^3, the concentration was found to be 6.8 x10^{-3} *M*. Similarly, the same calculations were done at other temperatures to develop the chart in Figure 5.32. Although the trends show a low regression R^2 = ±0.75, trends appear linear.

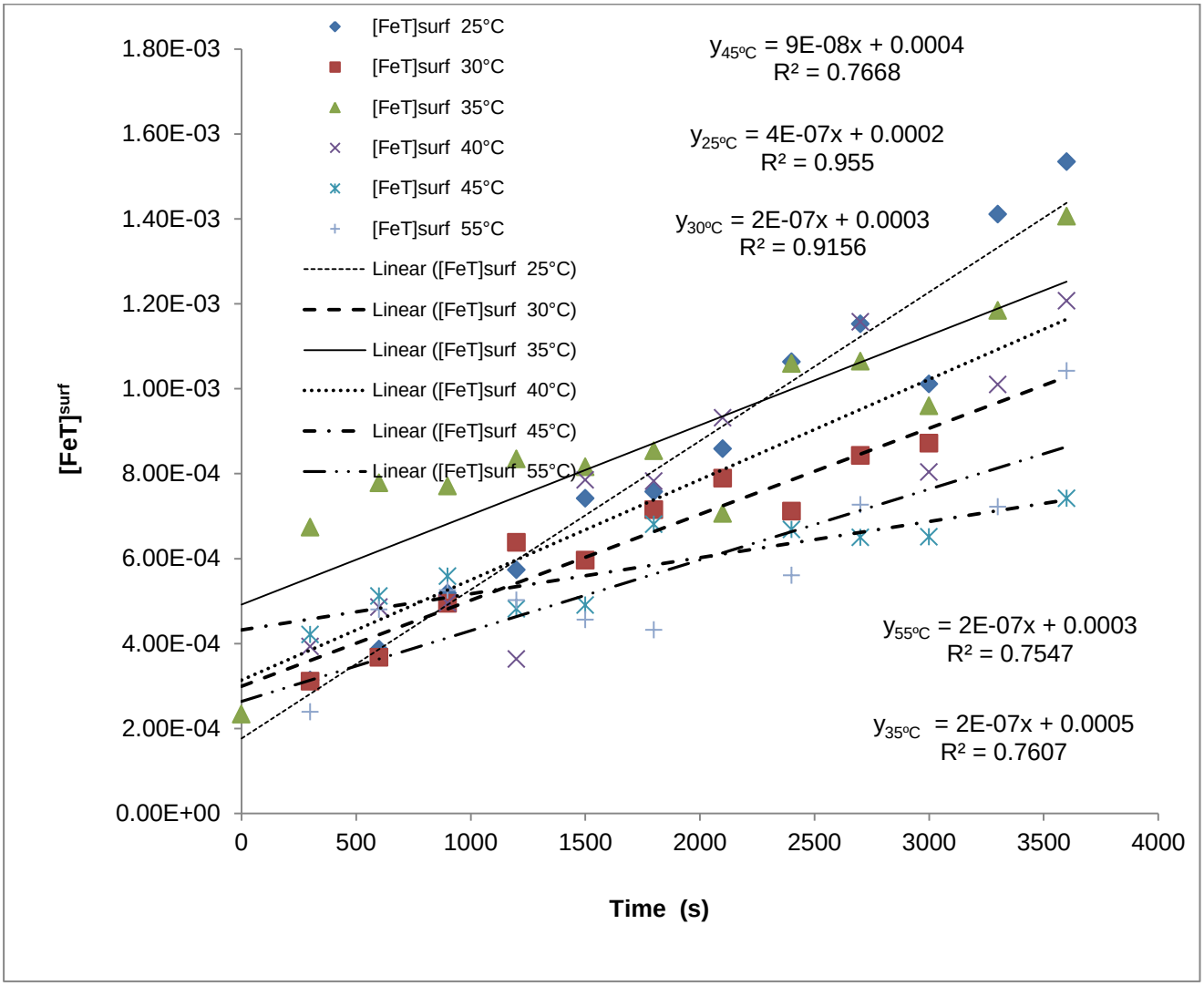

Figure 5.32 The Total Iron Concentration Trends

The low R^2 value maybe due to the curvature in the beginning of the EC for experiments at 35°C; 40°C; 45°C; 50°C, and 55°C. Experiments at 25°C and 30°C have straight lines with R^2 > 0.9 as expected (Faraday's Law).

5.9 Residual Ferrous Iron

Figure 5.33, residual ferrous irons follow similar trends as that of total iron but in opposite directions such that peaks in total iron are troughs in the ferrous trends. This is expected because ferrous iron reacts with various species in the effluent including water and oxygen forming various total iron products as shown in Figure 5.33. Ferrous iron was produced in the first 5 minutes and was then consumed in the next 15 minutes for experiments at 25^{o}C; 30^{o}C; 40^{o}C; 45^{o}C and 50^{o}C shown Figure 5.33. This was followed by gradual rise of concentrations of ferrous iron to maximum concentrations at about 1200s and 2400s for all experiments and dropping to below 1.0x10^{-5} mol/L for some experiments as shown in Figure 5.33.

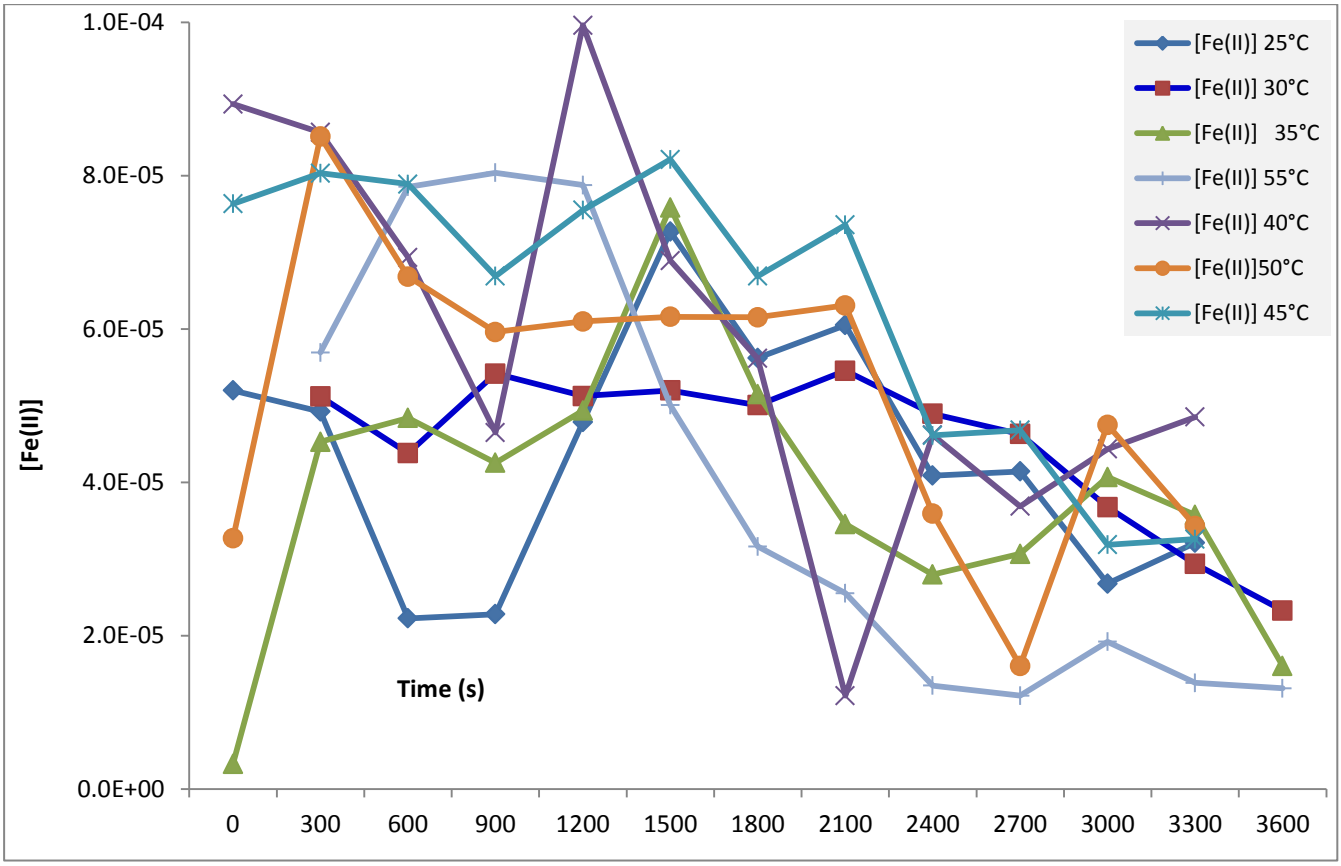

Figure 5.33 Residual Ferrous Iron

Chapter 6 : SUMMARY OF FINDINGS AND CONCLUSIONS

6.1. Summary of Textile Effluent Characterization

6.1 Conclusions about Characterization of Textile Effluent Using Commercial Sample Dyeing Machines

The reactive dyebath textile effluents originating from cotton pre-bleaching and dyeing with reactive dyes by commercial sample dyeing machines were characterized and found to have the following levels of pollution: The highest pH effluent was 11.6 ± 4.0 at 10:1 and 10.9 ±1.89 at 20:1 liquor ratios. The electrical conductivity and the TDS were 14.9 mS/cm ± 6.4 and 8.8 mg/LTSS ± 4.8 at 10:1 and 13.1 mS/cm ± 6.3 and 6.5 mg/LTSS ± 3.1 at 20:1.

- Turbidity and total suspended solids also varied from sample to sample: 133 ±52 NTU and 162.0 ±28 TSS for 10:1 and 37 NTU ± 13, 81 mg/L TSS ± 11
- 3873 mg/L COD ±525 and 2048 mg/LCOD ±356 for 10:1 and 20:1 liquor ratios.

A batch monopolar iron EC with 6 stainless steel 318 SS electrodes treated a 3.5 litre reactive dyes textile effluents coming out of the 20:1 liquor ratio dyeing. The 20:1 reactive dyeing textile effluents were characterised before EC and was found to have the following initial average and standard deviations values:

- pH_i between = 3 and 6 ±1, after adjustment to low starting pH electrocoagulation
- Conductivity κ_i of about = 8.9 mS/cm ±2.8;
- Resistivity (ρ_i) = 134.0 Ω.m ±55.8;
- COD_i = 2527 mg/LO_2 ± 601;
- Absorbance = 2.8 ± 0.60;
- True Hazen Colour (Pt-Co) = 4783, Pt-Co ± 1079;
- Turbidity = 74 NTU ± 20
- Total Suspended Solids (TSS) = 82 mg/L ±26
- Chlorides =128 mg/L ±56.0

The batch monopolar iron EC reactor was successful in treating textile effluents originating from cotton pre-bleaching and reactive dyes dyeing processes to lowest final treated effluent concentrations levels as follows:

- Conductivity κ_i stayed relatively constant with a small decrease in the low temperature range and a small increase in the high temperature range but averaged at = 9 mS/cm ±2.
- A slight decrease is resistivity (ρ_o) to 102 Ω.m, ±23.
- COD_0 = 732 mg/L ±293 with average 72% ±6; removal efficiency and a maximum, 81% at 40ºC.
- Absorbance = 0.1±0.04; at 98.0 % ±1.2 removal efficiency, Maximum 99% at 30ºC; 35ºC and 50ºC. Saravanan, *et al*., (2010) achieved more than 95% colour removal.
- True Hazen Colour (Pt-Co) = 418.3 Pt-Co ± 207.5; at 91.2% ±4.1 removal efficiency
- Turbidity = 20.2 NTU ± 11.5 at 72.6% ±15.4 removal efficiency and 89% maximum at 35ºC.
- Chlorides were removed to an average of 22.2 mg/L ±17.8 at 84.5% ±12.6, maximum removal efficiency of 99% at 25ºC.
- The pH was raised to pH_f = 8.0 ±0.7

Maximum COD removals could be achieved in 30 minutes and at low range temperatures between 25°C and 40°C to about 500 mg/LCOD with 81% removal, similar to findings of Arslan-Alaton *et al.* (2007). Kobya *et al.* (2003) required about 30 minutes for a good efficiency rate with iron electrocoagulation.

The final COD concentration was 500 mg/L and it was within some agencies' environmental limits from textile mills (Savin & Butnaru, 2008), 485 mg/L COD, (Azzi, *et al*., 2006) and 1632 mg/L COD (Naeem, *et al*., 2009). Our own Environmental Authority, DWA-SA, is very stringent (DWAF, 1996) 30-75 mg/L COD. The closest COD limit to that of DWA-SA was 80 mg/L COD, quoted in Yusuff and Sonibare (2004) for the FMENV[16]. In addition, 99% hazen and absorbance removals were achieved at 35°C, 40°C and 45°C as was in the case of Arslan-Alaton *et al.* (2007). In this research, 99% colour removals were achieved at 30°C, 40°C and 45°C.

Up to 7.03 $x10^{-3}$ g/L t-Fe dissolved residual iron was recorded towards the end of the electrocoagulation. The most successful experiments in this research were at 40°C with initial pH of 3.7. 40°C is an environmentally allowable temperature standard for some textile mills

[16] Federal Ministry of Nigeria Environmental because the study took place in Nigeria, abbreviation was not described in the paper.

(Savin & Butnaru, 2008)[17] (Naeem, *et al*., 2009)[18]. It had been shown that; in iron EC the pH is a very strong parameter for EC efficiency, as was the case in the study of iron EC by Larue (2003). It can be concluded that pH must be controlled during the iron EC pH adjustment of initial pH should be made before EC starts and avoiding pH adjustment during EC as this has a potential of dissolving the already formed ferric products and floccs within electrocoagulation. The iron EC was able to swing pH while the iron EC was in progress to a pH above 6.0, a minimum pH at which ferrous and ferric precipitates could automatically form. The lowest values of TSS of about 32 NTU and were achieved with the experiment at 45^{o}C and could have passed the US-EPA (35.2) but failed our DWA-SA (25.0 mg/L) and ISO (AAFA)[19], 2010 (30mg/L).

6.2 Conclusion about Reaction Kinetics Studies and Validation of Assumptions

The main objective of this study was to determine the reaction constants (k_c) of various parameters such as COD, Absorbance, Chlorides and free chlorines and consequently their activation energies (E_A). The temperature range over which the activation energy determination was to be performed was chosen based on typical real textile effluents temperatures existing dyehouses and textile mills.

In the theoretical section (Chapter 3), various assumptions were made about the reaction kinetics in electrocoagulation that EC reaction rates are elementary, homogenous, irreversible and obey Arrhenius law plot. Perhaps these were over assumptions as k_c values were found to be out range or produced curvatures when fitted with the Arrhenius Law plots. The deviations from Arrhenius law plot while determining the Activation energy were used to discuss the overall reaction kinetics. Eyrings plot was further used to determine other thermodynamics parameters such as enthalpy, entropies and Gibbs free energy of the transition state. The success for the determination of these parameters was used as a gauge to confirm successes of the reaction kinetics studies and discuss the deviations that were noted. The determinations of reaction constants were successful and they follow first order reaction model with respect to COD, chloride, total chlorine and absorbance removal.

[17] Based on NTPA standard but the acronym was not described in (Savin & Butnaru, 2008), Probably Romanian Environmental protection Agency
[18] For the Pakistan environmental agency
[19] Global Textile Effluent guidelines used by WHO, European National Standards and US-EPA

Although, literature convincingly influenced the conclusions made in this research that the COD and Absorbance removal follow first order reaction kinetics (Arslan-Alaton, *et al*., 2007; Rajkumar & Kim, 2006, Martinez, *et al*., 2012 and Hmani, *et al*., 2012); the data in this research also gave close fit into the second order model for COD removal and zero order for absorbance removal. As previously described in section 3.1.1, (Nauman, 2002) and Sparks, (1999) used Arrhenuis plot deviations to conlude on the conflicting reaction order models. The second order model was possible for COD removal, because on the contrary, other research reported second order model for electrocoagulation, conventional chemical coagulation and flocculation studies (Pernitsky, 2003, Rincon, 2011, Vasudevan, *et al*., 2009 and Mahmoud & Ahmed, 2014). Chemical coagulation and flocculation are integral mechanisms in electrochemical coagulation.

It was determined whether, the reaction kinetics were mass transfer controlled or not by calculations of current efficiency and limiting current density and it was concluded that iron EC reactions were mass transfer controlled. Mass transfer controlled reaction rates do not obey Arrhenius law and Eyring law plots (Bard & Faulkner, 2000; Clayden , 2000 and Nauman, 2002). The reaction rates are different for the temperatures of 25°C; 30°C; 35°C and 40°C with k_c values ranging between -1.17 x10^{-4}/s and -1.51 x10^{-4}/s and reaction rates at 45°C; 50°C and 55°C with k_c values ranging between -3.19x10^{-4}/s to -4.69 x10^{-4}/s. It was impossible to determine reaction rate constant for some parameters such as; free chorines, ferrous and ferric ions from bulk concentration because they did not fit any model.

This is possible because they might be multiple reaction mechanisms in EC including adsorption and mass transfer activities (Nauman, 2002; Schmidt, 1998 and Sparks , 1999). This might be caused by passivation. There were evidences of passivation on the electrodes surfaces especially for the cathodes at high temperatures. The electrodes appeared black after electrocoagulation. The black colour could be other forms of iron oxide called black oxides mainly magnetite (Fe_3O_4) (Reade(R), 2014) or $FeO{\cdot}Fe_2O_3$, (FAO, 2014). Fe_3O_4 is used as a commercial black pigment 11 (C.I. No.77499)) (FAO, 2014). However, the cathodes and anodes were alternated between runs to remove passivation but this could be the reasons for poor performance of some experimental runs and low current efficiencies.

Faster reaction rate takes place at lower temperatures range, probably due kinetic controlled reactions because Activation energy of 13.2 kJ/mol) ≤ 25 kJ/mol (Robertson, *et al*., 2005) and slow COD removal reactions rates at higher temperatures range with activation energy due to kinetic controlled reaction rates at activation energy of 34.4 ≥ 25 kJ/mol (Robertson, *et*

al., 2005). Chlorides removal reaction rate follow first order model. The kc values varied between 7.0x10^{-4}/s at 25ºC and 4.0x10^{-4}/s at 45ºC with overall activation energy of 32 kJ/mol, same as the enthalpy of reaction ($\Delta H^{\#}$) of the transition state. The enthalpy of reaction ($\Delta H^{\#}$) is positive indicating that the reactions are endothermic. The overall activation energy for chlorides (32 kJ/mol) is almost the same as that of COD (34 kJ/mol) at experimental temperatures between 45°C and 55°C. The reaction kinetic regression values were low for experiments at 50ºC and 55ºC and their reaction kinetic data ultimately failed to fit, the model neither the first order nor the second order reaction kinetics. However, the reaction kinetics data for chlorides obeyed Arrhenius plots.

The absorbance removal followed first order reaction kinetics with k_c values ranging from 7.71 x10^{-4}/s to 1.69 x 10^{-3}/s and -39 kJ/mol and -42 kJ/mol of activation energy and the enthalpy of reaction respectively. The zeroth order reaction constants are for total chlorines. They range from 1.4 x10^{-8} at 25ºC to 2.25 x10^{-8} at 50ºC. The total chlorine reactions required activation energy, enthalpy and entropy of the transition state of -15.7 kJ/mol; -13.3 kJ/mol and -438.8 J/K respectively.

Limiting current density plots showed plateau that normally indicate regions of mass transfer activities at which maximum limiting current densities were estimated and to be about -1.8 x10^{-3} A/cm^2 to -1.4 x10^{-3} A/cm^2 for both chlorides and COD removals. These limiting current densities were found to be less than the applied current density of 9.75 x10^{-3} A/cm^2 and the reaction rates were mass transfer controlled. The k_m is very important because it was used to determine the limiting current density (i_L). The i_L was useful for determination of concentrations of species at the surface of the electrodes and the concentration overpotential, E_{conc}. The low current efficiencies, high concentration overpotentials and high limiting current densities could have been contributed by the following:

- The electrolyte was dirty (effluent).
- Progressive deposition of iron into the bulk of the solution without its removal (batch reactor).
- The cathode surfaces were not smooth; therefore, a passivation layer could easily be deposited.
- Complex colloids formation floccs by electrostatic processes, producing stable Colloids (less charged ions than before at the beginning stage of the electrocoagulation).
- Precipitates were less charged and hence less conductivity than before.

- Formation of gaseous electrolysis products like oxygen, hydrogen and chlorine gases that hinder charge transfer (electrons) and ions at the surface of the electrodes, as was evident by bubbles at surface of the electrodes.
- Electro-active species that contribute to conductivity are transformed into products such as metal chlorides and chlorine gases hence conductivity decreased during electrocoagulation.
- A lot of electrolysis employed in generating heat, leading to thermal overpotential.
- The surfaces of the electrodes were treated before electrolysis.

6.3 Recommendations

As it seems, EC reactor performance was affected by pH (favoured low initial pH_i but how low?); and EC time (15 to 35 min); temperatures between 25°C and 40°C and high conductivities. The interaction of these parameters to achieve the optimum operating conditions needs to be established. The iron EC experiments were performed at constant applied current density (i_A); may be the reactor could have performed better at higher current densities. There seemed to be secondary NTU and TSS contaminations of the treated effluent water by the accumulations of sludge, perhaps, the electrocoagulators can be made narrow (tall) so that sampling can the done in the middle where there is less sludge or the reactor could have an extended conical bottom for temporary accumulation or recovery of sludge.

Electrochemical dozing of coagulant (electrodes dissolution) needs be monitored such as by online analyses or further studies of reactor modelling to avoid excessive electrode dissolution that may contaminate treated effluents. Passivation of electrodes could be the reasons for poor performance of the some experimental runs and low current efficiencies. The electrocoagulator power supply needs to be a pulsing DC supplier so that the electrodes can be automatically alternated by a DC programmable rectifier (Cifuentes, *et al*., 2001)

REFERENCES

1 Abdel-Aal, A. K., Zohdy, K. M. & Kareem, A. M., 2010. Hydrogen Production Using Sea Water Electrolyses. The Open Fuel Cells Journal, 2010,, Volume 3, pp. 1-7.

2 Abdel-Gawad, S. A., Amin, B. M. & Kawther , A., 2012. Removal of Some Pesticides from the Simulated Waste Water by Electrocoagulation Method Using Iron Electrodes.. International Journal of Electrochemical Science, Volume 7, pp. 6654 - 6665.

3 Acar, F. N. & Eren, ,. Z., 2006. Adsorption of Reactive Black 5 from an aqueous solution equilibrium and kinetic studies. Desalination, Volume 194, p. 1–10.

4 Adinew, B., 2012. Textiel Effluent Treatment and decolourization Techniques – A Review. Chemistry: Bulgarian Journal of Science Education, Volume 21, Number 3, 2012.

5 Ahmed , S. N. & Saad , A. A., 2013. Combination of Electrocoagulation and Electro-Oxidation Processes of Textile Wastewaters Treatment. Civil and Environmental Research, 3(13), pp. 61 - 74.

6 Ali, N., Abdul, H. & Ahmed, S., 2009. Physiochemical characterization and bioremediation perspective of textile effluent dyesand metals by indigenous bacteria. Journal of Harzadous Chemicals, Volume 164, p. 322–328.

7 Alinsafia, A., et. al., 2005. Electro-coagulation of reactive textile dyes and textile wastewater. Chemical Engineering and Processing , Volume 44, p. 461–470.

8 Arslan, I., et. al. 2001 . Treatability of a simulated disperse dye-bath by ferrous iron coagulation, ozonation, and ferrous iron-catalyzed ozonation. Journal of Hazardous Materials(, Volume B85 , p. 229–241.

9 Arslan-Alaton, I., Kabdas¸ Hanba, I., Deniz & Kuybu, E., 2007. Electrocoagulation of a real reactive dyebath effluent using aluminum and stainless steel electrodes. Journal of Hazardous Materials, Volume 150, p. 166–173.

10 Aslam, M. M. et al., 2004.. Textiel wastewater characterization and reduction of its COD & BOD by oxidation. Electronic Journal of Environmental; Agriculture and Food Chemistry, 3(6), pp. 804-811.

11 Asouhidou, D. D., Triantafyllidis, K. S., Lazaridis, N. K. & Matis, K. A., 2009. Absoption of Remozol Red 3BS from acqueous solutions using APTES- and cyclodextrin -modified HMS mesoporous silicas.. Volume 346, pp. 83-90.

12 Avlonitisa I, S. A. et al., (2008). Simulated cotton dye effluents treatment and reuse by nanofiltration. Desalination, Volume 221, p. 259–267.

13 Azzi, M., Saib, E. N. & Zaroul, C. Z., 2006. Contribution to the study of electro coagulation mechanism in basic textile effluent". Journal of Hazardous Materials. , Volume B 131, pp. 73-78.

14 Babu, R. R. et al., 2007. Treatment Of Tannery Wastewater By Electrocoagulation. Journal of the University of Chemical Technology and Metallurgy,, 42(2), pp. 201-206.

15 Bamford, C. H., Tipper, C. F. & Compton, G. R., 1986. Electrode Kinetics: Principles and Methodology: Principles and Methodology. s.l.:Elsevier.

16 Banchuen, T., 2002. Oxidation-Reduction (REDOX) Reaction Potentials.

17 Barclay, S., Buckley, C., Foure, P. & Lun, ,. K., 2005. Cleaner Production in Textile Manufacture – Results of Cleaner Textile Production Project and activities to create an ongoing awareness and demand for Textile Products produced in a more environmentally responsible manner..

18 Bard, A. J. & Faulkner, L. R., 2000. Electrochemical Methods : Fundamentals and Applications. Second Edition ed. s.l.:Johny Wiley.

19 Barrow, G. M., 1988. Physical Chemistry, 5th edition. s.l.:s.n.

20 Barrow, G. M., 1988. Physical Chemistry. New York: McGraw Hill.

21 Beagles , 2004. Electrocoagulation (EC) – Science and Applications.

22 Beesabathuni,, S. N. *et al*., 2013. Modeling of the Electrical Current of the Polyaniline.

23 Bonakdarpour,. B, V *et al,* 2011. Comparison of the performance of one stage and two stage sequential anaerobic biological processes for the treatment of reactive-azo-dye-containing synthetic wastewaters. International Biodeterioration & Biodegradation, Vol. 65, pp. 591 -599.

24 Canizares, P.,et. al., 2004. Combined adsorption and electrochemical processes for the treatment of acidic aqueous phenol wastes. Journal of Applied Electrochemistry : 1, . 111, Volume 34, p. 11–117.

25 CCT, 2007. Long-term water conservation and water demand management strategy:water & sanitation, Cape Town: Government, Available Online .

26 Cecil, S., 2010. Determining Activation Energy of activation Parameters from Dynamic NMR. In: Physical Chemistry - Mechanisms of Chemical Reactions. s.l.:s.n.

27 Chaturvedi, 2013. Electrocoagulation: A Novel Waste Water Treatment Method. International Journal of Modern Engineering Research (IJMER), 3(1), pp. 93-100.

28 Chen, G., 2004 . Electrochemical technologies in wastewater treatment. Separation and Purification Technology , Volume 38, p. 11–41.

29 Cheng, H. et al., 2006. Preatment of wastewater from traizine Manufacturing by coagulation electrolysisand internal microelectrolysis. Journal of Hazardous Materials, 146(1–2), p. 385–392.

30 Chequer, F. M. et al., 2013. Textile Dyes: Dyeing Process and Environmental Impact. Intech Open Source, pp. 151 - 176.

31 Cho, K. et al., 2014. Effects of Anodic Potential and Chloride Ion on Overall Reactivity in Electrochemical Reactors Designed for Solar-Powered Wastewater Treatment. Environmental Science Technology, Volume 48, p. 2377–2384.

32 Cifuentes, ,. L., Torrealba, J. & Crisós, G., 2001. Production of Ferric Hydroxide by Anodic Dissolution of Carbon Steel.

33 City of Cape Town, 2006. City of Cape Town Wastewater and Industrial Effluent Bylaw, Cape Town: s.n.

34 Clariant Colour Chronicle, 2005. Optimization of exhaust dyeing processes for cotton with reactive dyes., s.l.: Clariant.

35 Clark, M., 2011. Handbook of Textile and Industrial Dyeing: Principles, Processes And Types.. s.l.:Woodhead Publishing Limited.

36 Clayden , J., Greeves, N., Warren , . S. & Wothers, P., 2000. Organic Chemistry. 2ND ed. s.l.:Oxford University Press.

37 Daneshvar, N., et. al, 2006. Decolariztion of basic dyes solutions by Electrocoagulation: An investigation of the effect of operational parameters.Journal of Harzadous Material B129 (2006) 116-122.. Journal of Hazardous Materials (2006), October, Volume B129, p. 116–122.

38 Danilov, F. I., Pretsenko, V. S. & Ubiikon, A. V., 2004. Kinetic regularities governing the Reaction of electrocoagulationof iron From solutiona of citrate complexes of Iron (III). Russian Journal of Electrochmistry, 27 December.pp. 1439 - 1446.

39 Davis, M. L. & Cornwell, D., 2008. Introduction to Environmental Engineering. 5th ed. s.l.: McGraw-Hill.

40 del Río, A. I., Molina, . J., Bonastre, J. & Cases , . F., 2009. Influence of electrochemical reduction and oxidation processes on the decolourisation and degradation of C.I. Reactive Orange 4 solutions.

41 Drouiche, N. et al., 2009. Study on the treatment of photovoltaic wastewater using electrocoagulation:Fluoride removal with aluminium electrodes. Characteristics of products. Journal of Hazardous Materials , Volume 169, p. 65–69.

42 DWAF, 1996. South African Water Quality Guidelines : Industrial wate Use, Pretoria: Department of Water Affairs and Forestry.

43 DWAF, 1997. Draft White paper on Water Services,, s.l.: s.n.

44 DWAF, 1999. National Water Act Act No 36 of 1998, Pretoria: Government Gazette 20615 12 November 1999.

45 DWEA, 2010. National Environmental Management ACT. 1998, PRETORIA: s.n.

46 DyStar, 2007. DyStar's newest innovative systems for scouring, and bleaching of cellulosic fibers., s.l.: s.n.

47 DyStar, 2010. Sustainability in textile processing: Machinery manufacturer collaborations. s.l.:s.n.

48 Ebru, O., 2007. . An alternative method for the removal of surfactants from water: Electrocoagulation.. Separation and Purification Technology (2007)., Volume 52, pp. 527-532.

49 Econometric Institute, 2000. A Framework For Response Surface Methodology For Simulation Optimization, Rotterdam: Econometric Institute.

50 El-Shazly , A., Al-Zahrani , A. & Alhamed, Y., 2013. Kinetics and Performance Analysis of Batch Electrocoagulation Unit Used for the Removal of a Mixture of Phosphate and Nitrate Ions from Industrial Effluents.. International Journal of ectrochemical science.

51 El-Shazly, A. H. & Daous , M. A., 2013. Investigation and Kinetics Study for the Effect of Solution Flow Rate on the Performance of Electrocoagualtion Unit Used for Nutrients removal. International Journal of Electrochemistry.

52 Ersoy, B., Tosun, I., Gunay, A. & Dikmen, S., 2009. Turbidity removal from Wastewater of Natural Stone processing by Coagualtion/flocculation Methods. Clean, Volume 37, pp. 225-232.

53 Essadki, A. H. et al., 2007. Electrocoagulation/Electroflotation in an external-loop airlift reactor - Application to the decolarisation of Textiel dye wastewater.: Acase study. Chemical Engineering and Processing, 19 April, Volume 47, pp. 1211 - 1223.

54 Essadki, A. H., 2014. Electrochemical Probe for Frictional Force and Bubble Measurements in Gas-Liquid-Solid Contactors and Innovative Electrochemical Reactors for Electrocoagulation Electrocoagualtion/Electroflotation .

55 FAO, 2013. FAO. http://www.fao.org/[Online][Accessed 04 10 2014].

56 FAO, 2014. http://www.fao.org/(Accessed 02 2014].

57 Fil, B. A., Yilmaz, et al., 2014. Investigation of adsortion of dyestuff Astrozon Red Violet 3RN (Basic Violet 16) on Montmorillonite clay. Brazilian Journal of Chemical Engineering, Volume 31, pp. 171 - 182.

58 Fogler, S. H., 2006. Elements of Chemical Reaction Engineering. Michigan: Pearson Education International.

59 Fouad, Y., 2008. Performance of an electrocoagulation cell with horizontally oriented electrodes in

oil separation compared to a cell with vertical electrodes. Chemical Engineering Journal. .

60 Ganesan, , P., Lakshmi,, J., Sozhan, G. & Vasudevan, S., 2012. Removal of Manganese from Water by Electrocoagulation: Adsorption, Kineticsand Thermodynamic Studies.

61 Geethakarthi, A. & Phanikumar, B. R., 2011 . Characterization of the textile anthraquinone dye Reactive Blue 4. International Journal of Water Resources and Environmental Engineering , 3(1), pp. 1-9.

62 Gendel, Y. & Lahav, O., 2008. A New approach to increasing the Efficiency of low-pH Fe-electro-coagulation applications. Journal of Hazadous Materials , pp. 1 - 28.

63 Ghanim,, . A. N. & Ajjam , S. K., 2013. Modeling Of Textile Wastewater Electrocoagulation Via Adsorption Isotherm Kinetics. The Iraqi Journal For Mechanical And Material Engineering, , 2013, Vol.13, (No.1).

64 Gilfillan, C. M., 1997. Water and Effluent Management in the South African Textile Industry, Durban: University of Natal.

65 Grygar, T., 1995. Kinetics of electrochemical reductive dissolution of iron (III) hydroxy-oxides. Academy of Sciences of the Czech Republic, Volume 60, pp. 1261 - 1273.

66 Gurses, A., Yalcina, M. & Dogarb, C., 2002. Electrocoagulation of some reactive dyes: a statistical investigation of some electrochemical variables. Waste Management 2002, Volume 22 , p. 491– 499.

67 Hach, 2007. A To Z Hach Chemical Analysis User Manual. S.L.:Hach Company, 2007.

68 HACH, 2007. A to Z procedures for DR2800, Available online, www.hach.com, s.l.: s.n.

69 HACH, 2013. Chlorination, Chloramination And Chlorine Measurement , s.l.: s.n.

70 Hamdaoui, M., Charfi, A. & Khoffi , F., 2012. Study of the Dyeing Kinetics: Influence of Pre-Treatments and Woven Fabric Structure. s.l.:s.n.

71 Harp, D. L., 2002. Current Technology of Chlorine Analysis for Water and Wastewater, s.l.: Hach Company.

72 Hector, A. et al., 2009. Electrochemical Reactions for Electrocoaguation Using Iron Electrodes. Industria Engineering Chemistry, 14 01.pp. 2275 - 2282.

73 Henrik , H., et. al., 2006. Electrocoagulation as a remediation tool for wastewaters containing arsenic. Minerals Engineering.. pp. 521–524.. Journal of Environmental Management, 151(C), pp. 326-342..

74 Hmani , E., et. al., 2012. Electrochemical degradation of auramine-O dye at boron-doped diamond and lead.

75 Hokmes-Farley, R., 2008. Reef Aquarium Water Parameters. Available Online, at: http://reefkeeping.com, [Accessed 03 11 2011].

76 Holt, P. K., Barton, G. W. & Mitchell, C. A., 2004. The future of electrocoagulation as a localisedwater teratement. Chemosphere, 19 October, xxx(xxx), pp. 1-13.

77 Holt, P., 2002. Electrocoagulation: Unravelling And Synthesising The Mechanisms Behind Awater Treatment Process, Sydney: University of Sydney.

78 Hong, X. U. et al., 2008. Effect of configuration on Mass Transfer in a Filter-press Type Electrochemical Cell. Chinese Journal of Chemical Engineering.

79 Hong, X., Huang, W. & Xing, Y., 2008. Effect of configuration on Mass Transfer in a Filter -press Type Electrochemical Cell.

80 Hussain, T., 2012. Exhaust Dyeing with Reactive Dyes. Availble Online.https://www.academia.edu. , [Accessed 10 04 2015].

81 IC Controls, 2005. CHLORINE THEORY & MEASUREMENT, s.l.: IC Controls.

82 Jiang, J.-Q., 2002. Laboratory study of electro-coagulation–flotation for water treatment. Water Research., Volume 36, p. 4064–4078.

83 Jiang, J.-Q., Grahama, N. & Andrea, C., 2002. Laboratory study of electro-coagulation–flotation for water treatment. Water Research , Volume 36, p. 4064–4078.

84 Joshi, M., Bansal, R. & Purwar, r., 2003. Colour Removal from Textile effluents. Volume 29.

85 Kazakevičiūtė, G., et. al., 2004. Reducing Pollution in Wet Processing of Cotton/Polyester Fabrics.

86 Khue, V. A. et al., 2014. Removal of copper and fluoride from wastewater by thecoupling of electrocoagulation, fluidized bed andmicro-electrolysis (EC/FB/ME) process.

87 Kim, T.-H.,et. al., (2004. Comparison of disperse and reactive dye removals by chemical coagulation and Fenton oxidation. Journal of Hazardous Materials, Volume B112, p.95–103.

88 Kobya, M. et al., 2006 . Treatment of potato chips manufacturing wastewater by electrocoagulation. Desalination , 17 October, Volume 190 , p. 201–211.

89 Kobya, M., Bayramoglu, M. & Can, T. O., 2003. Decolorization of Reactive Dye Solution by Electrocoagulation Using Aluminium electrodes. Volume 42, pp. 3391 - 3396.

90 Kobya, M., et. al., 2007. Techno-economic evaluation of electrocoagulation for textile wastewater usind different electrodes. journal of Hazadous Materials , 17 February, Volume 148, pp. 311v - 318.

91 Kurt, U., Gonullu, R. T., Ihlan, F. & Varinca, K., 2008. Treatment of domestic wastewater byy Electrocoagulation in a cell with Fe-Fe electrodes..

92 Lacasse, K. & Baumann, W., 2001. Textile Chemicala : Environmental Facts and Data. s.l.:Springer.

93 Lahav, O. & Levi, N., 2009. Kinetic investigation of low-pH Fe(II) oxidation and the development of a method for Fe(III) generation as part of process aimed at H2S removal.

94 Lakshmana, D., Clifford, D. & Gautam, S., 2009. Ferrous and Ferric Ion Generation During Iron Electrocoagulation.

95 Larue, O. e. a., 2003. Electrocoagualtion and coagulation by iron of latax particles in aqueous solution.. Separation and Purification Technology , Volume 31, pp. 177-192..

96 Lechevallier, M. W.,et. al, 1981. Effect of Turbidity on Chlorination Efficiency and Bacterial Persistence in Drinking Water. Applied And Environmental Microbiology,,Vol. 42,(1), pp. 159-167.

97 Lekhlif, B. et al., 2013. Study of the electrocoagulation of electroplating industry wastewaters charged by nickel (II) and chromium (VI).

98 Levenspiel, O., 1999. Chemical Reaction Engineeing. s.l.:s.n.

99 Lopes, A. et al., 2004. Degradation of a Textile Dye C.I. Direct Red 80 by Electrochemical Processes.

100 Maharaj, D., George, . W. & Buckley, C., 2002. Cleaner Production In The Textile Industry Lessons From The Danish Experience, s.l.s.n.

101 Mahmoud, S. S. & Ahmed, M. M, 2014. Removal of surfactants in wastewater by electrocoagulation method using iron electrodes. Physical Science Research International , 2(2), pp. 28 - 34.

102 Mahmoud, S. S. & Ahmed, M. . M., 2014. Removal of surfactants in wastewater by electrocoagulation method using iron electrodes.

103 Mahvi, A. H., 2007. Removal of Cadmium from Industrial Effluents by Electrocoagulation Process Using Aluminium Electrodes. World Applied Sciences Journal , pp. 34-39,.

104 Martinez, G. F. et al., 2012. Kinetic Aspect of Gold and Silver Recovery in Cementation With Zinc Power and Electrocoagulaytion Iron Process.

105 Mazumder, D., 2011. Process eveluation and treatability of wastewater in a Textile Dyeing Industry. International Journal of Energy and Environment .

106 Mbolekwa, Z. & BUCKLEY, C. A., 2008. The Removal Of Reactive Dyes From Dye Liquor Using Activated Carbon For The Reuse Of Salt, Water And Energy.

107 McGraw-Hill , 2008.

108 Merck, 2011. Programming data for Spectroquant Test Kits for DR2800 DR3800 and DR3900 photometers from Hach, s.l.: MERCK.

109 Mollah, M. Y. et al., 2004. Fundamentals, present and future perspectives of electrocoagulation. Journal of Hazardous Materials, Volume B114 , p. 199–210.

110 Montiel, V., 2008. Electrocoagulation of a synthetic textile effluent powered by photovoltaic energy without batteries: direct connection behaviour.. Volume 92, pp. 291-297.

111 Moore, W. J., 1983. Basic Physical Chemistry. USAPrentice Hall International : s.n.

112 Moraes, ,. P. B. & Bertazzoli, R., 2005. Electrodegradation of landfill leachate in a flow electrochemical reactor. Chemosphere, Volume 58 , p. 41–46.

113 Moran, C. e. a., 1997. Effects of sewage treatment on textile effluent.. pp. 272-274.

114 Moreno-Casillas, H. A. et al., 2007. Electrocoagulation mechanism for COD removal. Separation and Purification Technology, Volume 56, p. 204–211.

115 Mrowiec, B., 2010. The Impact Of Textile Wastewater On Nutrients Removal.

116 Myron L, C., 2010. Oxidation Reduction Potenitial.

117 Naeem, A., et. at, 2009. Physiochemical characterization and bioremediation perspective of textile effluent dyesand metals by indigenous bacteria. Journal of Harzadous Chemicals.

118 Nauman, B. E., 2002. Chemical Reactors, Design, Optimization and Scale up. New York s.n.

119 Ntengwe, F., Mazana, N. & Samadi, F., 2010. The effect of impuries and other factors on the Current Density in electro-Chemical Reactors. 2(2), pp. 1289 - 1300.

120 Ntuli, 2009. Characterization of Effluent from Textile Wet Finishing Operations. World Congress on Engineering and Computer Science. Vol. 1

121 OilTrap Environmental INC, 2011. Electrocoagulation Stormwater Treatment : The Future of Water Treatment, Tumwater, USA: OilTrap Environmental.

122 Okafor, J. O., 2011. physico-chemical characteristics of effluents from garri processing industries in bida, niger state, nigeria. Bayero Journal of Pure and Applied Sciences,, 4(2), p. 150 – 154.

123 Panizza , M. & Giacomo , 2010. Applicability of electrochemical methods to carwash wastewaters for reuse.Part : Anodic oxidation with diamond and lead dioxide anodes.

124 Papagiannakis, I., 2005. Studying and Improving the Efficiency of Water Electrolysis Using a Proton Exchange Membrane Electrolyser.

125 Parvinzadeh, M. & Najafi, H., 2008. Textile Softeners on cotton Dyed with Direct Dyes: Reflectance and Fastness Assessments..

126 Pernitsky, D. J., 2003. Coagualtion 101. Assiciated Engieering .

127 Pilatowsky, I. et al., 2011. Cogeranation Ful Cell-Soption Air conditioning systems. s.l.:Springer.

128 Pintauro, P. N., 2007. Principles and Applications of Electrochemical Engineering. In: Albright Handbook of Chemical Engineering . s.l.:s.n.

129 Pletcher, D. & Walsh, F. C., 1990. Industrial Electrochemistry. s.l.:Chapman and Hall.

130 Population Institute, 2010. Population.

131 Powell Water Systems, Inc., 2001. Powell Electrocoagulation: Sustainable Technology For The Future, Centennial,: Us & World Wide Patents & Patents Pending.

132 Protsenko , V. S. & Danilov, F. I., 2010. Activation energy of electrochemical reaction measured at a constant value of electrode potential.

133 Purkait, M. K.,et. al. ., 2008. Decolourization of Crystal Violet Solution by Electrocoagulation. Journal of environmental Protection Science, pp. 25 - 35.

134 Quader, A. K., 2010. Treatment of Textile Watewater with Chlorine : An Effective Method.

135 Raghu, S. & Basha, A., 2007. Electrochemical Treatment of Procion Black 5B using cylindrical flow Reactor - A pilot plant study.

136 Rajkumar, D. & Kim, J. G., 2006. Oxidation of various reactive dyes with in situ electro-generated active chlorine for textile dyeing industry wastewater treatment.

137 Raju, B. G. et al., 2008. Treatment of wastewater from synthetic textile industry by electrocoagulation - electrooxidation.

138 Reade(R), SC R., 2014. [Online], Available at: http://www.reade.com/ ; [Accessed: 20-02-2014].

139 Reddy, S. S.,et. al., 2006. The Removal of Composite Reactive Dye from Dyeing Unit Effluent Using Sewage Sludge Derived Activated Carbon. Turkish Journal Engineering Environmental Science, 21 March, Volume 30, p. 367 – 373.

140 Republic of South Africa. DTI, 2007. Industrial Policy Action Plan: Implementation of Government's National Industrial Policy Framework:, Pretoria: RSA government publications.

141 Rincon, G., 2011. Kinetics of the electrocoagulation of oil and grease..

142 Robertson, S., et al., 2005. An Introductory Electrochemical Approach to Studying Hydrometallurgical Reactions.

143 Roy, R. et al., 2010. Characterization of Textile Industrial Effluents and its Effects on Aquatic Life. Bangladesh ournal of Scientific and industrial research, 54(1), pp. 79-84.

144 Sala, M. & Gutiérrez-Bouzán, C., 2012. Electrochemical Techniques in Textile Processes and Wastewater Treatment. International Journal of Photoenergy.

145 Salunke, K. . A., Bhave, P. P. & Mata, M. . D., 2005. Performance Status common effluent treamtent plant, CETP in India. International Journal of Research in Engineering and Technology, 03(09).

146 Saravanan, M., Pabmanavhan, N., Sambhamurthy & Sivarajan, M., 2010. Treatment of Acid Blue

113 Dye Solution Using Iron Electrocoagulation. CLEAN – Soil, Air, Water, 38(5-6).

147 Savin, I.-I. & Butnaru, R., 2008. Wastewater Characteristics in Textile Finishing Mills. Evironmental Engineering and Management Journal , Volume 7, p. 859 to 864.

148 Scherer, M. M., Westall, J. C., Ziomek-Moroz, M. & Tratnyek, P. G., 1997. Kinetics of Carbon Tetrachloride Reduction at an Oxide-Free Iron.

149 Schmidt, L. D., 1998. The Engineering of Chemical reactions. s.l.:s.n.

150 Scholz, F., 2010. Thermodyanamics of Electrochmical Reaction.

151 SEDA, 2012. Research on the performance of the Manufacturing Sector. Samml Enterprice Development Agency.

152 Seif, H. & Malak, M., 2001. Textile Wastewater Treatment. Sixth International Water Technology Conference, IWTC 2001, Alexandria, Egypt.

153 Sengil, A. I. & Ozacar, M., 2008. The decolorization of C.I. Reactive Black 5 in aqueous solution by electrocoagulation using sacrificial iron electrodes.

154 Sheng, H. & Peng, C. F., 1996. Continuous Treatment of textile wastewater by combined coagulation, Electrochemical oxidisation and activated sludge. Water Resource Vol , 587- 592, 1996,. Water Research , 30(3), pp. 587-592.

155 Shi, B. et al., 2007. Removal of direct dyes by coagulation: The performance of preformed polymeric aluminum species. Journal of Hazardous Materials , Volume 143, p. 567–574.

157 Spagni, A., et. al., 2010. Treatment of a simulated textile wastewater containing the azo-dye reactive orange 16 in an anaerobic-biofilm anoxiceaerobic membrane bioreactor. International Bio-deterioration & Biodegradation , Volume 64, p. 676 to 681.

158 Sparks , D., 1999. Kinetics and Mechanisms of Chemical Reactions at the Soils Mineral/Water Interphase.

159 Steininger, J. M. & Pareja, C., 1996. Orp Sensor Response In Chlorinated Water. Volume NSPI Symposium Series Vol. I.

160 Suteu, D. & Bilba, D., 2005. Equilibrium and Kinetic Study of Reactive Dye Brilliant Red HE-3B Adsorption by Activated Charcoal.

161 Tezcan, U., 2006. Electrocoagulation of olive mill wastewaters. Volume 52., p. 136–141.

165 UNICEF, W. H. O. a., 2006. Meeting the MDG drinking water and sanitation target : the urban and rural challenge of the decade..

166 US-EPA, 2013. www.ecfr.gov.. [Online], [Accessed 13 May 2013].

167 Valeedi-Perez, R. et. al.., 2001. Current-voltage curves for an electrodialyses reversal pilot plant: determination of limiting current.

168 Valero, D. et al., 2008. Electrocoagulation of a Synthetic Textile Effluent Powered By Photovoltaic Energy Without Batteries: Direct connection behaviour. Solar Energy Materials & Solar Cells, Volume 92, p. 291–297.

169 Van Hege, K., et. al., 2004. Electro-oxidative abatement of low-salinity reverse osmosis membrane concentrates. s.l.:s.n.

170 Vandevivere, P. C.et. al., 1998. Treatment and Reuse of Wastewater from the Textile Wet-Processing Industry: Review of Emerging Technologies. Journal Chemical Technology and Biotechnology, Volume 72, pp. 289-302.

171 Vasudevan, S.,et. al., 2009. Studies on the Removal of Iron from Drinking Water by Electrocoagulation – A Clean Process. Clean , 37((1)), p. 45 – 51.

172 Venkatesh, S., et. al., 2013. Treatment and Reuse of Dye Wastewater from the Textile Industry A Review of Advanced Treatment Technologies.

173 Vepsäläinen, M., 2012. Electrocoagulation in the treatment of industrial waters and wastewaters.

174 Wamser, C. C., 2000. Organic Chemistry . In: Organic Chemistry . s.l.:s.n.

175 Water Services , 2000. Chemistry at Work.

176 WHO, 1966. Water Pollution Control , Geneva: World Health Organization .

177 WRC, 2010. Water Wheel , s.l.: CSIR.

178 www.100people.org/, 1990. http://www.100people.org/statistics_100stats.php?section=statistics. [Online], [Accessed 12 09 2013].

179 Yildiz, Y. & Koporal A. S, K. B., 2007. Effect of initial pH and supporting electrolyte on the treatment of water containing high concentration of humic acid substances by electrocoagulation.. Chemical engineering Journal .

180 Yousuf, M. et al., 2007. Electrocoagulation (EC)—science and applications. Journal of Hazardous Materials B, Volume B84, p. 29–41.

181 YSI , 2001. Measurng ORP on YSI 6-series, Sondes Tips, Cautions and Limitations, s.l.: YSI Environmental Techincal note.

182 Yun, S.-H.et al., 2012. Estimation of approximate acivation energy loss and mass transfer coefficient from a polarization curve of a polymer fuel cell. Korean Journal of Chemical Engineering, September, 29(9), pp. 1158-1162.

183 Yusuff, R. O. and Sonibare, J. A., 2004. Characterisation of Textile Industries Effluent in Kaduna, Nigeria. p. 217.

184 Zahrim, A. Y., Tizaoui, C. & Hilal, N., 2011. Coagulation with polymers for nanofiltration pre-treatment of highly concentrated dyes: A review. Desalination, Volume 266 , p. 1–16.

185 Zayas, T. et al., 2007. Applicability of coagulation and electrochemical processes to the purification of biologically treated vinasse effluent. Separation and Purification Technology, Vol. 57, p. 270–276.

186 Zhang, X., Xu., W., Shoesmith, D. & Wren, J. C., 2007. Kinetics of H2O2 reaction with oxide films on carbon steel.

187 Zidane, F. et al., 2008. Decolourization of dye-containing effluent using mineral coagulants produced by electrocoagulation. Journal of Hazardous Materials , 21 November 2007, Volume 155, p.153–163.

188 Zoulias, E. et al., 2001. A review of water electrolysis, Greece: European Union.

APPENDICES

Appendices A1 is pre-bleaching and dyeing at a liquor ratio of 20:1 and the data presented comes from triplicates dyeing experiments with averages on top and standard deviations at the bottom for each textile-processing step. The average values are light shaded and the standard deviations are bold shaded.

APPENDIX A.1 Textile pre-bleaching and dyeing at a liquor ratio of 20:1

Prebleaching and Dyeing Steps	pH	Cond	TDS	Resistivity	Turbo	TSS	Absorb
After Pre-bleaching. Average	**13.017**	**16.873**	**8.530**	**59.0**	**212.9**	**224**	
Effluent #_25/10/2011	12.608	15.75	8.016	62.6	162.0	155	
Effluent #_31./05/2011	12.934	18.350	9.315	53.9	30.8	32	
Effluent #7-09/09/2012	13.510	16.520	8.258	60.5	446.0	484	
After Pre-bleaching. STDdev	0.457	1.336	0.691	4.540	212.234	234	
Cold Rinse, Average	**12.137**	**2.111**	**3.044**	**492.0**	**67.0**	**75**	
Effluent #_25/10/2011	12.15	3.708	1.86	269.0	74.1	68	
Effluent #_31./05/2011	12.205	2.624	4.228	117.0	73.9	78	
Effluent #7-09/09/2012	12.055	0.001	5.567	1090.0	52.9	79	
Cold Rinse, ATDdev.	0.076	1.906	1.674	523.430	12.183	6.1	
Effluent after Cold Rinse Average	**12.662**	**7.545**	**2.428**	**134.3**	**102.6**	**120**	
Effluent #_25/10/2011	12.291	7.768	3.917	128.0	113.0	106	
Effluent #_31/05/2011	12.639	8.544	0.197	117.0	47.8	41	
Effluent #7-09/09/2012	13.055	6.322	3.169	158.0	147.0	214	
After cold rinse. STDdev	0.383	1.128	1.968	21.221	50.411	87.4	
Hot Rinse Average	**11.086**	**0.708**	**37.555**	**2542.0**	**24.5**	**37**	
Effluent #_25/10/2011	10.583	1.735	0.868	576.0	21.3	49	
Effluent #_31./05/2011	11.390	0.390	0.197	2550.0	38.2	42	
Sample 3_Date	11.286	0.000	111.600	4500.0	14.0	19	
After Hot rinse. STDdev	0.439	0.910	64.126	1962.0	12.413	15.7	
Effluent. after Hot Rinse, Average	**12.463**	**4.306**	**2.157**	**243.3**	**42.5**	**71**	
Effluent #_25/10/2011	**12.085**	**3.118**	**1.575**	**319.0**	**40.0**	**37**	
Effluent #_31./05/2011	12.421	5.330	2.656	188.0	45.0	32	
Effluent #7-09/09/2012	12.883	4.469	2.241	223.0	92.3	143	
Effluent After Hot rinse. STDdev	0.401	1.115	0.545	67.826	3.536	62.7	
Acid Rinse, Average	**4.719**	**0.935**	**0.508**	**2740.0**	**32.7**	**9**	
Effluent #_25/10/2011	4.871	0.5037	0.253	1880.0	88.0	9	
Effluent #_31./05/2011	5.6	2.300	0.100	3400.0	6.5	13	
Sample 3_Date	3.685	0.000	1.170	2940.0	3.7	5	
After Acid rinse. STDdev	0.967	1.209	0.579	779.487	47.900	4.000	
Effluent. after acid rinse, Average	**11.857**	**32.153**	**18.850**	**291.3**	**47.7**	**64**	**2**
Effluent #_25/10/2011	11.929	3.127	1.547	323.0	69.4	64	

Effluent #_31./05/2011	12.411	9.149	4.578	109.9	25.9	47	2.385
Effluent #7-09/09/2012	11.230	1.841	9.224	540.0	47.8	82	
Effluent after acid rinse. STDdev	0.594	5.392	23.636	265.971	21.750	18	
Cold Rinse, Average	**6.827**	**0.203**	**13.669**	**3693.3**	**27.5**	**29**	
Effluent #_25/10/2011	5.414	0.2235	0.1147	4390.0	59.2	53	
Effluent #_31./05/2011	10.609	0.182	0.092	5460.0	20.3	27	
Sample 3_Date	4.459	$8.17x10^{-6}$	40.800	1230.0	3.0	6	
Cold rinse. STDdev	3.310	0.030	23.496	2199.371	28.805	24	
Effluent after cold rinse, average	**11.727**	**18.213**	**9.375**	**265.4**	**29.0**	**48**	
Effluent #_25/10/2011	12.491	39	19.520	15.6	23.3	67	2.404
Effluent #_31./05/2011	11.800	14.230	7.900	70.5	26.9	11	0.518
Effluent #7-09/09/2012	10.889	1.409	0.705	710.0	36.7	66	
Effluent after Cold rinse. STDdev	0.804	19.109	9.494	386.041	6.935	32	1.334
After dyeing, Average	**12.078**	**34.763**	**16.035**	**136.9**	**45.5**	**25**	**2.444**
Effluent #_25/10/2011	11.769	2.608	1.288	388.0	6.4	10	2.404
Effluent #_31./05/2011	12.447	93.420	46.400	10.8	23.2	30	2.483
Sample 3_Date	12.018	8.260	0.418	12.0	107.0	35	
Dyeing Effluent. STDdev	0.343	50.877	26.300	217.431	53.890	13	0.056
Effluent After dyeing , Average	**10.067**	**17.339**	**8.606**	**72.3**	**36.3**	**69**	**1.160**
Effluent #_25/10/2011	12.25	20.82	10.42	48.0	30.8	61	1.904
Effluent #_31./05/2011	12.342	22.600	11.100	45.0	26.6	54	0.416
Effluent #7-09/09/2012	5.608	8.597	4.298	124.0	51.6	92	
Effluent after Dyeing. STDdev	3.862	7.623	3.746	44.770	13.387	20	1.052
1st Cold Rinse, Average	**11.609**	**5.867**	**4.070**	**76.1**	**78.6**	**87**	**0.880**
Effluent #_25/10/2011	11.400	7.33	3.701	17.5	58.1	141	0.872
Effluent #_31./05/2011	12.142	1.560	5.120	96.9	49.6	86	0.888
Sample 3_Date	11.285	8.710	3.390	114.0	128.0	35	
1st Cold Rinse Effluent. STDdev	0.465	3.793	0.922	51.493	43.021	53.013	0.011
Effluent after cold 1st rinse, average	**11.883**	**17.307**	**8.669**	**58.3**	**42.0**	**78**	**0.984**
Effluent #_25/10/2011	12.165	15.82	7.920	63.2	48.7	93	1.415
Effluent #_31./05/2011	12.327	16.36	8.143	61.2	36.4	57	0.553
Effluent #7-09/09/2012	11.158	19.740	9.944	50.4	40.8	83	
Effluent after 1st cold rinse STDdev	0.633	2.125	1.110	6.886	6.232	19	0.610
Hot Rinse, Average	**10.912**	**1.492**	**0.863**	**712.0**	**30.5**	**46**	**0.284**
Effluent #_25/10/2011	10.583	1.735	0.868	576.0	21.3	49	0.333
Effluent #_31./05/2011	11.702	1.720	0.858	582.0	24.9	31	0.235
Sample 3_Date	10.450	1.022	0.511	978.0	45.3	59	
1st Hot Rinse Effluent. STDdev	0.688	0.407	0.007	230.382	12.943	14	0.069
Effluent after hot Rinse, Average	**11.787**	**12.571**	**6.920**	**85.4**	**35.8**	**70**	**0.750**
Effluent #_25/10/2011	11.96	7.182	3.584	139.0	35.0	79	1.091
Effluent #_31./05/2011	12.292	17.960	8.940	56.1	36.5	56	0.409
Effluent #7-09/09/2012	11.108	16.32	8.235	61.0	38.0	74	

Effluent after 1st hot rinse. STDdev	0.611	7.621	2.910	46.512	1.061	12	0.482	
Soaping Acid Rinse, Average	**3.983**	**0.581**	**0.282**	**1259.0**	**72.4**	**94**	**0.414**	
Effluent #_25/10/2011	4.206	0.617	0.308.8	2136.0	87.1	129	0.209	
Effluent #_31./05/2011	3.759	0.711	0.357	1400.0	112.0	138	0.618	
Effluent #7-09/09/2012	3.984	0.416	0.208	241.0	18.2	16		
Soap & Acid Rinse Effl.t. STDdev	0.224	0.151	0.106	955.336	48.590	67	0.289	
Effluent after soap & acid, average	**7.744**	**4.949**	**3.750**	**1887.9**	**29.0**	**57**	**0.671**	
Effluent #_25/10/2011	8.025	1.738	3.937	126.0	31.9	72	0.867	
Effluent #_31./05/2011	9.692	0.250	0.8767	5460.0	28.7	50	0.474	
Effluent #7-09/09/2012	5.516	12.860	6.437	77.7	26.5	50		
Effluent after Soap-Acid Rinse. STDdev	2.102	6.891	2.785	3093.624	2.715	12	0.278	
Cold Rinse, Average	**4.732**	**1.165**	**0.567**	**2901.0**	**17.5**	**24**	**0.224**	
Effluent #_25/10/2011	4.45	3.139	1.519	3900.0	12.9	16	0.028	
Effluent #_31./05/2011	5.590	0.253	0.1312	3840.0	26.8	44	0.419	
Sample 3_Date	4.156	0.104	0.051	963.0	12.7	12		
Cold Rinse Effluent. STDdev	0.757	1.711	0.825	1678.625	8.084	17	0.276	
Effluent. after cold Rinse, Average	**8.254**	**8.870**	**4.425**	**125.4**	**72.6**	**66**	**0.302**	
Effluent #_25/10/2011	**7.296**	**5.884**	**2.944**	**174.0**	**25.2**	**59**	**0.686**	
Effluent #_31./05/2011	11.833	12.500	6.222	80.2	47.7	55	0.17	
Sample 3_Date	5.632	8.226	4.109	122.0	145.0	85	0.051	
Effluent after Cold Rinse. STDdev	3.210	3.355	1.662	46.9	63.692	16	0.338	
Softener, Average	**6.622**	**5.739**	**4.180**	**2809.0**	**118.8**	**127**	**0.248**	
Effluent #_25/10/2011	4.78	0.1215	0.0612	8190.0	145.0	88		
Effluent #_31./05/2011	10.375	17.030	12.148	87.0	92.5	101	0.248	
Effluent #7-09/09/2012	4.712	0.067	0.332	150.0	133	191		
Softener Effluent. STDdev	3.250	9.778	6.901	4660.2	37.1	56		**COD**
Effluent after softener, Average	**9.818**	**5.895**	**2.933**	**365.7**	**29.6**	**69**	**0.805**	**1720**
Effluent #_25/10/2011	7.841	3.227	1.613	310.0	14.9	60	0.488	1342
Effluent #_31./05/2011	10.725	13.050	6.481	77.0	37.2	81	0.439	2048
Effluent #7-09/09/2012	10.889	1.409	0.705	710.0	36.7	66	1.489	1769
Softener Effluent. STDdev	1.714	6.262	3.106	320.2	12.7	11	0.593	356

Appendices A2 is the pre-bleaching and dyeing data at a liquor ratio of 10:1 and is presented as triplicates dyeing experiments with averages on top and standard deviations at the bottom of the columns for each textile-processing step.

APPENDIX A.2 Textile pre-bleaching and dyeing at a liquor ratio of 10:1

Preparation and Dyeing Steps	pH	Conduct.	TDS	Resistivity	Turb	TSS	Abs.
After Pre-treatment Liq. Ave	**12.700**	**11.528**	**5.840**	**95.1**	**314.5**	**309**	
Effluent #6_15/08/2011	13.161	21.28	10.440	46.9	109.0	118	
Sample 2_Date	12.356	7.976	3.988	125.0	390.0	391	
Effluent #4-11/08/2011	13.044	15.080	7.692	65.1	239.0	228	
After Pre-treatment Liq. STDdev	0.435	5.023	3.238	42.356	140.631	137	
Cold Rinse.	**11.827**	**1.119**	**2.686**	**813.0**	**89.7**	**187**	
Effluent #6_15/08/2011	12.162	1.650	8.250	606.0	22.8	46	
Sample 2_Date	11.270	0.001	4.253	1180.0	47.4	215	
Effluent #4-11/08/2011	12.383	2.238	1.118	446.0	132.0	159	
Cold Rinse Liq. STDdev	0.589	1.160	3.575	386.0	57.281	86	
Effluent after Cold Rinse.	**12.436**	**36.835**	**3.435**	**234.0**	**146.0**	**208**	
Effluent #6_15/08/2011	12.804	9.059	4.512	110.0	37.8	62	
Sample 2_Date	12.048	63.741	1.886	366.0	77.0	199	
Effluent #4-11/08/2011	12.823	9.928	4.984	102.0	215.0	218	
Effluent after Cold Rinse Liq.	0.442	31.323	1.669	150.2	93.077	85	
Hot Rinse.	**10.938**	**0.229**	**2.765**	**3602.0**	**20.7**	**22**	
Effluent #6_15/08/2011	10.850	0.000	0.120	4080.0	3.4	8	
Sample 2_Date	10.165	0.000	7.834	6580.0	17.9	23	
Effluent #4-11/08/2011	11.800	0.687	0.342	146.0	40.9	36	
Hot Rinse Liq. STDdev	0.821	0.396	4.391	3243.525	18.924	14	
Effluent. after Hot Rinse.	**12.057**	**3.017**	**1.516**	**231.7**	**88.6**	**110**	
Effluent #6_15/08/2011	12.480	5.683	2.867	176.0	96.9	140	
Sample 2_Date	11.890	2.680	1.340	373.0	128.0	153	
Effluent #4-11/08/2011	11.800	0.687	0.342	146.0	40.9	36	
Effluent. after Hot Rinse Liq.	0.369	2.515	1.272	123.3	44.1	64	
Acid Rinse.	**2.864**	**5.486**	**1.910**	**1977.3**	**47.4**	**51**	
Effluent #6_15/08/2011	2.403		1.731	2900.0	8.3	19	
Sample 2_Date	3.586		1.236	2850.0	2.9	2	
Effluent #4-11/08/2011	2.603	5.486	2.762	182.0	131.0	134	
Acid Rinse Liq. STDdev	0.633		0.779	1555.0	72.470	72	
Effluent after acid Rinse.	**10.123**	**2.658**	**3.905**	**414.7**	**88.6**	**112**	
Effluent #6_15/08/2011	11.853	3.626	1.750	285.0	89.0	135	
Sample 2_Date	6.311	1.725	8.657	579.0	91.1	111	
Effluent #4-11/08/2011	12.205	2.624	1.307	380.0	85.7	89	
Effluent. after Acid Rinse Liq.	3.306	0.951	4.122	150.0	2.722	23	
Cold Rinse.	**3.498**	**34.918**	**17.101**	**152.7**	**4.6**	**5**	
Effluent #7_15/08/2011	3.148	5.908	2.897	173.0	6.5	7	
Sample 2_Date	4.019	98.310	48.140	103.0	2.8	3	
Effluent #4-11/08/2011	3.328	0.537	0.266	182.0			

Effluent After Acid Rinse Liquor.	0.460	54.964	26.913	43.2	2.567	2.8	
Cold Rinse Liquor.	**10.115**	**2.438**	**1.228**	**484.0**	**102.3**	**100**	
Effluent #6_15/08/2011	11.598	2.138	1.066	469.0	133.0	109	
Sample 2_Date	6.212	1.394	0.698	717.0	71.5	91	
Effluent #4-11/08/2011	12.534	3.782	1.920	266.0			
Effluent After Cold Rinse. STDdev	3.412	1.222	0.627	225.874	43.487	12	
After Dyeing Liquor	**11.087**	**34.647**	**2.764**	**254.9**	**34.3**	**68**	**2.468**
Effluent #6_15/08/2011	11.947	5.873	3.255	645.6	28.1	75	2.468
Sample 2_Date	10.336	88.810	0.415	12.1	38.5	59	
Effluent #4-11/08/2011	10.978	9.257	4.621	107.0	36.2	72	
Dyeing Liquor STDdev	0.811	46.937	2.146	341.7	5.463	9	
Effluent After dyeing	**5.445**	**8.304**	**4.261**	**229.5**	**66.5**	**108**	**1.545**
Effluent #6_15/08/2011	6.436	8.096	4.086	124.0	75.0	115	
Sample 2_Date	5.076	5.817	2.909	472.0	40.7	57	1.545
Effluent #4-11/08/2011	4.824	11.000	5.789	92.6	83.9	151	
Effluent After Dyeing, STDdev	0.867	2.598	1.448	210.568	22.811	47	
Cold Rinse	**10.823**	**20.246**	**10.151**	**131.6**	**73.2**	**141**	**1.943**
Effluent #6_15/08/2011	11.232	4.295	2.152	232.0	33.9	54	0.976
Sample 2_Date	10.228	7.033	3.520	142.0	101.0	198	2.909
Effluent #4-11/08/2011	11.009	49.410	24.780	20.7	84.6	170	
Cold rinse Liquor, STDdev	0.527	25.294	12.688	106.0	34.981	76	
Effluent after Cold Rinse	**11.109**	**26.257**	**13.183**	**149.3**	**51.7**	**114**	**4.175**
Effluent #_31./05/2011	11.932	27.580	14.090	368.0	35.0	81	3.15
Sample 2_Date	10.352	21.640	10.870	46.1	52.6	118	5.2
Effluent #4-11/08/2011	11.042	29.550	14.590	33.8	67.5	144	
Cold Rinse Effluent , STDdev	0.792	4.118	2.019	189.5	16.269	32	
Hot Rinse	10.547	1.011	0.602	203.8	27.6	51	0.883
Effluent #6_15/08/2011	10.483	0.760	0.361	1.3	29.1	30	1.025
Sample 2_Date	10.406	0.138	0.370	135.0	22.2	45	0.741
Effluent #4-11/08/2011	10.753	2.135	1.074	475.0	31.6	78	
Hold Rinse Liquor , STDdev	0.182	1.022	0.409	244.2	4.869	25	
Effluent after hot Rinse	**11.028**	**18.725**	**9.272**	**55.6**	**45.8**	**94**	**1.860**
Effluent #6_15/08/2011	11.784	21.390	10.610	46.6	33.5	65	2.690
Sample 2_Date	10.301	13.650	6.827	73.3	44.5	94	1.030
Effluent #4-11/08/2011	11.000	21.135	10.380	47.0	59.3	122	
Effluent after Hot Rinse , STDdev	0.742	4.397	2.121	15.3	12.947	29	
Acid Rinse	**3.404**	**1.193**	**2.562**	**549.3**	**95.4**	**129**	**0.671**
Effluent #6_15/08/2011	3.137	0.981	0.451	110.0	237.0	316	0.471
Sample 2_Date	3.670	1.268	0.636	787.0	4.7	4	0.87
Effluent #4-11/08/2011	3.405	1.330	6.600	751.0	44.5	67	
Acid-soap-Rinse Liqour ,STDdev	0.267	0.186	3.498	380. 9	124.241	165	
Effluent after acid Rinse	**4.416**	**6.992**	**6.354**	**307.5**	**42.4**	**71**	**1.208**
Effluent #6_15/08/2011	4.866	10.560	8.158	61.6	40.2	86	2.166
Sample 2_Date	4.976	9.087	4.550	110.0	25.6	59	0.250
Effluent #4-11/08/2011	3.405	1.330		751.0	44.5	67	
Effluent after acid-soap ,STDdev	0.877	4.959	2.551	384.8	3.041	14	
Cold Rinse	**3.822**	**0.310**	**0.455**	**352.0**	**11.1**	**20**	**0.116**
Effluent #6_15/08/2011	3.500	0.209	0.994	496.0	14.4	32	0.100

Sample 2_Date	4.277	0.360	0.180	278.0	6.7	6	0.131	
Effluent #4-11/08/2011	3.690	0.362	0.192	282.0	12.1	24		
Cold Rinse Liquor , STDdev	0.405	0.088	0.466	124.7	3.969	13		
Effluent after cold Rinse	**4.881**	**11.377**	**5.711**	**94.8**	**31.3**	**68**	**1.207**	
Effluent #6_15/08/2011	4.789	13.470	6.731	74.6	36.2	74	0.638	
Sample 2_Date	4.998	7.440	3.713	135.0	22.3	50	1.776	
Effluent #4-11/08/2011	4.855	13.220	6.690	74.9	35.3	80		
Effluent After Cold Rinse , STDdev	0.107	3.412	1.731	34.8	7.778	16		
Softener	**4.333**	**49.424**	**29.340**	**748.3**	**309.9**	**268**	**0.634**	
Effluent #6_15/08/2011	3.953	0.163	0.073	654.0	634.0	533	0.300	
Sample 2_Date	4.950	0.109	0.546	917.0	229.0	120	0.551	
Effluent #4-11/08/2011	4.097	148.000	87.400	674.0	66.7	152	1.050	COD
Effluent after softener	**7.557**	**6.382**	**2.490**	**204.5**	**74.6**	**113**	**1.414**	**2509**
Effluent #6_15/08/2011	11.598	2.138	1.066	469.0	133.0	109	1.772	2859
Sample 2_Date	10.225	7.895	0.040	12.7	30.2	162	2.411	3130
Effluent #4-11/08/2011	4.824	11.000	5.789	92.6	83.9	151	0.501	3873
Effluent After Cold Rinse , STDdev	3.581	4.497	3.066	243.7	51.417	28	0.972	525

The following pages contain data Appendices B1 to B7. Each Appendix, B1, B2, B3, B4, B5, B6 and B7 present the data for electrocoagulation experiments at 25°C, 30°C, 35°C, 40°C, 45°C, 30°C respectively. At each temperature setting three experiments A, B and C were performed and are presented in Appendix B. In the top row are average values and the bottom rows show standard deviations for each parameter.

APPENDIX B 1: Iron Electrocoagulation Process of Reactive Dyebaths Textile Effluent at Various Temperatures

Table B.1 Iron Electrocoagulation Process of Reactive Dyebaths Textile Effluent at 5.0A and 25^{o}C

Time (min)	0	5	10	15	20	25	30	35	40	45	50	55	60	MAX	MIN
T. (^{o}C)	**25.0**	**25.6**	**25.1**	**25.1**	**25.9**	**25.8**	**25.6**	**25.4**	**25.3**	**25.4**	**25.3**	**25.1**	**25.3**	**25.9**	**25.1**
25deg Exp A	22.8	24.9	24.8	24.9	25.4	25.6	25.8	25.8	25.7	25.7	25.6	25.6	25.4	25.8	24.8
25deg Exp B	25.0	25.8	25.7	25.2	25.7	25.8	24.9	25.5	25.3	25.5	25.4	25.0	25.3	25.8	24.9
25deg Exp C	27.3	26.2	24.9	25.1	26.7	26.1	26.0	25.0	24.8	25.0	24.9	24.6	25.2	26.7	24.6
Std Dev	2.3	0.7	0.5	0.2	0.7	0.3	0.6	0.4	0.5	0.4	0.4	0.5	0.1	0.5	0.2
pH	**8.3**	**9.2**	**9.0**	**7.9**	**7.1**	**5.8**	**6.1**	**6.7**	**7.1**	**6.1**	**7.0**	**7.3**	**7.5**	**9.2**	**5.8**
25deg Exp A	5.7	6.4	7.0	7.3	7.0	8.0	6.8	7.5	8.5	5.3	6.4	6.9	7.2	8.5	5.3
25deg Exp B	11.8	11.7	10.6	9.0	8.3	2.1	3.7	4.4	5.2	5.0	6.1	6.3	6.4	11.7	2.1
25deg Exp C	7.4	9.4	9.5	7.5	6.0	7.3	7.9	8.3	7.4	7.9	8.3	8.6	8.9	9.5	6.0
Std Dev	3.2	2.6	1.9	1.0	1.1	3.2	2.2	2.0	1.7	1.6	1.2	1.2	1.2	1.6	2.1
κ (mS/cm)	**6.2**	**6.4**	**6.4**	**6.6**	**7.0**	**6.8**	**6.5**	**6.6**	**6.8**	**7.0**	**7.1**	**7.5**	**7.8**	**7.8**	**6.4**
25deg Exp A	6.7	6.9	6.7	6.8	6.9	6.9	7.0	7.1	7.2	7.4	7.4	7.4	7.4	7.4	6.7
25deg Exp B	5.9	6.6	6.7	7.0	7.3	7.5	6.6	6.7	6.8	6.9	6.9	7.1	6.9	7.5	6.6
25deg Exp C	5.9	5.8	5.9	5.9	6.9	5.9	5.9	6.1	6.3	6.8	7.0	8.0	9.0	9.0	5.8
Std Dev	0.5	0.6	0.5	0.6	0.2	0.8	0.6	0.5	0.4	0.3	0.3	0.5	1.1	0.9	0.5
ρ (ohm)	**109.3**	**105.4**	**101.7**	**100.0**	**97.9**	**105.3**	**106.3**	**105.0**	**104.8**	**102.3**	**101.9**	**101.2**	**101.9**	**106.3**	**97.9**
25deg Exp A	72.7	75.7	75.8	75.8	75.8	75.9	75.9	75.9	76.0	76.0	76.0	75.9	75.9	76.0	75.7
25deg Exp B	169.0	156.0	146.0	140.0	134.0	156.0	158.0	156.0	155.0	148.0	146.0	143.0	144.0	158.0	134.0
25deg Exp C	86.1	84.5	83.3	84.2	84.0	84.0	85.0	83.1	83.5	83.0	83.7	84.7	85.8	85.8	83.0
Std Dev	52.2	44.0	38.5	34.9	31.5	44.1	45.0	44.3	43.6	39.7	38.4	36.5	36.8	44.8	31.8
TDS (g/L)	**4.1**	**4.1**	**4.3**	**4.3**	**4.3**	**4.6**	**4.3**	**4.3**	**4.3**	**4.4**	**4.4**	**4.4**	**4.4**	**4.6**	**4.1**
25deg Exp A	3.4	3.4	3.5	3.5	3.5	3.6	3.6	3.6	3.6	3.7	3.7	3.7	3.7	3.7	3.4
25deg Exp B	3.0	3.2	3.4	3.5	3.5	4.2	3.3	3.3	3.4	3.4	3.5	3.5	3.4	4.2	3.2
25deg Exp C	6.1	5.8	5.9	6.0	6.0	6.0	6.0	6.0	6.0	6.0	6.0	6.1	6.1	6.1	5.8
Std Dev	1.7	1.4	1.5	1.4	1.5	1.3	1.5	1.5	1.5	1.4	1.4	1.4	1.4	1.2	1.4

U_{out}	**0.0**	**4.1**	**5.2**	**6.3**	**7.1**	**3.8**	**3.7**	**3.6**	**5.6**	**3.6**	**3.6**	**3.6**	**3.6**	**7.1**	**3.6**
25deg Exp A	0.0	4.6	5.0	4.9	4.8	4.4	4.2	4.0	3.9	3.8	3.8	3.8	3.7	5.0	3.7
25deg Exp B	0.0	4.6	7.5	10.9	13.6	4.0	3.9	3.9	9.9	3.9	3.9	3.9	3.9	13.6	3.9
25deg Exp C	0.0	3.2	3.1	3.1	3.1	3.1	3.1	3.0	3.0	3.0	3.0	3.1	3.1	3.2	3.0
Std Dev	0.0	0.8	2.2	4.1	5.6	0.7	0.6	0.5	3.7	0.5	0.5	0.4	0.4	5.5	0.5
Turbidity (NTU)	**59.7**	**49.9**	**43.5**	**42.9**	**37.9**	**34.6**	**23.3**	**26.6**	**30.7**	**29.5**	**22.5**	**39.6**	**59.9**	**59.9**	**22.5**
25deg Exp A	53.0	19.6	23.5	16.8	27.3	13.2	1.4	1.4	11.6	3.5	13.1	62.2	99.8	99.8	1.4
25deg Exp B	67.0	93.0	70.0	90.0	71.0	65.0	53.0	64.0	73.0	75.0	44.0	31.0	36.0	93.0	31.0
25deg Exp C	59.0	37.1	37.0	21.8	15.5	25.5	15.5	14.3	7.5	9.9	10.3	25.5	43.9	43.9	7.5
Std Dev	**7.0**	**38.3**	**23.9**	**40.9**	**29.2**	**27.1**	**26.7**	**33.1**	**36.7**	**39.6**	**18.7**	**19.8**	**34.8**	**30.5**	**15.6**
TSS (mg/L)	69.0	58.3	52.0	54.3	54.0	30.5	25.3	38.0	30.3	30.5	23.2	26.5	44.2	58.3	23.2
25deg Exp A	59.0	35.0	41.0	38.0	69.0	4.0	4.0	15.0	13.0	6.0	13.0	40.0	59.0	69.0	4.0
25deg Exp B	67.0	93.0	70.0	90.0	71.0	65.0	53.0	64.0	73.0	75.0	44.0	31.0	36.0	93.0	31.0
25deg Exp C	81.0	47.0	45.0	35.0	22.0	22.5	19.0	35.0	5.0	10.5	12.5	8.5	37.5	47.0	5.0
Std Dev	11.1	30.6	15.7	30.9	27.7	31.3	25.1	24.6	37.2	38.6	18.0	16.2	12.9	23.0	15.3
Color (Pt-Co)	**4103**	**3421**	**3601**	**2971**	**2245**	**1614**	**1462**	**1203.**	**863.0**	**1165**	**415**	**410**	**425**	**3601**	**4103**
25deg Exp A	3950	3814	4150	4456.0	4406	3438.	3592.0	2555.0	1931	1248	856	478	198	4456	198
25deg Exp B	3906.	3262	3804	2197	707	587.0	109.0	668.0	306.0	1485.0	22.0	393.0	483.0	3804.0	22.0
25deg Exp C	4452	3186	2850	2260	1621	817.0	684.0	386.0	352.0	761.0	366.0	360.0	595.0	3186.0	352.0
Std Dev	303.3	342.7	673.3	1287	1926.8	1583.8	1867.2	1179.3	925.2	369.1	419.1	60.9	204.7	635.1	165.1
$\Lambda_{\lambda 560nm}$	**3.1**	**2.9**	**2.7**	**2.0**	**1.7**	**0.7**	**0.6**	**0.4**	**0.3**	**0.3**	**0.2**	**0.2**	**0.1**	**2.9**	**0.1**
25deg Exp A	3.1	2.9	2.9	3.0	2.1	1.0	0.8	0.6	0.4	0.4	0.2	0.2	0.0	3.0	0.0
25deg Exp B	3.0	2.9	2.9	1.9	2.1	1.0	0.8	0.6	0.4	0.4	0.2	0.2	0.0	2.9	0.0
25deg Exp C	3.1	2.8	2.4	1.0	0.8	0.3	0.2	0.1	0.1	0.1	0.2	0.3	0.2	2.8	0.1
Std Dev	0.0	0.0	0.2	0.8	0.6	0.4	0.3	0.3	0.1	0.1	0.0	0.1	0.1	0.1	0.0
COD (mg/L)	**1929.7**	**1489.7**	**1433.8**	**1072.3**	**1219.8**	**1089.2**	**988.0**	**860.0**	**693.3**	**689.0**	**622.0**	**556.3**	**463.3**	**1489.7**	**463.3**
25deg Exp A	1928.0	1158.0	1119.0	838.0	789.0	607.0	548.0	494.0	476.0	496.0	421.0	455.0	394.0	1158.0	394.0
25deg Exp B	1960.0	1560.0	1632.0	1484.0	1373.5	1299.5	1208.0	1044.0	606.0	753.0	671.0	550.0	480.0	1632.0	480.0
25deg Exp C	1901.0	1751.0	1550.5	895.0	1497.0	1361.0	1208.0	1042.0	998.0	818.0	774.0	664.0	516.0	1751.0	516.0
Std Dev	24.1	247.1	225.1	292.0	308.8	341.9	311.1	258.8	221.9	139.0	148.2	85.4	51.2	256.4	51.2

(Cℓ) (mg/L)	**73.7**	**80.6**	**62.4**	**73.1**	**38.0**	**20.9**	**13.1**	**31.0**	**27.3**	**17.0**	**16.3**	**47.7**	**0.9**	**80.6**	**0.9**
25deg Exp A	24.0	19.6	10.0	11.7	13.1	18.4	16.1	15.3	8.2	1.8	1.3	0.6	0.4	19.6	0.4
25deg Exp B	173.0	197.0	146.8	191.0	96.5	24.4	20.9	75.1	70.2	46.0	41.5	141.4	1.1	197.0	1.1
25deg Exp C	24.2	25.2	30.5	16.5	4.4	19.8	2.2	2.6	3.6	3.2	6.1	1.1	1.4	30.5	1.1
Std Dev	70.2	82.4	60.2	83.4	41.5	2.6	7.9	31.6	30.4	20.5	17.9	66.3	0.4	81.2	0.3
t-Cl_2 (mg/L)	**0.5**	**0.4**	**1.0**	**1.6**	**1.8**	**2.5**	**2.9**	**1.6**	**1.0**	**0.8**	**0.9**	**1.6**	**0.3**	**2.9**	**0.3**
25deg Exp A	0.5	1.0	1.2	2.4	2.5	3.8	2.9	4.2	2.5	0.5	0.4	2.1	0.8	4.2	0.4
25deg Exp B		0.3	0.2	0.3	0.8	0.2	1.7	0.0	0.0	1.2	1.4	0.9	0.1	1.7	0.0
25deg Exp C		0.0	1.5	2.1	2.2	3.5	4.1	0.4	0.3	0.8	0.8	1.7	0.1	4.1	0.0
Std Dev	0.0	0.4	0.5	1.0	0.8	1.6	1.0	1.9	1.1	0.3	0.4	0.5	0.3	1.2	0.2
f-Cl_2 (mg/L)	**0.1**	**1.5**	**1.6**	**1.2**	**0.3**	**0.6**	**0.8**	**0.2**	**0.2**	**0.3**	**0.3**	**0.1**	**0.1**	**1.6**	**0.1**
25deg Exp A	0.1	0.0	0.0	0.1	0.2	0.0	0.1	0.1	0.0	0.1	0.1	0.0	0.1	0.2	0.0
25deg Exp B		4.5	4.8	3.3	0.5	1.7	2.3	0.4	0.5	0.7	0.6	0.3	0.2	4.8	0.2
25deg Exp C		0.0	0.0	0.1	0.2	0.1	0.1	0.1	0.1	0.1	0.2	0.1	0.1	0.2	0.0
Std Dev	0.0	2.1	2.2	1.5	0.1	0.8	1.0	0.2	0.2	0.3	0.2	0.1	0.0	2.2	0.1
t-Cl_2 (mg/L)	**0.5**	**1.9**	**2.1**	**2.1**	**1.3**	**1.9**	**2.4**	**1.6**	**1.1**	**0.8**	**0.9**	**1.1**	**0.4**	**2.4**	**0.4**
25deg Exp A	0.5	1.0	1.2	2.5	2.6	3.8	3.0	4.3	2.6	0.5	0.6	2.1	0.8	4.3	0.5
25deg Exp **B**		4.8	5.0	3.6	1.2	1.9	4.0	0.4	0.6	1.9	2.1	1.2	0.2	5.0	0.2
25deg Exp C		0.0	0.0	0.1	0.2	0.1	0.1	0.1	0.1	0.1	0.2	0.1	0.1	0.2	0.0
Std Dev	0.0	2.1	2.1	1.5	1.0	1.5	1.6	1.9	1.1	0.8	0.8	0.8	0.3	2.2	0.2
Fe(III) (mg/L)		**0.2**	**-0.3**	**2.7**	**3.4**	**4.1**	**1.2**	**4.2**	**3.3**	**4.8**	**1.7**	**4.5**	**4.0**	**4.8**	**-0.3**
25deg Exp A		0.0	0.0	1.4	2.9	3.0	0.0	0.8	1.4	2.8	2.9	2.3	2.2	3.0	0.0
25deg Exp B		-0.1	-1.5	2.7	4.5	4.9	2.6	6.8	3.8	6.4	-1.0	5.8	3.7	6.8	-1.5
25deg Exp C		0.8	0.7	3.9	2.9	4.5	0.9	5.0	4.7	5.3	3.3	5.4	6.2	6.2	0.7
Std Dev		0.4	0.9	1.0	0.7	0.8	1.1	2.5	1.4	1.5	2.0	1.6	1.6	1.7	0.9
Fe(II) (mg/L)		**4.1**	**4.1**	**1.4**	**1.5**	**1.6**	**4.1**	**1.2**	**3.1**	**1.1**	**3.0**	**1.4**	**1.3**	**4.1**	**1.1**
25deg Exp A		4.0	4.1	3.2	1.2	2.7	4.9	3.0	4.8	3.1	3.4	3.6	3.0	4.9	1.2
25deg Exp B		4.1	4.0	0.6	1.6	1.0	3.7	0.3	2.2	0.1	2.8	0.2	0.4	4.1	0.1
25deg Exp C		4.1	4.0	0.6	1.6	1.0	3.7	0.3	2.2	0.1	2.8	0.2	0.4	4.1	0.1
Std Dev		0.1	0.0	1.2	0.2	0.8	0.5	1.3	1.2	1.5	0.3	1.6	1.2	0.4	0.6

t-Fe (mg/L)		**4.3**	**3.8**	**4.1**	**4.9**	**5.7**	**5.3**	**5.4**	**6.4**	**5.9**	**4.7**	**5.9**	**5.3**	**6.4**	**3.8**
25deg Exp A		3.9	4.2	4.6	4.1	5.7	4.9	3.9	6.2	5.9	6.4	5.9	5.3	6.4	3.9
25deg Exp B		4.0	2.6	3.2	6.1	5.9	6.3	7.1	6.0	6.4	1.7	6.0	4.1	7.1	1.7
25deg Exp C		5.0	4.7	4.5	4.5	5.4	4.7	5.3	6.9	5.4	6.1	5.6	6.6	6.9	4.5
Std Dev		0.5	0.9	0.6	0.8	0.2	0.7	1.3	0.4	0.4	2.1	0.2	1.0	0.4	1.2
ORP, mV	**11.0**	**123.0**	**65.8**	**37.7**	**25.7**	**112.2**	**114.5**	**93.0**	**86.5**	**90.7**	**108.3**	**95.5**	**122.7**	**123.0**	**25.7**
25deg Exp A		163.0	139.5	142.0	98.0	82.5	51.5	51.0	65.5	79.0	103.0	95.5	145.0	163.0	51.0
25deg Exp B	11.0	-42.0	-66.0	-70.0	-76.0	185.0	266.0	206.0	142.0	120.0	119.0	90.0	78.0	266.0	-76.0
25deg Exp C		248.0	124.0	41.0	55.0	69.0	26.0	22.0	52.0	73.0	103.0	101.0	145.0	248.0	22.0
Std Dev		149.1	114.4	106.0	90.6	63.4	131.8	98.9	48.5	25.6	9.2	5.5	38.7	55.0	66.6

Table B.2 Iron Electrocoagulation Process of Reactive Dyebaths Textile Effluent at 5.0A and 30^{o}C

Time	**0**	**5**	**10**	**15**	**20**	**25**	**30**	**35**	**40**	**45**	**50**	**55**	**60**	MAX	MIN
T. (^{o}C)	**30.5**	**30.1**	**30.0**	**30.0**	**29.9**	**30.1**	**30.1**	**30.2**	**30.5**	**30.7**	**30.8**	**30.9**	**30.8**	**30.9**	**29.9**
30deg Exp A	30.6	28.9	29.0	28.9	29.0	29.6	29.9	30.3	30.8	31.1	31.4	31.7	31.9	**31.9**	**28.9**
30deg Exp B	30.0	30.4	29.8	29.9	30.0	30.3	30.1	30.2	30.6	31.0	31.1	31.1	30.5	**31.1**	**29.8**
30deg Exp C	31.0	31.0	31.2	31.1	30.8	30.4	30.4	30.2	30.2	30.1	30.0	30.0	30.1	**31.2**	**30.0**
Std Dev	0.5	1.1	1.1	1.1	0.9	0.4	0.3	0.1	0.3	0.6	0.7	0.9	0.9	0.4	0.6
pH	**8.3**	**8.8**	**9.1**	**8.9**	**8.4**	**7.7**	**7.9**	**8.1**	**8.2**	**8.2**	**8.1**	**8.2**	**8.4**	**9.1**	**7.7**
30deg Exp A	5.3	9.3	9.7	9.2	8.8	6.6	7.1	7.3	7.5	7.5	7.7	7.9	8.1	**9.7**	**6.6**
30deg Exp B	11.7	6.6	6.4	6.5	6.8	7.2	7.5	7.9	8.1	8.0	7.8	7.7	8.0	**8.1**	**6.4**
30deg Exp C	7.9	10.4	11.2	11.0	9.5	9.2	9.2	9.1	9.1	9.1	8.9	9.0	9.0	**11.2**	**8.9**
Std Dev	2.7	2.7	3.4	3.2	1.8	1.4	1.2	0.8	0.7	0.7	0.8	0.9	0.7	2.2	1.8
κ (mS/cm)	**11.3**	**11.4**	**11.3**	**11.3**	**11.4**	**11.1**	**11.0**	**11.1**	**10.8**	**10.7**	**10.6**	**10.8**	**10.7**	**11.4**	**10.6**
30deg Exp A	10.3	11.0	11.0	11.1	11.5	11.1	11.2	11.2	11.2	11.2	11.2	11.2	11.2	**11.5**	**11.0**
30deg Exp B	12.9	12.4	12.4	12.3	12.4	12.3	12.4	12.5	12.5	12.5	12.5	12.5	12.5	**12.5**	**12.3**
30deg Exp C	10.6	10.7	10.6	10.5	10.3	9.8	9.4	9.5	8.6	8.5	8.1	8.7	8.4	**10.7**	**8.1**
Std Dev	1.4	0.9	0.9	1.0	1.0	1.3	1.5	1.5	2.0	2.1	2.3	1.9	2.1	0.9	2.2
ρ (ohm)	**110.1**	**84.4**	**85.5**	**85.8**	**85.0**	**85.2**	**85.4**	**85.5**	**85.9**	**86.4**	**87.5**	**87.6**	**91.8**	**91.8**	**84.4**

30deg Exp A	97.4	89.6	90.1	90.6	90.2	89.9	90.0	90.2	91.0	91.6	92.3	92.9	93.3	**93.3**	**89.6**
30deg Exp B	87.0	79.1	79.5	79.5	79.2	79.5	79.6	79.5	79.6	79.6	79.6	79.6	79.6	**79.6**	**79.1**
30deg Exp C	146.0	84.5	86.9	87.2	85.7	86.1	86.6	86.7	87.1	87.9	90.7	90.2	102.4	**102.4**	**84.5**
Std Dev	31.5	5.3	5.4	5.7	5.5	5.3	5.3	5.5	5.8	6.1	6.9	7.0	11.5	11.5	5.3
TDS (g/L)	**5.7**	**5.0**	**5.7**	**5.6**	**5.6**	**5.5**	**5.5**	**5.5**	**5.4**	**5.4**	**5.3**	**5.4**	**5.3**	**5.7**	**5.0**
30deg Exp A	5.1	3.5	5.6	5.5	5.5	5.5	5.6	5.6	5.6	5.6	5.6	5.6	5.6	**5.6**	**3.5**
30deg Exp B	6.5	6.2	6.2	6.2	6.2	6.2	6.2	6.2	6.2	6.3	6.2	6.3	6.2	**6.3**	**6.2**
30deg Exp C	5.3	5.3	5.3	5.2	5.1	4.9	4.7	4.7	4.3	4.2	4.0	4.4	4.2	**5.3**	**4.0**
Std Dev	0.7	1.4	0.4	0.5	0.5	0.7	0.7	0.8	1.0	1.0	1.1	1.0	1.0	0.5	1.4
U_{out}	**0.0**	**3.1**	**3.1**	**3.1**	**2.8**	**3.0**	**3.0**	**3.0**	**3.0**	**3.0**	**3.0**	**3.0**	**3.0**	**3.1**	**2.8**
30deg Exp A	0.0	3.0	2.8	2.9	2.1	2.8	2.8	2.8	2.7	2.7	2.7	2.7	2.7	**3.0**	**2.1**
30deg Exp B	0.0	2.8	2.8	2.8	2.8	2.7	2.7	2.7	2.7	2.7	2.7	2.7	2.6	**2.8**	**2.6**
30deg Exp C	0.0	3.5	3.6	3.6	3.6	3.6	3.6	3.6	3.6	3.6	3.5	3.6	3.5	**3.6**	**3.5**
Std Dev	0.0	0.4	0.4	0.4	0.7	0.5	0.5	0.5	0.5	0.5	0.5	0.5	0.5	0.4	0.7
Turbidity	**53.3**	**55.0**	**34.2**	**25.6**	**32.6**	**13.7**	**13.8**	**10.1**	**16.0**	**11.0**	**7.9**	**7.5**	**10.4**	**55.0**	**7.5**
30deg Exp A	53.0	44.0	31.6	18.7	62.7	17.0	14.3	11.2	22.0	7.1	2.8	5.6	4.1	**62.7**	**2.8**
30deg Exp B	39.0	66.0	25.0	21.0	18.0	13.0	7.0	4.0	3.0	8.0	6.0	4.0	12.0	**66.0**	**3.0**
30deg Exp C	68.0	55.0	46.0	37.0	17.0	11.0	20.0	15.0	23.0	18.0	15.0	13.0	15.0	**55.0**	**11.0**
Std Dev	14.5	11.0	10.7	10.0	26.1	3.1	6.5	5.6	11.3	6.1	6.3	4.8	5.6	5.6	4.7
TSS (mg/L)	**49.0**	**64.0**	**37.3**	**21.7**	**26.0**	**9.0**	**6.3**	**3.7**	**5.0**	**5.0**	**3.7**	**2.3**	**6.7**	**64.0**	**2.3**
30deg Exp A	59.0	61.0	42.0	26.0	54.0	9.0	7.0	3.0	8.0	4.0	1.0	1.0	2.0	**61.0**	**1.0**
30deg Exp B	39.0	66.0	25.0	21.0	18.0	13.0	7.0	4.0	3.0	8.0	6.0	4.0	12.0	**66.0**	**3.0**
30deg Exp C	49.0	65.0	45.0	18.0	6.0	5.0	5.0	4.0	4.0	3.0	4.0	2.0	6.0	**65.0**	**2.0**
Std Dev	10.0	2.6	10.8	4.0	25.0	4.0	1.2	0.6	2.6	2.6	2.5	1.5	5.0	2.6	1.0
Color (Pt-Co)	**6314.7**	**2847.0**	**2521.7**	**2202.0**	**608.7**	**886.3**	**759.0**	**582.0**	**240.7**	**610.0**	**286.0**	**218.0**	**261.7**	**2847.0**	**218.0**
30deg Exp A	3906.0	2918.0	2978.0	2752.0	1392.0	429.0	413.0	366.0	284.0	451.0	229.0	109.0	71.0	**2978.0**	**71.0**
30deg Exp B	4452.0	3250.0	3051.0	2530.0	0.0	2002.0	1631.0	865.0	139.0	1080.0	473.0	459.0	590.0	**3250.0**	**0.0**
30deg Exp C	10586.0	2373.0	1536.0	1324.0	434.0	228.0	233.0	515.0	299.0	299.0	156.0	86.0	124.0	**2373.0**	**86.0**
Std Dev	3709.1	442.8	854.4	768.4	712.2	971.4	760.5	256.2	88.4	414.1	166.0	209.0	285.6	448.9	45.9
$A_{\lambda 560nm}$	**3.2**	**2.4**	**1.9**	**1.7**	**0.8**	**0.1**	**0.1**	**0.1**	**0.1**	**0.1**	**0.0**	**0.0**	**0.1**	**2.4**	**0.0**

30deg Exp A	3.3	2.5	2.4	2.2	1.5	0.1	0.1	0.1	0.1	0.0	0.0	0.0	0.0	**2.5**	**0.0**
30deg Exp B	3.5	3.2	2.5	2.3	0.8	0.1	0.1	0.1	0.0	0.1	0.0	0.0	0.1	**3.2**	**0.0**
30deg Exp C	2.8	1.6	0.9	0.4	0.1	0.1	0.1	0.1	0.1	0.1	0.0	0.0	0.1	**1.6**	**0.0**
Std Dev	0.3	0.8	0.9	1.1	0.7	0.0	0.0	0.0	0.0	0.0	0.0	0.0	0.0	0.8	0.0
COD (mg/L)	**1966.0**	**1755.7**	**1619.7**	**1180.7**	**1120.7**	**899.0**	**800.7**	**634.0**	**671.7**	**621.0**	**613.0**	**662.3**	**601.0**	**1755.7**	**601.0**
30deg Exp A	1928.0	1817.0	1786.0	1285.0	1651.0	1065.0	1005.0	597.0	691.0	565.0	548.0	516.0	531.0	**1817.0**	**516.0**
30deg Exp B	1998.0	1848.0	1660.0	1307.0	950.0	898.0	680.0	599.0	635.0	605.0	622.0	833.0	655.0	**1848.0**	**599.0**
30deg Exp C	1972.0	1602.0	1413.0	950.0	761.0	734.0	717.0	706.0	689.0	693.0	669.0	638.0	617.0	**1602.0**	**617.0**
Std Dev	35.4	134.0	189.7	200.1	468.9	165.5	177.9	62.4	31.8	65.5	61.0	159.9	63.5	134.0	53.9
($C\ell^-$) (mg/L)	**180.3**	**99.9**	**114.0**	**97.4**	**88.6**	**72.0**	**45.5**	**31.5**	**33.0**	**18.0**	**21.8**	**18.2**	**13.2**	**114.0**	**13.2**
30deg Exp A	138.0	99.8	96.1	77.1	87.3	79.0	54.5	36.0	26.0	21.0	18.0	15.0	14.0	**99.8**	**14.0**
30deg Exp B	144.0	104.0	122.0	114.0	97.5	71.0	32.0	23.5	32.0	4.0	16.5	7.5	7.5	**122.0**	**4.0**
30deg Exp C	259.0	96.0	124.0	101.0	81.0	66.0	50.0	35.0	41.0	29.0	31.0	32.0	18.0	**124.0**	**18.0**
Std Dev	68.2	4.0	15.6	18.7	8.3	6.6	11.9	6.9	7.5	12.8	8.0	12.6	5.3	13.4	7.2
t-Cl_2 (mg/L)	**0.3**	**1.4**	**0.7**	**0.6**	**0.7**	**44.8**	**0.6**	**0.5**	**0.3**	**0.3**	**0.8**	**0.4**	**0.7**	**44.8**	**0.3**
30deg Exp A	1.0	1.3	1.1	0.1	0.1	0.4	0.1	0.1	0.1	0.0	0.0	0.2	0.2	**1.3**	**0.0**
30deg Exp B	0.0	1.0	0.3	0.2	0.7	0.0	0.4	0.1	0.5	0.3	0.1	0.3	0.2	**1.0**	**0.0**
30deg Exp C	0.0	2.0	0.7	1.3	1.3	133.9	1.4	1.3	0.4	0.7	2.4	0.7	1.7	**133.9**	**0.4**
Std Dev	0.6	0.5	0.4	0.7	0.6	77.2	0.7	0.7	0.2	0.3	1.3	0.3	0.8	76.6	0.2
f-Cl_2 (mg/L)	**0.1**	**0.3**	**0.1**	**0.1**	**0.1**	**0.1**	**0.2**	**0.1**	**0.1**	**0.1**	**0.1**	**0.1**	**0.1**	**0.3**	**0.1**
30deg Exp A	0.3	0.7	0.3	0.1	0.0	0.0	0.2	0.0	0.0	0.2	0.1	0.0	0.0	**0.7**	**0.0**
30deg Exp B	0.0	0.1	0.1	0.1	0.1	0.1	0.1	0.1	0.1	0.0	0.1	0.2	0.0	**0.2**	**0.0**
30deg Exp C	0.0	0.1	0.1	0.1	0.1	0.1	0.1	0.1	0.1	0.1	0.1	0.1	0.2	**0.2**	**0.1**
Std Dev	0.2	0.4	0.1	0.0	0.0	0.0	0.0	0.1	0.0	0.1	0.0	0.1	0.1	0.3	0.0
t-Cl_2 (mg/L)	**0.4**	**1.0**	**0.6**	**0.2**	**0.3**	**0.2**	**0.3**	**0.2**	**0.2**	**0.2**	**0.2**	**0.2**	**0.2**	**1.0**	**0.2**
30deg Exp A	1.2	2.0	1.4	0.2	0.1	0.4	0.2	0.1	0.1	0.2	0.2	0.2	0.3	**2.0**	**0.1**
30deg Exp B	0.0	1.0	0.3	0.3	0.8	0.1	0.5	0.3	0.6	0.3	0.2	0.4	0.2	**1.0**	**0.1**
30deg Exp C	0.0	0.1	0.1	0.1	0.1	0.1	0.1	0.1	0.1	0.1	0.1	0.1	0.2	**0.2**	**0.1**
Std Dev	0.7	1.0	0.7	0.1	0.4	0.2	0.2	0.1	0.3	0.1	0.0	0.2	0.0	0.9	0.0
Fe(III) (mg/L)	**0.0**	**1.0**	**1.8**	**1.4**	**2.6**	**1.3**	**1.7**	**1.0**	**1.1**	**1.6**	**2.2**	**0.7**	**0.7**	**2.6**	**0.7**

30deg Exp A	0.0	0.4	0.6	2.2	2.8	1.7	1.2	0.8	2.1	0.8	2.4	0.5	-0.1	**2.8**	**-0.1**
30deg Exp B	0.0	1.0	2.5	0.6	2.3	0.1	1.1	1.1	0.7	2.6	1.3	0.9	1.3	**2.6**	**0.1**
30deg Exp C	0.0	1.5	2.2	1.5	2.8	2.2	3.0	1.1	0.6	1.4	3.1	0.7	1.0	**3.1**	**0.6**
Std Dev	0.0	0.6	1.0	0.8	0.3	1.1	1.1	0.2	0.8	0.9	0.9	0.2	0.7	0.2	0.3
Fe(II) (mg/L)	**0.0**	**2.9**	**2.4**	**3.0**	**2.9**	**2.9**	**2.8**	**3.0**	**2.7**	**2.6**	**2.1**	**1.6**	**1.3**	**3.0**	**1.3**
30deg Exp A	0.0	0.5	0.2	3.8	3.3	4.0	2.8	3.0	3.1	2.0	2.3	1.9	1.8	**4.0**	**0.2**
30deg Exp B	0.0	3.2	3.7	2.4	1.4	1.1	3.2	3.5	2.2	3.5	1.6	1.1	0.7	**3.7**	**0.7**
30deg Exp C	0.0	4.9	3.4	2.8	3.9	3.6	2.4	2.7	2.9	2.3	2.3	1.9	1.4	**4.9**	**1.4**
Std Dev	0.0	2.2	1.9	0.7	1.3	1.6	0.4	0.4	0.5	0.8	0.4	0.5	0.6	0.6	0.6
t-Fe (mg/L)	**0.0**	**3.8**	**4.3**	**4.5**	**5.5**	**4.2**	**4.5**	**4.0**	**3.8**	**4.2**	**4.3**	**2.4**	**2.0**	**5.5**	**2.0**
30deg Exp A	0.0	0.8	0.9	6.0	6.1	5.7	4.0	3.8	5.2	2.7	4.7	2.4	1.8	**6.1**	**0.8**
30deg Exp B	0.0	4.2	6.3	3.0	3.7	1.2	4.2	4.6	2.9	6.1	2.9	2.0	2.0	**6.3**	**1.2**
30deg Exp C	0.0	6.4	5.6	4.4	6.7	5.8	5.4	3.8	3.4	3.8	5.4	2.7	2.4	**6.7**	**2.4**
Std Dev	0.0	2.8	3.0	1.5	1.6	2.6	0.8	0.5	1.2	1.7	1.3	0.3	0.3	0.3	0.8
ORP, mV	**63.3**	**73.0**	**85.7**	**94.3**	**98.7**	**73.7**	**59.3**	**84.7**	**36.7**	**18.3**	**57.7**	**70.0**	**114.0**	**114.0**	**18.3**
30deg Exp A	0.0	62.0	127.0	159.0	139.0	143.0	130.0	91.0	132.0	96.0	127.0	72.0	148.0	**159.0**	**62.0**
30deg Exp B	44.0	40.0	61.0	68.0	158.0	144.0	92.0	231.0	66.0	53.0	103.0	240.0	129.0	**240.0**	**40.0**
30deg Exp C	146.0	117.0	69.0	56.0	-1.0	-66.0	-44.0	-68.0	-88.0	-94.0	-57.0	-102.	65.0	**117.0**	**-102**
Std Dev	74.9	39.7	36.0	56.3	86.8	121.0	91.5	149.6	112.9	99.6	100.0	171.0	43.5	62.5	89.0

Table B.3. Iron Electrocoagulation Process of Reactive Dyebaths Textile Effluent at 5.0A and 35^{o}C

Time	**0**	**5**	**10**	**15**	**20**	**25**	**30**	**35**	**40**	**45**	**50**	**55**	**60**	MAX	MIN
T. (^{o}C)	**36.1**	**35.5**	**35.7**	**35.7**	**35.6**	**35.2**	**35.7**	**35.4**	**35.3**	**35.2**	**34.8**	**35.4**	**34.9**	35.7	34.8
35deg Exp A	35.5	35.7	35.6	35.7	35.1	34.1	35.7	34.9	34.7	35.5	33.5	33.9	34.1	35.7	33.5
35deg Exp B	36.5	35.5	36.2	35.9	36.2	35.9	35.6	35.6	35.5	34.3	35.2	36.2	35.5	36.2	34.3
35deg Exp C	36.4	35.4	35.3	35.6	35.6	35.6	35.7	35.8	35.8	35.8	35.8	36.0	35.0	36.0	35.0
Std Dev	0.6	0.2	0.5	0.2	0.6	1.0	0.1	0.5	0.6	0.8	1.2	1.3	0.7	0.3	0.8
pH	**5.5**	**5.4**	**7.0**	**7.6**	**8.1**	**8.1**	**8.8**	**8.4**	**8.7**	**8.9**	**8.9**	**5.8**	**5.8**	8.9	5.4

35deg Exp A	4.5	5.7	6.4	7.8	7.5	7.8	8.5	6.3	6.8	7.4	7.6	7.7	7.5	8.5	5.7
35deg Exp B	7.8	8.0	9.3	9.0	10.0	9.1	9.4	9.4	9.5	9.5	9.5	0.0	0.0	10.0	0.0
35deg Exp C	4.2	2.7	5.4	6.0	6.7	7.5	8.5	9.5	9.7	9.7	9.7	9.7	9.9	9.9	2.7
Std Dev	2.0	2.6	2.0	1.5	1.7	0.8	0.5	1.8	1.6	1.3	1.2	5.1	5.2	0.8	2.8
κ (mS/cm)	**11.8**	**11.6**	**11.6**	**11.5**	**11.5**	**11.5**	**11.4**	**11.3**	**11.5**	**11.5**	**11.5**	**11.5**	**11.5**	11.6	11.3
35deg Exp A	12.1	12.0	11.9	11.9	11.8	11.8	11.8	11.3	11.9	11.8	11.8	11.7	11.9	12.0	11.3
35deg Exp B	11.6	11.5	11.6	11.5	11.5	11.5	11.5	11.5	11.6	11.6	11.7	11.7	11.7	11.7	11.5
35deg Exp C	11.7	11.4	11.4	11.2	11.2	11.2	11.1	11.0	11.0	11.0	10.9	11.0	10.9	11.4	10.9
Std Dev	0.3	0.3	0.3	0.3	0.3	0.3	0.3	0.2	0.4	0.4	0.5	0.4	0.5	0.3	0.3
ρ (ohm)	**83.8**	**84.6**	**84.3**	**85.0**	**84.9**	**84.9**	**85.5**	**84.8**	**85.3**	**85.3**	**85.2**	**85.0**	**85.3**	85.5	84.3
35deg Exp A	81.0	81.4	81.0	83.8	83.2	82.9	84.5	82.8	84.1	84.8	84.0	83.1	83.6	84.8	81.0
35deg Exp B	84.8	84.9	84.4	84.8	85.3	85.4	85.4	85.0	85.2	84.6	84.9	85.2	85.5	85.5	84.4
35deg Exp C	85.6	87.6	87.4	86.3	86.3	86.4	86.7	86.5	86.7	86.5	86.7	86.7	86.9	87.6	86.3
Std Dev	2.5	3.1	3.2	1.3	1.6	1.8	1.1	1.9	1.3	1.0	1.4	1.8	1.7	1.5	2.7
TDS (g/L)	**5.9**	**5.8**	**5.8**	**5.8**	**5.7**	**5.7**	**5.7**	**5.7**	**5.7**	**5.7**	**5.7**	**5.7**	**5.7**	5.8	5.7
35deg Exp A	6.1	6.0	6.0	5.9	5.9	5.9	5.9	5.9	5.9	5.9	5.9	5.9	6.0	6.0	5.9
35deg Exp B	5.8	5.8	5.8	5.7	5.7	5.7	5.7	5.7	5.8	5.8	5.9	5.9	5.8	5.9	5.7
35deg Exp C	5.8	5.7	5.7	5.6	5.6	5.6	5.5	5.5	5.5	5.5	5.4	5.5	5.5	5.7	5.4
Std Dev	0.1	0.2	0.1	0.2	0.2	0.2	0.2	0.2	0.2	0.2	0.3	0.2	0.3	0.1	0.2
U_{out}	**10.0**	**3.2**	**3.1**	**3.1**	**3.0**	**3.0**	**3.0**	**2.9**	**2.9**	**2.9**	**3.0**	**3.0**	**3.0**	3.2	2.9
35deg Exp A	15.0	2.7	2.6	2.6	2.6	2.6	2.7	2.6	2.7	2.7	2.7	2.7	2.7	2.7	2.6
35deg Exp B	0.0	2.9	2.9	2.8	2.9	2.9	2.8	2.8	2.8	2.8	2.9	2.8	2.8	2.9	2.8
35deg Exp C	15.0	4.0	4.0	3.7	3.6	3.5	3.4	3.3	3.3	3.3	3.3	3.4	3.4	4.0	3.3
Std Dev	8.7	0.7	0.7	0.6	0.5	0.4	0.4	0.4	0.3	0.3	0.3	0.4	0.4	0.7	0.3
Turbidity (NTU)	**65.2**	**50.7**	**52.3**	**14.1**	**13.2**	**15.4**	**25.6**	**14.5**	**27.6**	**20.5**	**18.8**	**20.8**	**23.2**	52.3	13.2
35deg Exp A	14.0	11.2	13.9	7.0	20.5	22.0	35.9	12.3	9.4	10.5	7.3	10.1	7.5	35.9	7.0
35deg Exp B	159.0	120.0	122.0	23.0	16.0	13.0	33.0	16.0	33.0	39.0	41.0	37.0	54.0	122.0	13.0
35deg Exp C	22.6	20.8	21.0	12.4	3.1	11.3	7.8	15.3	40.3	11.9	8.2	15.3	8.2	40.3	3.1
Std Dev	81.3	60.2	60.5	8.1	9.0	5.8	15.5	2.0	16.1	16.1	19.2	14.3	26.6	48.5	5.0
TSS (mg/L)	**76.3**	**57.0**	**63.0**	**43.8**	**11.3**	**12.3**	**19.0**	**10.3**	**23.3**	**16.7**	**17.0**	**16.7**	**24.3**	63.0	10.3

35deg Exp A	26.0	18.0	25.0	87.3	10.0	12.0	18.0	3.0	10.0	3.0	4.0	6.0	7.0	87.3	3.0
35deg Exp B	159.0	120.0	122.0	23.0	16.0	13.0	33.0	16.0	33.0	39.0	41.0	37.0	54.0	122.0	13.0
35deg Exp C	44.0	33.0	42.0	21.0	8.0	12.0	6.0	12.0	27.0	8.0	6.0	7.0	12.0	42.0	6.0
Std Dev	72.2	55.1	51.8	37.7	4.2	0.6	13.5	6.7	11.9	19.5	20.8	17.6	25.8	40.1	5.1
Colour (Pt-Co)	**4593**	**3910**	**3036.7**	**3050.0**	**1824.0**	**1512.0**	**1979.0**	**1432.3**	**1045.7**	**1120.0**	**812.0**	**682.3**	**645.3**	3910.3	645.3
35deg Exp A	3625.	2744	2886	2657	371.0	195.0	384.0	93.0	148.0	813.0	124.0	155.0	221.0	2886.0	93.0
35deg Exp B	5569.	4173	1518	1843	1307.	795.0	530.0	439.0	175.0	217.0	283.0	186.0	147.0	4173.0	147.0
35deg Exp C	4584	4814	4706	4650	3794	3546	5023	3765	2814	2330	2029	1706	1568.	5023.0	1568
Std Dev	972.	1060	1599	444.2	1769.	1787	2637	2028	1532	1089	1057	887	800	1075.9	836.4
$A_{\lambda 560nm}$	**2.6**	**1.9**	**1.3**	**0.6**	**0.5**	**0.3**	**0.2**	**0.2**	**0.1**	**0.1**	**0.1**	**0.1**	**0.1**	1.9	0.1
35deg Exp A	2.2	2.1	1.6	1.2	0.8	0.1	0.1	0.1	0.1	0.0	0.0	0.0	0.1	2.1	0.0
35deg Exp B	3.0	3.0	1.9	0.2	0.1	0.1	0.1	0.2	0.2	0.3	0.2	0.2	0.2	3.0	0.1
35deg Exp C	2.6	0.5	0.5	0.5	0.5	0.5	0.5	0.3	0.2	0.1	0.1	0.1	0.1	0.5	0.1
Std Dev	0.4	1.3	0.7	0.5	0.3	0.2	0.2	0.1	0.1	0.1	0.1	0.1	0.1	1.2	0.0
COD (mg/L)	**1951.**	**1225.1**	**1061.7**	**966.0**	**940.0**	**971.7**	**893.0**	**822.0**	**584.0**	**514.7**	**695.3**	**652.7**	**632.0**	1225.1	514.7
35deg Exp A	1879	1219.	918.0	653.0	343.0	556.0	886.0	380.0	276.0	362.0	374.0	376.0	482.0	1219.0	276.0
35deg Exp B	1749	440.2	290.0	337.0	769.0	785.0	371.0	728.0	272.0	0.0	670.0	651.0	637.0	785.0	0.0
35deg Exp C	2226	2016.	1977.0	1908	1708.	1574.	1422.	1358.	1204.	1182.	1042.	931.0	777.0	2016.0	777.0
Std Dev	247	787.9	852.6	831.0	698.4	534.1	525.5	495.7	536.9	605.6	334.7	277.5	147.6	624.4	393.9
(Cℓ) (mg/L)	**168.7**	**120.8**	**105.9**	**85.3**	**80.0**	**82.3**	**63.7**	**60.2**	**55.3**	**42.3**	**44.7**	**48.7**	**49.7**	120.8	42.3
35deg Exp A	199.	171.9	149.7	137.0	97.0	137.0	99.1	94.6	87.9	89.0	52.0	89.0	99.2	171.9	52.0
35deg Exp B	227.	132.0	114.0	80.0	109.0	76.0	70.0	66.0	59.0	20.8	50.0	44.0	35.0	132.0	20.8
35deg Exp C	80.0	58.5	54.0	39.0	34.0	34.0	22.0	20.0	19.0	17.0	32.0	13.0	15.0	58.5	13.0
Std Dev	78.1	57.5	48.4	49.2	40.3	51.8	38.9	37.6	34.6	40.5	11.0	38.2	44.0	57.5	20.6
C-Cl_2 **(mg/L)**	**1.0**	**4.2**	**3.5**	**2.5**	**2.4**	**2.5**	**1.8**	**1.4**	**1.0**	**0.8**	**0.4**	**0.3**	**0.7**	4.2	0.3
35deg Exp A	0.0	3.6	4.2	2.8	2.7	1.2	0.9	0.6	0.7	0.3	0.2	0.5	0.7	4.2	0.2
35deg Exp B	0.0	4.2	2.0	1.1	1.2	1.5	1.6	0.8	0.8	1.1	0.0	0.0	0.7	4.2	0.0
35deg Exp C	3.1	5.0	4.4	3.6	3.3	4.8	2.9	3.0	1.4	0.9	0.9	0.5	0.7	5.0	0.5
Std Dev	1.8	0.7	1.4	1.3	1.0	2.0	1.0	1.3	0.4	0.4	0.5	0.3	0.0	0.4	0.2
f-Cl_2 (mg/L)	**0.5**	**0.4**	**0.5**	**0.7**	**1.1**	**0.1**	**0.5**	**0.1**	**0.2**	**0.1**	**0.0**	**0.1**	**0.1**	1.1	0.0

35deg Exp A	0.0	0.0	0.0	0.1	0.1	0.1	0.2	0.1	0.2	0.1	0.0	0.1	0.2	0.2	0.0
35deg Exp B	0.0	0.2	0.1	0.0	0.0	0.1	0.2	0.1	0.1	0.0	0.1	0.0	0.1	0.2	0.0
35deg Exp C	1.6	1.2	1.3	2.1	3.2	0.1	1.3	0.1	0.3	0.3	0.1	0.3	0.1	3.2	0.1
Std Dev	0.9	0.6	0.8	1.2	1.8	0.0	0.6	0.0	0.1	0.1	0.0	0.1	0.1	1.7	0.0
t-Cl_2 (mg/L)	**1.6**	**4.7**	**4.0**	**3.2**	**3.5**	**2.6**	**2.4**	**1.5**	**1.1**	**0.9**	**0.4**	**0.4**	**0.8**	4.7	0.4
35deg Exp A	0.0	3.6	4.2	2.8	2.8	1.2	1.1	0.6	0.9	0.4	0.2	0.6	0.9	4.2	0.2
35deg Exp B	0.0	4.4	2.0	1.1	1.2	1.6	1.8	0.9	0.8	1.1	0.1	0.0	0.7	4.4	0.0
35deg Exp C	4.7	6.1	5.8	5.7	6.4	4.9	4.2	3.0	1.6	1.1	1.0	0.7	0.8	6.4	0.7
Std Dev	2.7	1.3	1.9	2.3	2.7	2.0	1.6	1.3	0.4	0.4	0.5	0.4	0.1	1.2	0.3
Fe(III) (mg/L)	**3.1**	**4.0**	**4.0**	**3.7**	**3.7**	**2.2**	**3.4**	**2.9**	**3.8**	**3.1**	**3.4**	**4.6**	**6.7**	6.7	2.2
35deg Exp A	0.0	3.6	2.1	2.3	3.0	2.8	2.8	3.8	1.1	2.9	-0.4	1.7	1.4	3.8	-0.4
35deg Exp B	0.0	2.4	3.1	3.4	1.6	1.7	2.7	1.1	1.3	0.8	1.4	0.0	0.5	3.4	0.0
35deg Exp C	9.2	6.0	6.7	5.5	6.5	2.2	4.7	3.8	9.1	5.5	9.1	12.1	18.3	18.3	2.2
Std Dev	5.3	1.8	2.4	1.6	2.6	0.6	1.1	1.6	4.5	2.3	5.0	6.6	10.0	8.5	1.4
Fe(II) (mg/L)	**0.2**	**2.5**	**2.7**	**2.4**	**2.8**	**4.2**	**2.9**	**1.9**	**1.6**	**1.7**	**2.3**	**2.0**	**0.9**	4.2	0.9
35deg Exp A	0.0	3.4	4.3	3.9	2.8	3.1	3.6	1.6	1.6	3.5	2.3	2.0	1.3	4.3	1.3
35deg Exp B	0.0	4.2	3.2	3.0	3.7	3.4	3.3	2.7	2.2	0.8	4.2	0.0	1.1	4.2	0.0
35deg Exp C	0.6	0.1	0.6	0.3	1.8	6.2	1.8	1.5	0.9	0.9	0.3	4.0	0.3	6.2	0.1
Std Dev	0.3	2.2	1.9	1.9	1.0	1.7	1.0	0.7	0.7	1.5	1.9	2.0	0.5	1.1	0.7
t-Fe (mg/L)	**3.3**	**6.5**	**6.7**	**6.1**	**6.4**	**6.5**	**6.3**	**4.8**	**5.4**	**4.8**	**5.6**	**6.6**	**7.6**	7.6	4.8
35deg Exp A	0.0	6.9	6.4	6.2	5.8	5.9	6.4	5.4	2.7	6.3	1.9	3.7	2.7	6.9	1.9
35deg Exp B	0.0	6.6	6.4	6.4	5.3	5.1	6.0	3.8	3.5	1.6	5.6	0.0	1.6	6.6	0.0
35deg Exp C	9.8	6.1	7.3	5.7	8.3	8.4	6.4	5.3	10.0	6.4	9.4	16.1	18.6	18.6	5.3
Std Dev	5.6	0.4	0.5	0.4	1.6	1.7	0.2	0.9	4.0	2.7	3.7	8.4	9.5	6.8	2.7
ORP, mV	**-3.7**	**264.4**	**152.0**	**244.9**	**252.1**	**120.3**	**173.0**	**135.3**	**207.4**	**102.6**	**70.0**	**75.3**	**106.2**	264.4	70.0
35deg Exp A	0.0	335.0	208.0	133.0	103.0	63.0	199.0	112.0	95.0	111.0	105.0	119.0	116.0	335.0	63.0
35deg Exp B	0.0	440.2	227.0	72.7	103.2	53.9	97.0	96.9	71.3	20.8	0.0	0.0	86.5	440.2	0.0
35deg Exp C	-11.0	18.0	21.0	529.0	550.0	244.0	223.0	197.0	456.0	176.0	105.0	107.0	116.0	550.0	18.0
Std Dev	6.4	219.8	113.8	247.9	258.0	107.2	66.9	54.0	215.6	77.9	60.6	65.5	17.0	107.5	32.4

Table B.4. Iron Electrocoagulation Process of Reactive Dyebaths Textile Effluent at 5.0A and 40°C

Time	0	5	10	15	20	25	30	35	40	45	50	55	60	MAX	MIN
T. (°C)	**41.8**	**41.8**	**42.0**	**41.5**	**41.2**	**40.6**	**40.3**	**39.6**	**39.7**	**39.6**	**38.2**	**39.5**	**38.9**	**42.0**	**38.2**
40deg Exp A	44.5	44.5	44.6	42.9	41.9	41.8	41.1	39.1	39.4	39.1	38.9	39.2	40.5	**44.6**	**38.9**
40deg Exp B	39.7	39.9	40.2	40.0	40.2	39.1	39.3	39.2	40.1	40.3	39.8	40.3	40.3	**40.3**	**39.1**
40deg Exp C	41.1	41.1	41.3	41.7	41.4	41.0	40.6	40.6	39.7	39.3	36.0	39.0	36.0	**41.7**	**36.0**
Std Dev	2.5	2.4	2.3	1.5	0.9	1.4	0.9	0.8	0.4	0.6	2.0	0.7	2.5	2.2	1.7
pH	**7.7**	**8.0**	**8.1**	**7.9**	**7.7**	**7.4**	**7.6**	**8.1**	**8.2**	**7.5**	**7.9**	**8.0**	**8.1**	**8.2**	**7.4**
40deg Exp A	9.4	4.6	5.9	5.8	6.3	6.6	6.6	6.9	6.8	6.7	6.8	6.9	6.9	**6.9**	**4.6**
40deg Exp B	7.5	9.9	10.2	10.3	8.4	8.3	8.4	9.4	9.5	9.8	9.9	9.9	10.0	**10.3**	**8.3**
40deg Exp C	6.2	9.5	8.2	7.6	8.3	7.4	7.8	8.0	8.3	6.2	6.9	7.2	7.3	**9.5**	**6.2**
Std Dev	1.6	3.0	2.1	2.3	1.2	0.8	0.9	1.3	1.4	1.9	1.8	1.7	1.7	1.8	1.9
κ (mS/cm)	**12.0**	**11.7**	**11.7**	**11.7**	**11.7**	**11.7**	**11.7**	**11.7**	**11.6**	**11.7**	**11.7**	**11.6**	**11.6**	**11.7**	**11.6**
40deg Exp A	12.7	12.4	12.5	12.5	12.5	12.5	12.6	12.6	12.4	12.5	12.4	12.5	12.5	12.6	12.4
40deg Exp B	11.8	11.5	11.5	11.5	11.5	11.6	11.6	11.5	11.4	11.5	11.5	11.2	11.2	11.6	11.2
40deg Exp C	11.6	11.2	11.1	11.1	11.1	11.1	11.1	11.0	11.0	11.1	11.2	11.2	11.1	11.2	11.0
Std Dev	0.6	0.6	0.7	0.7	0.7	0.7	0.8	0.8	0.7	0.7	0.6	0.7	0.7	0.7	0.7
ρ (ohm)	**83.1**	**83.6**	**83.2**	**83.2**	**82.8**	**82.7**	**82.8**	**83.1**	**83.6**	**83.7**	**83.7**	**83.8**	**84.0**	**84.0**	**82.7**
40deg Exp A	78.6	77.5	77.4	76.8	76.8	76.8	76.5	76.7	77.1	77.6	78.0	78.0	78.5	78.5	76.5
40deg Exp B	84.3	87.1	85.0	86.0	84.3	84.0	84.6	85.0	85.7	85.6	86.2	86.5	86.8	87.1	84.0
40deg Exp C	86.4	86.3	87.1	86.9	87.3	87.2	87.3	87.5	88.1	87.8	87.0	86.8	86.8	88.1	86.3
Std Dev	4.0	5.3	5.1	5.6	5.4	5.3	5.6	5.7	5.8	5.4	5.0	5.0	4.8	5.3	5.1
TDS (g/L)	**6.0**	**5.8**	**5.8**	**5.8**	**5.8**	**5.8**	**5.9**	**5.8**	**5.8**	**5.8**	**5.9**	**5.8**	**5.8**	**5.9**	**5.8**
40deg Exp A	6.4	6.2	6.2	6.2	6.2	6.2	6.3	6.3	6.2	6.2	6.2	6.2	6.2	6.3	6.2
40deg Exp B	5.9	5.8	5.7	5.7	5.8	5.8	5.7	5.7	5.7	5.7	5.8	5.7	5.8	5.8	5.7
40deg Exp C	5.8	5.6	5.5	5.5	5.5	5.5	5.5	5.5	5.5	5.6	5.6	5.6	5.6	5.6	5.5
Std Dev	0.3	0.3	0.4	0.4	0.4	0.4	0.4	0.4	0.4	0.3	0.3	0.3	0.3	0.4	0.3
U_{out}	**10.0**	**2.9**	**2.6**	**2.6**	**2.6**	**2.6**	**2.6**	**2.6**	**2.9**	**2.7**	**2.7**	**2.6**	**2.7**	**2.9**	**2.6**
40deg Exp A	15.0	3.5	2.6	2.6	2.6	2.6	2.6	2.6	3.6	3.1	3.1	2.6	3.0	3.6	2.6

40deg Exp B	15.0	2.7	2.7	2.7	2.7	2.7	2.7	2.6	2.6	2.6	2.6	2.6	2.5	2.7	2.5
40deg Exp C	0.0	2.6	2.6	2.6	2.6	2.6	2.6	2.6	2.6	2.5	2.5	2.6	2.6	2.6	2.5
Std Dev	8.7	0.5	0.1	0.1	0.1	0.1	0.1	0.0	0.6	0.3	0.3	0.0	0.3	0.5	0.0
Turbidity (NTU)	**52.0**	**42.7**	**42.8**	**36.2**	**22.5**	**15.6**	**14.0**	**7.0**	**15.2**	**34.0**	**30.5**	**31.4**	**25.3**	**42.8**	**7.0**
40deg Exp A	55.1	42.6	38.0	35.4	30.2	27.0	20.1	13.8	9.5	8.3	8.2	48.5	47.4	48.5	8.2
40deg Exp B	58.0	48.0	46.0	33.0	17.0	9.0	13.0	2.0	30.0	38.0	44.0	2.0	8.0	48.0	2.0
40deg Exp C	43.0	37.6	44.4	40.2	20.3	10.9	9.0	5.3	6.2	55.7	39.2	43.8	20.6	55.7	5.3
Std Dev	8.0	5.2	4.2	3.7	6.9	9.9	5.6	6.1	12.9	24.0	19.4	25.6	20.1	4.3	3.1
TSS (mg/L)	**55.3**	**43.7**	**45.3**	**26.3**	**19.3**	**10.2**	**10.7**	**4.6**	**35.7**	**51.7**	**42.3**	**16.4**	**11.1**	**51.7**	**4.6**
40deg Exp A	41.0	34.0	35.0	33.0	30.0	14.5	15.1	9.9	73.0	64.0	58.0	4.2	4.2	73.0	4.2
40deg Exp B	58.0	48.0	46.0	33.0	17.0	9.0	13.0	2.0	30.0	38.0	44.0	2.0	8.0	48.0	2.0
40deg Exp C	67.0	49.0	55.0	13.0	11.0	7.0	4.0	2.0	4.0	53.0	25.0	43.0	21.0	55.0	2.0
Std Dev	13.2	8.4	10.0	11.5	9.7	3.9	5.9	4.6	34.8	13.1	16.6	23.1	8.8	12.9	1.3
T-C (Pt-Co)	**4118.0**	**3512.0**	**2644.3**	**2153.0**	**769.7**	**332.0**	**322.7**	**137.0**	**156.3**	**144.0**	**227.3**	**135.7**	**120.7**	**3512.0**	**120.7**
40deg Exp A	4856	3432	3066	3041	350	132	284	183	75	58	433	16	7	3432	7
40deg Exp B	3749	3552	1807	1074	558	560	419	0	205	223	127	167	228	3552	0
40deg Exp C	3749	3552	3060	2344	1401	304	265	228	189	151	122	224	127	3552	122
Std Dev	639.1	69.3	725.2	997.3	556.6	215.4	84.0	120.8	70.9	82.7	178.1	107.5	110.6	69.3	68.5
$\Lambda_{\lambda 560nm}$	**1.9**	**2.6**	**2.2**	**1.2**	**0.4**	**0.2**	**0.3**	**0.1**	**0.2**	**0.2**	**0.3**	**0.1**	**0.1**	**2.6**	**0.1**
40deg Exp A	2.8	2.5	1.9	1.2	0.6	0.5	0.6	0.4	0.3	0.3	0.2	0.1	0.2	2.5	0.1
40deg Exp B	0.0	2.2	2.2	2.3	0.3	0.1	0.2	0.0	0.1	0.2	0.0	0.0	0.0	2.3	0.0
40deg Exp C	3.0	2.9	2.5	0.2	0.2	0.1	0.1	0.0	0.0	0.2	0.6	0.1	0.1	2.9	0.0
Std Dev	1.7	0.3	0.3	1.0	0.2	0.3	0.3	0.2	0.2	0.1	0.3	0.1	0.1	0.3	0.1
COD (mg/L)	**2539**	**2144**	**1801**	**1556**	**1255**	**942**	**758**	**633**	**559**	**532**	**514**	**485**	**489**	**2144**	**485**
40deg Exp A	2238	1928	1794	1670	1559	1228	873	636	571	551	538	529	513	1928	513
40deg Exp B	2690	2215	1788	1590	990	789	765	694	678	695	675	656	656	2215	656
40deg Exp C	2690	2290	1820	1407	1217	810	637	568	428	351	329	270	299	2290	270
Std Dev	261.0	191.1	17.0	134.8	286.4	247.6	118.1	63.1	125.4	172.8	174.2	196.7	179.7	191.1	195.1
($C\ell^-$) (mg/L)	**51.3**	**42.0**	**42.0**	**46.5**	**16.6**	**17.6**	**6.3**	**6.6**	**5.5**	**4.1**	**2.8**	**2.7**	**1.9**	**46.5**	**1.9**
40deg Exp A	128.0	117.0	109.0	125.0	49.0	36.0	18.0	17.0	16.0	11.0	7.0	6.0	5.0	125.0	5.0

40deg Exp B	12.9	0.0	0.0	0.0	0.0	0.0	0.0	0.0	0.0	0.0	0.0	0.0	0.0	0.0	0.0
40deg Exp C	12.9	9.1	16.9	14.6	0.7	16.8	0.9	2.9	0.6	1.2	1.4	2.0	0.6	16.9	0.6
Std Dev	66.5	65.1	58.7	68.4	28.1	18.0	10.1	9.1	9.1	6.0	3.7	3.1	2.7	67.8	2.7
t-Cl_2 (mg/L)	**0.0**	**0.5**	**0.3**	**0.2**	**0.2**	**0.1**	**0.1**	**0.2**	**0.0**	**-0.1**	**0.1**	**0.1**	**0.1**	**0.5**	**-0.1**
40deg Exp A	0.0	0.84	0.00	0.23	0.29	0.11	0.13	0.38	0.02	-0.21	0.05	0.08	0.10	0.8	-0.2
40deg Exp B	0.0	0.12	0.10	0.05	0.05	0.04	0.08	0.08	0.00	0.02	0.07	0.09	0.04	0.1	0.0
40deg Exp C	0.0	0.51	0.65	0.25	0.17	0.04	0.13	0.03	0.03	0.04	0.07	0.06	0.07	0.7	0.0
Std Dev	0.0	0.4	0.4	0.1	0.1	0.0	0.0	0.2	0.0	0.1	0.0	0.0	0.0	0.4	0.1
f-Cℓ_2 (mg/L)	**0.0**	**0.13**	**0.02**	**0.14**	**0.09**	**0.09**	**0.08**	**0.08**	**0.05**	**0.17**	**0.10**	**0.09**	**0.09**	**0.2**	**0.0**
40deg Exp A	0.0	0.27	0.00	0.15	0.01	0.13	0.15	0.14	0.08	0.36	0.09	0.12	0.03	0.4	0.0
40deg Exp B	0.0	0.00	0.03	0.11	0.11	0.07	0.05	0.05	0.04	0.08	0.11	0.06	0.11	0.1	0.0
40deg Exp C	0.0	0.11	0.04	0.16	0.16	0.07	0.05	0.05	0.04	0.06	0.11	0.09	0.12	0.2	0.0
Std Dev	0.0	0.1	0.0	0.0	0.1	0.0	0.1	0.1	0.0	0.2	0.0	0.0	0.0	0.1	0.0
t-Cℓ_2 (mg/L)	**0.0**	**0.62**	**0.27**	**0.32**	**0.26**	**0.15**	**0.20**	**0.24**	**0.07**	**0.12**	**0.17**	**0.17**	**0.16**	**0.6**	**0.1**
40deg Exp A	0.0	1.11	0.00	0.38	0.30	0.24	0.28	0.52	0.10	0.15	0.14	0.20	0.13	1.1	0.0
40deg Exp B	0.0	0.12	0.13	0.16	0.16	0.11	0.13	0.13	0.04	0.10	0.18	0.15	0.15	0.2	0.0
40deg Exp C	0.0	0.62	0.69	0.41	0.33	0.11	0.18	0.08	0.07	0.10	0.18	0.15	0.19	0.7	0.1
Std Dev	0.0	0.5	0.4	0.1	0.1	0.1	0.1	0.2	0.0	0.0	0.0	0.0	0.0	0.5	0.0
Fe(III) (mg/L)	**0.0**	**1.09**	**2.08**	**2.42**	**1.25**	**1.02**	**1.55**	**2.35**	**1.03**	**3.24**	**1.85**	**2.18**	**2.89**	**3.2**	**1.0**
40deg Exp A	0.0	0.5	2.4	2.5	0.0	0.2	1.3	1.8	0.0	4.6	0.0	1.0	3.3	4.6	0.0
40deg Exp B	0.0	0.73	1.94	1.43	0.66	0.03	0.46	2.27	0.00	2.42	2.68	3.06	2.59	3.1	0.0
40deg Exp C	0.0	2.08	1.92	3.35	3.10	2.83	2.94	2.97	3.09	2.70	2.86	2.51	2.80	3.4	1.9
Std Dev	0.0	0.9	0.3	1.0	1.6	1.6	1.3	0.6	1.8	1.2	1.6	1.1	0.4	0.8	1.1
Fe(II) (mg/L)	**0.0**	**4.99**	**4.78**	**3.87**	**2.60**	**5.56**	**3.85**	**3.14**	**0.68**	**2.58**	**2.06**	**2.48**	**2.71**	**5.6**	**0.7**
40deg Exp A	0.0	5.3	4.0	4.2	0.0	9.0	4.5	3.1	0.0	0.5	0.0	1.8	2.3	9.0	0.0
40deg Exp B	0.0	4.81	5.19	4.45	5.67	5.08	4.60	4.00	0.00	4.34	4.24	3.45	4.26	5.7	0.0
40deg Exp C	0.0	4.88	5.13	2.98	2.12	2.64	2.45	2.27	2.04	2.95	1.94	2.15	1.60	5.1	1.6
Std Dev	0.0	0.3	0.7	0.8	2.9	3.2	1.2	0.9	1.2	2.0	2.1	0.9	1.4	2.1	0.9
t-Fe (mg/L)	**0.0**	**6.29**	**6.86**	**6.29**	**3.85**	**6.59**	**5.40**	**5.49**	**1.71**	**5.82**	**3.91**	**4.66**	**5.60**	**6.9**	**1.7**
40deg Exp A	0.0	6.4	6.4	6.7	0.0	9.2	5.8	5.0	0.0	5.1	0.0	2.8	5.6	9.2	0.0

40deg Exp B	0.0	5.54	7.13	5.88	6.33	5.11	5.06	6.27	0.00	6.76	6.92	6.51	6.85	7.1	0.0
40deg Exp C	0.0	6.96	7.05	6.33	5.22	5.47	5.39	5.24	5.13	5.65	4.80	4.66	4.40	7.1	4.4
Std Dev	0.0	0.7	0.4	0.4	3.4	2.3	0.3	0.7	3.0	0.9	3.5	1.9	1.2	1.2	2.5
ORP, mV	**0.0**	**110.7**	**89.3**	**63.7**	**91.3**	**107.8**	**96.7**	**98.7**	**133.3**	**114.3**	**110.0**	**102.0**	**109.0**	**133.3**	**63.7**
40deg Exp A	0.0	136.0	134.0	59.0	98.0	133.5	136.0	124.0	146.0	129.0	117.0	92.0	109.0	146.0	59.0
40deg Exp B	0.0	60.0	0.0	73.0	78.0	103.0	85.0	97.0	108.0	85.0	96.0	97.0	109.0	109.0	0.0
40deg Exp C	0.0	136.0	134.0	59.0	98.0	87.0	69.0	75.0	146.0	129.0	117.0	117.0	109.0	146.0	59.0
Std Dev	0.0	43.9	77.4	8.1	11.5	23.6	35.0	24.5	21.9	25.4	12.1	13.2	0.0	21.4	34.1

Table B.5. Iron Electrocoagulation Process of Reactive Dyebaths Textile Effluent at 5.0A and 45^{o}C

Time	**0**	**5**	**10**	**15**	**20**	**25**	**30**	**35**	**40**	**45**	**50**	**55**	**60**	MAX	MIN
T. (^{o}C)	**45.3**	**45.1**	**45.5**	**45.6**	**45.4**	**45.8**	**45.8**	**45.7**	**45.7**	**45.7**	**45.5**	**45.3**	**45.2**	**45.8**	**45.1**
45deg Exp A	45.0	44.0	45.4	45.4	45.4	46.0	46.6	46.6	46.3	45.8	44.9	44.9	44.8	46.6	44.0
45deg Exp B	46.0	46.9	46.7	46.0	45.5	45.3	45.4	45.4	45.4	45.5	45.4	45.5	45.5	46.9	45.3
45deg Exp C	45.0	44.5	44.5	45.4	45.4	46.0	45.3	45.0	45.4	45.9	46.1	45.6	45.2	46.1	44.5
Std Dev	0.6	1.6	1.1	0.3	0.1	0.4	0.7	0.8	0.5	0.2	0.6	0.4	0.4	0.4	0.7
pH	**11.6**	**3.9**	**4.6**	**5.3**	**5.6**	**6.4**	**6.9**	**5.8**	**6.5**	**6.1**	**6.5**	**6.4**	**6.8**	**6.9**	**3.9**
45deg Exp A	12.0	5.1	5.9	7.4	7.6	8.6	8.9	4.8	6.3	6.5	7.0	6.2	6.9	8.9	4.8
45deg Exp B	11.3	3.0	3.6	4.0	4.3	4.9	5.5	5.9	6.3	6.8	7.0	7.0	7.1	7.1	3.0
45deg Exp C	11.5	3.7	4.1	4.7	5.0	5.6	6.3	6.8	7.0	5.0	5.5	6.0	6.3	7.0	3.7
Std Dev	0.3	1.1	1.2	1.8	1.7	2.0	1.8	1.0	0.4	1.0	0.9	0.6	0.4	1.1	0.9
κ (mS/cm)	**6.9**	**7.3**	**7.3**	**7.2**	**7.2**	**7.2**	**7.1**	**7.4**	**7.4**	**7.7**	**7.6**	**7.6**	**7.5**	**7.7**	**7.1**
45deg Exp A	5.3	5.7	5.6	5.4	5.3	5.2	5.1	6.2	6.1	6.0	5.9	5.9	5.7	6.2	5.1
45deg Exp B	7.9	8.6	8.6	8.6	8.6	8.7	8.7	8.7	8.7	8.7	8.5	8.5	8.4	8.7	8.4
45deg Exp C	7.6	7.7	7.6	7.7	7.7	7.6	7.6	7.5	7.4	8.3	8.4	8.4	8.3	8.4	7.4
Std Dev	1.4	1.5	1.5	1.6	1.7	1.8	1.9	1.3	1.3	1.5	1.4	1.4	1.5	1.4	1.7
ρ(ohm)	**222.7**	**161.7**	**163.0**	**167.0**	**167.0**	**145.7**	**115.0**	**105.1**	**87.1**	**89.0**	**89.7**	**89.7**	**89.3**	**167.0**	**87.1**
45deg Exp A	388.0	178.0	182.0	187.0	189.0	197.0	199.0	169.0	120.0	120.0	121.0	121.0	120.0	199.0	120.0
45deg Exp B	126.0	114.0	116.0	116.0	116.0	113.0	110.0	110.0	111.0	111.0	112.0	112.0	112.0	116.0	110.0

45deg Exp C	154.0	193.0	191.0	198.0	196.0	127.0	36.0	36.3	30.4	36.1	36.0	36.0	35.9	198.0	30.4
Std Dev	143.9	42.0	41.0	44.5	44.3	45.0	81.6	66.5	49.3	46.1	46.7	46.7	46.4	47.6	49.1
TDS (g/L)	**3.5**	**3.6**	**3.6**	**3.6**	**3.6**	**3.6**	**3.6**	**3.7**	**3.7**	**3.8**	**3.8**	**3.8**	**3.7**	**3.8**	**3.6**
45deg Exp A	3.2	2.9	2.8	2.7	2.7	2.6	2.5	3.1	3.0	3.0	2.9	3.0	2.9	3.1	2.5
45deg Exp B	4.0	4.3	4.3	4.3	4.3	4.3	4.4	4.3	4.3	4.1	4.2	4.2	4.2	4.4	4.1
45deg Exp C	3.2	3.5	3.8	3.8	3.8	3.8	3.8	3.7	3.7	4.1	4.2	4.2	4.2	4.2	3.5
Std Dev	0.4	0.7	0.8	0.8	0.8	0.9	0.9	0.6	0.6	0.7	0.7	0.7	0.8	0.7	0.8
U_{out}	**15.3**	**3.2**	**2.6**	**2.9**	**2.8**	**2.7**	**3.1**	**3.0**	**3.0**	**3.0**	**3.0**	**3.1**	**3.1**	**3.2**	**2.6**
45deg Exp A	16.0	3.4	2.3	3.3	2.3	2.3	3.3	3.0	3.1	3.1	3.2	3.4	3.4	3.4	2.3
45deg Exp B	15.0	2.8	2.7	2.7	2.7	2.6	2.6	2.6	2.6	2.8	2.6	2.7	2.7	2.8	2.6
45deg Exp C	15.0	3.5	2.8	2.7	3.4	3.2	3.3	3.3	3.3	3.1	3.1	3.1	3.1	3.5	2.7
Std Dev	0.6	0.3	0.3	0.3	0.6	0.5	0.4	0.3	0.3	0.2	0.3	0.4	0.4	0.3	0.2
Turbidity (NTU)	**110.3**	**50.0**	**44.8**	**53.7**	**37.7**	**31.4**	**47.4**	**89.1**	**101.3**	**44.7**	**63.0**	**72.3**	**70.7**	**101.3**	**31.4**
45deg Exp A	115.0	27.0	24.4	50.1	37.0	16.2	20.8	17.3	68.9	98.1	122.0	107.0	109.0	122.0	16.2
45deg Exp B	60.0	60.0	65.0	75.0	50.0	25.0	10.3	5.0	5.0	10.0	15.0	10.0	20.0	75.0	5.0
45deg Exp C	156.0	63.0	45.0	36.0	26.0	53.0	111.0	245.0	230.0	26.0	52.0	100.0	83.0	245.0	26.0
Std Dev	48.2	20.0	20.3	19.7	12.0	19.2	55.4	135.2	115.9	46.9	54.3	54.1	45.8	87.8	10.5
TSS (mg/L)	**109.3**	**66.0**	**66.0**	**73.0**	**50.0**	**41.7**	**44.4**	**104.3**	**95.3**	**61.3**	**71.0**	**75.0**	**74.0**	**104.3**	**41.7**
45deg Exp A	122.0	68.0	57.0	76.0	51.0	20.0	17.0	30.0	84.0	118.0	126.0	115.0	128.0	128.0	17.0
45deg Exp B	60.0	60.0	65.0	75.0	50.0	25.0	10.3	5.0	5.0	10.0	15.0	10.0	20.0	75.0	5.0
45deg Exp C	146.0	70.0	76.0	68.0	49.0	80.0	106.0	278.0	197.0	56.0	72.0	100.0	74.0	278.0	49.0
Std Dev	44.4	5.3	9.5	4.4	1.0	33.3	53.4	150.9	96.5	54.2	55.5	56.8	54.0	105.3	22.7
Color (Pt-Co)	**5739**	**5901**	**4199**	**2568**	**3495**	**2639**	**2431**	**1938**	**1361**	**1830**	**1558**	**886.0**	**678.0**	**5901**	**678.0**
45deg Exp A	8881	9681	5371	2136	1280	510.0	388.0	347.0	207.0	721.0	728.0	275.0	407.0	9681	207.0
45deg Exp B	3946	3803	4758	2931	5273	3707	4584	3542	2655	235.0	246.0	202.0	164.0	5273	164.0
45deg Exp C	4390.	4220.0	2467.	2638.	3931.	3700.	2320.	1924.	1220.	4534.	3700.	2181.	1463.	4534.	1220.
Std Dev	2730.	3279.9	1530.	402.1	2031.	1843.	2100.	1597.	1230.	2354.	1870.	1122.	690.6	2782.	597.7
$A_{\lambda 560nm}$	**2.9**	**1.7**	**1.6**	**1.4**	**1.5**	**1.0**	**1.0**	**0.7**	**0.5**	**0.4**	**0.3**	**0.3**	**0.1**	**1.7**	**0.1**
45deg Exp A	2.1	2.0	1.9	1.6	1.9	0.9	0.4	0.3	0.2	0.1	0.1	0.1	0.0	2.0	0.0
45deg Exp B	2.5	2.6	2.4	2.1	2.1	1.9	2.1	1.3	1.0	0.9	0.7	0.6	0.1	2.6	0.1

45deg Exp C	4.2	0.5	0.5	0.4	0.4	0.3	0.4	0.5	0.3	0.1	0.2	0.3	0.1	0.5	0.1
Std Dev	1.1	1.1	1.0	0.9	0.9	0.8	1.0	0.5	0.4	0.4	0.3	0.2	0.1	1.1	0.0
COD (mg/L)	**3000.**	**2673.0**	**2237.**	**2233.**	**1996.**	**1867.**	**1736.**	**1406.**	**1474.**	**1179.**	**1365.**	**1079.**	**981.0**	**2673.**	**981.0**
45deg Exp A	3196.	3046.0	2493.	2215.	2066.	1940.	2065.	1414.	1982.	1219.	1859.	952.0	843.0	3046.	843.0
45deg Exp B	3115.	2848.0	2304.	2608.	2140.	1866.	1543.	1109.	882.0	835.0	782.0	622.0	416.0	2848.	416.0
45deg Exp C	2691.	2125.0	1915.	1878.	1782.	1797.	1601.	1696.	1560.	1484.	1455.	1663.	1684.	2125.	1455.
Std Dev	271.2	484.8	294.7	365.4	189.0	71.5	286.1	293.6	554.9	326.3	544.1	532.0	645.2	484.8	522.2
(Cℓ) (mg/L)	**154.4**	**140.8**	**97.6**	**84.7**	**85.5**	**88.6**	**102.9**	**92.6**	**85.7**	**55.3**	**29.5**	**40.6**	**44.6**	**140.8**	**29.5**
45deg Exp A	175.0	179.0	120.0	35.0	80.2	62.5	72.5	80.0	97.5	22.5	10.0	9.0	12.0	179.0	9.0
45deg Exp B	139.0	129.0	90.0	134.2	77.6	114.9	175.2	130.6	106.9	79.2	74.1	68.7	70.9	175.2	68.7
45deg Exp C	149.2	114.3	82.8	84.8	98.6	88.5	60.9	67.1	52.6	64.1	4.5	44.1	51.0	114.3	4.5
Std Dev	18.6	33.9	19.7	49.6	11.4	26.2	62.9	33.6	29.0	29.4	38.7	30.0	30.0	36.3	35.8
f-Cℓ_2 (mg/L)	**1.0**	**2.6**	**3.6**	**1.4**	**2.0**	**2.0**	**1.8**	**1.6**	**0.7**	**0.2**	**0.2**	**0.4**	**0.4**	**3.6**	**0.2**
45deg Exp A	1.1	1.3	0.5	0.2	0.5	0.5	0.1	0.2	0.2	0.3	0.1	0.3	0.2	1.3	0.1
45deg Exp B	1.0	5.6	4.5	3.8	3.8	4.2	4.4	3.8	2.0	0.1	0.4	0.7	0.7	5.6	0.1
45deg Exp C	0.9	0.9	5.7	0.1	1.8	1.3	1.0	0.7	0.0	0.1	0.0	0.1	0.2	5.7	0.0
Std Dev	0.1	2.6	2.7	2.1	1.6	1.9	2.2	1.9	1.1	0.1	0.2	0.3	0.3	2.5	0.0
f-Cℓ_2 (mg/L)	**0.2**	**0.4**	**0.4**	**0.7**	**0.3**	**0.2**	**0.3**	**0.3**	**0.2**	**0.2**	**0.4**	**0.2**	**0.2**	**0.7**	**0.2**
45deg Exp A	0.1	0.7	0.5	0.9	0.1	0.0	0.3	0.3	0.2	0.0	0.2	0.1	0.1	0.9	0.0
45deg Exp B	0.5	0.1	0.4	0.8	0.6	0.1	0.3	0.3	0.2	0.2	0.9	0.3	0.3	0.9	0.1
45deg Exp C	0.1	0.6	0.3	0.5	0.2	0.6	0.3	0.4	0.2	0.2	0.2	0.1	0.1	0.6	0.1
Std Dev	0.2	0.3	0.1	0.2	0.3	0.3	0.0	0.1	0.0	0.1	0.4	0.1	0.1	0.1	0.0
f-Cℓ_2 (mg/L)	**1.2**	**3.1**	**3.9**	**2.1**	**2.3**	**2.3**	**2.1**	**1.9**	**1.0**	**0.3**	**0.6**	**0.5**	**0.6**	**3.9**	**0.3**
45deg Exp A	1.2	2.0	1.0	1.1	0.6	0.5	0.5	0.5	0.4	0.3	0.3	0.4	0.3	2.0	0.3
45deg Exp B	1.5	5.7	4.9	4.5	4.3	4.3	4.7	4.1	2.2	0.3	1.2	0.9	1.0	5.7	0.3
45deg Exp C	1.0	1.5	5.9	0.6	2.0	2.0	1.3	1.1	0.3	0.4	0.2	0.2	0.4	5.9	0.2
Std Dev	0.3	2.3	2.6	2.1	1.9	1.9	2.2	1.9	1.1	0.0	0.6	0.4	0.4	2.2	0.1
Fe(III) (mg/L)	**0.0**	**1.5**	**1.6**	**2.2**	**1.5**	**0.8**	**2.0**	**2.7**	**1.5**	**1.9**	**2.5**	**1.2**	**2.5**	**2.7**	**0.8**
45deg Exp A	0.0	0.8	0.7	1.3	1.0	0.8	1.3	2.0	1.4	2.1	2.6	2.3	3.6	3.6	0.7
45deg Exp B	0.0	1.0	1.6	2.7	1.9	0.1	2.5	3.3	1.8	1.8	2.3	0.1	1.5	3.3	0.1

45deg Exp C	0.0	2.6	2.4	2.5	1.5	1.5	2.2	2.7	1.3	1.9	2.5	1.2	2.5	2.7	1.2
Std Dev	0.0	1.0	0.8	0.8	0.5	0.7	0.6	0.7	0.2	0.1	0.2	1.1	1.1	0.5	0.5
Fe(II) (mg/L)	**0.0**	**4.3**	**4.5**	**4.4**	**3.7**	**4.2**	**4.6**	**3.7**	**4.1**	**2.6**	**2.6**	**1.8**	**1.8**	**4.6**	**1.8**
45deg Exp A	0.0	5.5	4.3	5.6	2.2	2.6	4.8	4.1	4.5	2.8	3.8	2.9	1.2	5.6	1.2
45deg Exp B	0.0	3.5	5.3	3.8	5.2	5.1	5.3	4.5	4.4	2.0	1.4	0.6	2.5	5.3	0.6
45deg Exp C	0.0	3.8	3.8	3.9	3.9	4.9	3.6	2.6	3.4	2.9	2.6	1.8	1.8	4.9	1.8
Std Dev	0.0	1.1	0.8	1.0	1.5	1.4	0.9	1.0	0.6	0.5	1.2	1.2	0.6	0.3	0.6
t-Fe (mg/L)	**0.0**	**5.7**	**6.0**	**6.6**	**5.2**	**5.0**	**6.6**	**6.4**	**5.6**	**4.5**	**5.1**	**3.0**	**4.4**	**6.6**	**3.0**
45deg Exp A	0.0	6.3	5.0	6.8	3.1	3.4	6.1	6.1	5.9	4.8	6.5	5.2	4.8	6.8	3.1
45deg Exp B	0.0	4.5	7.0	6.5	7.1	5.2	7.8	7.8	6.2	3.8	3.7	0.7	3.9	7.8	0.7
45deg Exp C	0.0	6.4	6.2	6.4	5.3	6.4	5.8	5.3	4.8	4.8	5.1	3.0	4.4	6.4	3.0
Std Dev	0.0	1.1	1.0	0.2	2.0	1.5	1.1	1.3	0.8	0.6	1.4	2.2	0.4	0.7	1.3
ORP, mV	**30.7**	**200.0**	**183.7**	**139.3**	**114.7**	**67.7**	**56.3**	**-18.3**	**-22.3**	**18.7**	**38.0**	**39.7**	**24.0**	**200.0**	**-22.3**
45deg Exp A	12.0	135.0	82.0	38.0	15.0	-5.0	-15.0	41.0	9.0	-47.0	43.0	73.0	73.0	135.0	-47.0
45deg Exp B	71.0	304.0	243.0	191.0	166.0	149.0	121.0	-55.0	-15.0	-15.0	-2.0	-25.0	-1.0	304.0	-55.0
45deg Exp C	9.0	161.0	226.0	189.0	163.0	59.0	63.0	-41.0	-61.0	118.0	73.0	71.0	0.0	226.0	-61.0
Std Dev	35.0	91.0	88.5	87.8	86.3	77.4	68.2	51.9	35.6	87.5	37.7	56.0	42.4	84.6	7.0

Table B.6. Iron Electrocoagulation Process of Reactive Dyebaths Textile Effluent at 5.0A and 50^{o}C

Time	**0**	**5**	**10**	**15**	**20**	**25**	**30**	**35**	**40**	**45**	**50**	**55**	**60**	MAX	MIN
T. (^{o}C)	**49.4**	**50.2**	**50.5**	**50.5**	**50.6**	**50.7**	**50.6**	**50.4**	**50.4**	**50.6**	**50.4**	**50.3**	**50.3**	**50.7**	**50.2**
50deg Exp A	50.0	50.0	50.2	50.1	49.9	49.7	49.7	49.3	49.1	49.0	49.0	49.0	49.2	50.2	49.0
50deg Exp B	50.0	51.6	51.6	51.5	51.6	51.4	51.0	50.7	50.4	50.1	49.9	49.8	49.6	51.6	49.6
50deg Exp C	48.1	49.0	49.7	49.9	50.4	50.9	51.1	51.1	51.7	52.7	52.2	52.2	52.2	52.7	49.0
Std Dev	1.1	1.3	1.0	0.9	0.9	0.9	0.8	0.9	1.3	1.9	1.7	1.7	1.6	1.3	0.3
pH	**8.8**	**5.9**	**6.7**	**7.2**	**4.9**	**5.5**	**5.9**	**5.7**	**6.4**	**6.6**	**6.8**	**7.5**	**7.3**	**7.5**	**4.9**
50deg Exp A	11.4	3.0	3.7	4.5	5.2	5.7	6.1	6.4	6.8	7.1	7.3	9.4	9.6	9.6	3.0
50deg Exp B	11.4	10.2	10.3	10.2	1.9	2.8	3.5	4.3	5.1	5.6	6.0	6.0	6.1	10.3	1.9
50deg Exp C	3.7	4.5	6.2	6.9	7.5	7.9	8.1	6.5	7.2	7.2	7.1	7.0	6.2	8.1	4.5

Std Dev	4.4	3.8	3.3	2.9	2.8	2.6	2.3	1.2	1.1	0.9	0.7	1.7	2.0	1.1	1.3
κ (mS/cm)	**6.5**	**7.4**	**7.5**	**7.2**	**7.7**	**7.6**	**7.6**	**7.6**	**7.6**	**7.6**	**7.3**	**7.8**	**8.1**	**8.1**	**7.2**
50deg Exp A	4.8	5.9	5.9	5.9	5.9	5.8	5.7	5.7	5.6	5.6	5.6	5.6	5.6	5.9	5.6
50deg Exp B	4.8	6.4	6.6	5.7	7.4	7.3	7.3	7.4	7.4	7.3	6.3	7.2	7.2	7.4	5.7
50deg Exp C	10.0	10.0	9.9	9.9	9.8	9.7	9.6	9.6	9.7	9.7	10.1	10.4	11.4	11.4	9.6
Std Dev	3.0	2.2	2.2	2.4	2.0	2.0	2.0	2.0	2.0	2.1	2.4	2.4	3.0	2.8	2.3
ρ (ohm)	**78.2**	**128.0**	**171.3**	**190.7**	**182.7**	**144.0**	**145.0**	**127.9**	**121.7**	**128.4**	**127.1**	**125.7**	**122.7**	**190.7**	**121.7**
50deg Exp A	67.3	165.0	164.0	166.0	166.0	168.0	171.0	172.0	173.0	173.0	174.0	174.0	174.0	174.0	164.0
50deg Exp B	67.3	119.0	119.0	119.0	114.0	115.0	114.0	114.0	113.0	114.0	114.0	114.0	114.0	119.0	113.0
50deg Exp C	100.0	100.0	231.0	287.0	268.0	149.0	150.0	97.7	79.1	98.3	93.3	89.0	80.0	287.0	79.1
Std Dev	18.9	33.4	56.4	86.7	78.3	26.9	28.8	39.1	47.6	39.4	41.9	43.7	47.6	85.7	42.7
TDS (g/L)	**4.3**	**3.7**	**3.7**	**3.6**	**3.8**	**3.8**	**3.8**	**3.8**	**3.8**	**3.8**	**3.9**	**4.0**	**4.0**	**4.0**	**3.6**
50deg Exp A	4.0	3.0	3.0	3.0	3.0	2.9	2.8	2.9	2.8	2.8	2.8	2.8	2.8	3.0	2.8
50deg Exp B	4.0	3.2	3.3	2.8	3.7	3.6	3.7	3.7	3.7	3.7	3.6	3.6	3.6	3.7	2.8
50deg Exp C	5.0	5.0	4.9	4.9	4.9	4.8	4.8	4.8	4.9	5.0	5.2	5.7	5.7	5.7	4.8
Std Dev	0.6	1.1	1.1	1.2	1.0	1.0	1.0	1.0	1.0	1.1	1.2	1.5	1.5	1.4	1.1
U_{out}	**16.0**	**3.1**	**3.2**	**3.2**	**2.8**	**2.8**	**2.8**	**2.8**	**2.8**	**2.8**	**2.8**	**2.8**	**2.8**	**3.2**	**2.8**
50deg Exp A	16.0	3.3	3.2	3.2	3.1	3.1	3.1	3.2	3.2	3.2	3.2	3.2	3.2	3.3	3.1
50deg Exp B	16.0	3.4	3.7	3.7	2.7	2.8	2.8	2.7	2.7	2.7	2.7	2.7	2.8	3.7	2.7
50deg Exp C	16.0	2.8	2.6	2.6	2.6	2.6	2.6	2.6	2.6	2.5	2.5	2.4	2.4	2.8	2.4
Std Dev	0.0	0.3	0.6	0.6	0.3	0.3	0.3	0.3	0.3	0.3	0.4	0.4	0.4	0.5	0.4
Turbidity (NTU)	**91.0**	**48.9**	**51.9**	**35.1**	**75.4**	**80.7**	**62.7**	**45.9**	**37.4**	**23.0**	**23.9**	**46.4**	**44.3**	**80.7**	**23.0**
50deg Exp A	85.0	43.0	43.0	37.0	136.0	168.0	124.0	55.0	22.0	11.0	11.0	9.0	13.0	168.0	9.0
50deg Exp B	140.0	62.0	56.0	56.0	88.0	70.0	63.0	67.0	89.0	56.0	49.0	82.0	107.0	107.0	49.0
50deg Exp C	48.1	41.8	56.6	12.2	2.3	4.2	1.2	15.8	1.1	2.0	11.8	48.1	13.0	56.6	1.1
Std Dev	46.2	11.3	7.7	22.0	67.7	82.4	61.4	26.8	45.9	28.9	21.7	36.5	54.3	55.8	25.7
TSS (mg/L)	**126.3**	**68.3**	**70.7**	**94.0**	**93.0**	**92.7**	**54.7**	**34.7**	**37.7**	**31.3**	**41.7**	**39.7**	**53.0**	**94.0**	**31.3**
50deg Exp A	140.0	62.0	38.0	45.0	164.0	201.0	98.0	30.0	12.0	7.0	8.0	8.0	11.0	201.0	7.0
50deg Exp B	140.0	62.0	56.0	56.0	88.0	70.0	63.0	67.0	89.0	56.0	49.0	82.0	107.0	107.0	49.0
50deg Exp C	99.0	81.0	118.0	181.0	27.0	7.0	3.0	7.0	12.0	31.0	68.0	29.0	41.0	181.0	3.0

Std Dev	23.7	11.0	42.0	75.5	68.6	99.0	48.0	30.3	44.5	24.5	30.7	38.1	49.1	49.5	25.5
Color (Pt-Co)	**6781.**	**4832.**	**3406.**	**2551.**	**3610.**	**2424.**	**2889.**	**2783.**	**2090.**	**1734.**	**1087.**	**655.0**	**356.0**	**4832.**	**356.0**
50deg Exp A	6982.	5903.	4669.	2963.	4452.	1905.	4050.	4083.	3616.	2284.	1327.	845.0	459.0	5903.	459.0
50deg Exp B	6982.	2996.	2668.	2768.	4798.	4766.	4148.	3944.	2402.	1951.	1727.	952.0	450.0	4798.	450.0
50deg Exp C	6379.	5599.	2883.	1922.	1582.	603.0	470.0	323.0	253.0	967.0	209.0	168.0	159.0	5599.	159.0
Std Dev	348.1	1597.	1098.	553.4	1765.	2129.	2095.	2131.	1703.	684.8	786.8	425.1	170.7	570.8	170.7
$A_{\lambda 560nm}$	**3.4**	**2.4**	**2.1**	**1.6**	**1.2**	**0.7**	**0.4**	**0.2**	**0.1**	**0.0**	**0.1**	**0.0**	**0.0**	**2.4**	**0.0**
50deg Exp A	3.8	2.8	2.3	2.3	1.6	1.2	0.4	0.2	0.1	0.0	0.0	0.0	0.0	2.8	0.0
50deg Exp B	3.8	2.4	2.5	1.5	1.1	0.9	0.7	0.3	0.1	0.1	0.1	0.1	0.0	2.5	0.0
50deg Exp C	2.7	1.9	1.3	1.2	0.8	0.0	0.0	0.0	0.0	0.0	0.0	0.0	0.0	1.9	0.0
Std Dev	0.7	0.5	0.6	0.6	0.4	0.6	0.3	0.1	0.0	0.0	0.0	0.0	0.0	0.5	0.0
COD mg/L)	**2429.**	**2267.**	**2287.**	**2324.**	**2244.**	**2048.**	**1868.**	**1676.**	**1408.**	**1209.**	**1227.**	**928.3**	**1120.**	**2324.**	**928.3**
50deg Exp A	2220.	1960.	1976.	2971.	2829.	1947.	2138.	1993.	1666.	1395.	1356.	715.0	771.0	2971.	715.0
50deg Exp B	2690.	2880.	2676.	1937.	1937.	2138.	1666.	1395.	1356.	988.0	1056.	741.0	851.0	2880.	741.0
50deg Exp C	2379.	1962.	2210.	2066.	1966.	2061.	1802.	1642.	1203.	1244.	1270.	1329.	1739.	2210.	1203.
Std Dev	239.0	530.4	356.4	563.3	506.7	96.1	243.0	300.5	235.9	205.7	154.5	347.2	537.3	415.6	274.5
(Cℓ) (mg/L)	**219.7**	**175.8**	**114.5**	**58.4**	**130.2**	**99.4**	**62.1**	**75.7**	**69.9**	**71.4**	**28.9**	**30.0**	**55.1**	**175.8**	**28.9**
50deg Exp A	370.0	340.0	280.0	80.0	270.0	160.0	110.0	100.0	70.0	75.0	60.0	10.0	15.0	340.0	10.0
50deg Exp B	129.0	97.3	27.9	29.1	80.5	28.1	39.3	92.1	111.8	109.2	15.7	53.9	101.2	111.8	15.7
50deg Exp C	160.0	90.0	35.5	66.0	40.0	110.0	37.0	35.0	28.0	30.0	11.0	26.0	49.0	110.0	11.0
Std Dev	131.1	142.3	143.4	26.3	122.8	66.6	41.5	35.5	41.9	39.7	27.0	22.2	43.4	132.3	3.0
t-Cℓ_2 (mg/L)	**4.6**	**3.9**	**3.8**	**2.7**	**3.0**	**1.6**	**1.3**	**1.5**	**0.5**	**0.6**	**0.1**	**0.8**	**1.1**	**3.9**	**0.1**
50deg Exp A	5.1	0.4	0.8	5.4	2.2	0.2	0.2	1.8	0.0	0.8	0.2	0.4	0.0	5.4	0.0
50deg Exp B	5.9	5.5	6.0	2.5	6.1	4.1	3.5	2.1	1.4	0.6	0.1	1.5	2.9	6.1	0.1
50deg Exp C	2.8	5.9	4.6	0.2	0.8	0.5	0.2	0.5	0.1	0.5	0.1	0.4	0.3	5.9	0.1
Std Dev	1.6	3.1	2.7	2.6	2.8	2.1	1.9	0.8	0.8	0.1	0.1	0.7	1.6	0.4	0.1
f-Cl_2 (mg/L)	**0.7**	**0.5**	**0.5**	**1.2**	**0.3**	**0.5**	**0.8**	**0.3**	**0.7**	**0.3**	**0.2**	**0.1**	**0.2**	**1.2**	**0.1**
50deg Exp A	1.3	1.0	1.1	0.0	0.8	0.7	1.9	0.0	1.7	0.5	0.3	0.3	0.4	1.9	0.0
50deg Exp B	0.6	0.2	0.4	3.5	0.2	0.6	0.6	0.7	0.5	0.4	0.4	0.1	0.2	3.5	0.1
50deg Exp C	0.3	0.5	0.0	0.0	0.1	0.1	0.0	0.2	0.0	0.0	0.1	0.0	0.0	0.5	0.0

Std Dev	0.5	0.4	0.5	2.0	0.4	0.3	1.0	0.3	0.9	0.2	0.1	0.1	0.2	1.5	0.1
t-Cl_2 (mg/L)	**5.3**	**4.5**	**4.3**	**3.9**	**3.4**	**2.1**	**2.1**	**1.7**	**1.2**	**0.9**	**0.4**	**0.9**	**1.2**	**4.5**	**0.4**
50deg Exp A	6.5	1.3	1.8	5.4	2.9	1.0	2.1	1.8	1.7	1.3	0.5	0.6	0.4	5.4	0.4
50deg Exp B	6.5	5.7	6.4	6.0	6.3	4.6	4.1	2.7	1.9	1.0	0.5	1.6	3.0	6.4	0.5
50deg Exp C	3.1	6.4	4.7	0.2	0.9	0.7	0.3	0.7	0.1	0.6	0.1	0.4	0.3	6.4	0.1
Std Dev	1.9	2.7	2.3	3.2	2.7	2.2	1.9	1.0	1.0	0.4	0.2	0.6	1.5	0.6	0.2
Fe(III) (mg/L)	**0.0**	**0.7**	**1.9**	**2.4**	**2.3**	**1.1**	**1.8**	**1.1**	**2.1**	**2.4**	**2.7**	**1.6**	**1.3**	**2.7**	**0.7**
50deg Exp A	0.0	-0.6	1.7	2.7	2.0	0.5	1.4	0.6	1.6	2.2	2.6	1.4	0.9	2.7	-0.6
50deg Exp B	0.0	0.7	1.9	1.1	1.8	-0.1	1.0	-0.4	1.7	2.4	2.7	0.8	3.1	3.1	-0.4
50deg Exp C	0.0	2.1	1.9	3.4	3.1	2.8	2.9	3.0	3.1	2.7	2.9	2.5	0.0	3.4	0.0
Std Dev	0.0	1.3	0.1	1.2	0.7	1.6	1.0	1.7	0.9	0.2	0.1	0.9	1.6	0.3	0.3
Fe(II) (mg/L)	**0.0**	**3.4**	**4.8**	**3.7**	**3.3**	**3.4**	**3.4**	**3.4**	**3.5**	**3.5**	**2.3**	**2.7**	**1.9**	**4.8**	**1.9**
50deg Exp A	0.0	0.6	4.7	3.7	3.8	1.2	2.4	1.9	4.5	3.1	0.8	2.4	2.6	4.7	0.6
50deg Exp B	0.0	4.8	4.4	4.5	4.0	6.4	5.5	6.2	4.0	4.3	4.2	3.5	3.1	6.4	3.1
50deg Exp C	0.0	4.9	5.1	3.0	2.1	2.6	2.5	2.3	2.0	3.0	1.9	2.2	0.0	5.1	0.0
Std Dev	0.0	2.5	0.4	0.8	1.1	2.7	1.8	2.4	1.3	0.8	1.8	0.7	1.7	0.9	1.6
t-Fe (mg/L)	**0.0**	**4.2**	**6.6**	**6.1**	**5.6**	**4.5**	**5.2**	**4.5**	**5.6**	**5.9**	**5.0**	**4.2**	**3.2**	**6.6**	**3.2**
50deg Exp A	0.0	0.0	6.4	6.4	5.8	1.7	3.7	2.5	6.1	5.3	3.4	3.8	3.5	6.4	0.0
50deg Exp B	0.0	5.5	6.4	5.6	5.8	6.3	6.5	5.8	5.7	6.8	6.9	4.3	6.2	6.9	4.3
50deg Exp C	0.0	7.0	7.1	6.3	5.2	5.5	5.4	5.2	5.1	5.7	4.8	4.7	0.0	7.1	0.0
Std Dev	0.0	3.7	0.4	0.4	0.4	2.4	1.4	1.8	0.5	0.8	1.8	0.4	3.1	0.3	2.5
ORP, mV	**117.0**	**92.3**	**49.0**	**72.3**	**67.3**	**70.0**	**60.3**	**68.3**	**75.0**	**56.3**	**101.7**	**110.7**	**152.0**	**152.0**	**49.0**
50deg Exp A	82.0	70.0	0.0	65.0	62.0	68.0	42.0	58.0	70.0	80.0	80.0	76.0	63.0	80.0	0.0
50deg Exp B	109.0	67.0	38.0	61.0	69.0	81.0	92.0	98.0	94.0	0.0	100.0	86.0	178.0	178.0	0.0
50deg Exp C	160.0	140.0	109.0	91.0	71.0	61.0	47.0	49.0	61.0	89.0	125.0	170.0	215.0	215.0	47.0
Std Dev	39.6	41.3	55.3	16.3	4.7	10.1	27.5	26.1	17.1	49.0	22.5	51.6	79.3	69.8	27.1

Table B.7. Iron Electrocoagulation Process of Reactive Dyebaths Textile Effluent at 5.0A and 55^{o}C

Time	**0**	**5**	**10**	**15**	**20**	**25**	**30**	**35**	**40**	**45**	**50**	**55**	**60**	MAX	MIN

T. (°C)	**55.0**	**54.8**	**54.7**	**54.8**	**55.0**	**55.0**	**55.2**	**54.8**	**54.6**	**54.8**	**54.8**	**55.1**	**55.2**	55.2	54.6
55deg Exp A	55.0	56.4	55.8	55.4	55.1	54.8	54.6	54.5	54.4	54.4	54.4	54.5	54.5	56.4	54.4
55deg Exp B	55.0	54.4	55.6	55.9	55.7	55.1	55.2	54.7	54.7	55.1	55.5	55.5	55.2	55.9	54.4
55deg Exp C	55.0	53.5	52.6	53.2	54.2	55.1	55.9	55.1	54.7	54.8	54.5	55.4	55.8	55.9	52.6
Std Dev	0.0	1.5	1.8	1.4	0.8	0.2	0.7	0.3	0.2	0.4	0.6	0.6	0.7	0.3	1.0
pH	**10.4**	**5.4**	**5.8**	**6.2**	**6.5**	**7.0**	**7.3**	**7.2**	**7.9**	**8.0**	**8.1**	**8.1**	**8.1**	8.1	5.4
55deg Exp A	10.4	5.3	6.0	6.6	7.2	8.0	8.5	9.0	9.2	9.5	9.6	9.8	9.9	9.9	5.3
55deg Exp B	10.4	4.4	5.1	5.6	6.0	6.6	7.1	7.4	7.6	7.8	8.0	8.0	8.1	8.1	4.4
55deg Exp C	10.4	6.6	6.4	6.5	6.3	6.3	6.3	5.2	6.8	6.7	6.6	6.4	6.4	6.8	5.2
Std Dev	0.0	1.1	0.7	0.5	0.6	0.9	1.1	1.9	1.2	1.4	1.5	1.7	1.8	1.5	0.5
κ (mS/cm)	**5.4**	**6.6**	**6.5**	**6.4**	**6.5**	**6.4**	**6.6**	**6.4**	**6.4**	**6.4**	**6.3**	**6.5**	**6.1**	6.6	6.1
55deg Exp A	5.4	6.8	6.7	6.7	6.9	6.7	6.6	6.5	6.3	6.4	6.3	6.2	6.3	6.9	6.2
55deg Exp B	5.4	6.5	6.3	6.1	6.1	5.9	6.6	6.2	5.8	5.6	5.6	5.2	5.2	6.6	5.2
55deg Exp C	5.4	6.5	6.6	6.6	6.6	6.6	6.5	6.6	7.1	7.1	7.0	8.0	6.9	8.0	6.5
Std Dev	0.0	0.1	0.2	0.3	0.4	0.4	0.0	0.2	0.7	0.7	0.7	1.4	0.9	0.8	0.7
ρ (ohm)	**201.0**	**140.3**	**141.0**	**139.3**	**139.3**	**138.7**	**139.0**	**139.3**	**140.3**	**141.3**	**143.0**	**143.0**	**144.0**	144.0	138.7
55deg Exp A	201.0	140.0	140.0	139.0	139.0	138.0	140.0	141.0	142.0	143.0	146.0	147.0	149.0	149.0	138.0
55deg Exp B	201.0	139.0	141.0	139.0	138.0	138.0	137.0	138.0	140.0	142.0	143.0	142.0	142.0	143.0	137.0
55deg Exp C	201.0	142.0	142.0	140.0	141.0	140.0	140.0	139.0	139.0	139.0	140.0	140.0	141.0	142.0	139.0
Std Dev	0.0	1.5	1.0	0.6	1.5	1.2	1.7	1.5	1.5	2.1	3.0	3.6	4.4	3.8	1.0
TDS (g/L)	**2.7**	**3.3**	**3.3**	**3.2**	**3.2**	**3.2**	**3.3**	**3.2**	**3.2**	**3.2**	**3.2**	**3.1**	**3.1**	3.3	3.1
55deg Exp A	2.7	3.4	3.4	3.4	3.4	3.4	3.3	3.2	3.2	3.2	3.2	3.1	3.1	3.4	3.1
55deg Exp B	2.7	3.3	3.2	3.0	3.0	3.0	3.3	3.1	2.9	2.8	2.8	2.6	2.6	3.3	2.6
55deg Exp C	2.7	3.3	3.3	3.3	3.3	3.3	3.3	3.3	3.6	3.5	3.5	3.5	3.5	3.6	3.3
Std Dev	0.0	0.1	0.1	0.2	0.2	0.2	0.0	0.1	0.3	0.4	0.4	0.4	0.5	0.1	0.4
U_{out}	**0.0**	**3.0**	**3.2**	**3.1**	**3.0**	**3.0**	**3.0**	**3.0**	**2.9**	**2.9**	**2.9**	**2.9**	**2.9**	3.2	2.9
55deg Exp A	0.0	2.8	2.8	2.8	2.8	2.8	2.7	2.8	2.8	2.8	2.8	2.8	2.8	2.8	2.7
55deg Exp B	0.0	2.9	2.9	2.8	2.8	2.8	2.8	2.8	2.8	2.8	2.9	2.9	2.9	2.9	2.8
55deg Exp C	0.0	3.2	3.8	3.6	3.6	3.6	3.6	3.6	3.2	3.1	3.1	3.0	3.0	3.8	3.0
Std Dev	0.0	0.2	0.5	0.5	0.5	0.5	0.5	0.5	0.2	0.2	0.1	0.1	0.1	0.5	0.1

Turbidity (NTU)	**64.3**	**36.5**	**35.9**	**67.6**	**85.9**	**52.9**	**36.6**	**101.0**	**37.0**	**77.5**	**52.6**	**39.2**	**56.4**	101.0	35.9
55deg Exp A	63.0	30.5	29.7	46.9	56.8	34.6	21.8	13.0	11.1	16.5	15.3	14.1	15.2	56.8	11.1
55deg Exp B	67.0	62.0	54.0	69.0	93.0	62.0	51.0	42.0	39.0	20.0	13.4	12.5	45.0	93.0	12.5
55deg Exp C	63.0	17.0	24.0	87.0	108.0	62.0	37.0	248.0	61.0	196.0	129.0	91.0	109.0	248.0	17.0
Std Dev	2.3	23.1	15.9	20.1	26.3	15.8	14.6	128.1	25.0	102.7	66.2	44.9	47.9	101.6	3.1
TSS (mg/L)	**67.0**	**49.0**	**41.2**	**82.5**	**110.2**	**110.2**	**60.7**	**93.5**	**55.5**	**91.3**	**60.8**	**150.7**	**77.5**	150.7	41.2
55deg Exp A	67.0	38.0	37.5	126.5	165.5	146.5	58.0	169.5	56.5	153.0	102.0	165.5	86.5	169.5	37.5
55deg Exp B	67.0	62.0	54.0	69.0	93.0	62.0	51.0	42.0	39.0	20.0	13.4	12.5	45.0	93.0	12.5
55deg Exp C	67.0	47.0	32.0	52.0	72.0	122.0	73.0	69.0	71.0	101.0	67.0	274.0	101.0	274.0	32.0
Std Dev	0.0	12.1	11.4	39.0	49.1	43.5	11.2	67.2	16.0	67.0	44.6	131.4	29.1	90.9	13.1
Color (Pt-Co)	**4335**	**3421**	**2655**	**3064**	**1857**	**1787**	**1526**	**1095**	**10425**	**8945**	**628**	**7328**	**500**	3421	500
55deg Exp A	4335	3692.	3398	2771	702	508	620	240	108	184	186	136	211	3692.0	108.0
55deg Exp B	4335	3038	2446	2308	1902	1489	1511	1263.0	1009.0	987.0	756.0	856.0	365.0	3038.0	365.0
55deg Exp C	4335	3533	2122.0	4113.0	2966.0	3363.0	2446.0	1781.0	2009.0	1511.0	941.0	1205.0	923.0	4113.0	923.0
Std Dev	0.0	341.1	663.3	937.5	1132.7	1450.6	913.1	784.2	950.9	668.4	393.5	545.1	374.6	541.7	416.7
$A_{\lambda 560nm}$	**1.6**	**1.4**	**1.2**	**1.0**	**1.3**	**0.7**	**0.4**	**0.0**	**0.0**	**0.0**	**0.0**	**0.0**	**0.0**	1.4	0.0
55deg Exp A	1.6	1.5	1.2	0.9	0.7	0.3	0.1	0.0	0.0	0.0	0.0	0.0	0.1	1.5	0.0
55deg Exp B	1.6	1.6	1.1	0.9	1.4	0.7	0.0	0.1	0.0	0.0	0.0	0.0	0.0	1.6	0.0
55deg Exp C	1.6	1.2	1.2	1.1	1.8	1.3	1.0	0.0	0.0	0.1	0.0	0.0	0.0	1.8	0.0
Std Dev	0.0	0.2	0.1	0.2	0.6	0.5	0.6	0.0	0.0	0.1	0.0	0.0	0.1	0.2	0.0
COD (mg/L)	**2401.3**	**2219.7**	**1947.0**	**1785.0**	**1604.7**	**1372.3**	**1157.0**	**1295.0**	**1191.3**	**942.0**	**978.7**	**811.0**	**787.7**	2219.7	787.7
55deg Exp A	2493.0	2404.0	1986.0	1586.0	1396.0	1410.0	1010.0	1386.0	1204.0	482.0	428.0	174.0	234.0	2404.0	174.0
55deg Exp B	2493.0	2272.0	1970.0	1890.0	1745.0	1538.0	1430.0	1307.0	1316.0	1399.0	1508.0	1239.0	1199.0	2272.0	1199.0
55deg Exp C	2218.0	1983.0	1885.0	1879.0	1673.0	1169.0	1031.0	1192.0	1054.0	945.0	1000.0	1020.0	930.0	1983.0	930.0
Std Dev	158.8	215.3	54.3	172.4	184.3	187.4	236.7	97.6	131.5	458.5	540.3	562.4	498.0	215.3	531.4
($C\ell^-$) (mg/L)	**120.4**	**104.9**	**103.6**	**178.8**	**109.8**	**109.0**	**122.6**	**86.4**	**105.5**	**99.4**	**74.2**	**80.5**	**49.0**	178.8	49.0
55deg Exp A	131.0	215.0	215.8	391.8	132.0	240.0	199.2	130.6	175.3	212.0	136.6	134.9	54.6	391.8	54.6
55deg Exp B	90.3	50.4	18.3	44.7	87.3	37.6	72.1	37.0	38.1	17.7	17.7	40.7	37.8	87.3	17.7
55deg Exp C	140.0	49.4	76.8	99.9	110.1	49.4	96.4	91.6	103.0	68.4	68.3	65.9	54.6	110.1	49.4
Std Dev	26.5	95.3	101.4	186.5	22.4	113.6	67.5	47.0	68.6	100.8	59.7	48.8	9.7	169.6	20.0

t-Cℓ_2 (mg/L)	**2.1**	**3.0**	**2.4**	**2.3**	**-54.5**	**1.1**	**-0.4**	**0.9**	**1.4**	**0.7**	**0.2**	**0.9**	**-0.6**	3.0	-54.5
55deg Exp A	2.1	5.1	1.7	2.3	-168.1	0.5	-2.3	0.7	1.1	0.5	0.8	1.0	1.1	5.1	-168.1
55deg Exp B	2.1	2.3	4.6	3.5	4.1	2.7	1.0	1.1	1.9	1.5	1.7	-2.0	0.1	4.6	-2.0
55deg Exp C	2.1	1.7	0.9	1.1	0.3	0.1	0.1	0.9	1.2	0.1	-1.9	3.8	-2.9	3.8	-2.9
Std Dev	0.0	1.8	1.9	1.2	98.3	1.4	1.7	0.2	0.4	0.7	1.9	2.9	2.1	0.7	95.6
f-Cl_2 (mg/L)	**0.5**	**1.5**	**1.3**	**1.5**	**58.9**	**1.7**	**2.7**	**0.7**	**0.7**	**0.9**	**2.0**	**2.2**	**2.1**	58.9	0.7
55deg Exp A	0.5	0.1	2.8	3.7	174.5	2.5	4.2	0.9	0.6	1.4	2.2	1.3	1.0	174.5	0.1
55deg Exp B	0.5	3.6	0.9	0.3	1.5	0.9	2.0	1.2	1.2	0.3	1.2	3.2	2.4	3.6	0.3
55deg Exp C	0.5	0.8	0.3	0.4	0.8	1.7	2.0	0.1	0.3	1.0	2.7	2.2	2.9	2.9	0.1
Std Dev	0.0	1.9	1.3	1.9	100.1	0.8	1.3	0.5	0.4	0.5	0.8	0.9	1.0	98.9	0.1
f-Cl_2 (mg/L)	**2.6**	**4.5**	**3.7**	**3.7**	**4.4**	**2.7**	**2.3**	**1.6**	**2.1**	**1.6**	**2.3**	**3.1**	**1.5**	4.5	1.5
55deg Exp A	2.6	5.1	4.4	6.0	6.4	2.9	1.8	1.5	1.7	1.9	3.0	2.3	2.0	6.4	1.5
55deg Exp B	2.6	5.9	5.5	3.8	5.6	3.6	3.0	2.3	3.1	1.8	2.9	1.2	2.6	5.9	1.2
55deg Exp C	2.6	2.5	1.2	1.5	1.1	1.8	2.0	1.1	1.5	1.1	0.9	6.0	0.0	6.0	0.0
Std Dev	0.0	1.8	2.2	2.2	2.9	0.9	0.6	0.6	0.9	0.4	1.2	2.5	1.3	0.3	0.8
Fe(III) (mg/L)	**0.0**	**0.5**	**2.4**	**2.5**	**1.7**	**2.1**	**2.3**	**2.5**	**4.6**	**5.0**	**2.7**	**4.2**	**6.3**	6.3	0.5
55deg Exp A	0.0	0.0	1.4	2.0	0.0	0.5	0.6	1.2	0.9	0.0	0.5	1.7	0.2	2.0	0.0
55deg Exp B	0.0	0.6	0.0	1.3	0.5	1.0	1.9	2.3	1.7	1.1	2.2	0.3	0.4	2.3	0.0
55deg Exp C	0.0	1.0	5.7	4.1	4.7	4.8	4.4	4.1	11.4	14.0	5.4	10.7	18.3	18.3	1.0
Std Dev	0.0	0.5	3.0	1.4	2.6	2.4	1.9	1.5	5.9	7.8	2.5	5.7	10.4	9.3	0.5
Fe(II) (mg/L)	**0.0**	**3.2**	**4.4**	**4.5**	**4.4**	**2.8**	**1.8**	**1.4**	**0.8**	**0.7**	**1.1**	**0.8**	**0.7**	4.5	0.7
55deg Exp A	0.0	0.0	5.3	4.0	5.5	2.0	1.1	1.0	0.3	0.5	0.4	0.0	0.4	5.5	0.0
55deg Exp B	0.0	5.5	6.6	5.5	6.2	5.4	3.3	2.3	1.4	1.2	2.5	0.8	0.5	6.6	0.5
55deg Exp C	0.0	4.1	1.2	3.9	1.4	1.1	0.9	1.0	0.6	0.4	0.4	1.5	1.4	4.1	0.4
Std Dev	0.0	2.8	2.8	0.9	2.6	2.3	1.3	0.7	0.5	0.4	1.2	0.7	0.6	1.3	0.2
f-Fe (mg/L)	**0.0**	**3.7**	**6.8**	**7.0**	**6.1**	**4.9**	**4.1**	**4.0**	**5.4**	**5.7**	**3.7**	**5.0**	**7.0**	7.0	3.7
55deg Exp A	0.0	0.0	6.7	6.0	5.6	2.5	1.7	2.2	1.2	0.5	0.8	1.7	0.6	6.7	0.0
55deg Exp B	0.0	6.1	6.7	6.8	6.7	6.4	5.2	4.6	3.0	2.2	4.6	1.1	0.8	6.8	0.8
55deg Exp C	0.0	5.0	7.0	8.0	6.1	5.9	5.3	5.1	12.0	14.5	5.8	12.2	19.7	19.7	5.0
Std Dev	0.0	3.3	0.2	1.0	0.6	2.1	2.0	1.5	5.8	7.6	2.6	6.2	11.0	7.5	2.7

ORP, mV	**146.0**	**149.0**	**183.3**	**165.3**	**97.3**	**54.3**	**44.0**	**15.3**	**0.3**	**-12.3**	**-11.0**	**-2.7**	**11.0**	183.3	-12.3
55deg Exp A	146.0	0.0	207.0	202.0	115.0	101.0	93.0	63.0	48.0	33.0	10.0	63.0	13.0	207.0	0.0
55deg Exp B	146.0	330.0	274.0	238.0	178.0	128.0	83.0	51.0	41.0	24.0	14.0	31.0	31.0	330.0	14.0
55deg Exp C	146.0	117.0	69.0	56.0	-1.0	-66.0	-44.0	-68.0	-88.0	-94.0	-57.0	-102.0	-11.0	117.0	-102.0
Std Dev	0.0	167.3	104.5	96.4	90.8	105.1	76.4	72.4	76.6	70.9	39.9	87.5	21.1	106.9	63.3